NOTICE

The quality of this microform is heavily dependent upon the quality of the original thesis submitted for microfilming. Every effort has been made to ensure the highest quality of reproduction possible.

If pages are missing, contact the university which granted the degree.

Some pages may have indistinct print especially if the original pages were typed with a poor typewriter ribbon or if the university sent us an inferior photocopy.

Reproduction in full or in part of this microform is governed by the Canadian Copyright Act, R.S.C. 1970, c. C-30, and subsequent amendments.

AVIS

La qualité de cette microforme dépend grandement de la qualité de la thèse soumise au microfilmage. Nous avons tout fait pour assurer une qualité supérieure de reproduction.

S'il manque des pages, veuillez communiquer avec l'université qui a conféré le grade.

La qualité d'impression de certaines pages peut laisser à désirer, surtout si les pages originales ont été dactylographiées à l'aide d'un ruban usé ou si l'université nous a fait parvenir une photocopie de qualité inférieure.

La reproduction, même partielle, de cette microforme est soumise à la Loi canadienne sur le droit d'auteur, SRC 1970, c. C-30, et ses amendements subséquents.

ISBN 0-315-53850-3

BEHAVIOR OF EARTHQUAKE RESISTANT SQUAT SHEAR WALLS

by
Claude F. Pilette

A thesis
submitted under the supervision of
Dr. Murat Saatcioglu

in partial fulfillment
of the requirements for the degree of
Master of Applied Science

Department of Civil Engineering
Faculty of Engineering
University of Ottawa
November 5, 1987

Abstract

Performance of slender reinforced concrete structural walls during strong seismic excitations has demonstrated that a ductile behavior can be attained by promoting flexural yielding of vertical reinforcement prior to shear failure. This can be achieved by providing shear strength in excess of the shear stress associated with the ultimate flexural capacity. However, in squat shear walls, the high ratio of shear force to bending moment may make this mechanism difficult to attain. The desirable flexural failure mode may be suppressed by a diagonal tension failure or by sliding of the wall at its base. It is apparent that the effectiveness of the vertical and horizontal wall reinforcement in resisting shear force and bending moment is unclear. Hence, more experimental data is required to attain full understanding of the load resisting mechanism in earthquake resistant squat walls.

In this investigation, two squat shear walls with an aspect ratio of one-half were designed, according to the current design codes, and tested. The main variable was the ultimate flexural capacity and associated nominal shear stress. An appropriate shear reinforcement was provided based on the maximum shear stress associated with the development of the full flexural capacity. Lateral displacement reversals were imposed and no axial load was applied to the specimens.

The test data were analytically studied. The load deflection relationships, crack patterns, moment-rotation and shear force-shear deformation relationships and general observations during the test were analyzed. Both specimens failed in a sliding shear mode prior to the attainment of their ultimate flexural capacities. A nominal shear stress of $0.45\sqrt{f'_c}$MPa and $0.69\sqrt{f'_c}$MPa was sustained by each wall respectively at 68% and 70% of their respective ultimate flexural capacity.

A finite element procedure and a software were developed to extend the experimental investigation of squat shear walls analytically. A good agreement with the test data was achieved.

Based on the experimental and analytical investigations and other researcher's findings, the behavior and failure modes of squat shear walls is presented.

Acknowledgements

The author wishes to express his gratitude to Dr. M. Saatcioglu who provided guidance and advice throughout the development and execution of this research project. I also wish to thank the assistance provided by Mr. Z. Wasiewicz and the technical staff of the Civil Engineering Department during the experimental part of this project.

The Financial assistance provided by the University of Ottawa and the Natural Sciences and Engineering Research Council of Canada is gratefully acknowledged.

Finally, I wish to thank my wife for her understanding and encouragement throughout the year.

Contents

List of Figures

List of Tables

Notations

E_c	=	modulus of elasticity of concrete (initial tangent stiffness)
f'_c	=	maximum compressive stress observed in a cylinder test (negative quantity)
f_{c1}	=	principal tensile stress in concrete (positive quantity)
f_{c2}	=	principal compressive stress in concrete (negative quantity)
f_{cr}	=	stress in concrete at cracking (positive quantity)
f_{cx}	=	stress in concrete in x-direction
f_{cy}	=	stress in concrete in y-direction
f_x	=	stress in reinforced concrete in x-direction
f_{sx}	=	average stress in x-reinforcement
f_{sy}	=	average stress in y-reinforcement
f_y	=	stress in reinforced concrete in y-direction
f_{yx}	=	yeild stress of x-reinforcement
f_{yy}	=	yield stress of y-reinforcement
f_u	=	ultimate stress of reinforcement
G	=	elastic shear modulus of concrete
S_θ	=	spacing of cracks inclined at θ
S_{mx}	=	average spacing of cracks perpendicular to the x-reinforcement
S_{my}	=	average spacing of cracks perpendicular to the y-reinforcement
v_{cxy}	=	shear stress in concrete relative to x, y axes
v_{xy}	=	shear stress in reinforced concrete relative to x, y axes
w	=	crack width
ϵ_1	=	maximum principal strain (positive quantity)
ϵ_2	=	minimum principal strain (negative quantity)
ϵ'_c	=	strain in concrete cylinder at peak stress f'_c (negative quantity)
ϵ_{cr}	=	strain in concrete at cracking (positive quantity)
ϵ_{sh}	=	strain at onset of strain hardening in reinforcement
ϵ_{sy}	=	yield strain of reinforcement
ϵ_{su}	=	ultimate strain in reinforcement
γ_{xy}	=	shear strain relative to x, y axes
θ	=	angle of inclination of principal strains to x-axis
θ_c	=	angle of inclination of principal stresses in concrete to x-axis
ν	=	Poisson ratio of reinforced concrete
ρ_{sx}	=	reinforcement ratio of reinforcing steel in x-direction
ρ_{sy}	=	reinforcement ratio of reinforcing steel in y-direction

Chapter 1

Introduction

1.1 General

The usefulness of reinforced concrete walls in earthquake resistant structures has long been recognized. When walls are located in advantageous positions, they can be very effective in providing the required strength and stiffness to lateral loads. Depending on geometric and functional requirements, structural walls are used in a number of different forms. Isolated walls provide lateral resistance through cantilever action. Coupled walls and frame wall systems show significant interaction of walls with other structural members. Furthermore, depending on wall aspect ratio (height-to-width ratio), the governing mode of deformation and hence the structural response to cyclic loading can be quite different.

Structural walls with an aspect ratio of less than two are called squat shear walls. They are often used in low-rise buildings where they play an important role in resisting earthquake forces. Squat walls may also be used in high-rise buildings where part of the lateral load may be assigned to them.

The philosophy of earthquake resistant design for buildings has been well established [14,15,16]. Three basic design criteria that the designer aims to

achieve, when using structural walls in earthquake resistant structures, are put forward as follows:

1. To provide adequate stiffness so that during low intensity earthquakes, the elastic response of a shear wall can ensure near full protection against damage of non-structural components.
2. To provide adequate strength to ensure that moderate earthquakes do not result in more than superficial structural damage.
3. To provide adequate ductility and capability to dissipate energy in the event of a severe earthquake.

The performance of shear walls during severe earthquakes has often been questioned especially when prevention of total collapse is a prerequisite. For this reason, higher design earthquake loads are specified in the National Building Code of Canada [7,8] for shear wall structures. The increase in design load is introduced through an augmentation of the numerical coefficient, K, which reflects the material and type of construction, damping, ductility and energy-absorptive capacity of shear walls.

Performance of structural walls during recent earthquakes has demonstrated that a ductile behavior can be attained under strong seismic excitations. Slender walls are especially capable of developing the required ductility [24]. Ductile behavior can be attained by promoting flexural yielding of vertical reinforcement prior to shear failure. This is easily achieved by designing the walls for shear strength in excess of that corresponding to flexural yielding. However, in squat shear walls, the high ratio of shear force to bending moment may make this mechanism difficult to attain. The mode of failure at ultimate load may be unpredictable. Indeed the desirable flexural failure mode described previously may be suppressed by a diagonal tension failure or by sliding of the wall at its base. Also, high lateral loads can induce a diagonal compression failure, characterized by crushing of concrete in the compression zone of the wall.

It is apparent that the effectiveness of the vertical and horizontal wall reinforcement in resisting shear force and bending moment reversals is unclear.

More experimental data is required to attain full understanding of the load resisting mechanism in earthquake resistant squat walls.

1.2 Literature review of experimental studies

Considerable research has been carried out to investigate the performance of structural walls found in high-rise buildings. However, only a limited amount of this research is relevant to squat shear walls. The performance of squat walls is often compared with that of deep beams due to their geometric similarities. However the application of the load, generating shear stresses, is different in these two types of structural members. In squat walls, the load is introduced as a line load along the joint between the floor slab and the wall, or foundation and the wall. In deep beams, the load(s) and reactions are directly applied to the faces of the member. This considerably enhances the load resisting mechanism of the beam through an arch action. Therefore the extensive studies of reinforced concrete deep beams, conducted in the past, are not applicable to squat shear walls.

In 1957, Benjamin et al. [13] tested 2.44 m high 3.66 m long plain and reinforced concrete panels. The purpose of the investigation was to develop design data for shear walls resisting atomic blast loading. Monotonically shear force was applied in the plane of the wall through a member at the top which distributed the load along the panel length. Tension and compression columns were provided at either end of the specimens. They observed that panel reinforcement was affecting the cracked wall behavior. On a series of tests conducted on panels with aspect ratio varying between 0.32 and 1.25, they concluded that the panel height-to-length ratio had a direct and pronounced influence on wall behavior.

Tests were carried out at University of Canterbury by Beekhuis [12] in 1971 on three 500 mm by 500 mm cantilever shear walls. He studied the behavior of squat shear walls under cyclic loading. The effects of flexural and shear reinforcement on the mode of failure and ductility were investigated. It was suggested that, for a ductile failure mechanism in low-rise shear walls,

the nominal shear stresses associated with flexural overturning of the wall should be limited. Also, because the flexural failure mechanism is associated with large cracks, no reliance should be placed on the contribution of concrete toward shear strength.

In 1973, Cardenal et al. [18] tested seven large scale specimens at the Portland Cement Association. Walls of 1.90 m by 1.90 m were subjected to static in-plane horizontal loads without any vertical loading. One of the specimens was subjected to ten cycles of load reversals. Its strength was found to be approximately 7% less than that for a similar wall subjected to monotonic loading. It was concluded that for walls with an aspect ratio of one, both vertical and horizontal shear reinforcement were effective in contributing to the shear strength of walls.

Barda et al. [9] tested eight specimens with boundary elements at the Portland Cement Association in 1977. Static and cyclic in-plane loading was applied. The length of the walls was kept constant at 1.90 m whereas the height was varied between 0.48 m and 1.90 m. The objective of this test program was to obtain data on the strength, energy absorption, performance under load reversals, and serviceability of low-rise shear walls with boundary elements. The walls contained sufficient flexural reinforcement to provide a moment capacity larger than the shear strength, forcing the walls to fail in shear. The results of this investigation may be summarized as follows:

1. The shear strength of walls was not affected by the amount of flexural reinforcement.
2. Load reversals decreased the strength by about 10%.
3. For an aspect ratio of one-half and less, horizontal wall reinforcement did not contribute to shear strength but was effective in producing a more uniform crack pattern.
4. The shear strengths of walls with aspect ratios of one-quarter and one-half were the same. However the strength was 20% lower in walls with an aspect ratio of one.

5. The shear force was transmitted from the top slab to the base of the wall by compressive struts.

Synge [35] in 1977, conducted reversed cyclic load tests at University of Canterbury on four reinforced concrete shear walls with a height-to-length ratio of one half. The units were 3 m long and 1.5 m high. Two walls had a rectangular cross section, and the other two were constructed with flanges. Some of these walls contained diagonal shear reinforcement. The following conclusions were made:

1. All walls resisted the applied load in a flexural manner. The corner to corner failure plane was suppressed by using shear reinforcement corresponding to its ultimate flexural capacity of the walls.
2. At high level of lateral deformations, approximately one half of the applied shear was carried by the horizontal reinforcement.
3. The magnitude of slipping of the wall along the wall foundation interface governed the extent to which ductile flexural yielding could occur in the wall.
4. The general hysteric performance of squat shear walls was substantially improved by diagonal shear reinforcement.

Hernandez et al. [25] at University of Mexico in 1980 studied the hysteretic behavior of reinforced concrete walls that were critical in shear. Twenty two models with 1:8 scale and a full scale wall were tested under alternating lateral loads. The test parameters included; aspect ratio, compressive strength of concrete, horizontal and vertical steel reinforcement, axial load, and boundary elements. They observed that structural walls, critical in shear, had an inadequate hysteretic behavior, showing progressive deterioration of strength under repeated load reversals. Also, the efficiency of boundary elements in terms of improving the hysteretic behavior was found to be low.

Two squat shear walls were tested at the University of Toronto by Wiradinata [40] in 1985. The main variable was the wall aspect ratio. The walls

were 2 m long 0.5 m and 1 m high respectively. The amount of reinforcement and the load reversal program used in both specimens were identical. It was concluded that:

1. The shear strength of squat shear walls increases with decreasing aspect ratio.
2. Sliding of the wall as a whole may govern the failure mode beyond a certain level of shear stress if the wall had previously yielded in flexure.
3. For walls with an aspect ratio of one half, a ductile flexural response is possible with the minimum horizontal steel depending on the flexural capacity of the wall.
4. Flexural and shear deformations are equally significant within the deformation range where no strength decay takes place under load reversals.
5. Hysteretic force-deformation curves of squat walls show significant pinching as characterized by shear deformations.
6. Stiffness degradation of walls take place under repeated load reversals.

Two squat shear walls were tested at the University of Ottawa by Wasiewicz [39] in 1987. The main objective of his research program was to suppress sliding shear failure in squat shear walls by special detailing of the reinforcement at the base of the wall. It was concluded that starting bars placed between flexural reinforcement up to 20% of the height of the wall were effective in preventing sliding shear failures.

1.3 Objective and scope

The objective of the research program is to investigate the failure modes in earthquake resistant squat shear walls. Both experimental and analytical investigations are included in the study of the shear wall behavior.

The following forms the scope of the investigation:

1. Review of previous research and current state of the art on aseismic design of squat shear walls.
2. Determination of the parameters that affect the failure modes and identification of those that have not been examined experimentally.
3. Design and construction of large scale test specimens to study the effect of selected parameters on the failure modes of shear walls.
4. Testing of wall specimens under simulated seismic loading.
5. Evaluation and presentation of the test results.
6. Development of a finite element procedure and a software to extend the parametric investigation of shear walls analytically.
7. Establishment of the relationships between the design parameters and failure modes.
8. Presentation of research findings.

Chapter 2

Behavior of Squat Shear Walls

2.1 Energy dissipation mechanism

The ability of a reinforced concrete structure to perform in the inelastic range has often been measured in terms of ductility. In general the term ductility is defined as the ratio of a specified deformation (displacement, rotation, distortion, etc...) at a particular stage of loading to that of yield point. The term ductility is a useful index to describe the energy absorption capability of a squat shear wall. However this holds true only in cases where the load capacity is maintained during load reversals without appreciable loss of strength and stiffness.

It is well recognized that it is uneconomical to design walls to resist lateral forces within the elastic limit during a severe earthquake. Consequently it is generally accepted that energy dissipation, involving considerable large excursions into the postelastic range, will have to be relied upon. As mentioned previously, prevention of collapse is one of the fundamental design criteria. Therefore it is necessary to ensure that plastic deformations in the wall can occur while the lateral load capacity is not significantly reduced.

In most situations involving large earthquake imposed displacements, en-

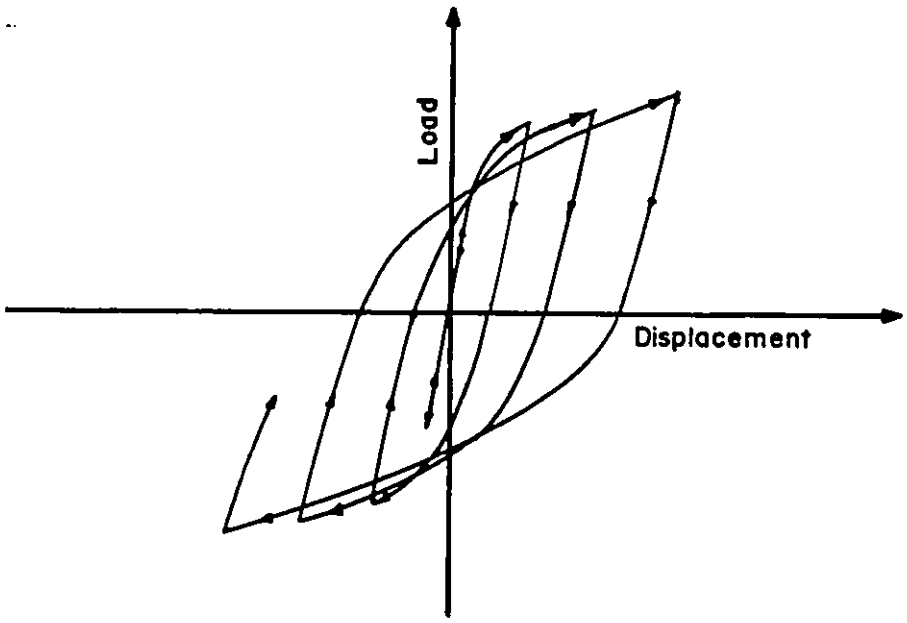

Figure 2.1: Load-Displacement response to cyclic loading of a ductile shear wall

ergy dissipation by hysteretic damping is a viable means by which survival of shear walls can be assured. To ensure the desired energy dissipation, the designer's primary aim will be to minimize the inevitable degradation in both stiffness and strength.

Hysteretic damping is readily available in reinforced concrete walls through inelastic flexural deformations. Although yielding of the flexural reinforcement is a good source of energy dissipation, inelastic deformation of concrete is not as efficient. Concrete being a brittle material will show a rapid strength degradation when subjected to cyclic loading. Contribution of concrete towards shear strength in plastic region should therefore be neglected in design. The desired response of a ductile wall subjected to lateral load reversals shows well rounded load-displacement hysteresis loops as depicted in Figure 2.1.

Shear distortions under inelastic cyclic shear loading are generally unsuit-

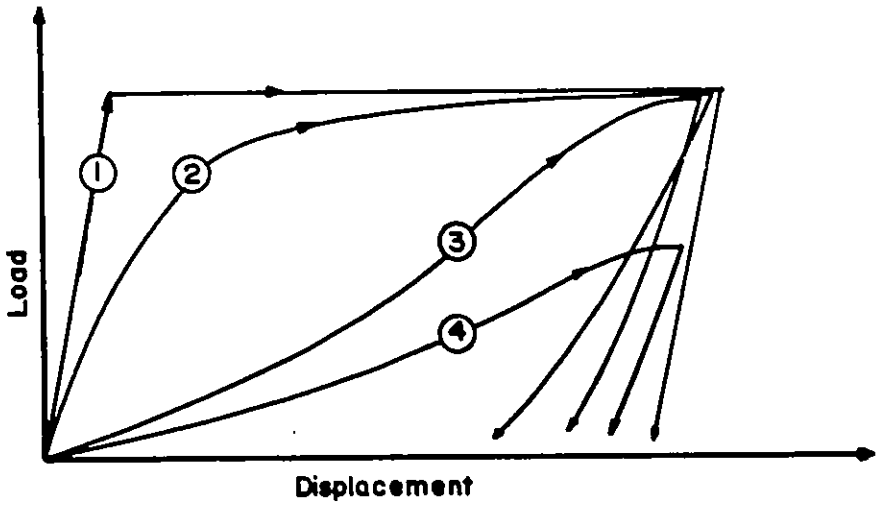

Figure 2.2: Load-Displacement response for (1) idealized elasto-plastic, (2) optimal,(3) (4) repeated shear affected conditions in reinforced concrete walls

able means for energy dissipation. Shear resistance after inelastic shear displacements is not so easily available. It can be attained only when the subsequently imposed displacement is larger than the largest previously applied displacement. Therefore inelastic tensile strains in reinforcement can never be recovered and consequently the width of diagonal cracks increases with progressive cyclic loading. Curves 3 and 4 of Figure 2.2 show typical load-displacement responses which have been affected by significant shear displacements. It is also seen that inelastic shear displacement results in strength and stiffness degradation.

From the features discussed previously it becomes clear that a realistic design procedure should attempt to minimize the probable occurrence of inelastic shear deformation and promote energy dissipation by flexural yielding.

2.2 Shear resistance mechanism

Various mechanisms of shear resistance that interfere with efficient energy dissipation in squat shear walls are reviewed in this section. Diagonal tension, diagonal compression and sliding shear failures are discussed with reference to squat shear walls. Before considering each of these failure modes, base fixity at the foundation level of squat shear walls needs to be examined.

The gravity load on squat walls may be very small, even nonexistent. Therefore the lateral load capacity may be limited by the stability requirement of statics. The full lateral load capacity of the wall can only be developed if significant resistance against overturning is achieved. This requires the foundation to be capable of developing tension associated with foundation uplift.

Reinforced concrete walls subjected to shear stresses develop principal tensile stresses with approximately 45° inclination. Failure associated with these tensile stresses is referred to as diagonal tension failure. Diagonal tension failure usually occur when the horizontal reinforcement is insufficient. The mode of load application at the top edge of squat walls has a significant effect on the diagonal tension strength of such walls. The usual 45° diagonal crack as shown in Figure 2.3(a) does not result in failure due to the tie beam or floor slab which acts as a huge stirrup. The load is transferred to the remainder of the wall by this top member, forcing it to develop a corner to corner failure plane as shown in Figure 2.3(b). However, for walls with aspect ratio varying between one and two, the 45° failure plane may control the failure mode.

As principal tensile stresses develop, principal compressive stresses also develop in the perpendicular plane. These stresses are transferred through compression struts between the diagonal cracks. Excessive compression in these struts may build up if diagonal tension failure is prevented. This may produce a diagonal compression failure by crushing the concrete under heavy compression. It usually takes place when the average shear stress in the wall section is high. Under reversed cyclic loading, two sets of di-

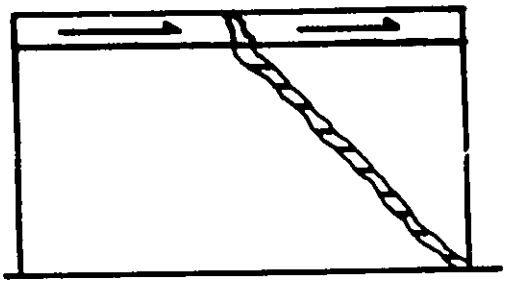

a) 45° diagonal tension failure

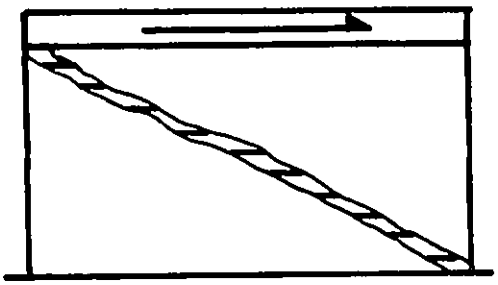

b) Diagonal tension failure

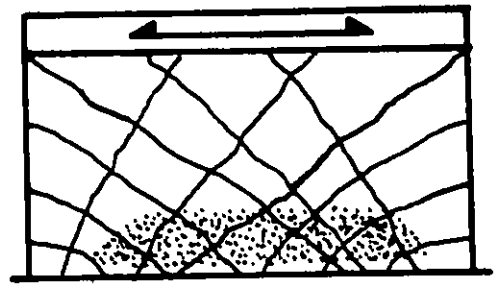

c) Diagonal compression failure

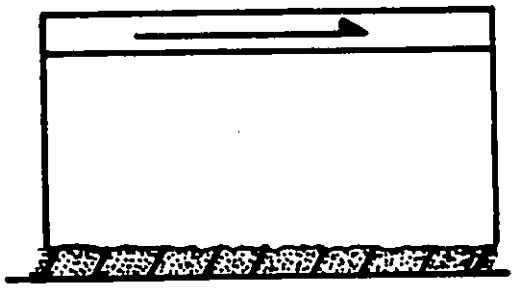

d) Sliding shear failure

Figure 2.3: Failure modes for squat shear walls.

agonal cracks develop in two opposite directions. Opening and closing of these diagonal cracks under cyclic loading reduces considerably the compression strength of concrete. Therefore, the diagonal compression failure may develop at a much lower average shear stress. As a result, crushing of concrete spreads rapidly over the entire length of the wall, as depicted in Figure 2.3(c), resulting in a drastic and irrecoverable loss of strength.

As described previously, the desired energy dissipation would be expected to come mainly from yielding of the vertical flexural reinforcement. However, after few inelastic cycles the phenomenon of sliding shear can occur. This mode of failure is characterized by sliding of the wall along its base due to flexural cracks which interconnect and form a continuous weak plane along the construction joint, as shown in Figure 2.3(d). Sliding shear is responsible for a significant reduction of stiffness and energy dissipation. This failure mode has been extensively studied by Wasiewicz [39].

2.3 Design philosophy for squat shear walls

For squat shear walls the assessment of flexural and shear strength cannot be based on the beam theory applicable to tall structural walls. Experiments with reinforced concrete tall walls with adequate shear reinforcement indicate that the shear force has little influence on the development of flexural capacity. This enables the designer to ignore the interaction of shear and flexure and to deal with them separately. Park and Pauley [28] showed, however, that an intimate relation does exist between flexure, shear, bond and anchorage in the region of high shear force and bending moment.

Even though the assumptions on which flexural response of tall walls are based [2], do not hold true in squat shear walls, the standard approach for the prediction of flexural strength is likely to be satisfactory for design purposes. In the derivation of the ultimate flexural capacity that can be mobilized during very large excursions in the postelastic range, the following factors need to be taken into account:

1. The ultimate moment resistance must be based on the contribution of all vertical bars that are present in the wall section, including vertical steel for shrinkage control.

2. The strength of the reinforcement must be based on the actual yield strength rather than on the nominal strength.

3. As large steel strains are expected, it is necessary to evaluate or approximate the additional strength develop due to strain hardening.

4. Some allowance may have to be made for the increase in concrete strength to a value larger than that used in the design.

For seismic design procedures the non-linearity of flexural strains, known to occur in deep beams, do not need to be taken into account for squat shear walls. It may be assumed that at ultimate curvature all flexural bars in the wall yield in tension or compression, as appropriate. Since earthquake type of loading will need to be resisted in both lateral directions, a symmetrical distribution of vertical flexural steel is the common practice. In most cases the amount of flexural reinforcement will be small because a relatively large internal lever arm may be utilized and the lateral load capacity of the wall may be limited by the inability of the foundation to resist the overturning moment. Therefore it will be more practical to distribute the vertical reinforcement uniformly over the full length of the wall with only a small increase at the vertical edges.

One prerequisite for ductile flexural response of squat walls, and hence for significant energy dissipation by plastic hinging, is that shear failure should be suppressed. If this principle is accepted, then every precaution must be taken to prevent a possible shear failure during a seismic disturbance of some duration [29]. Diagonal tension failure should be prevented by providing horizontal shear reinforcement capable of transferring across the potential failure plane a shear force in excess of that produced at attainment of the ultimate flexural capacity. Diagonal compression failure may be avoided by prescribing a maximum average shear stress value, limiting the ultimate flexural strength of the wall section as suggested by Aktan and Bertero [1]. If both diagonal tension and compression failures

are prevented, the full flexural capacity of the wall should be developed. Consequently excessive yielding of vertical reinforcement will occur, hence triggering the undesirable sliding shear phenomenon. The severity of sliding shear is considered to increase with an increase in expected ductility demand and a decrease in wall aspect ratio [41]. Unless specially detailed, all ductile squat shear walls are likely to fail in this mode.

2.4 Design building codes

Code recommendations used in the past have been mostly based on the early work of Benjamin and Williams [13] on low-rise shear walls. The work of Cardenas et al. [18] and Barda et al. [9] has contributed much toward the present understanding of squat shear wall resisting mechanism. In spite of their contributions, very little is said about squat shear walls in the American code and no address is made in the Canadian code. Therefore the designer most rely on the present state of the code for ductile flexural walls to design squat shear walls or seek additional informations elsewhere [29,30].

As far as special provisions for seismic design are concerned, the North American codes limit the maximum applied nominal shear stress for shear walls. This value has been accepted for many years in North America. Extensive experimental work, involving the testing of numerous low and high rise shear walls under monotonic static load, has shown this value to be conservative, as mentioned by Cardenas et al. [19] and Fiorato et al. [23]. However, the code limit for nominal shear stress was never meant for situations under seismic conditions [32]. Pauley [31] observed that shear stresses of this magnitude cannot be sustained across plastic hinges, which is likely to occur over the full height of squat walls, when cyclic loading is involved. Also, the contribution of concrete towards shear strength in plastic regions of shear walls shall not be taken into account, as stipulated by the Canadian code. Nevertheless the American code allows the designer to include and increase that contribution for walls with aspect ratio less than two.

Chapter 3

Experimental Program

3.1 Test specimens

Two reinforced concrete squat walls with rectangular sections were tested and analyzed in this investigation. These walls were part of an overall investigation on earthquake resistant squat walls and formed the fourth and fifth walls in the test program. Therefore they were labelled as Wall 4 and Wall 5. Both walls had a height-to-length ratio of one half with the same overall dimensions. The two specimens were designed and detailed as 1/3 scale models with orthogonal reinforcement arrangement in two layers. Both walls were subjected to cyclic load reversals without vertical loading. Walls 1 & 2 and 3 & 6 were reported by Wiradinata [40] and Wasiewicz [39] respectively.

A rectangular heavily reinforced beam was cast along the top horizontal edge of each wall. The purpose of this top beam was to simulate the actual floor-slab system and to provide a uniform load transfer. Also, a heavily reinforced base footing was provided for each wall. This bottom beam was used to provide fixity at the base and hence transfer the load uniformly from the wall to the footing. This footing was connected on to the strong floor of the structural laboratory by means of four 1800 mm long by 70 mm

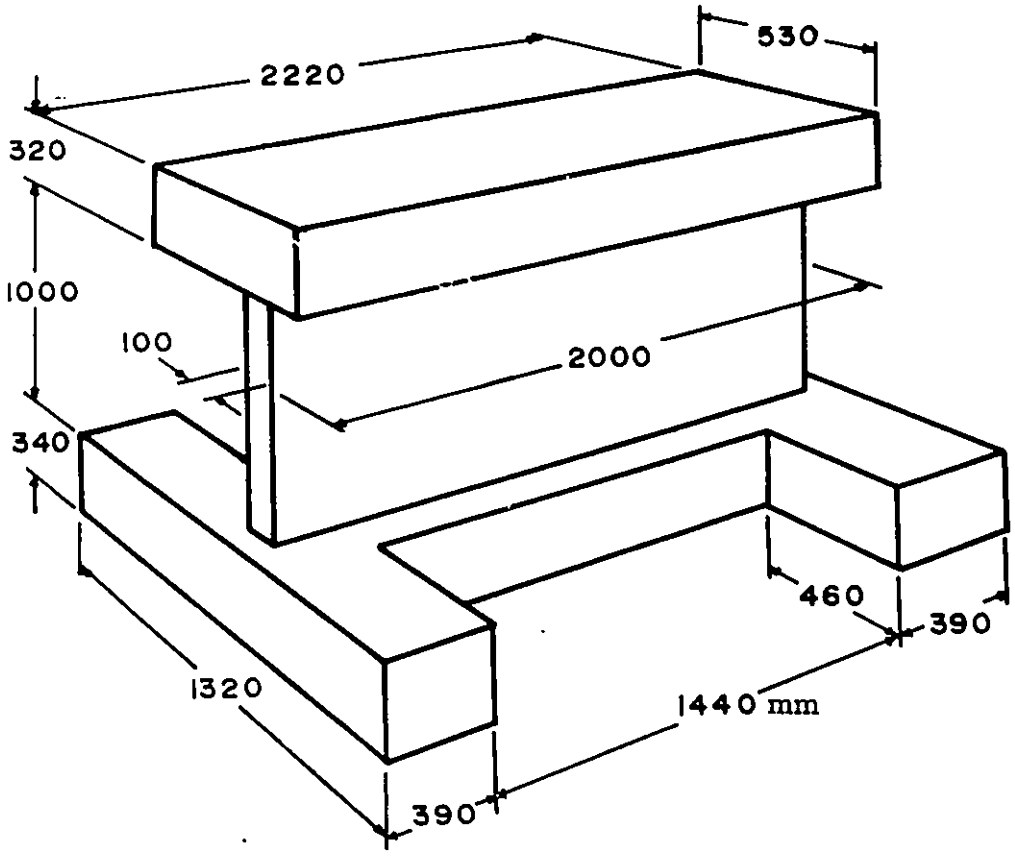

Figure 3.1: Schematic of Walls 4 and 5

diameter high strength bolts. The overall dimensions of Walls 4 and 5 are presented in Figure 3.1.

3.1.1 Design of Wall 4

Wall 4 was designed as a companion specimen to Wall 1 reported by Wiradinata [40]. The same arrangement of the vertical flexural reinforcement was used, resulting in a predicted applied shear stress of $0.67\sqrt{f'_c}$ MPa. The main objective of Wall 4 was to suppress the corner to corner failure plane observed in Wall 1 and hence to achieve a better ductile behavior.

Flexural strength was based on the vertical reinforcement provided, using the conventional beam theory and assuming that it applies to squat shear walls. A vertical reinforcement ratio of 0.8% of the gross cross-sectional area was used, resulting in eight pairs of 10M deformed bars placed symmetrically along the wall with only a nominal increase at the edges. Proper bar anchorage was provided into the bottom and top beams. Based on the measured material properties, the flexural capacity of the cross-section was found to be 698 kN·m. Detailed computations are presented in Appendix A.

From the predicted bending moment capacity, a design shear force of 612 kN was obtained. Neglecting concrete contribution towards shear strength, this resulted in a horizontal shear reinforcement ratio of 0.8%. Four pairs of 10M deformed bars were placed uniformly over the height of the wall for a design shear strength of 614 kN. It was believed that the diagonal tension failure observed in Wall 1, with a shear reinforcement ratio of 0.25%, could be suppressed by providing a shear strength capacity in excess of the shear force obtained at ultimate curvature.

Stirrups were provided at both ends of the wall to prevent premature buckling of the vertical bars in compression. These stirrups were made of 6.4 mm diameter plain steel and were spaced at 80 mm. The effect on confinement of concrete provided by these stirrups was not considered in design calculations.

The details of the reinforcement layout and sections of the footing, the wall and the top member are presented in Figure 3.2.

3.1.2 Design of Wall 5

Wall 5 was designed for a higher flexural capacity than Wall 4. It was designed to develop an applied shear stress of $1.01\sqrt{f'_c}$MPa which is higher than the maximum permissible value of $0.83\sqrt{f'_c}$MPa allowed by Design Building Codes [3,17]. Its flexural and shear strength capacities were based

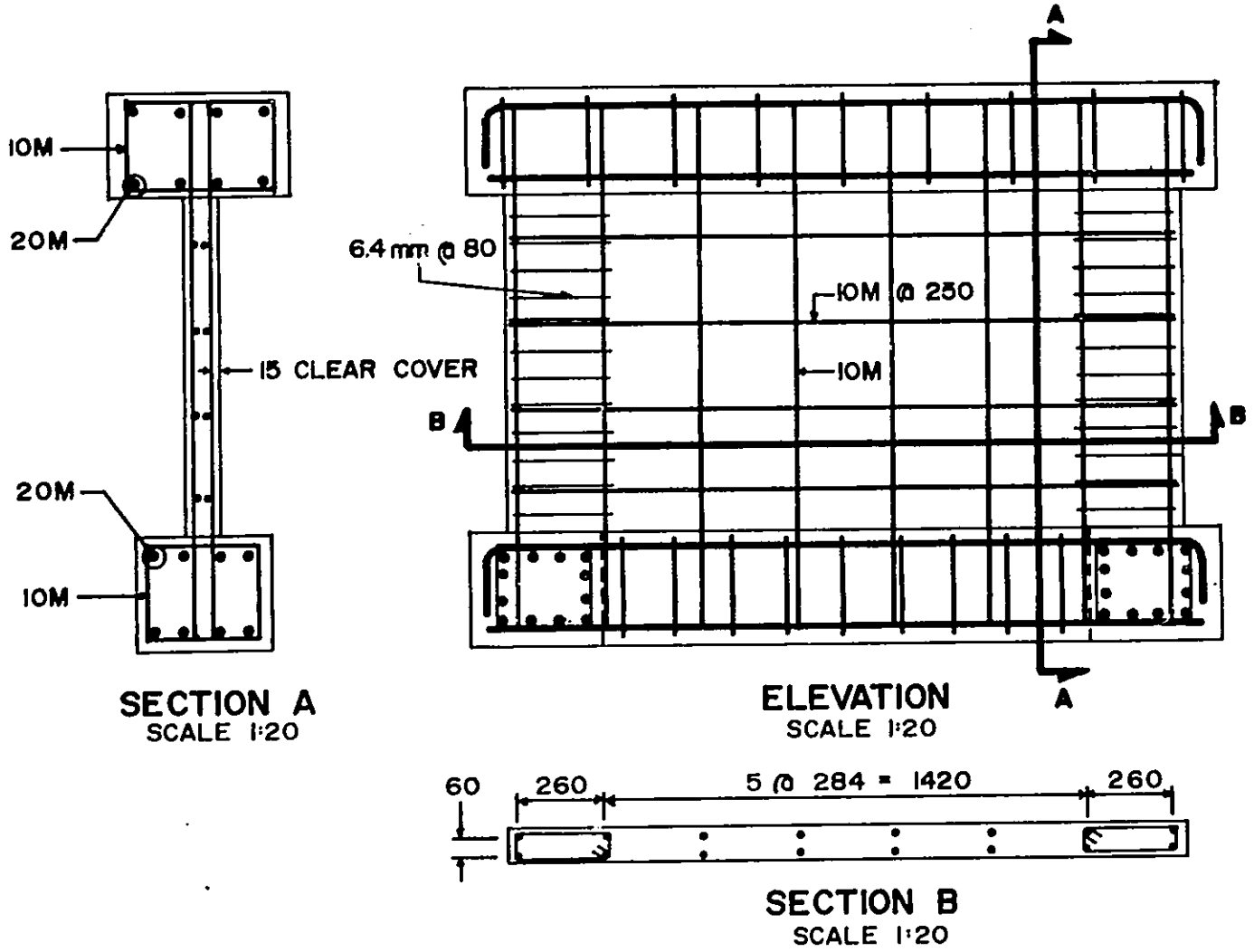

Figure 3.2: Reinforcement layout and sections of Wall 4

on the same design philosophy and assumptions as Wall 4.

A vertical reinforcement ratio of 1.2% of the gross cross-sectional area was used. Twelve pairs of 10M deformed bars were placed uniformly along the wall height and well anchored into the bottom and top members. Again, stirrups were provided at both ends of the wall to prevent premature buckling of the vertical bars in the compression zone. The predicted flexural capacity was found to be 955 kN·m. Detailed computations are presented in Appendix B.

From the predicted flexural capacity, a design shear of 838 kN was computed. A horizontal shear reinforcement ratio of 1.2% was used. Six pairs of 10M deformed bars were placed uniformely over the height of the wall providing a design shear capacity of 878 kN. The details of the reinforcement layout and sections of Wall 5 are presented in Figure 3.3.

3.2 Fabrication

The two test specimens were prepared in a wooden formwork made from 20 mm thick plywood. The formwork was painted and a light coat of form oil was applied prior to the placing of the reinforcement as a bond-breaker. The formwork was designed in such a way that it could be used for Walls 3, 4, 5 and 6.

The test specimens were constructed in two stages in order to simulate a construction joint at the wall base. The footing was cast first with the vertical wall reinforcement. The concrete was properly vibrated using a 25 mm diameter electrical vibrator. Concrete cylinders were also cast in accordance with CSA Standard CAN3-A23.2-M. An exposed aggregate construction joint was prepared on the top surface of the foundation beam as required by CSA Standard CAN3-A23.3-M84. After few hours, the specimen and the cylinders were wrapped in wet burlaps and polyethylene sheets for at least five days.

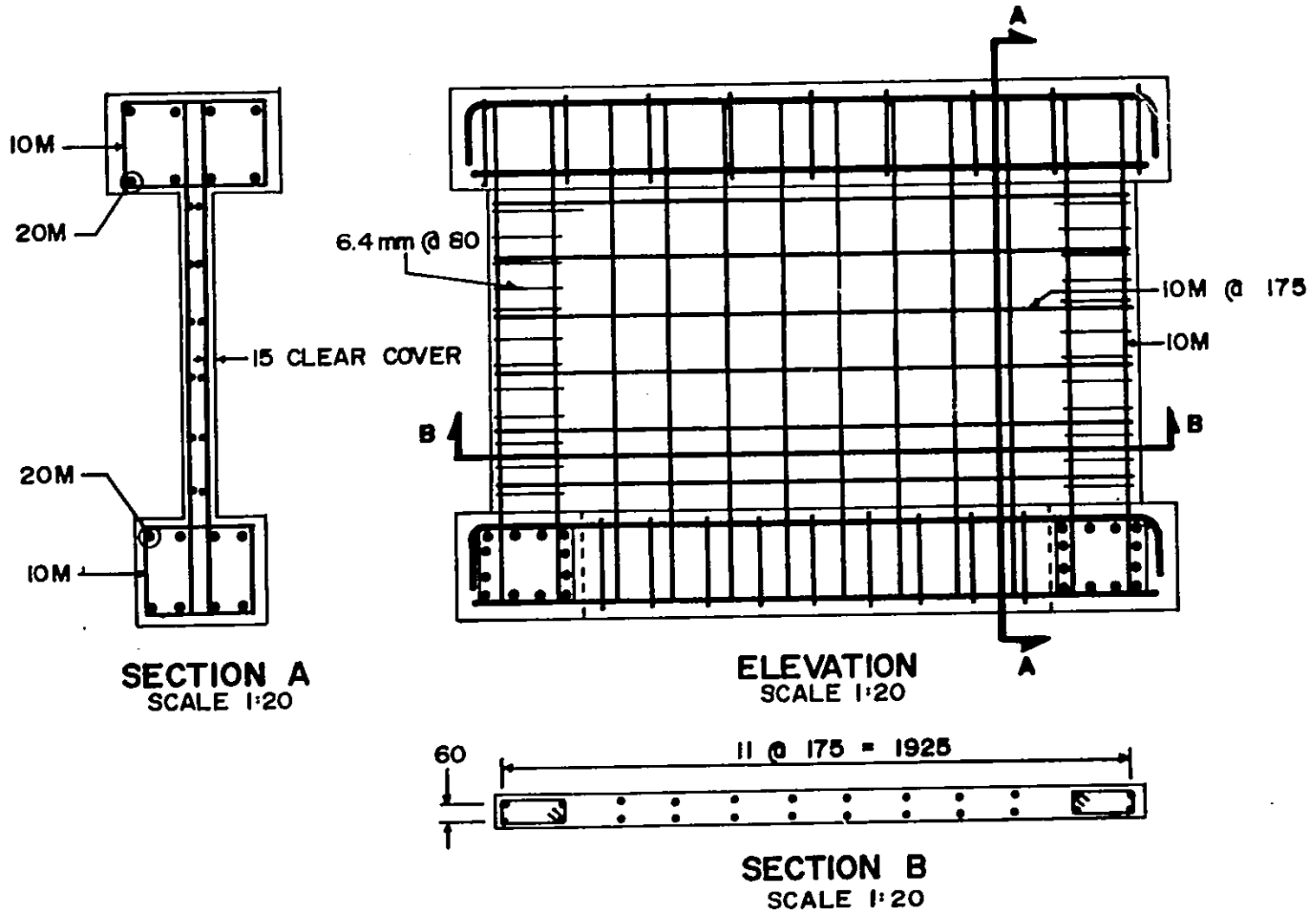

Figure 3.3: Reinforcement layout and sections of Wall 5

After removal of the bottom beam formwork, the horizontal reinforcing bars and stirrups were placed. Figures 3.4 and 3.5 present Walls 4 and 5 respectively at the end of the first construction stage. Also, a close-up of the end region of Wall 5 is shown in Figure 3.6.

The second construction stage was the casting of the wall and top beam in an upright position. Concrete cylinders were also cast and all concrete was vibrated using an electrical vibrator. After pouring of the concrete, the top surface of the top beam and the cylinders were wrapped with wet burlaps and polyethylene sheets. The formwork was stripped after seven and four days for Walls 4 and 5 respectively and the curing process was continued for another week by wrapping wet burlaps and polyethylene sheets around the whole specimen. Testing commenced after 164 and 102 days for Walls 4 and 5 respectively. Prior to testing, the specimens were painted with a thin coat of white paint to facilitate crack detection.

3.3 Material properties

3.3.1 Concrete

Ready mix concrete was obtained from a local plant and was used for both specimens. A 28-day target strength of 28 MPa, 100 mm slump and maximum aggregate size of 10 mm was ordered for each wall.

Several 150 × 300 mm cylinders from each batch were tested to determine the compressive strength, f'_c, and the tensile strength, f_{cr}, of the concrete. Also, stress-strain relationship of concrete cylinders under monotonic and cyclic compressive loading were determined. Figures 3.7 and 3.8 present these relationships for Walls 4 and 5 respectively. Concrete strain in cylinder tests was measured by two 10 mm stroke Linear Variable Differential Transformers (LVDT) mounted on two opposite sides of cylinders. The concrete properties are summarized in Table 3.1.

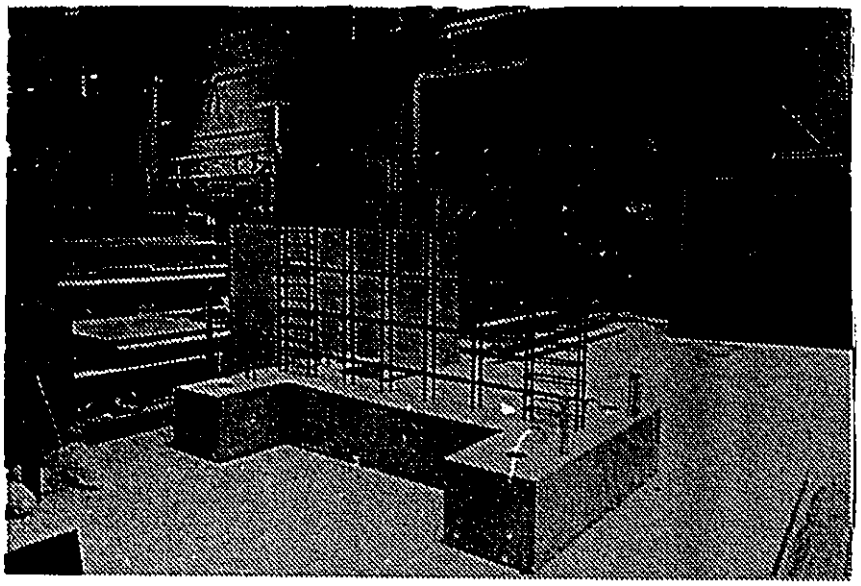

Figure 3.4: Wall reinforcement of Wall 4

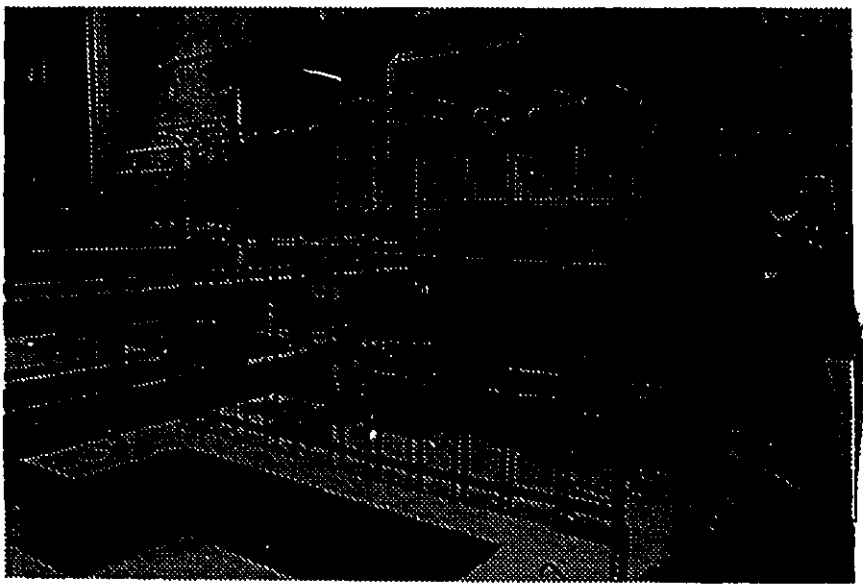

Figure 3.5: Wall reinforcement of Wall 5

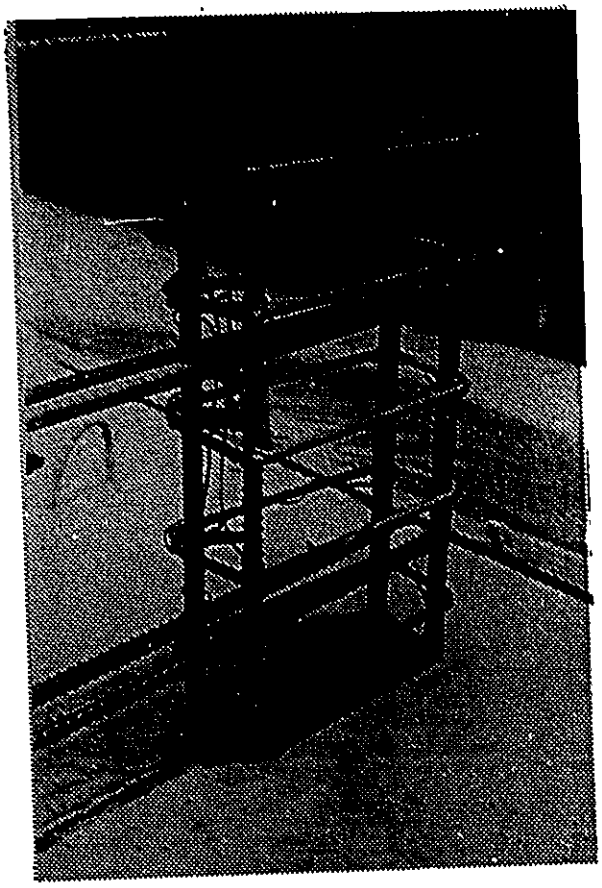

Figure 3.6: Edge details of Wall 5

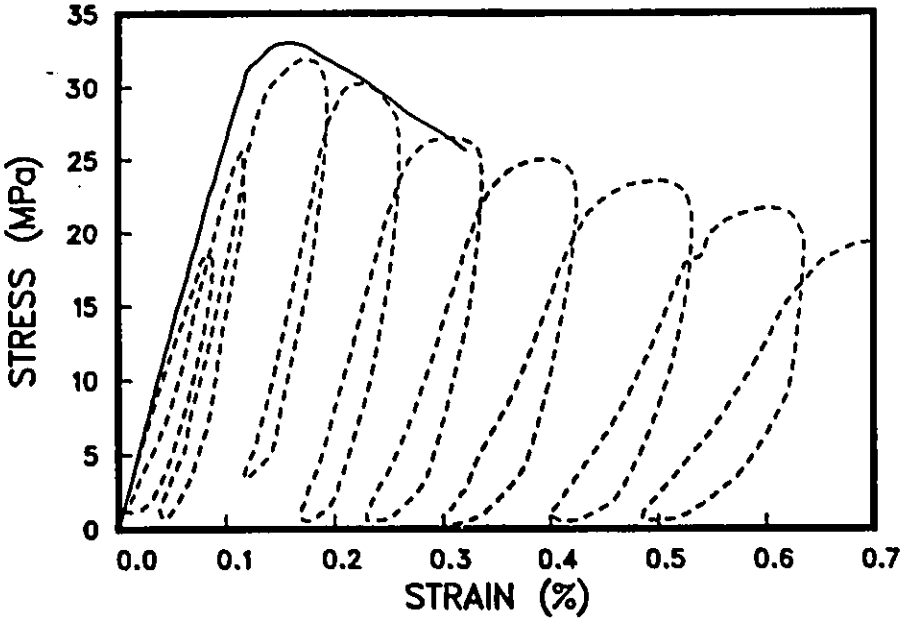

Figure 3.7: Stress-Strain relation of concrete for Wall 4

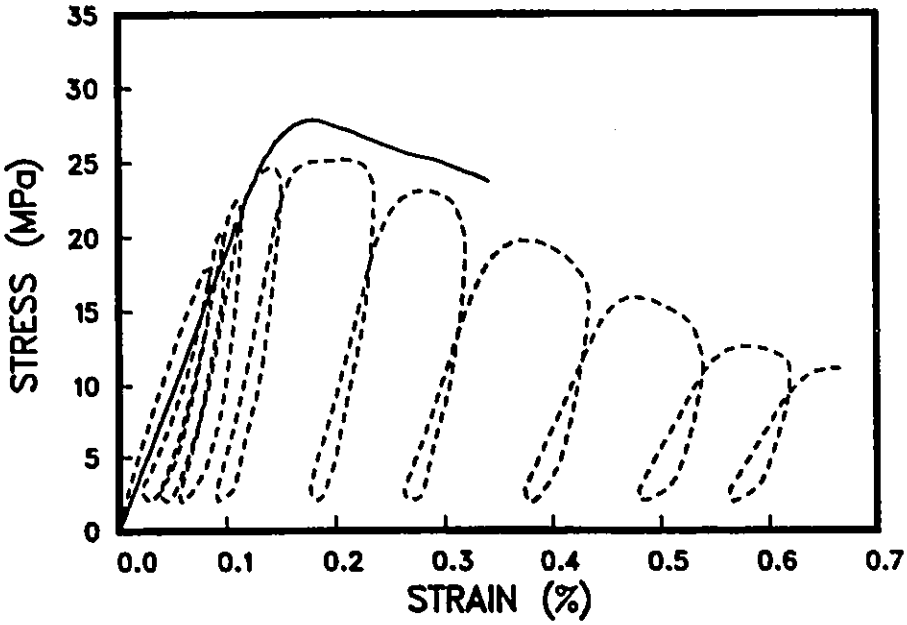

Figure 3.8: Stress-Strain relation of concrete for Wall 5

Concrete			
Wall	f'_c (MPa)	ϵ'_c (%)	f_{cr} (MPa)
4	-33	-0.17	3.5
5	-27	-0.18	3.4
Reinforcing steel			
Bar	f_{yy} (MPa)	ϵ_{sy} (%)	f_u (MPa)
6.4 mm	370	0.186	470
10M	480	0.240	770

Table 3.1: Material properties

3.3.2 Reinforcing steel

Vertical and horizontal reinforcement used for both specimens were made of Grade 400, 10M deformed bars obtained from the same batch. Coupons were tested under monotonic and cyclic tensile loading to determine the characteristics of the steel. Stirrups were made of 6.4 mm diameter mild plain steel. A 50 mm extensometer was used to obtained the stress-strain relationships presented in Figure 3.9. Steel properties are summarized in Table 3.1.

3.4 Instrumentation

During the test, readings of the applied load and vertical and horizontal deflections at selected locations on the specimens were recorded. All deflections were measured with respect to the foundation beam so that movement of the specimen on the floor would not affect the readings. Also, strains in selected vertical bars were measured by means of strain gauges.

Locations of the Linear Variable Differential Transformers (LVDT), used to measured deflections can be seen in Figure 3.10. Two different sizes of

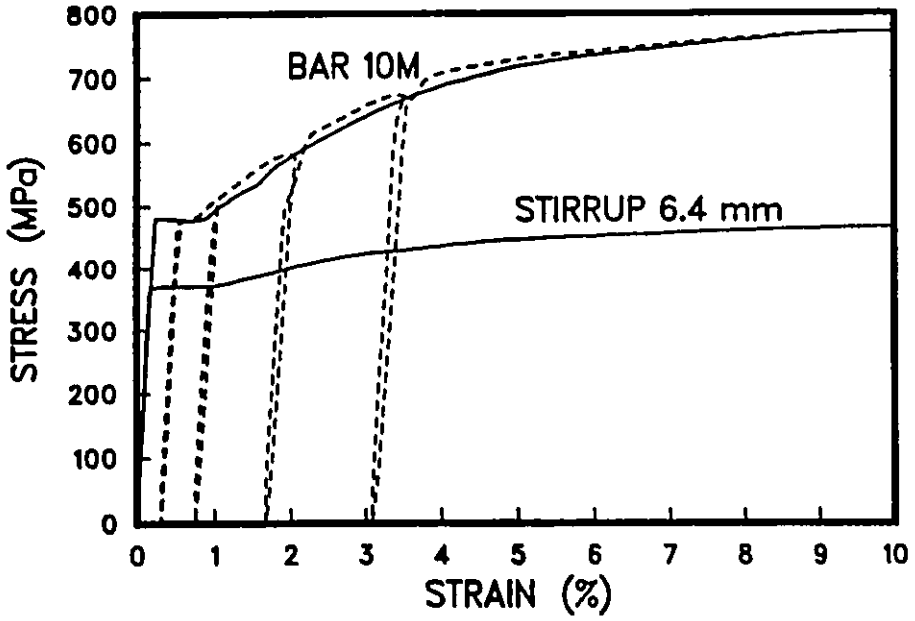

Figure 3.9: Stress-Strain relation of reinforcing steel

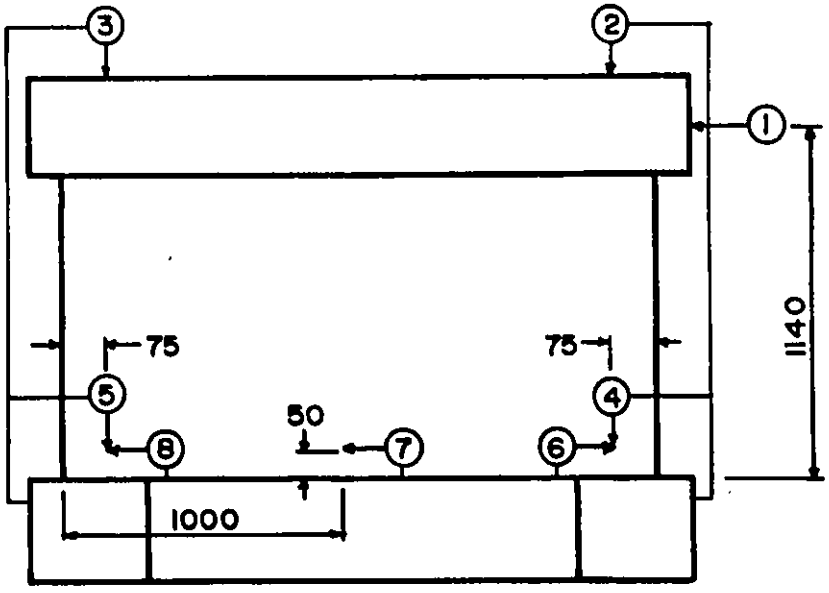

Figure 3.10: Schematic of the location of LVDTs on Walls 4 and 5

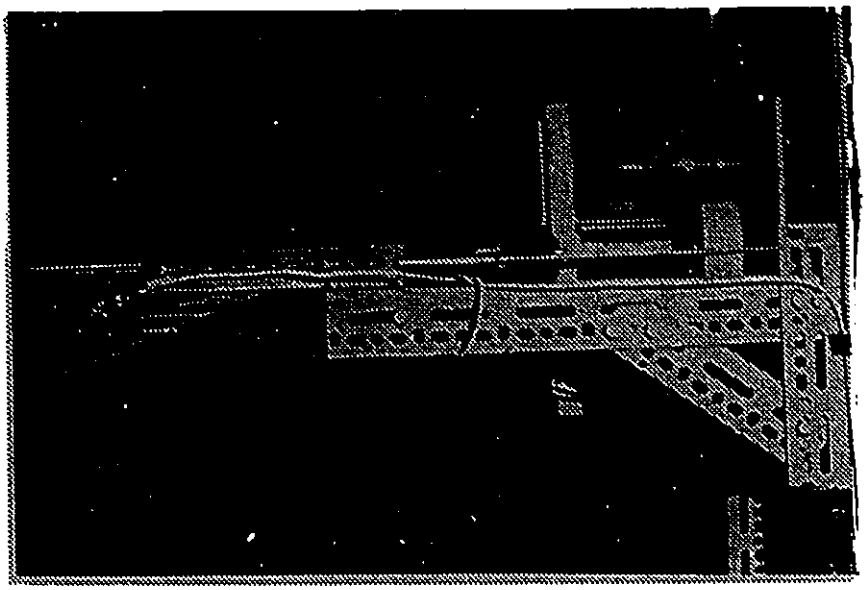

Figure 3.11: Picture of LVDT 1

LVDTs with 10 mm and 150 mm stroke capacities were used during the test. As depicted in Figure 3.10, LVDT 1 was used to measured the top horizontal deflection of the specimen whereas LVDTs 2 and 3 measured the vertical movement of the top beam. Figure 3.11 shows LVDT 1 mounted to a frame made of steel angles which was connected to the bottom beam. Vertical movements, resulting from the local slippage of the vertical bars in the foundation beam near the construction joint, were recorded with LVDTs 4 and 5. Slip of the wall along the construction joint was monitored with LVDTs 6, 7 and 8. Figure 3.12 shows a close-up of LVDTs 4 and 6.

Electrical resistance strain gauges were placed on most vertical bars at the construction joint level. The extreme vertical bars had gauges installed at 100 mm below and 200 mm above the construction joint level. All gauges were installed using the following procedure presented in Figure 3.13: (1)(2) the bar was first filed and cleaned, (3) the gauge and the terminal were bonded to the bar by the use of an adhesive agent and the wire was soldered to the terminal, (4) a thick layer of a water proofing agent was applied on the gauge and terminal, (5) a soft compound was used to

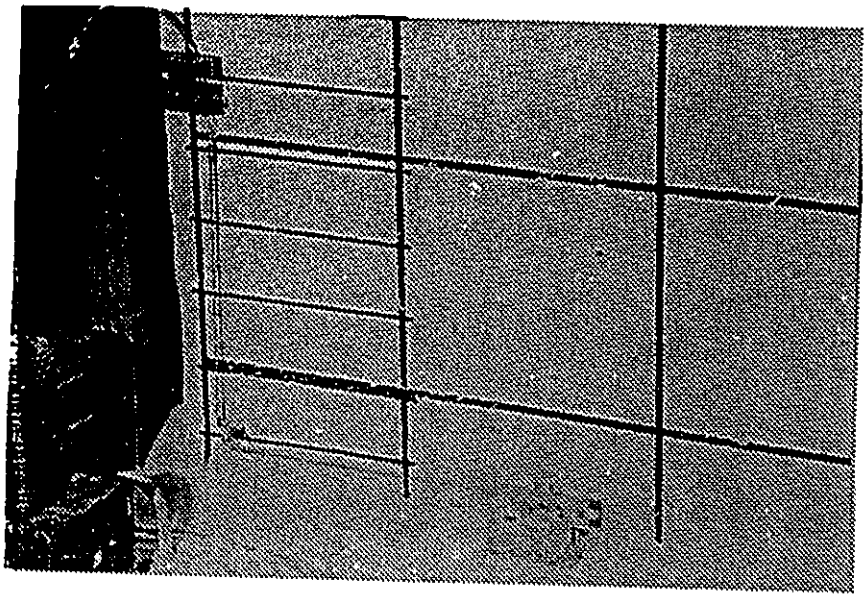

Figure 3.12: Picture of LVDTs 4 and 6

protect the gauge and the terminal against chocks and finally, (6) the whole area was wrapped around with electrical tape.

The applied load was measured with two 1250 kN load cells. Prior to the test the load cells were accurately calibrated. More details about the load measurement system are presented in section 3.5.

All voltages from the LVDTs, strain gauges and load cells were then fed into a Hewlett-Packard (HP) 3497A Data Acquisition Control Unit which in turn was controlled by an HP 9845B desktop computer. A software was written by the author to automatically take readings at prescribed load or deformation increment during the test. These voltages were then stored on a data cartridge and later transferred to the mainframe computer system of the University of Ottawa for data processing. Figure 3.14 shows the data acquisition system used during the tests.

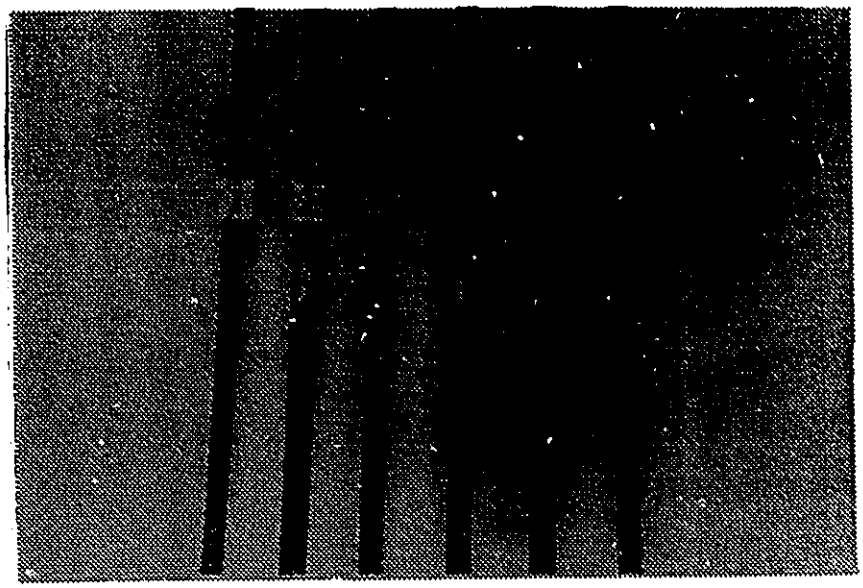

Figure 3.13: Strain gauge installation

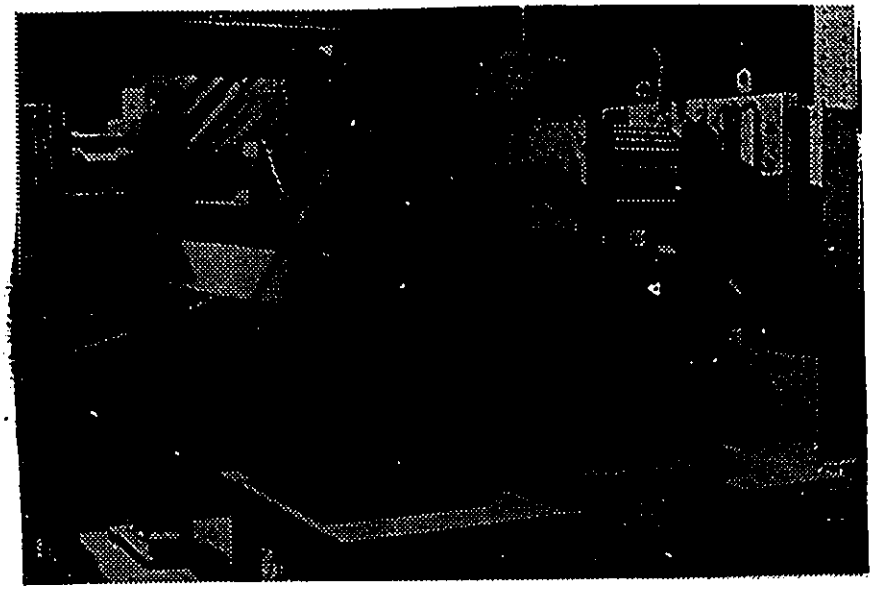

Figure 3.14: Data acquisition system

3.5 Test set-up

A plane view of the test set-up is presented in Figure 3.15. Lateral load reversals were applied to the test specimen by a hydraulic jack with a capacity of 1500 kN. The stroke of the jack was limited to 150 mm and was operated by an electrical hydraulic pressure oil pump. As depicted in Figure 3.16, the jack was mounted on two 'A frames' supported by four channel sections. This reaction frame was connected to the strong floor with six 1400 mm long by 70 mm diameter high strength bolts. This set-up was designed to accommodate squat shear walls with heights of 0.5 m and 1.0 m by simply moving the jack to the appropriate location. An overall view of the test set-up is presented in Figure 3.17.

The positive horizontal load (pushing) was applied by means of a rectangular steel shaft pin connected between the jack and the wall. The load was then transfer to the south end of the top beam through the load cell by two bearing plates as depicted in Figure 3.18. However, the negative horizontal load (pulling) was applied to the north end of the top beam by means of four Grade 400, 35M deformed bars. During the casting of the top beam, four plastic tubes were placed to permit the insertion of these four pulling bars prior to testing. The load was then measured by a load cell inserted between the end of the top beam and the bearing plate connecting the four 35M bars (see Figure 3.11). No prestressing force was applied to these bars.

3.6 Loading program

Determination of the appropriate loading program for use in quasi-static tests to simulate structural response to earthquakes has to be established carefully. Derecho et al. [22] discussed a quantitative description of a representative loading history for structural walls. A loading program shown in Figure 3.19 was established for Walls 4 and 5.

In the first three cycles the specimens were loaded to approximately half

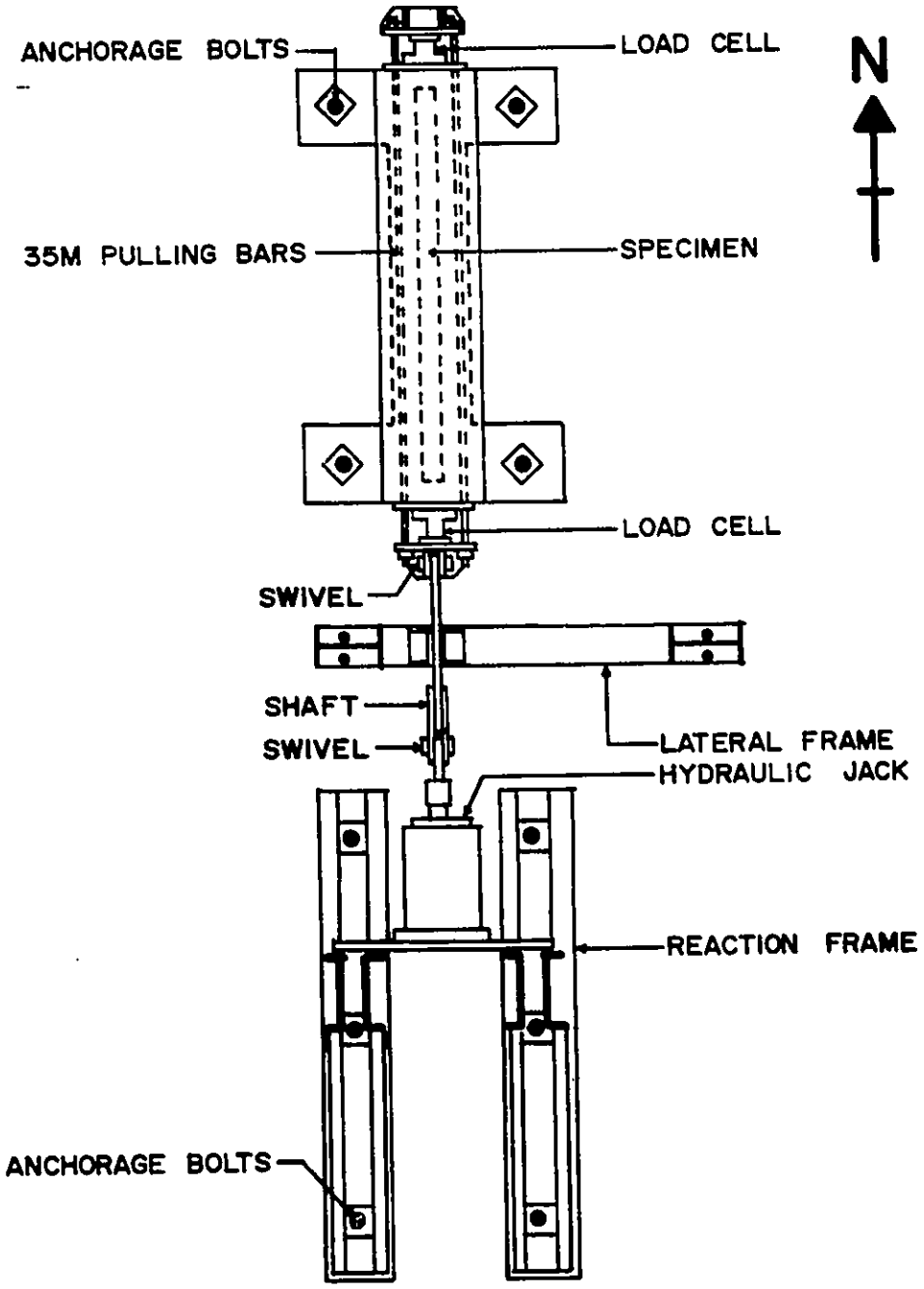

Figure 3.15: Plane view of test set-up

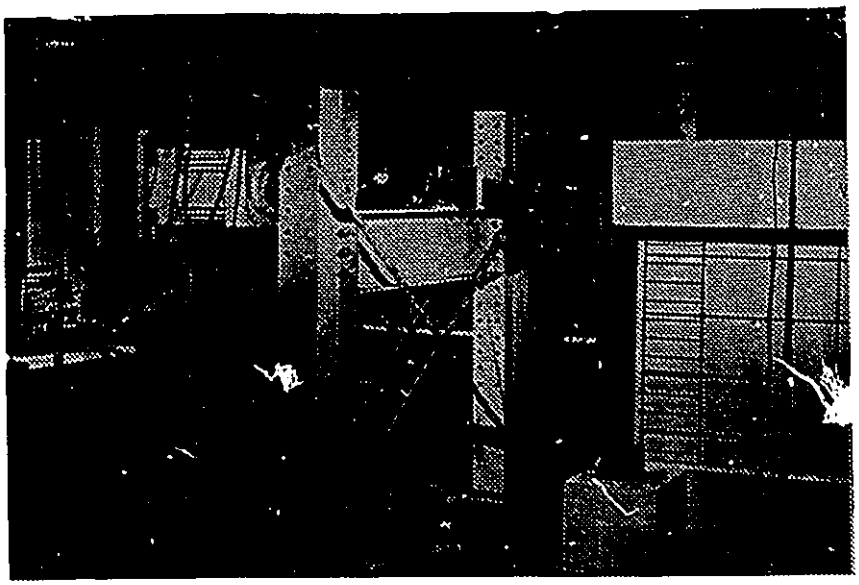

Figure 3.16: Loading reaction system

of the theoretical ultimate loads computed in Appendices A and B. This load stage represented initial elastic cycles beyond the cracking load. It is denoted by $\frac{1}{2}\Delta_y$ on Figure 3.19 where Δ_y represents the yield deflection of the specimen. The subsequent cycles beyond the elastic cycles were dependent upon the magnitude of the yield deflection. The yield deflection was defined as the deflection at which the member was yielding as a whole rather than the beginning of yielding at the critical section. This deflection level was assumed to correspond to yielding of half the vertical bars in the tension zone. It was experimentally determined from the strain gauges located on the vertical bars at the base level. From these readings, the neutral axis was located and the top deflection was increased until half of the vertical bars were yielding.

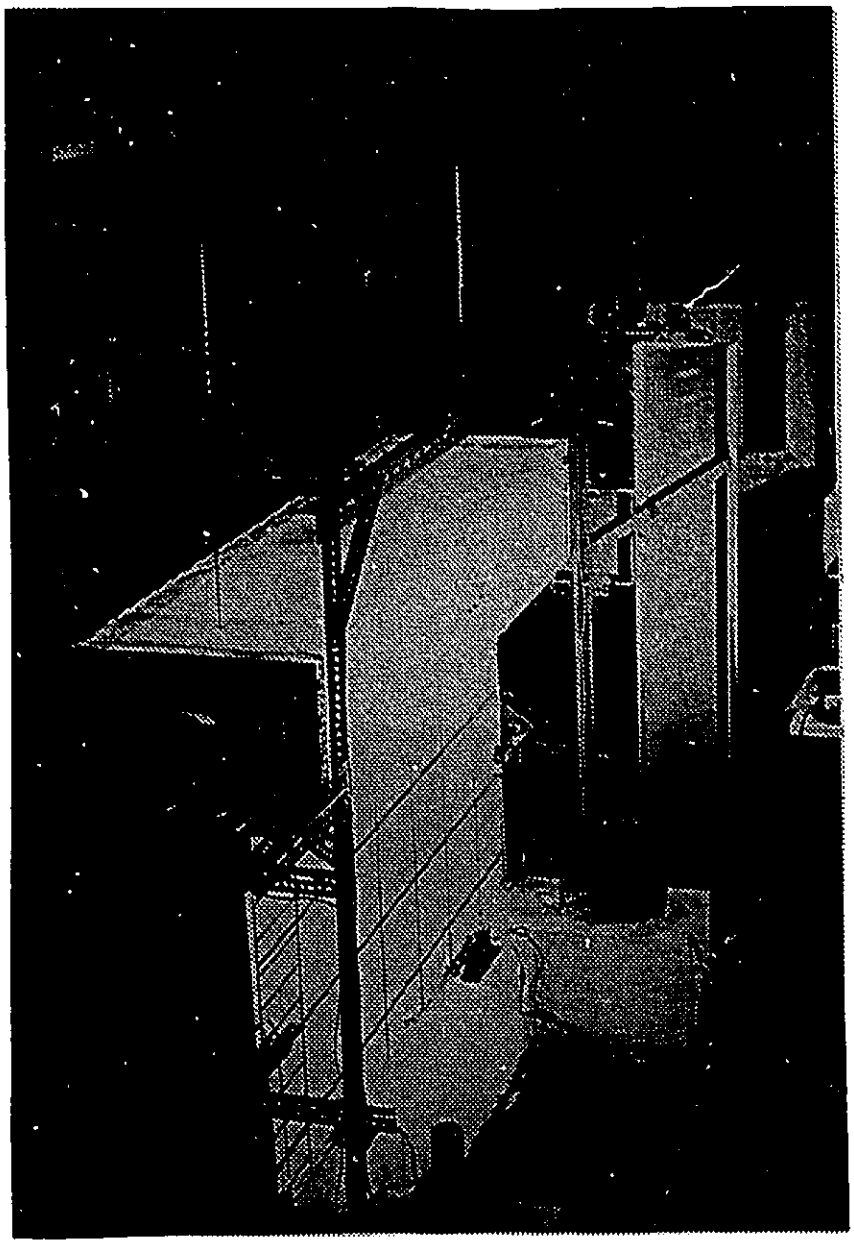

Figure 3.17: Overall view of the test set-up

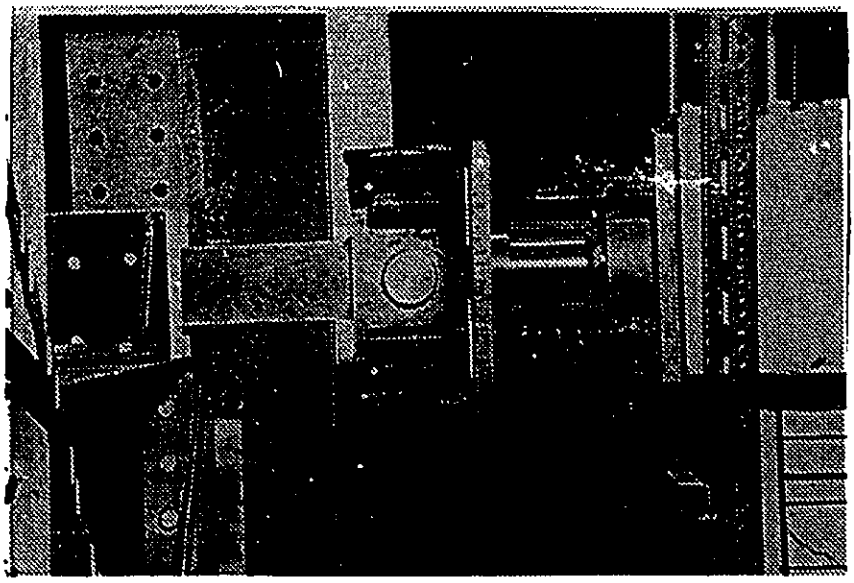

Figure 3.18: Picture of load cell

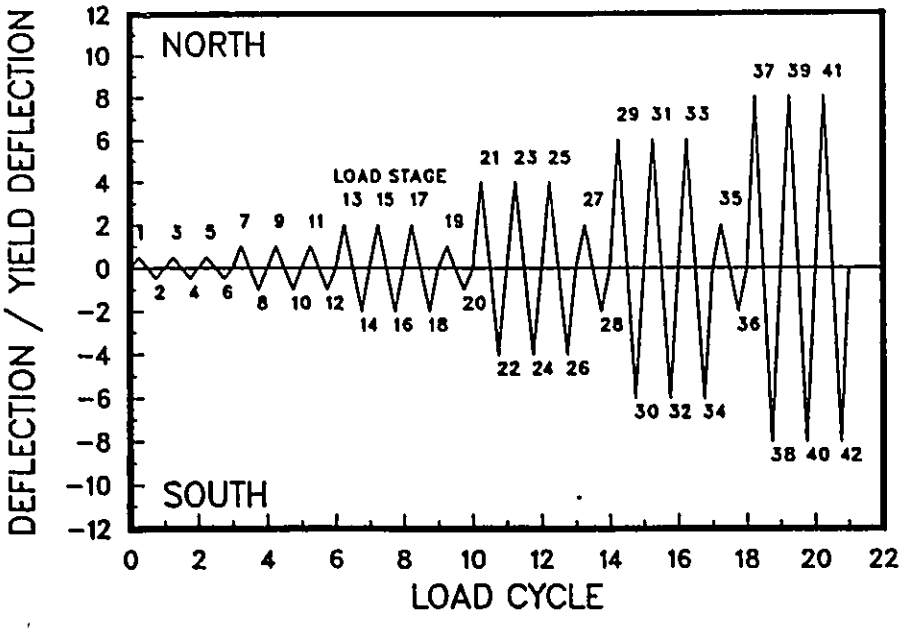

Figure 3.19: Intended loading program

Chapter 4

Test Results

4.1 Introduction

Test results for Walls 4 and 5 are reported in this chapter. The observed behavior of the walls during testing and the crack patterns are also presented. Relationships between the lateral load and wall displacements, including top displacement, base slip, bar slip and vertical displacement are reported. Strains measured in the vertical flexural bars at the construction joint level are also presented. Discussion of the test results is made in Chapter 5.

4.2 Wall 4

Wall 4, with an aspect ratio of one-half, was subjected to slowly applied displacement reversals as explained in Section 3.6. The actual loading program observed during the test is presented in Figure 4.1. The predicted ultimate shear force obtained from Appendix A is 612 kN. The details of the wall geometry, reinforcement detailing and material properties are given in

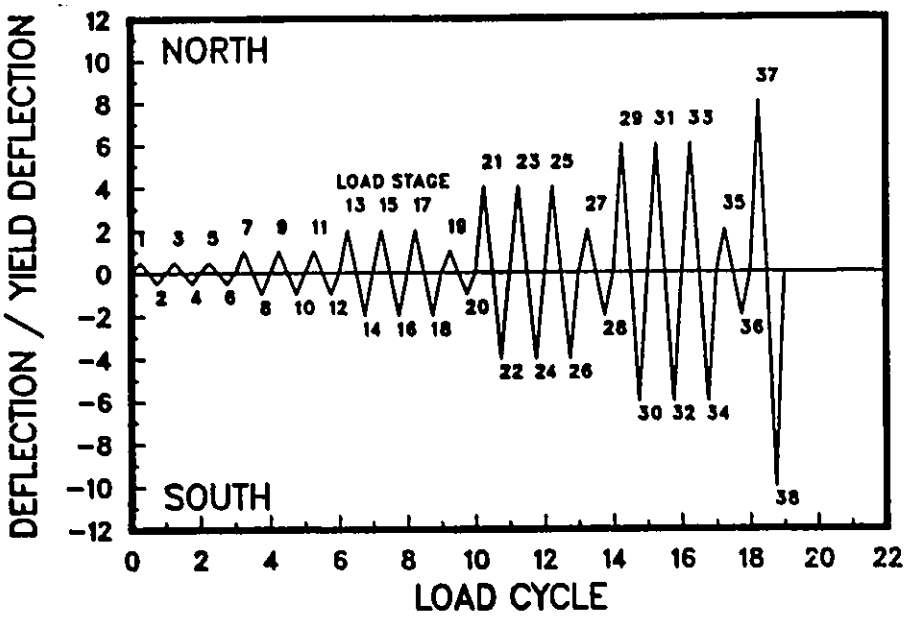

Figure 4.1: Actual loading program of Wall 4

Sections 3.2 and 3.3.

4.2.1 Load-Top displacement relationship and crack patterns

The load-top displacement hysteresis curves recorded during the test is presented in Figure 4.2. The displacement was monitored by LVDT 1 as depicted in Figure 3.10.

First, three elastic cycles were applied to the wall. The maximum loads recorded during the elastic cycles were 161 kN and -218 kN in the north and south directions respectively. The first set of diagonal shear cracks occurred at 161 kN during load stage 1. Also a flexural crack appeared at the construction joint level extending up to the third row of vertical tension steel. All the observed cracks were hair line cracks. Upon load reversal, symmetrical diagonal shear cracks appeared at -120 kN while loading to-

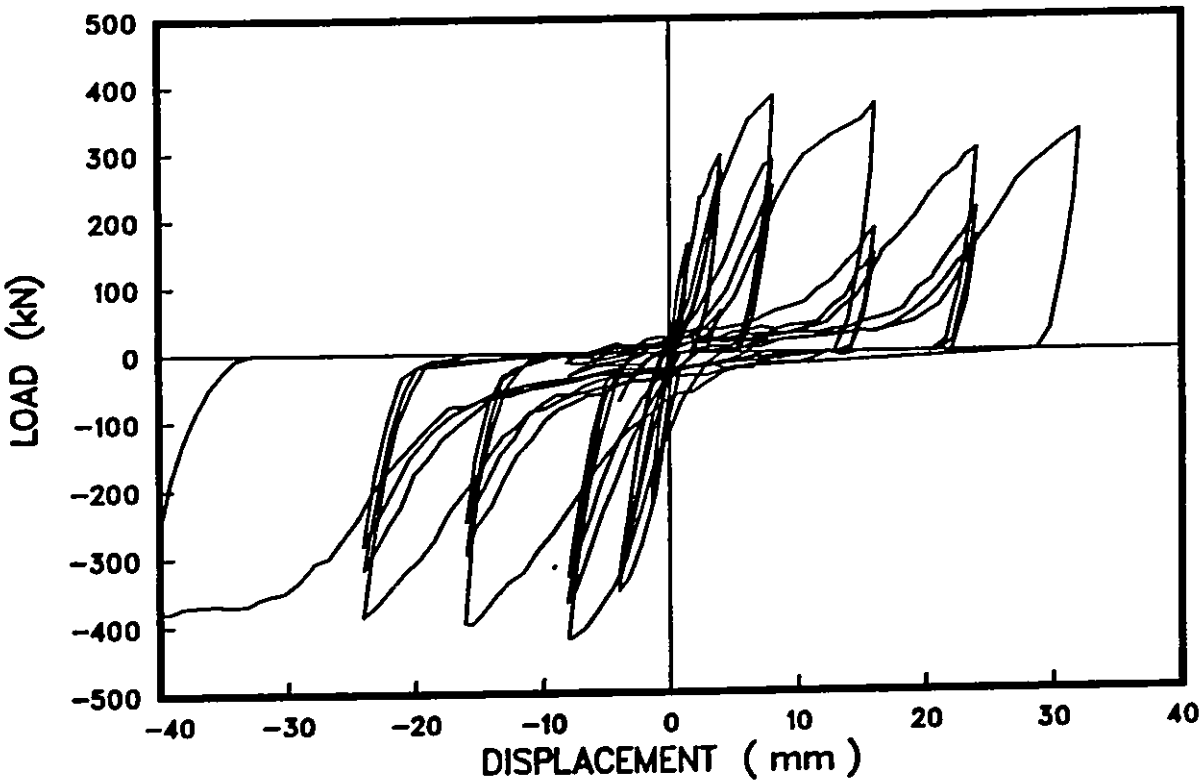

Figure 4.2: Load-Top displacement relationship of Wall 4

wards load stage 2. Few additional shear cracks occurred at load stage 3 and the subsequent load cycles did not produced additional cracks. The crack pattern at the end of the first three elastic cycles, end of load stage 6, is presented in Figure 4.3.

During the next three cycles, the wall was loaded up to a deformation level corresponding to the observed yield deflection, $1\Delta_y$. This deflection was experimentally obtained from the strain gauges installed on the vertical flexural bars at the construction joint level. During loading towards load stage 7, 39° diagonal shear cracks appeared at a load level of 180 kN. These cracks extended from the upper corner at the south end to the base of the wall. The yield deflection, Δ_y, was defined as 4.0 mm, and the corresponding yield load was 294 kN. At this stage , the previously existing flexural crack at the base did not further extend nor open. Symmetrical 39° diagonal shear cracks occurred while loading towards load stage 8 and additional steeper shear cracks appeared at -235 kN. A peak load of -345 kN was recorded at $-1\Delta_y$ at -4.0 mm. A flexural crack at the base of the wall opened by approximately 0.5 mm, extending up to the third row of vertical tension bars. The crack pattern at this stage is presented in Figure 4.4. As depicted, most of the cracks are diagonal shear cracks starting at the edge of the wall and extending to the base at approximately 39°, but none of these cracks widened at this deformation level. The remaining two cycles produced only a few additional shear cracks as depicted in Figure 4.5.

The next deformation level was $2\Delta_y$. Three cycles of 8.0 mm and -8.0 mm were applied to the wall. Upon loading towards load stage 13, additional shear cracks appeared at 285 kN. These cracks started along the top beam and extended toward the toe compression zone of the wall. A peak load of 383 kN was recorded at $2\Delta_y$. Horizontal flexural cracks appeared at approximately 200 mm above the construction joint level, extending up to the second row of vertical tension bars. The flexural base crack opened up to approximately 1 mm and extended up to the fourth row of vertical tension bars. Upon load reversal, symmetrical diagonal shear cracks occured at -355 kN. The maximum load of -419 kN was reached at $-2\Delta_y$, at load stage 14. The flexural base crack width was measured to be approximately 1.5 mm. This crack extended up to the fourth row of vertical tension bars and

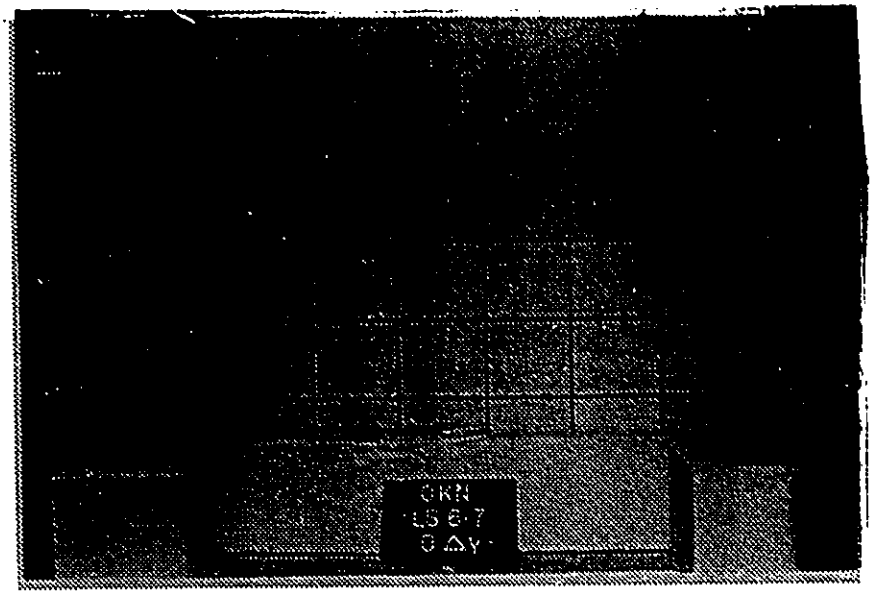

Figure 4.3: Wall 4 crack pattern at end of elastic cycles

Figure 4.4: Wall 4 crack pattern at $-1\Delta_y$

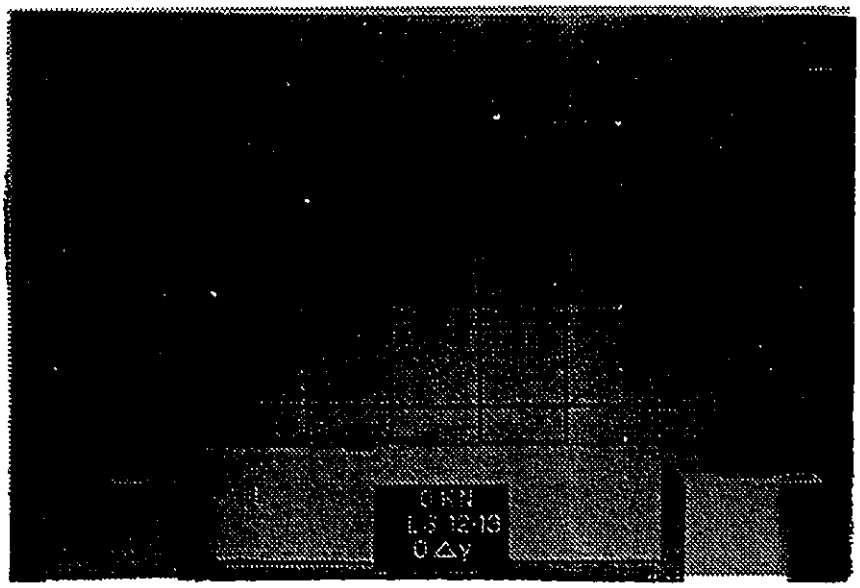

Figure 4.5: Wall 4 crack pattern at end of cycles at $1\Delta_y$

Figure 4.6: Wall 4 crack pattern at end of cycles at $2\Delta_y$

formed a continuous crack at the base of the wall. Also, horizontal flexural cracks were observed on the tension side of the wall. The width and length of these cracks decreased progressively from the base to the top of the wall. No additional cracks were observed during the remaining two cycles at $\pm 2\Delta_y$, but some visible damage could be observed at the construction joint due to base slip which explains the drop in load at peak deformation as depicted in Figure 4.2. Figure 4.6 presents the crack pattern at the end of cycles at $2\Delta_y$.

Immediately after the $2\Delta_y$ cycles, one cycle was imposed at $\pm 1\Delta_y$ as load stages 18 and 19. Peak loads of 62 kN and -71 kN respectively were recorded during the latter load stages.

The previously observed base slip was clearly visible after three cycles at $\pm 4\Delta_y$. Peak loads of 371 kN and -396 kN, recorded at load stages 21 and 22, were considerably reduced during the subsequent cycles. Flexural cracks at the base of the wall were measured to be approximately 2 mm. Spalling of the concrete cover at the base and kinking of the vertical bars were noticeable, as depicted in Figure 4.7. Flexural or shear cracks did not form during the $4\Delta_y$cycles. This can be seen in Figure 4.8.

The subsequent deformation cycle was at $\pm 2\Delta_y$, resulting in peak loads of 31 kN and -33 kN at load stages 27 and 28 respectively.

The base slip became more pronounced at a deformation level of $6\Delta_y$. The peak loads dropped to 301 kN and -386 kN at load stages 29 and 30 respectively. Kinking of the vertical bars at the base of the wall resulted in additional spalling of the concrete cover as shown in Figure 4.9. Figure 4.10 presents the crack pattern after three cycles at $\pm 6\Delta_y$. Additional cracks were not observed.

The next cycle at $\pm 2\Delta_y$, load stages 35 and 36, did not produce any resistance against lateral deformation but only aggravated the deterioration of the concrete at the base.

An increase in load resistance was observed at $+8\Delta_y$, load stage 37, up to a maximum load of 327 kN. Crushing of the concrete in the compression

Figure 4.7: Wall 4 kinking of vertical bars at $4\Delta_y$

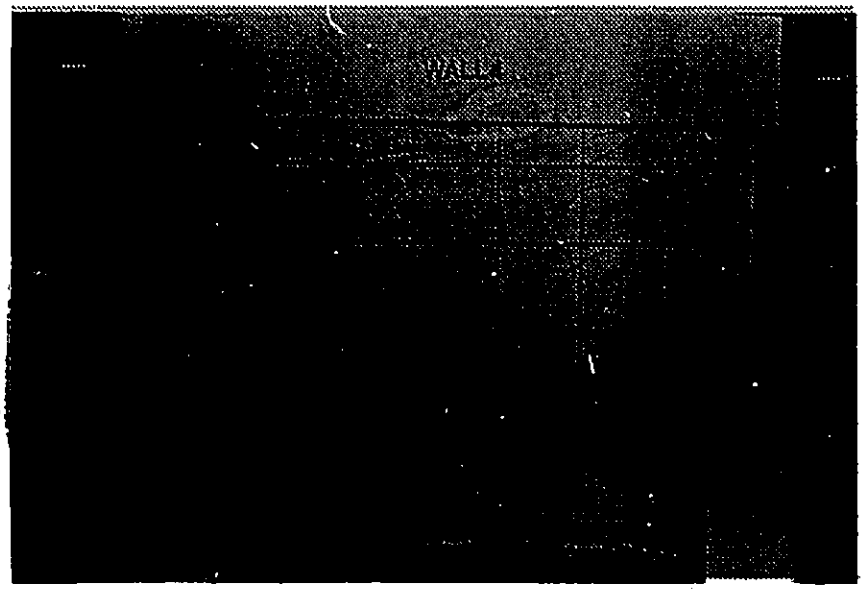

Figure 4.8: Wall 4 crack pattern at end of cycles at $4\Delta_y$

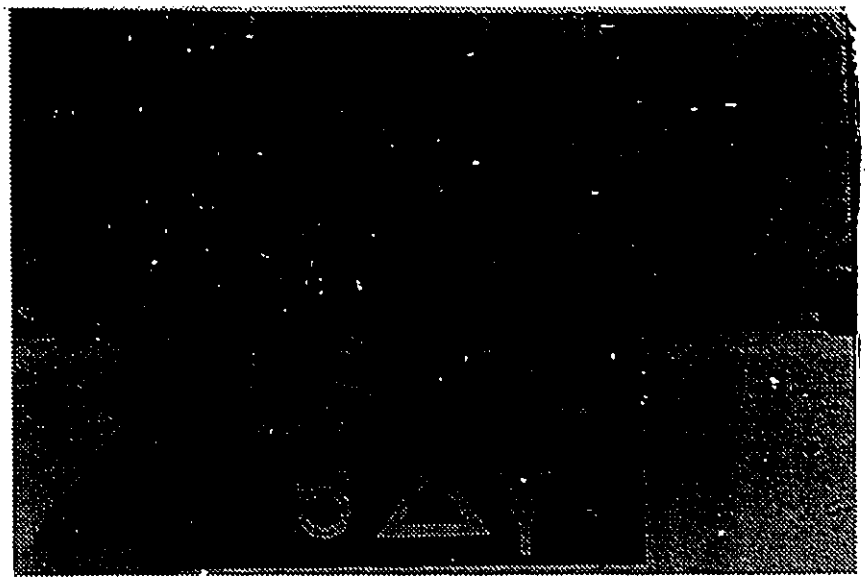

Figure 4.9: Wall 4 kinking of vertical bars at $6\Delta_y$

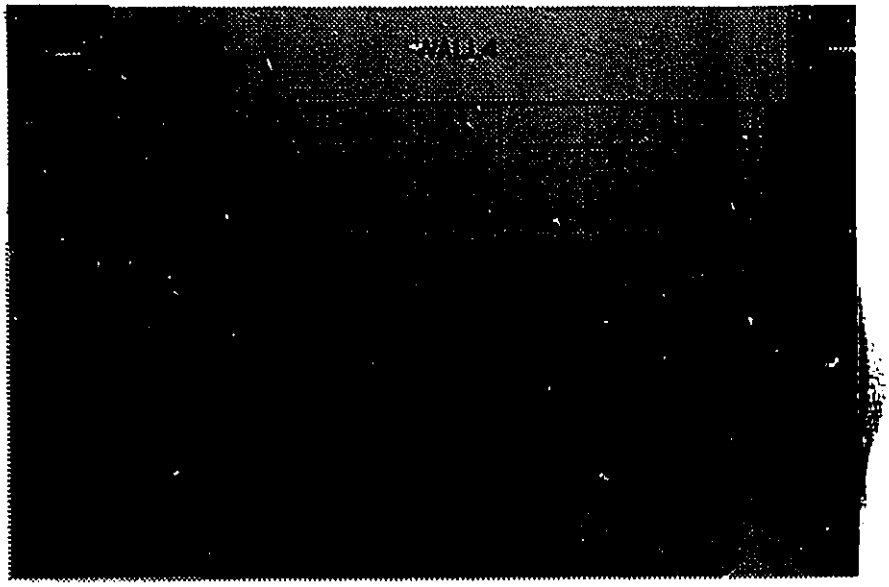

Figure 4.10: Wall 4 crack pattern at end of cycles at $6\Delta_y$

zone was observed and small additional shear cracks were noticed. Upon load reversal, extensive crushing of the concrete in the compression zone occured at $-8\Delta_y$. At this point, the wall started to show some sign of lateral instability, hence, it was decided to continue up to $-10\Delta_y$ and stop the test. The load reached a maximum of -375 kN and most of the flexural-shear cracks on the tension side were opened by 3 to 5 mm. Figure 4.11 presents the crack pattern at $-10\Delta_y$ which was the end of the test. A close-up of the end region of the wall is shown in Figure 4.12.

4.2.2 Load-Base slip relationship

The wall base slip along the construction joint was monitored by LVDTs 6, 7 and 8 as depicted in Figure 3.10. The displacement recorded by each of these LVDTs throughout the test are presented in Figures 4.13, 4.14 and 4.15 respectively.

Essentially, the base slip started to affect the top displacement hysteresis curves at $2\Delta_y$. Subsequent cycles at the same deformation level are characterized by an increase in base slip. It should be noted that the base slip recorded before $2\Delta_y$ was not base slip but, shear deformation occurring between the construction joint and the level at which the LVDTs were mounted.

4.2.3 Load-Wall displacement relationship

An average base slip was calculated from LVDTs 6, 7, 8 and subtracted from LVDT 1 to obtain the load-displacement relationship imposed on the wall. This is shown in Figure 4.16.

The hysteresis curves presented in Figure 4.16 consist of three horizontal displacement components. These components are due to flexure, shear and local slippage of vertical reinforcement in the foundation beam. A detailed analysis of these components is presented in Chapter 5.

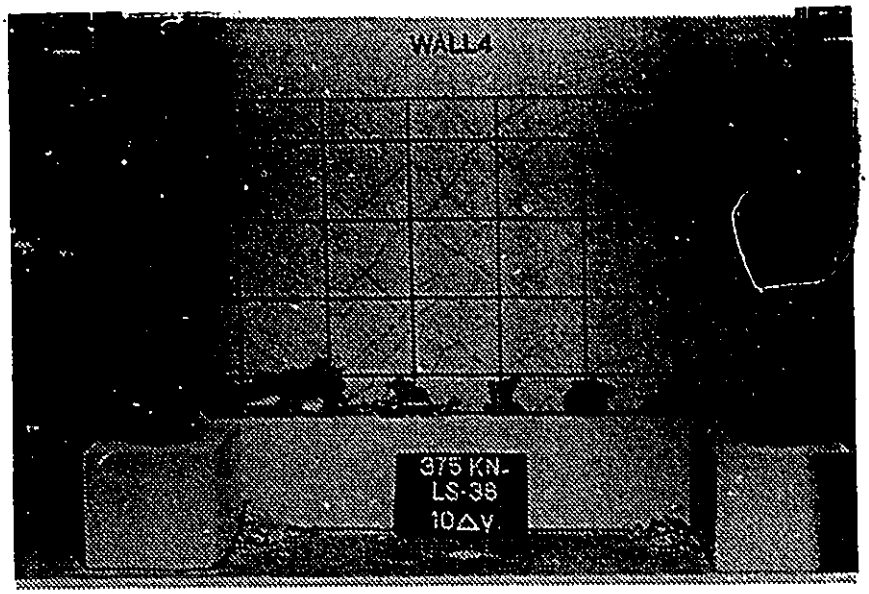

Figure 4.11: Wall 4 crack pattern at $-10\Delta_y$ and end of test

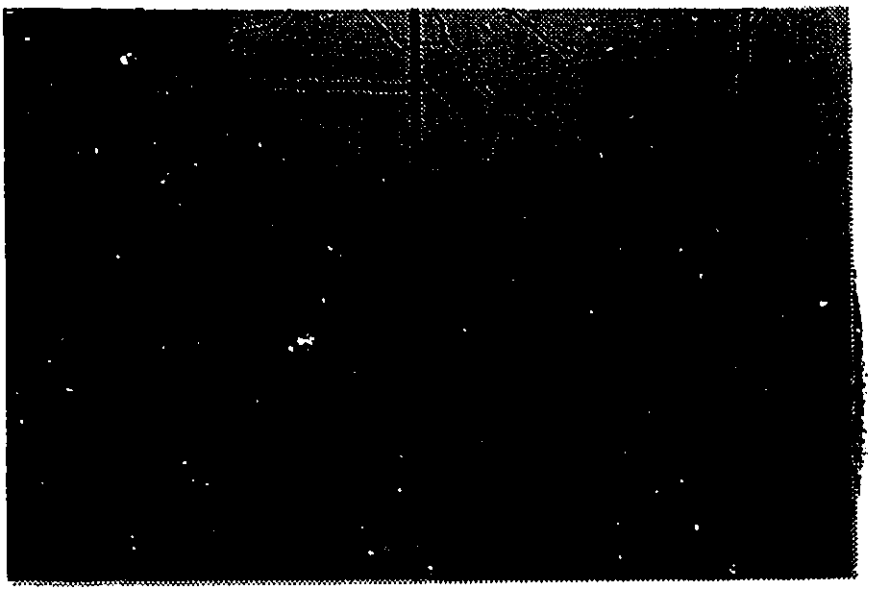

Figure 4.12: Wall 4 detail of end region at end of test

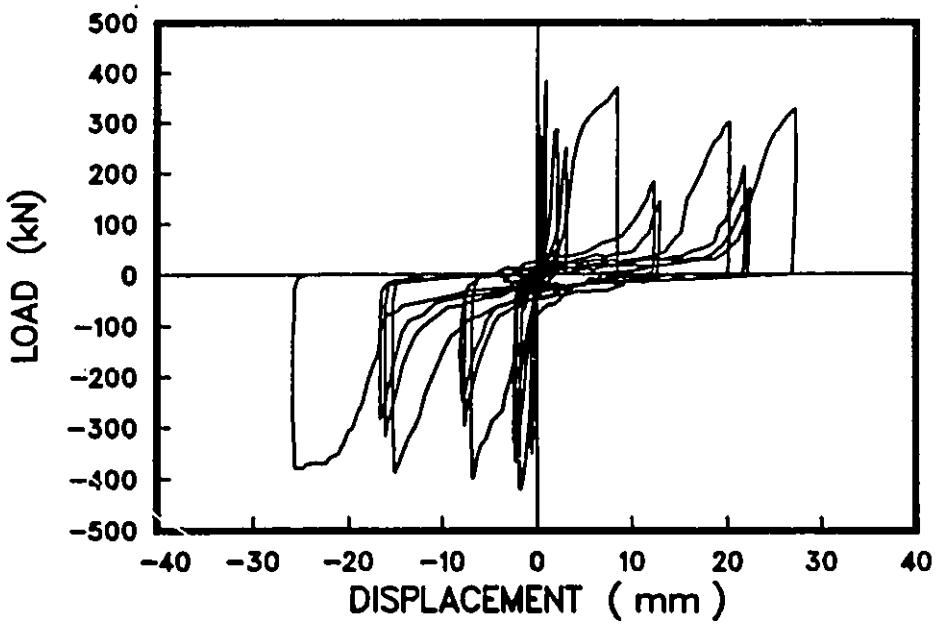

Figure 4.13: Load-Displacement relationship for LVDT 6 of Wall 4

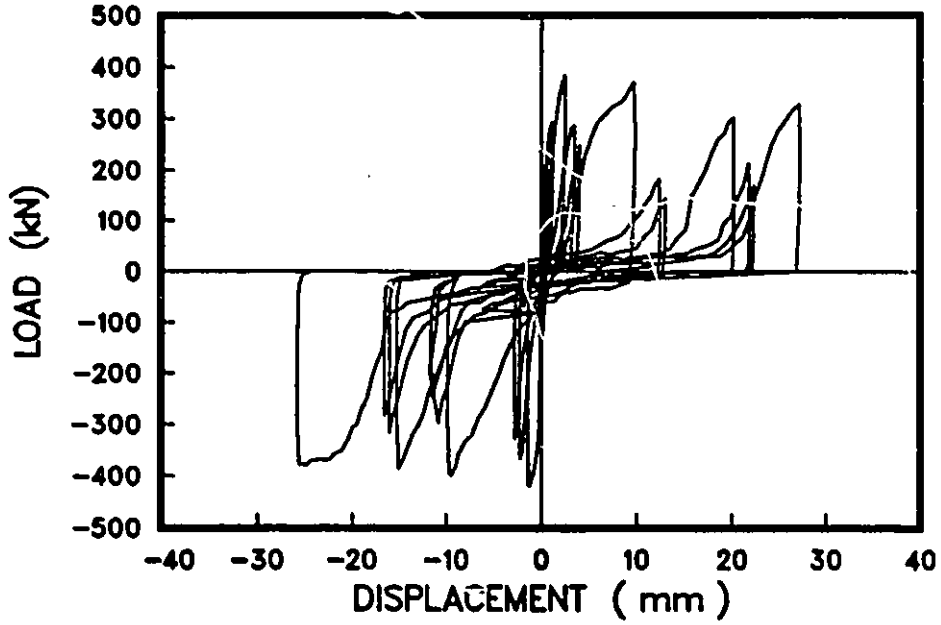

Figure 4.14: Load-Displacement relationship for LVDT 7 of Wall 4

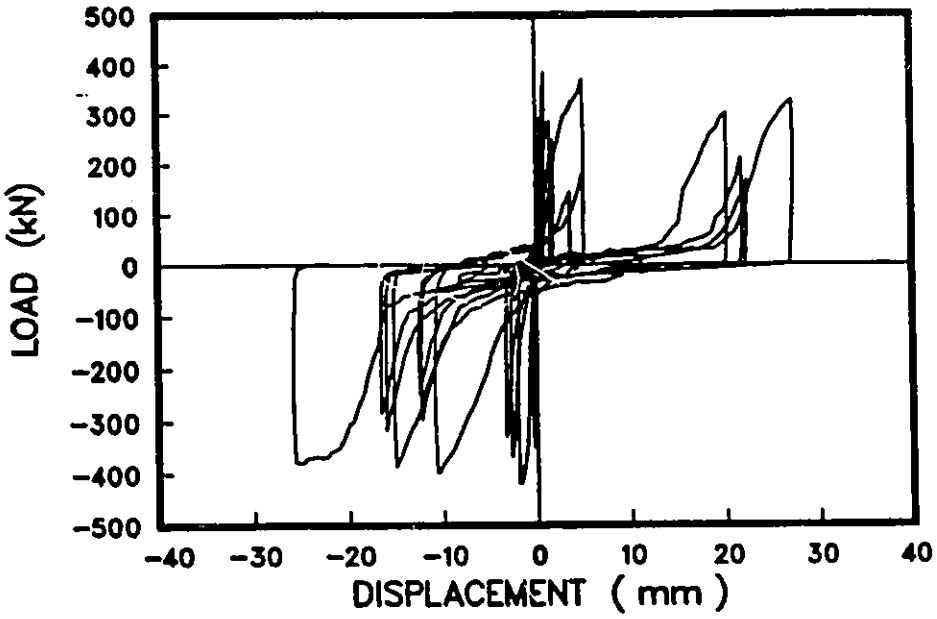

Figure 4.15: Load-Displacement relationship for LVDT 8 of Wall 4

4.2.4 Load-Bar slip relationship

The slippage of vertical reinforcement in the foundation beam was measured at both ends of the wall with LVDTs 4 and 5 as depicted in Figure 3.10. The displacements recorded during the test by these two LVDTs are presented in Figures 4.17 and 4.18 respectively. Unfortunately, LVDT 5 was malfunctioning after load stage 26. Consequently Figure 4.18 shows the load-bar slip hysteresis loops up to $4\Delta_y$.

The rotation of the wall at its base can be calculated from these two LVDTs by subtracting LVDT 4 from 5 and dividing this differential vertical movement by the distance separating the tow LVDTs. This base rotation is presented in Figure 4.19 up to $\pm 4\Delta_y$. At low load level, the base rotation is greatly affected by the continuous crushing of the concrete at the base due to sliding.

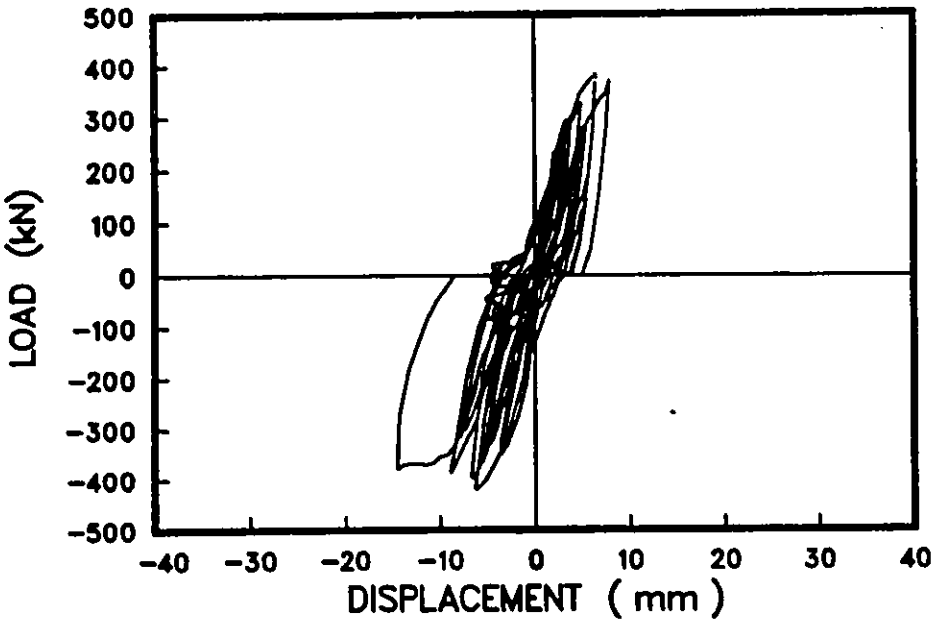

Figure 4.16: Load-Top wall displacement relationship of Wall 4 excluding displacements due to sliding shear

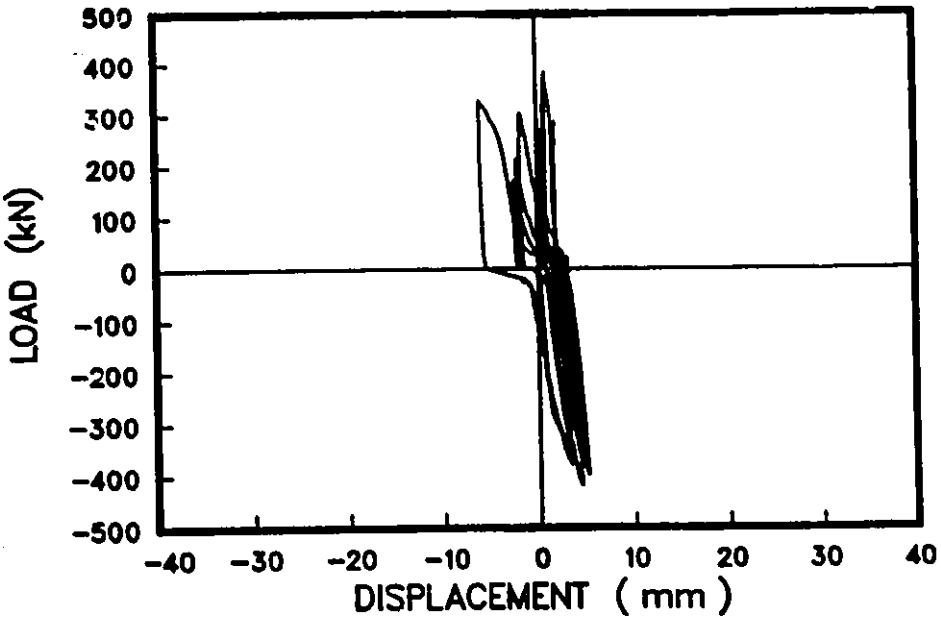

Figure 4.17: Load-Displacement relationship for LVDT 4 of Wall 4

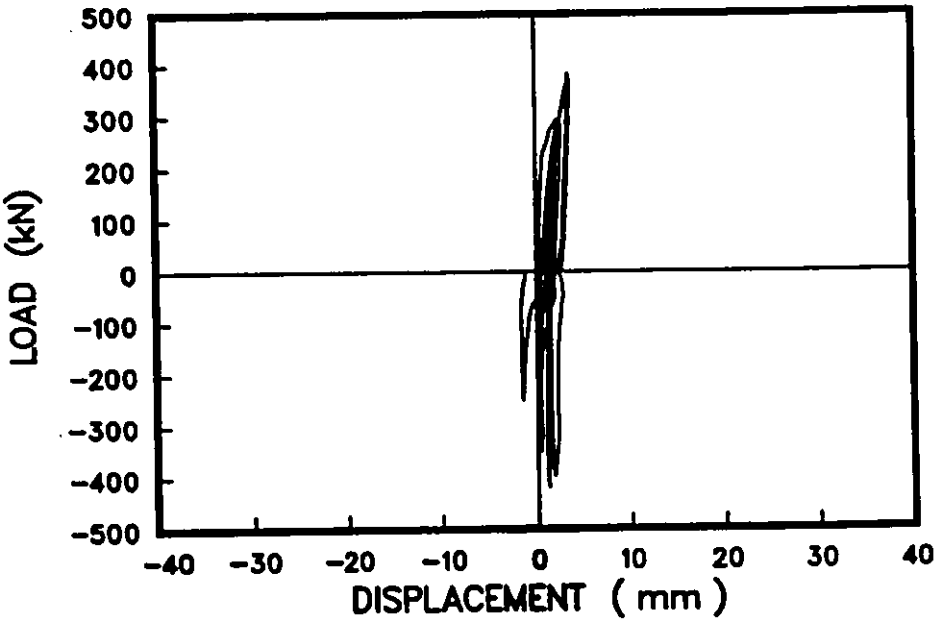

Figure 4.18: Load-Displacement relationship for LVDT 5 of Wall 4

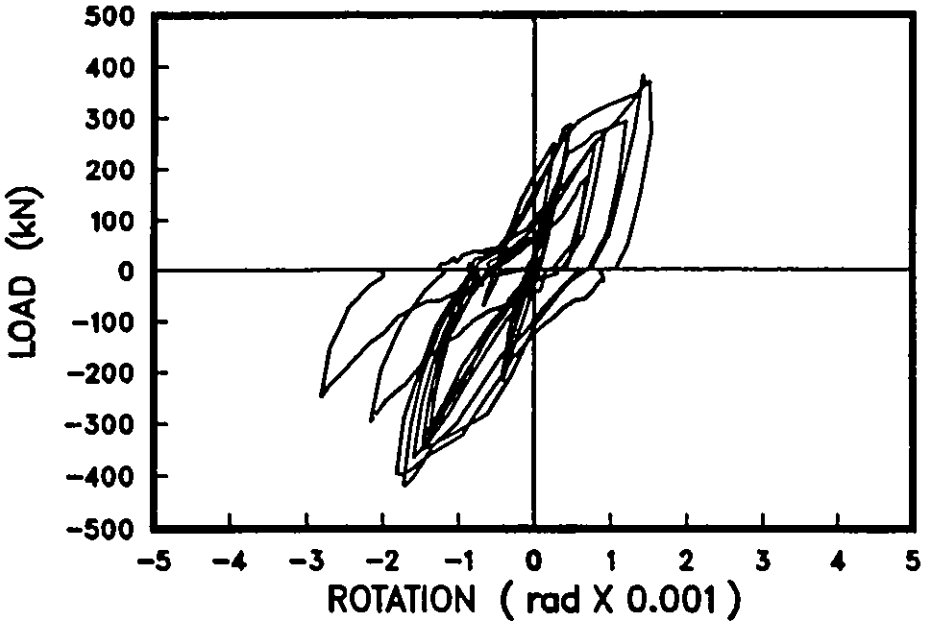

Figure 4.19: Load-Base rotation relationship for Wall 4

4.2.5 Load-Total vertical displacement relationship

The vertical movement of the top beam was monitored by LVDTs 2 and 3 as presented in Figure 3.10. The displacements recorded during the test by these LVDTs are presented in Figures 4.20 and 4.21 respectively. These displacements are composed of the bar slip described previously and the vertical displacement in the wall element due to flexure.

The total rotation of the top beam is calculated in the same way as the base rotation due to bar slip. This load-total rotation relationship can be seen in Figure 4.22 where well rounded curves are observed.

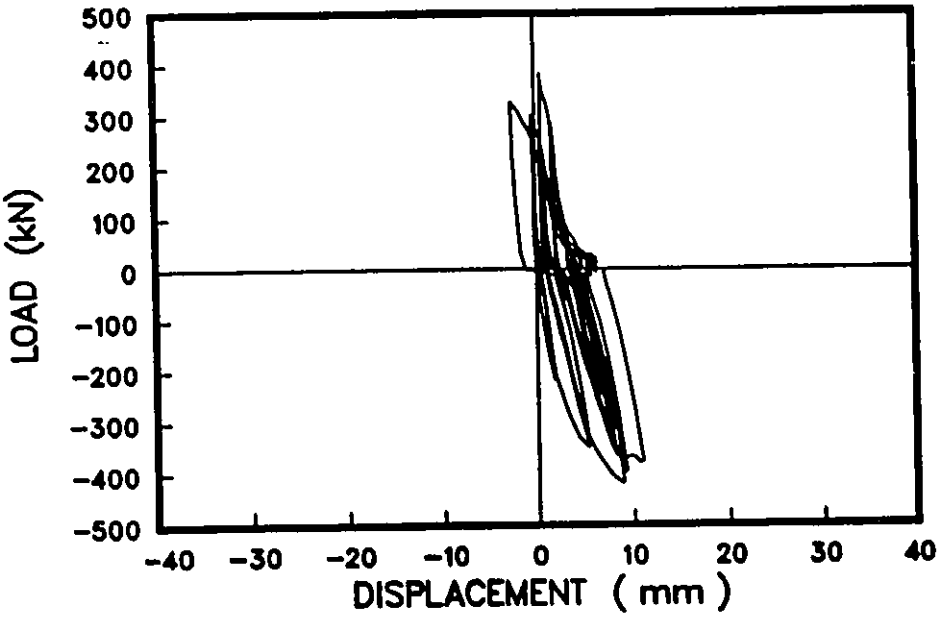

Figure 4.20: Load-Displacement relationship for LVDT 2 of Wall 4

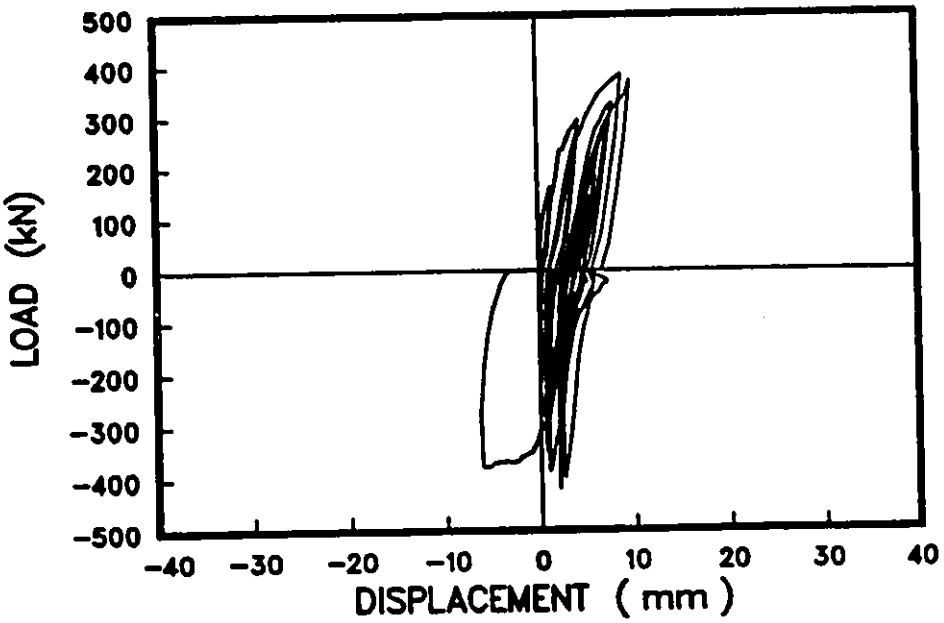

Figure 4.21: Load-Displacement relationship for LVDT 3 of Wall 4

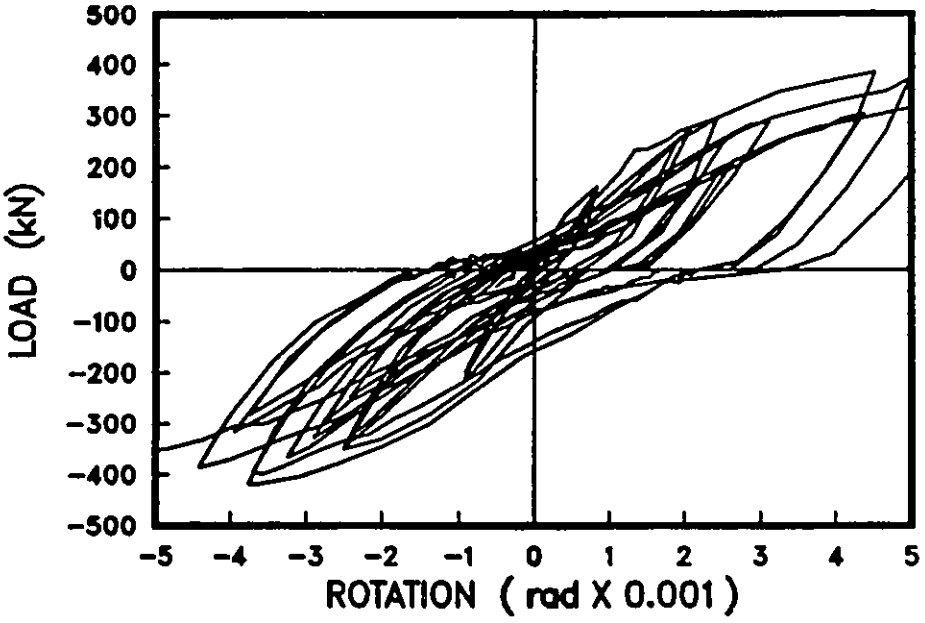

Figure 4.22: Load-Top rotation relationship for Wall 4

4.2.6 Strains in vertical flexural reinforcement

The strains in all vertical flexural bars were monitored at the construction joint level as mentioned in Section 3.4. Figure 4.23, 4.24, 4.25 and 4.26 present the load-strain relationship in selected bars.

Steel strain distributions along the base of the wall at different load levels are examined in more detail in Chapter 5.

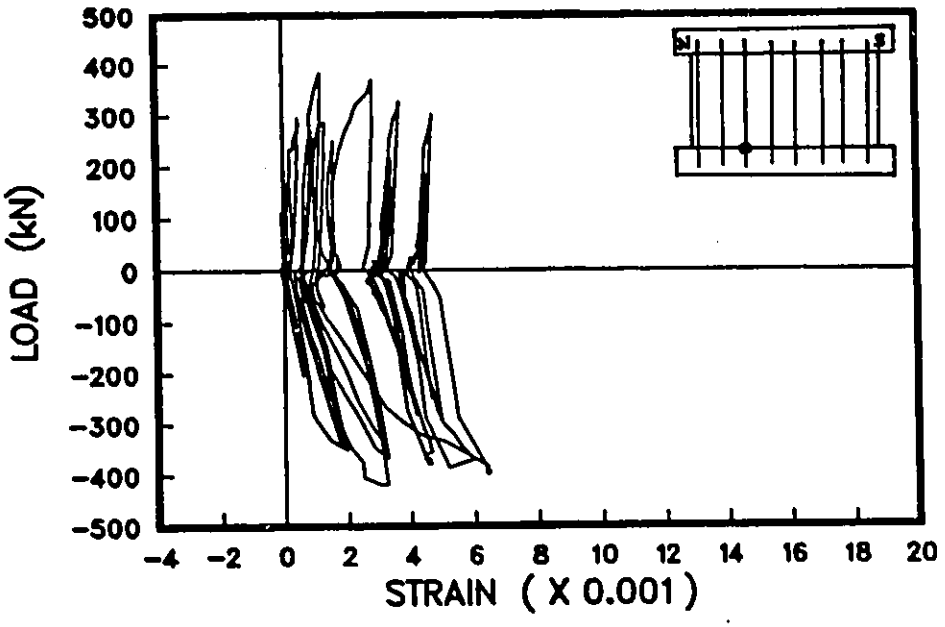

Figure 4.23: Load-Strain relationship in vertical bar of Wall 4

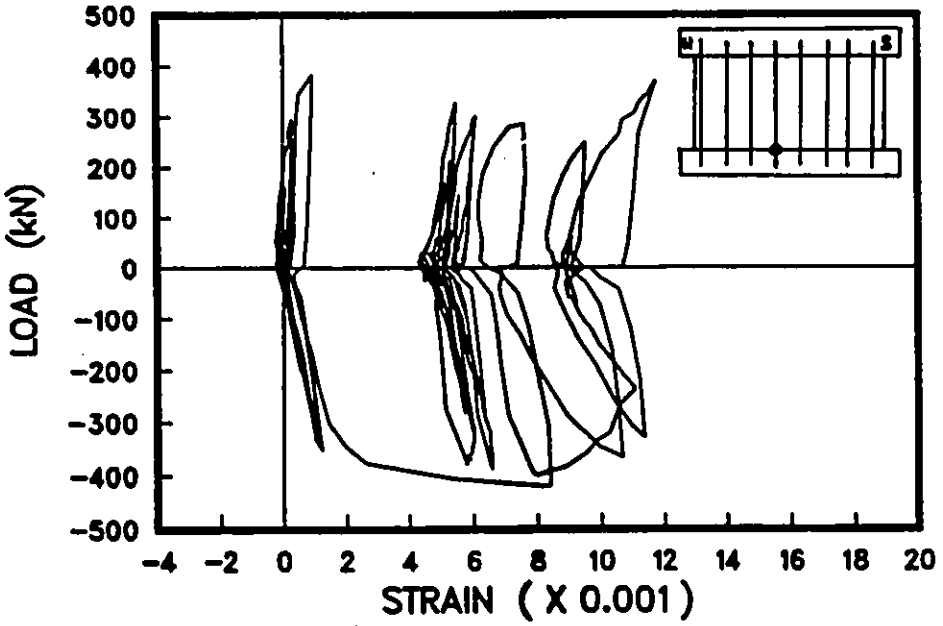

Figure 4.24: Load-Strain relationship in vertical bar of Wall 4

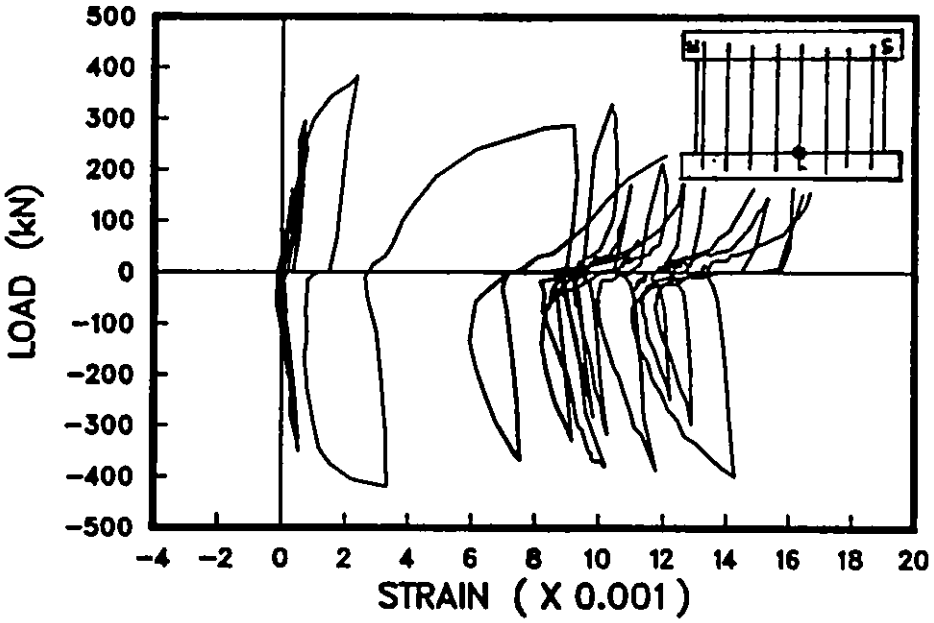

Figure 4.25: Load-Strain relationship in vertical bar of Wall 4

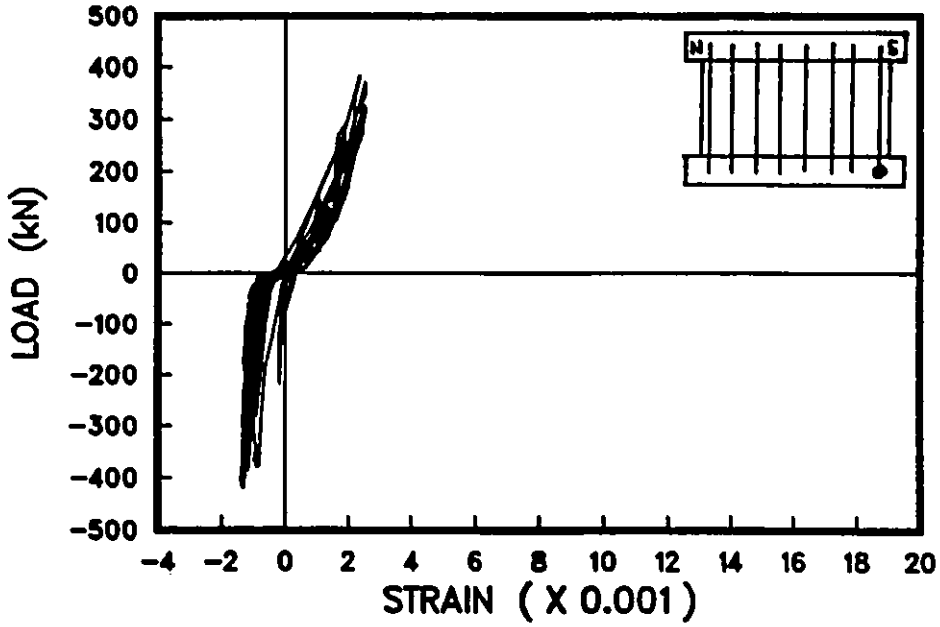

Figure 4.26: Load-Strain relationship in vertical bar of Wall 4

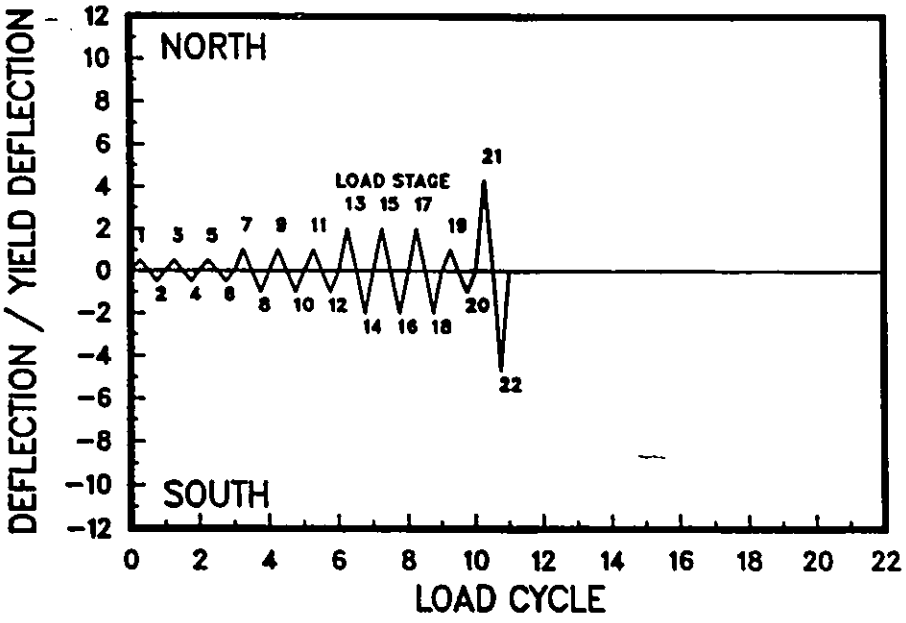

Figure 4.27: Actual loading program of Wall 5

4.3 Wall 5

Wall 5, with an aspect ratio of one-half, was subjected to slowly applied displacement reversals as explained in Section 3.6. The actual loading program observed during the test is presented in Figure 4.27. The predicted ultimate shear force obtained from Appendix B is 838 kN. The details of the wall geometry, reinforcement detailing and material properties are given in Sections 3.2 and 3.3.

4.3.1 Load-Top displacement relationship and crack patterns

The load-top displacement hysteresis curves recorded during the test is presented in Figure 4.28. As mentioned previously, LVDT 1 was used to monitor the top deflection of the wall.

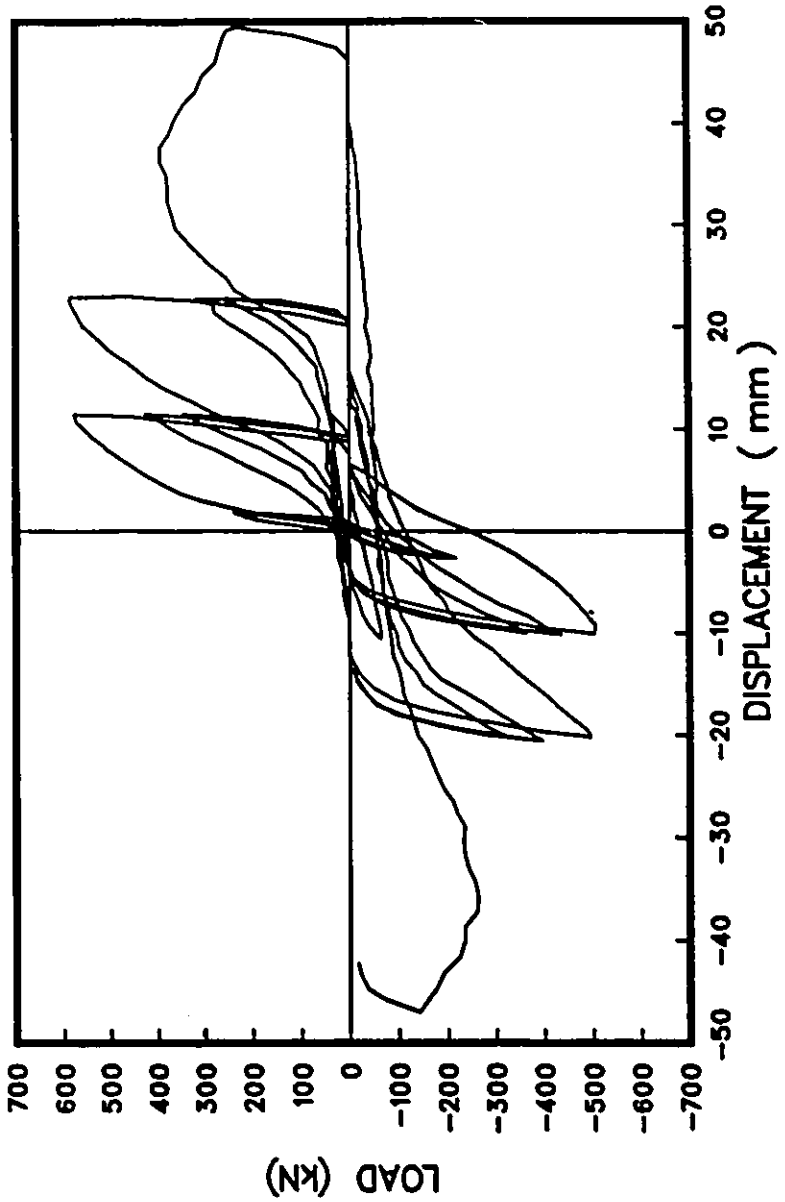

Figure 4.28: Load-Top displacement of Wall 5

First, three elastic cycles were applied to the wall. The maximum loads recorded were 238 kN at load stage 1 and -220 kN at load stage 2. The first set of diagonal shear cracks appeared at 155 kN while loading towards load stage 1. They formed with approximately 38° inclination with the horizontal, starting from the tension side of the wall. Upon load reversal towards load stage 2, a symmetrical diagonal crack pattern was observed at -145 kN. The observed crack pattern is shown in Figure 4.29. The subsequent two elastic cycles did not produce additional cracks. No sign of flexural cracking was observed during these cycles.

For the next three cycles, the wall was loaded up to a deformation level corresponding to the observed yield deflection, $1\Delta_y$. While loading towards load stage 7, additional diagonal shear cracks appeared at 290 kN. A flexural crack occured at the base of the wall at 415 kN. This crack extended up to the sixth row of vertical tension bars with a width of approximately 1 mm. Additional flexural cracks, with crack widths less than 1 mm, appeared on the tension side of the wall during the latter part of this load stage. The yield deflection, Δ_y, was arrived at 11.4 mm at a recorded load of 577 kN, at load stage 7. Upon load reversal, symmetrical sets of diagonal shear cracks and flexural base cracks occured at -255 kN and -405 kN respectively. The yield deflection, $-\Delta_y$, was slightly different than $+\Delta_y$ and was reached at -10.0 mm, at load stage 8. At this deformation level, the recorded load was -503 kN. A continuous flexural base crack was formed with some sign of spalling of the concrete cover in the compression zone. The subsequent cycles did not produce additional shear cracks but resulted in spalling of the concrete cover at the base due to sliding of the wall. The sliding of the wall produced considerable degradation of stiffness during the subsequent cycles. This can be seen in the hysteretic load deflection relationship given in Figure 4.28. The crack pattern at the end of the three cycles at $\pm 1\Delta_y$ is presented in Figure 4.30.

The next deformation level was $\pm 2\Delta_y$. Three cycles of 22.8 mm and -20.0 mm were applied in the north and south directions respectively. A peak load of 586 kN was recorded at load stage 13. Additional shear cracks were observed during this load stage. The flexural base crack width was measured to be approximately 7 mm. Crushing of the concrete in the compression zone was observed. Upon load reversal, a maximum load of -495

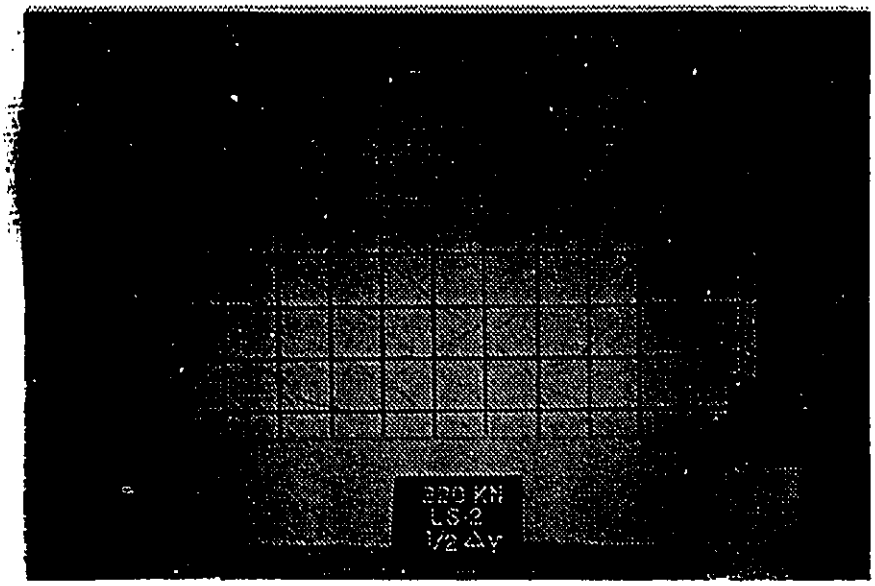

Figure 4.29: Wall 5 crack pattern after one elastic cycle

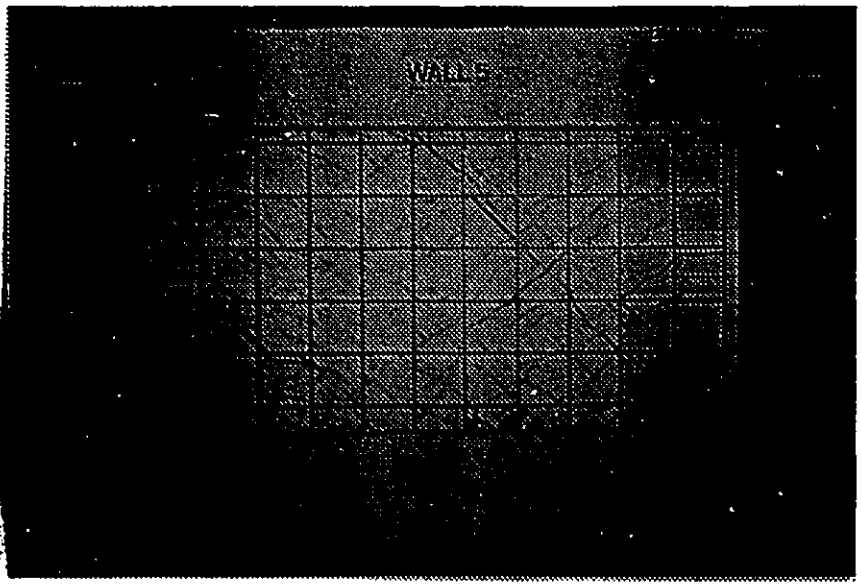

Figure 4.30: Wall 5 crack pattern at the end of cycles at $1\Delta_y$

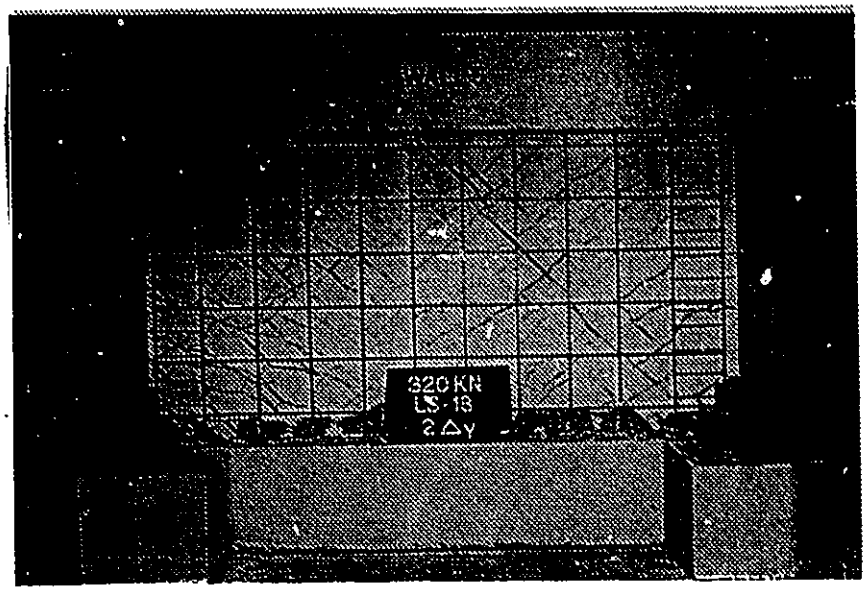

Figure 4.31: Wall 5 crack pattern at the end of cycles at $2\Delta_y$

kN was recorded at load stage 14. Additional shear cracks were observed on the wall. The concrete at the base was damaged due to wall sliding. The remaining two cycles aggravated this situations as depicted in Figure 4.31. Kinking of the vertical bars became apparent as shown in Figure 4.32. At the end of the $\pm 2\Delta_y$ cycles, complete deterioration of the base concrete at the wall ends was observed as presented in Figure 4.33.

One small cycle at $\pm 1\Delta_y$ was then imposed on the wall, as load stages 19 and 20. Very small lateral load resistance was recorded during this cycle.

While loading towards $4\Delta_y$, at load stage 21, excessive kinking of the vertical bars was observed at the base. A peak load of 395 kN was recorded at approximately $3\Delta_y$ followed by an extensive crushing of the concrete at the base. From thereon the lateral load resistance started to decrease till $4\Delta_y$ as shown in Figure 4.28. The same phenomenon occured upon load reversal. The load reached a peak of -265 kN at about $-3.5\Delta_y$ resulting in a general disintegration of the concrete at the base. The subsequent loading, close to $-5\Delta_y$, showed an irrecoverable loss in strength. Consequently, it

Figure 4.32: Wall 5 kinking of vertical bars at $2\Delta_y$

Figure 4.33: Wall 5 end detail at end of cycles at $2\Delta_y$

was decided to stop the test at this point. Figure 4.34 shows the specimen at the end of the test, at load stage 22. The complete deterioration of the concrete is clearly seen on Figure 4.35 where the loose pieces of concrete were removed.

4.3.2 Load-Base slip relationship

The wall base slip along the construction joint is presented in Figures 4.36, 4.37 and 4.38 for each of the three LVDTs used at the base of the wall. The exact location of these LVDTs were previously discussed and are illustrated in Figure 3.10.

The base slip became noticeable during the first cycle of $1\Delta_y$. Subsequent cycles at the same deformation level showed an increase in the base slip. The base slip recorded before $1\Delta_y$ was essentially the shear deformation that took place within the bottom portion of the wall where the LVDTs were mounted. No visible sliding was observed up to $1\Delta_y$.

4.3.3 Load-Wall displacement relationship

An average base slip was calculated from Figures 4.36, 4.37, 4.38 and subtracted from Figure 4.28 to obtain the load-displacement relationship imposed on the wall element. This is shown in Figure 4.39.

The hysteresis curves presented in Figure 4.39 consist of three horizontal top displacement components, namely flexure, shear and reinforcement slip displacements which are examined in more details in Chapter 5.

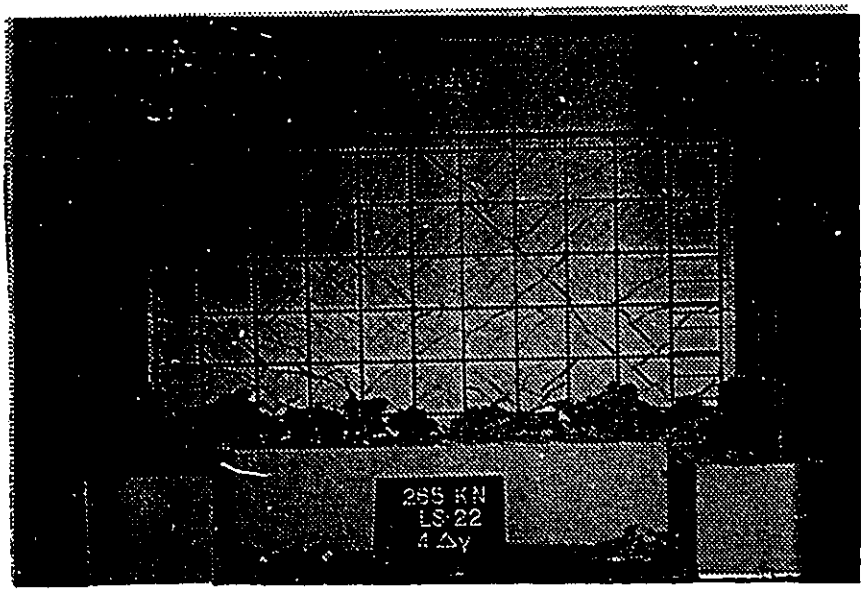

Figure 4.34: Wall 5 crack pattern at end of cycles at $4\Delta_y$ and end of test

Figure 4.35: Wall 5 detail of end region at end of test

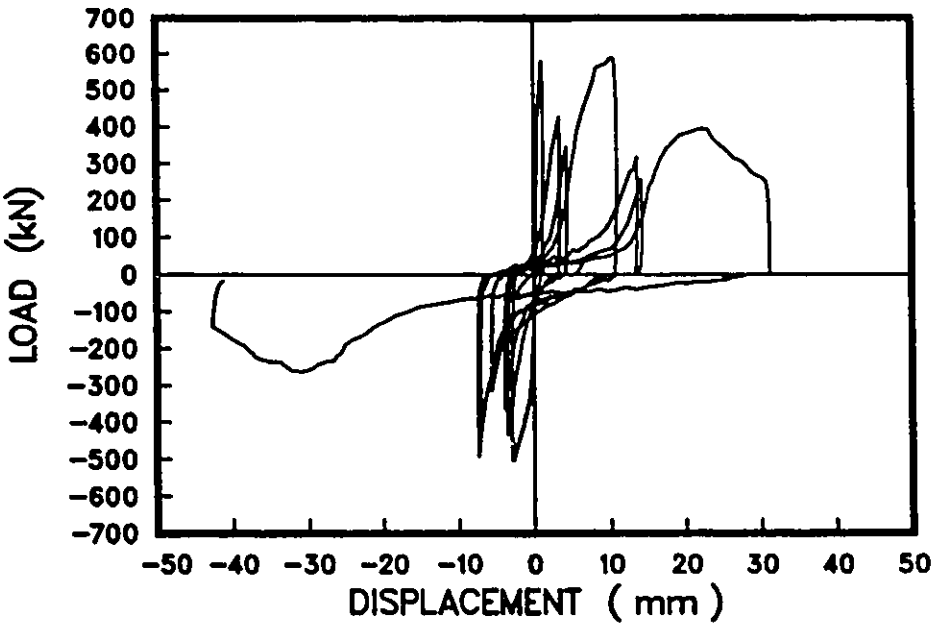

Figure 4.36: Load-Displacement relationship for LVDT 6 of Wall 5

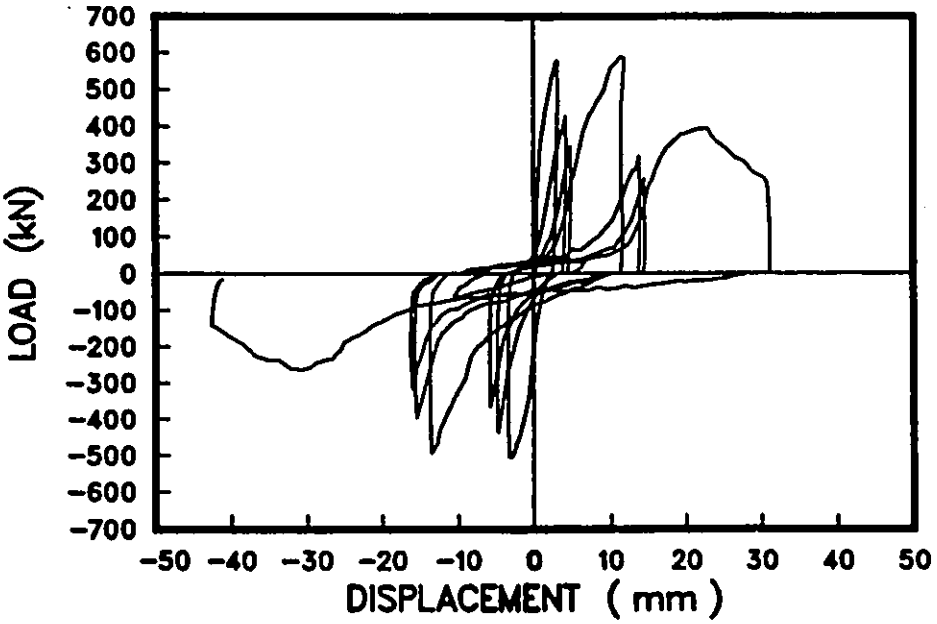

Figure 4.37: Load-Displacement relationship for LVDT 7 of Wall 5

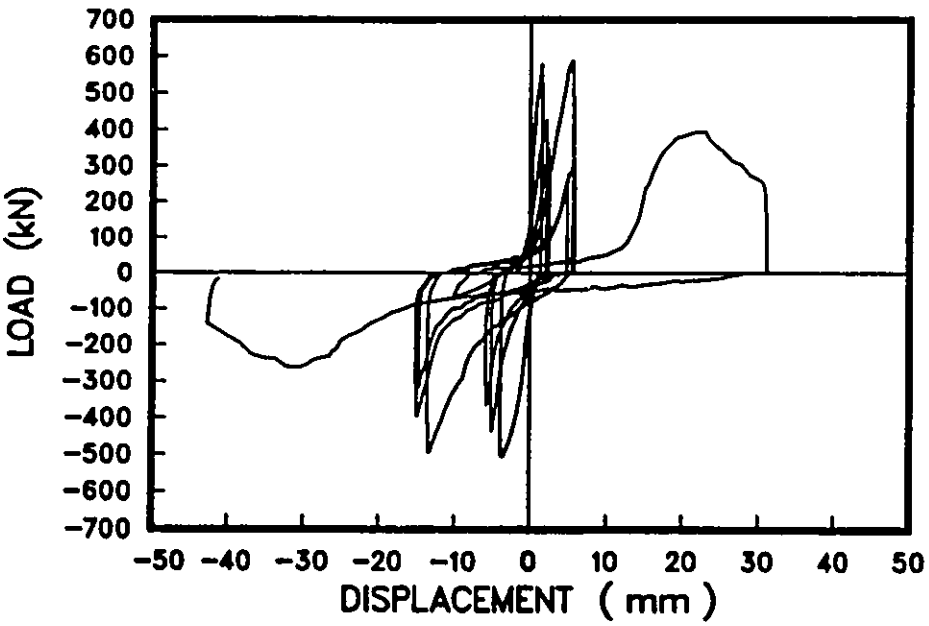

Figure 4.38: Load-Displacement relationship for LVDT 8 of Wall 5

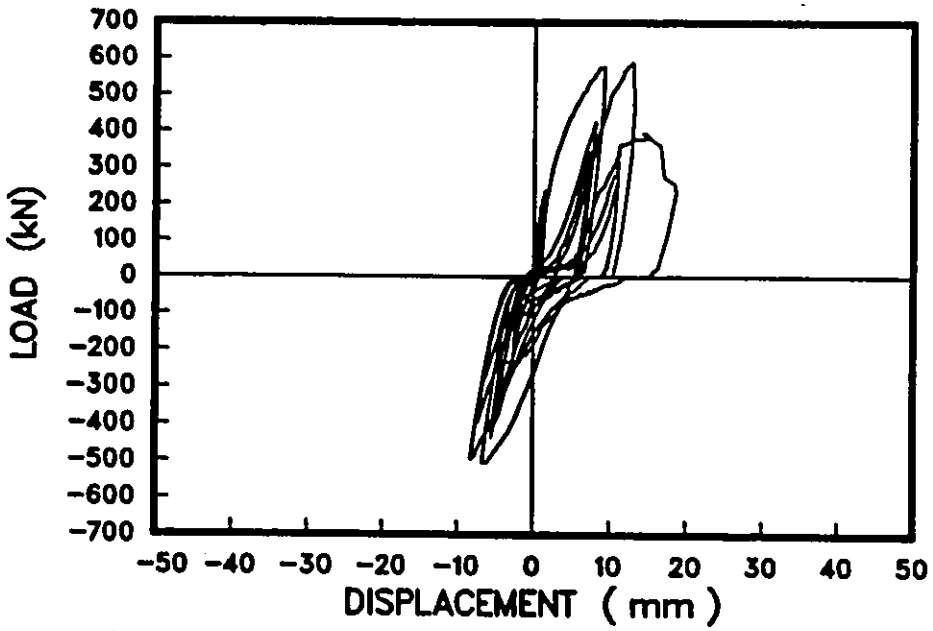

Figure 4.39: Load-Top wall displacement relationship for Wall 5 excluding displacements due to sliding shear

4.3.4 Load-Bar slip relationship

The slippage of vertical wall reinforcement in the foundation beam was recorded at both ends of the wall during the test. The test data are presented in Figures 4.40 and 4.41. As mentioned previously, the bar slip results from the penetration of steel stresses into the footing causing cumulative extension of the reinforcement at the wall footing interface.

Additional wall rotation resulting from the bar slip is calculated as described in Section 4.2.4 and is presented in Figure 4.42.

4.3.5 Load-Total vertical displacement relationship

The vertical movement at each end of the top beam is presented in Figures 4.43 and 4.44. These displacements are composed of the bar slip in the foundation beam and the vertical wall displacement resulting from flexure.

Lateral load versus total wall rotation hysteretic relationship is shown in Figure 4.45.

4.3.6 Strains in vertical flexural reinforcement

The strains in most of the vertical bars were monitored at the construction joint level as mentioned in Section 3.4. Figures 4.46, 4.47, 4.48 and 4.49 present the load-strain relationships at selected locations.

The steel strain distributions along the base of the wall are discussed in more detail in Chapter 5.

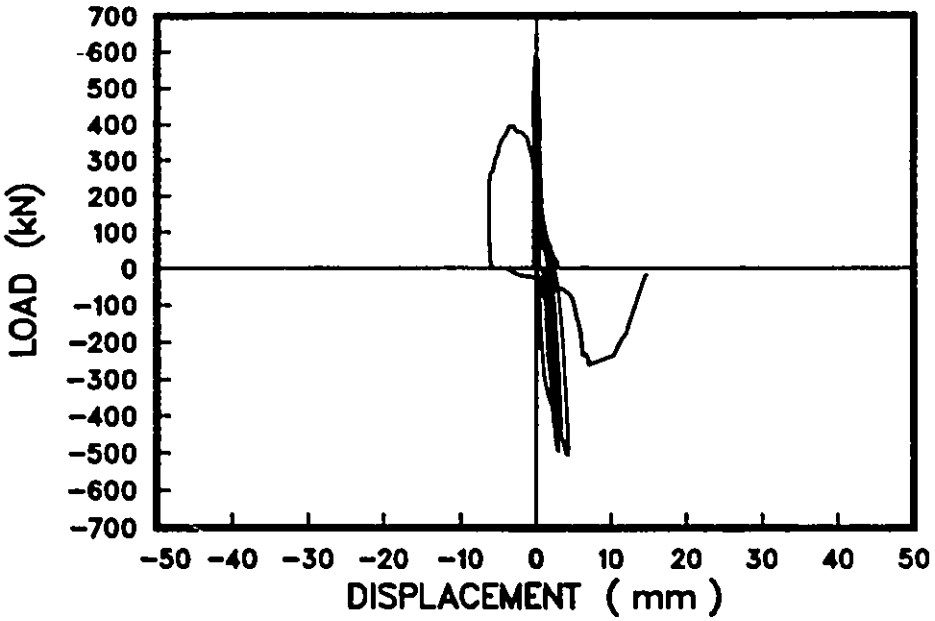

Figure 4.40: Load-Displacement relationship for LVDT 4 of Wall 5

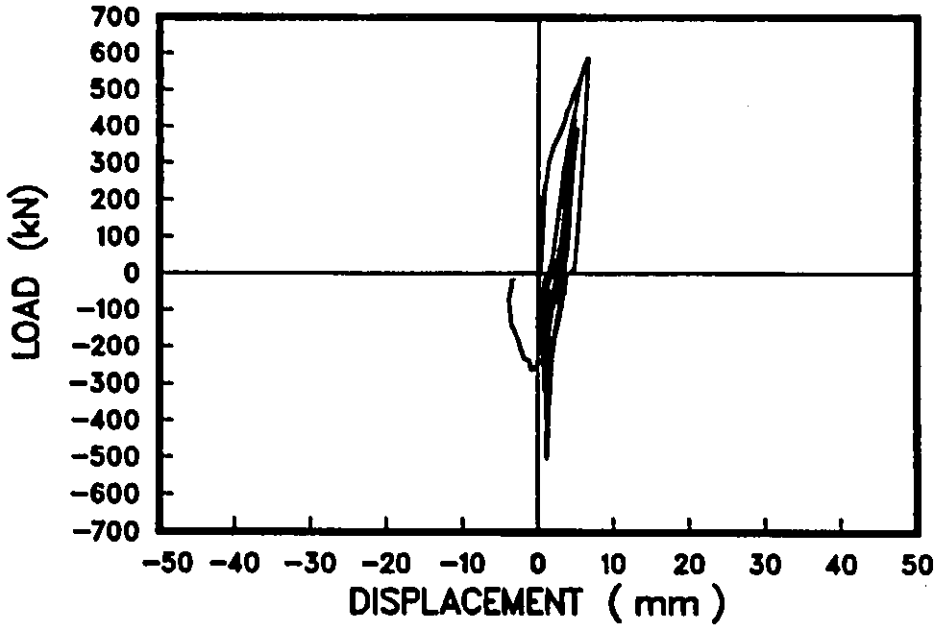

Figure 4.41: Load-Displacement relationship for LVDT 5 of Wall 5

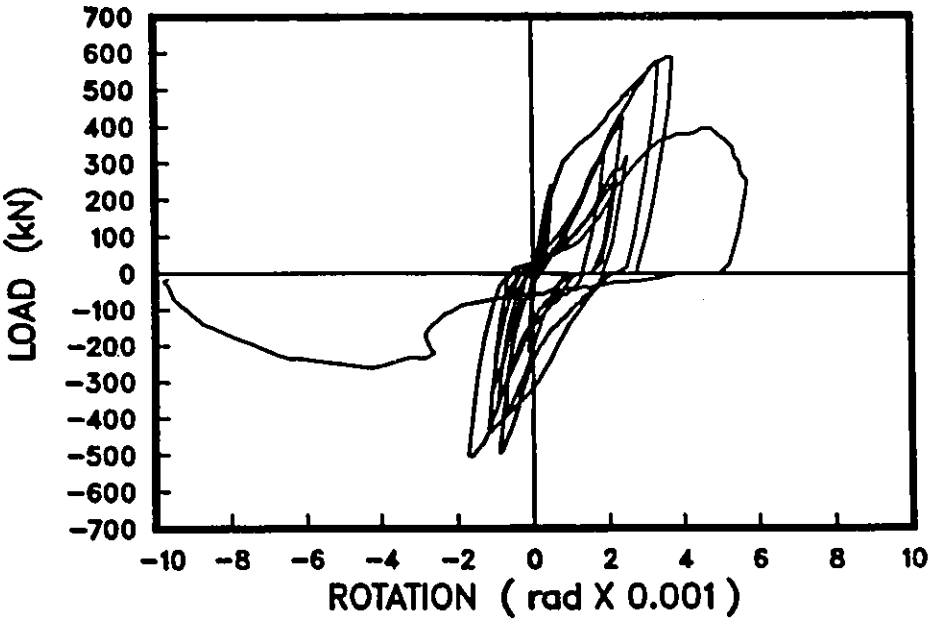

Figure 4.42: Load-Base rotation relationship of Wall 5

4.4 Discussion of test set-up

The overall performance of the test set-up was found to be satisfactory. The absence of prestressing on the high strength bolts connecting the specimen and the reaction frame to the strong floor resulted in some sliding of these components during testing. However these movements did not affect the displacement readings since the foundation beam was taken as the reference point. The instrumentation performed well throughout the testing. Some unexpected large displacements (base slip) were found to exceed the linear range of the LVDTs and had to be corrected manually.

At the attainment of the peak loads at $\pm 1\Delta_y$ and $\pm 2\Delta_y$, some unexpected deformations were noticed in the foundation beam. Figure 4.50 presents a schematic of the observed cracking in the foundation beam at the end of the test. A vertical deflection of approximately 10 mm was detected in the middle region of the beam which resulted in vertical flexural and diagonal shear cracks as depicted in Figure 4.50. These cracks were all hair

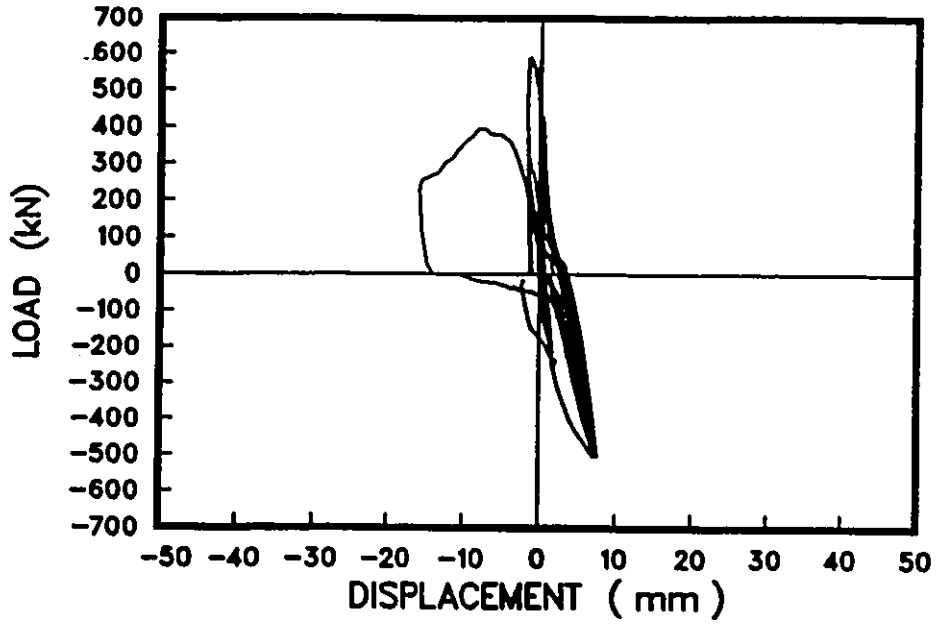

Figure 4.43: Load-Displacement relationship for LVDT 2 of Wall 5

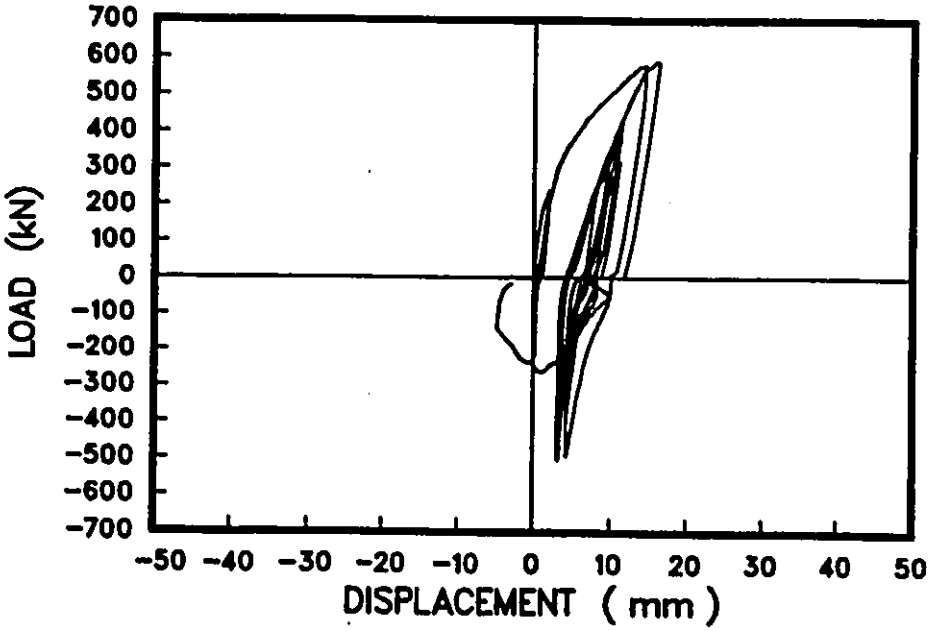

Figure 4.44: Load-Displacement relationship for LVDT 3 of Wall 5

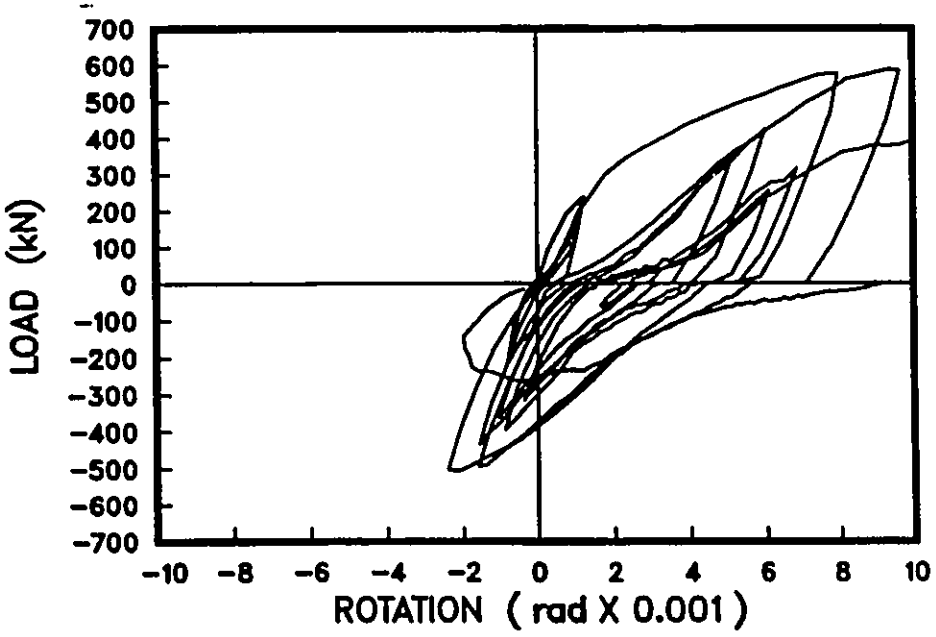

Figure 4.45: Load-Top rotation relationship of Wall 5

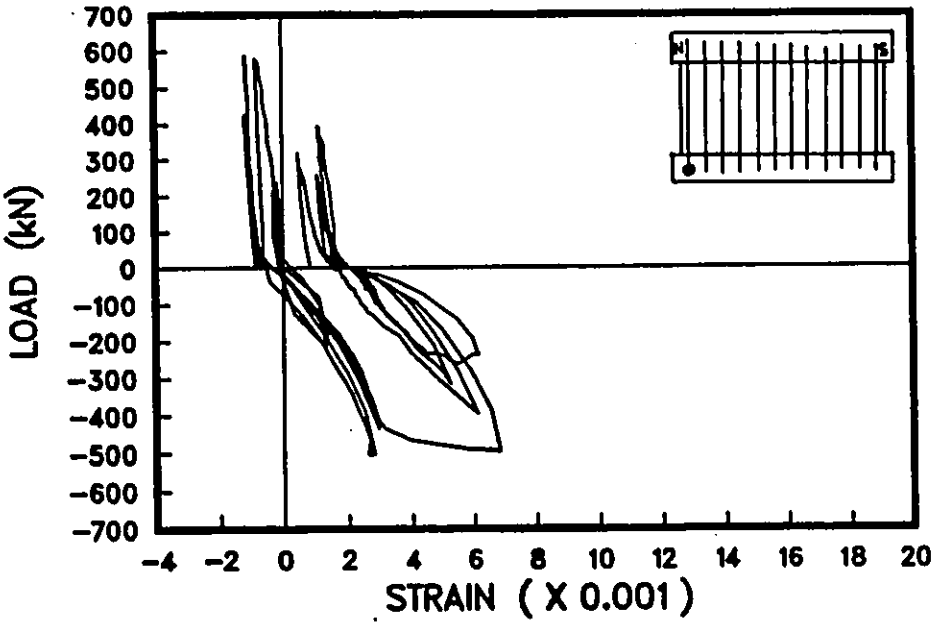

Figure 4.46: Load-Strain relationship of vertical bar of Wall 5

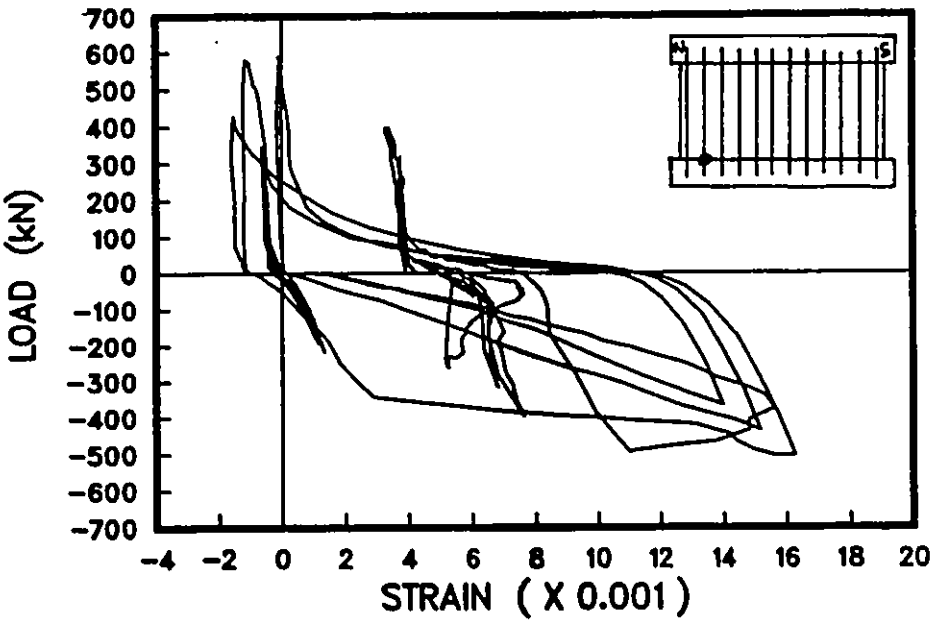

Figure 4.47: Load-Strain relationship of vertical bar of Wall 5

line cracks. Also some cracks were noticed on the transverse section at the ends of the foundation beam which indicates that bending took place in the transverse direction. The effect of the observed behavior of the foundation beam on the wall response is analyzed in Chapter 6.

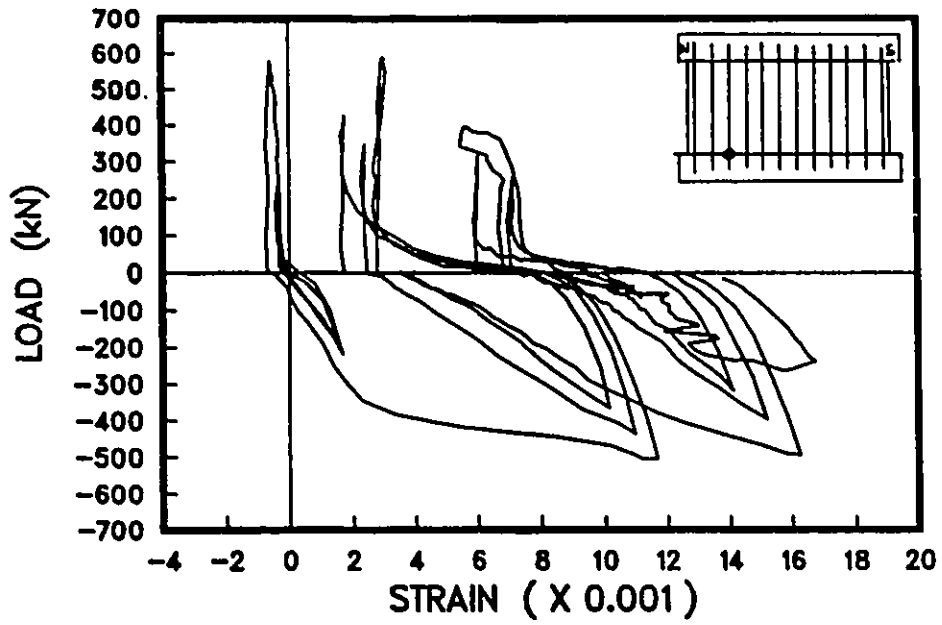

Figure 4.48: Load-Strain relationship of vertical bar of Wall 5

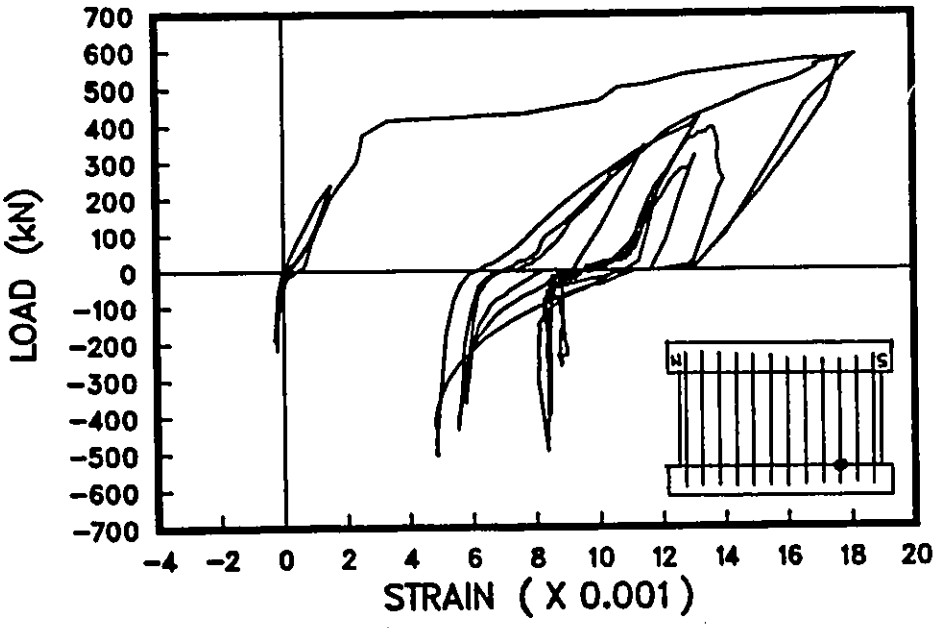

Figure 4.49: Load-Strain relationship of vertical bar of Wall 5

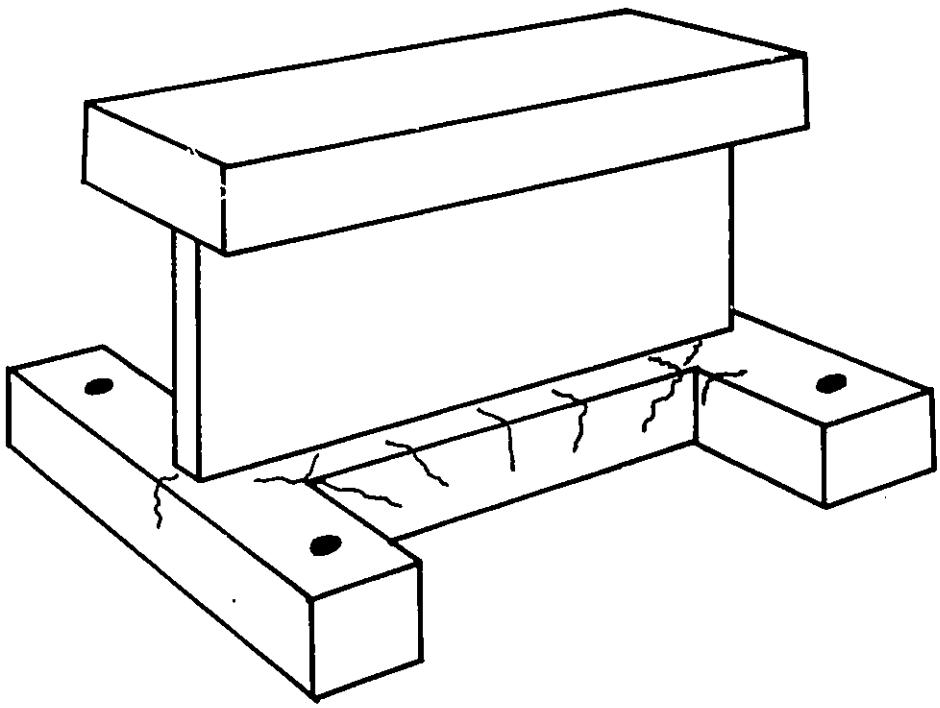

Figure 4.50: Schematic of cracks in foundation beam

Chapter 5

Discussion and Analysis of Test Results

5.1 Introduction

The behavior of Walls 4 and 5 are discussed in this chapter based on the test results presented in Chapter 4. Also a detailed analysis of the displacement components are presented, namely the contribution to the top horizontal displacement of the base slip, bar slip, shear and flexural deformations. Moment-curvature, moment-rotation, and shear force - shear distortion relationships are presented and compared with theoretical relationships. Flexural strains obtained from strain gauges are analyzed and finally the energy dissipation mechanism of each wall is discussed.

5.2 Behavior of specimens

5.2.1 Wall 4

Wall 4 was designed using a vertical steel reinforcement ratio of 0.8% with a predicted flexural capacity of 698 kN·m. Corresponding to this moment capacity, a predicted shear force of 612 kN was expected and an appropriate horizontal steel reinforcement ratio of 0.8% was provided. As explained in Section 3.1.1, Wall 4 was a companion specimen to Wall 1 reported by Wiradinata [40]. The same amount of vertical steel was used in Walls 1 and 4 resulting in similar ultimate flexural capacities. Wall 1 was designed with a minimum horizontal steel ratio of 0.25%. This resulted in a ductile behavior of the wall up to a top horizontal displacement of 10 mm followed by a corner-to-corner diagonal tension failure. Based on these observations, Wall 4 was expected to perform in a ductile manner throughout the intended loading program presented in Figure 3.19.

The load-top displacement hysteresis curves of Wall 4 are presented in Figure 4.2. This figure reveals that the wall did not reach its predicted design shear force of 612 kN. A maximum load of -419 kN was recorded at load stage 14, at a deformation level of $-2\Delta_y$. This load level corresponds to a shear stress level of $0.45\sqrt{f'_c}$MPa. At this point the wall was fully cracked as depicted in Figure 4.6. Some hair line flexural cracks were observed on both sides of the wall. Hence it would be expected that more load could be taken by the wall. In fact, the steep slope of the force-deformation relationship, shown in Figure 4.2, in the region of the maximum load, indicates the reserve capacity of the wall. Because the specimen was subjected to displacement controlled loading, the load was reversed at a prescribed displacement level. Cyclic loading produced excessive sliding of the wall along the construction joint, not giving the wall a chance to develop higher load resistance.

Upon displacement reversals at $\pm 4\Delta_y$, severe pinching of the hysteresis loops were observed. This pinching action was essentially due to the sliding of the wall along the construction joint. This can be seen by examining

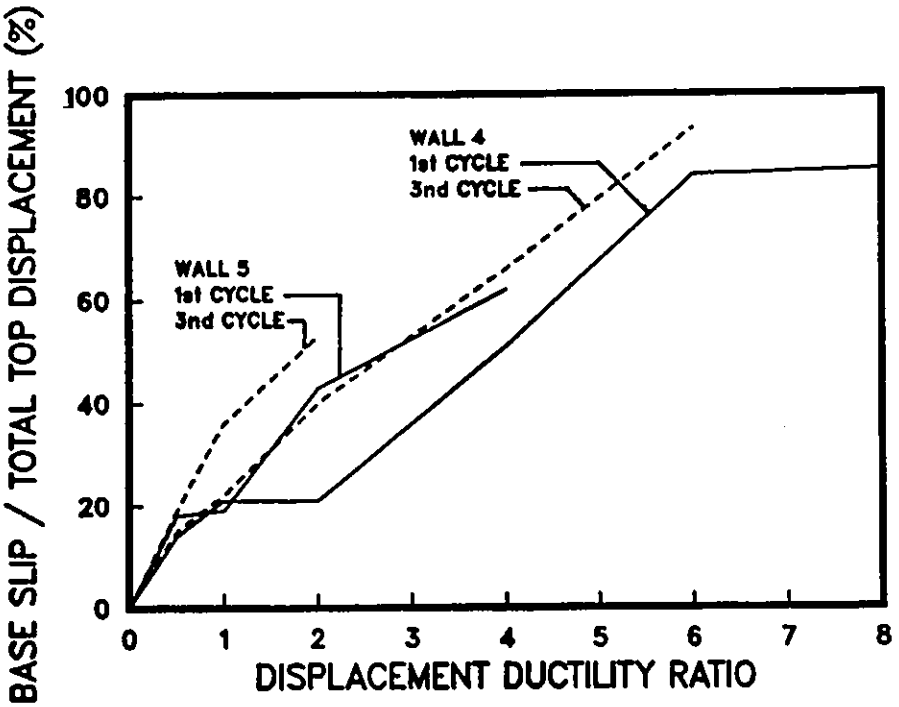

Figure 5.1: Contribution of base slip to the top displacement

Figures 4.13, 4.14 and 4.15. The observed pinching effect started at $2\Delta_y$ by the formation of a continuous crack at the base of the wall. Displacement reversals at $\pm 4\Delta_y$ resulted in partial crushing of the concrete and kinking of the vertical bars at the base of the wall as observed in Figure 4.7. The contribution of the base slip to the top horizontal displacement can be seen in Figure 5.1 at different displacement ductility ratios. The base slip recorded up to $1\Delta_y$ was essentially the shear deformation that took place within the bottom wall portion where the LVDTs were mounted. Subsequent cycles showed a distinct increase in the contribution of the base slip to the top displacement. The effect of this large base slip on the imposed ductility on the wall element is clearly seen in Figure 4.16. The wall element was subjected to very little inelastic deformation throughout the test which explains the relatively large stiffnesses observed on Figure 4.2 at peak deformations.

The behaviors of the wall in the north and south directions were slightly different. Higher loads were recorded at peak deformation while loading in the south direction. The magnitude of the loads were 5% to 25% higher in comparison with the north direction at the same displacement ductility

ratio. However strength degradation was more pronounced in the north direction. At low load level, ±50 kN, pinching effect due to severe base slip resulted in stiffness degradation.

In summary, the principal mode of failure of Wall 4 was due to sliding shear. A maximum average shear stress of $0.45\sqrt{f'_c}$MPa was reached at 68% of the predicted ultimate shear force. Base slip was initiated by the formation of a continuous flexural crack at the base of the wall.

5.2.2 Wall 5

Wall 5 was designed using a vertical steel reinforcement ratio of 1.2% with a predicted flexural capacity of 955 kN·m. Corresponding to this flexural capacity, a shear force of 838 kN was expected and appropriated horizontal shear reinforcement ratio of 1.2% was provided. Wall 5 was designed and constructed prior to the testing of Wall 4. Based on previous studies, Wall 5 was expected to develop its flexural capacity and fail due to sliding shear or diagonal compression failure. A high shear stress level of $1.01\sqrt{f'_c}$MPa was expected to be the cause of the failure mechanism.

The load-top displacement hysteresis curves of Wall 5 are presented in Figure 4.28. As depicted in this figure, the wall did not reach its predicted design shear force of 838 kN. A maximum load of 586 kN was recorded at load stage 13, at $2\Delta_y$. This level of load corresponds to a shear stress value of $0.69\sqrt{f'_c}$MPa. A similar load level was recorded at load stage 7, at $1\Delta_y$. At this deformation level, Wall 5 was fully cracked as shown in Figure 4.30. Flexural cracks less than 1 mm wide were observed on the tension side of the wall which explains the rounded shape of the hysteresis curve at $1\Delta_y$. However from the stiffness of the hysteresis curve an increase in lateral load capacity would be expected at a displacement ductility ratio of $2\Delta_y$.

Upon displacement reversals at $\pm 1\Delta_y$, noticeable displacements were recorded at the base of the wall as shown in Figures 4.36, 4.37 and 4.38. These observations are emphasized in Figure 5.1 where base slip contributes to 36% of the total top displacement at the third cycle at $1\Delta_y$. Also at this point a

continuous flexural cracks was present at the base of the wall. Subsequent cycles at $\pm 2\Delta_y$ and $\pm 4\Delta_y$ showed an increase in the contribution of the base slip to the top displacement. The effect of this large base slip is clearly seen in Figure 4.39. The imposed ductility on the wall element was very low in the north direction and inexistant in the south direction. The elastic behavior in the south direction can be seen in Figure 4.39 where high stiffnesses were recorded at peak deformations.

The overall behavior of the wall in the north and south directions was slightly different. Higher peak loads were recorded in the north direction. Loading in the north direction also showed a more pronounced strength degradation in comparison with the south direction at the same displacement ductility ratio. This confirms our previous observation that the wall element above the bottom LVDTs remained essentially elastic while loading in the south direction. Stiffness degradation due to pinching effect was not detected at $\pm 1\Delta_y$. However the pinching of the hysteresis loops at $2\Delta_y$ due to base slip was marked by a severe stiffness degradation at low load level.

In summary, the principal mode of failure of Wall 5 was due to sliding shear. A maximum shear stress level of $0.69\sqrt{f'_c}$MPa was obtained at 70% of the design shear force. Base slip was initiated by the formation of a continuous flexural crack at the base of the wall.

5.3 Displacement components

The load-top displacement hysteresis curves presented in Figures 4.2 and 4.28 can be decomposed into four displacement components: the base slip, the bar slip, the shear and flexural deformations.

The base slip component was defined as the sliding of the wall as a rigid body motion in the horizontal direction with respect to the foundation beam. This component was calculated as a weighted average of LVDTs 6, 7 and 8. The bar slip component was calculated from the load-base rotation relationship presented in Figures 4.19 and 4.42. The angle of

rotation measured at the base of the wall was multiplied by the wall height (the distance separating LVDT 1 and LVDTs 4 and 5 as shown in Figure 3.10) to obtain the top horizontal displacement resulting from the rigid body rotation of the wall with respect to the foundation. This component was caused by local deterioration of bond between concrete and steel in the foundation beam, and the resulting slippage of the vertical bars.

The shear displacement component was calculated from the vertical and horizontal displacements of the four corners of the wall. Using the general equation for plane section transformation

$$\epsilon_\theta = \epsilon_x \, cos^2\theta + \epsilon_y \, sin^2\theta - \gamma_{xy} \, sin\theta cos\theta$$

the shear distortion angle, γ_{xy}, was obtained. In the above expression, ϵ_x, ϵ_y and ϵ_θ are the calculated average strains in the horizontal, vertical and diagonal directions respectively. The angle θ was measured between the horizontal and diagonal directions. Multiplying the shear distortion γ_{xy} by the clear distance measured between the top beam and the bottom LVDTs, the shear contribution to the top deflection was approximated. Finally the flexural component was calculated by subtracting the base slip, bar slip and shear components from the total top deflection. Consequently the experimentally determined flexural component is less accurate than the other components since it includes any computational inaccuracy involved in the previous three components.

The hysteresis loops of each displacement components namely, the base slip, bar slip, shear and flexural deformations for Wall 4 are presented in Figures 5.2 to 5.5 respectively. As mentioned previously, LVDT 5 was malfunctioning at $6\Delta_y$ and $8\Delta_y$ during the testing of Wall 4, consequently, the hysteresis loops presented in Figures 5.3 to 5.5 are shown up to load stage 26.. Figures 5.6 to 5.9 present the hysteresis loops of each wall component for Wall 5.

The principal mode of failure of Wall 4 was due to sliding shear as depicted in Figure 5.2 where symmetrical hysteresis loops are noticed. The bar slip component presented in Figure 5.3 shows small hysteresis loops after the onset of flexural yielding at $+1\Delta_y$. The magnitude of the bar slip component at $\pm 2\Delta_y$ and $\pm 4\Delta_y$ shows a constant value of approximately

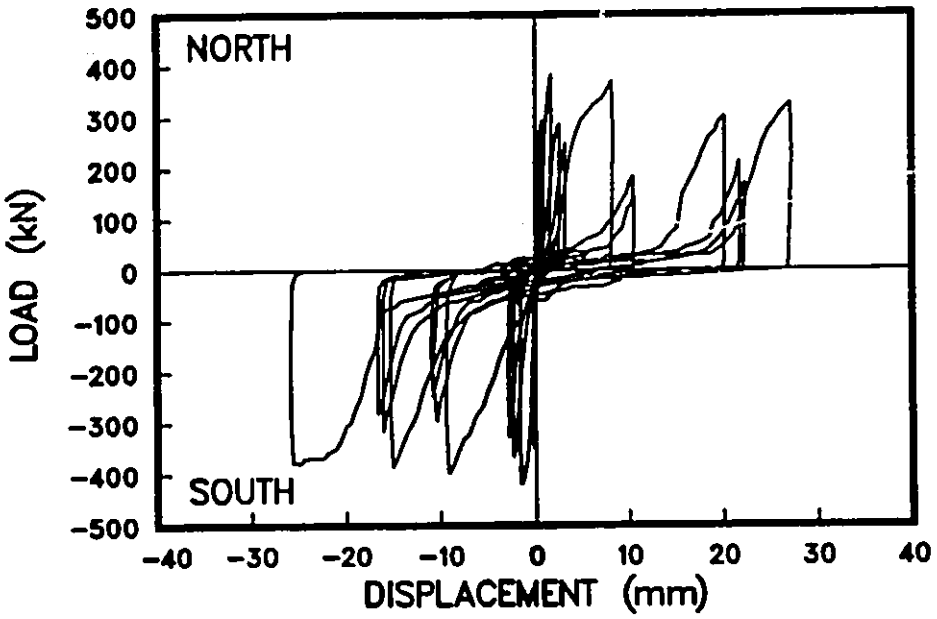

Figure 5.2: Wall 4 Load-Base slip relationship

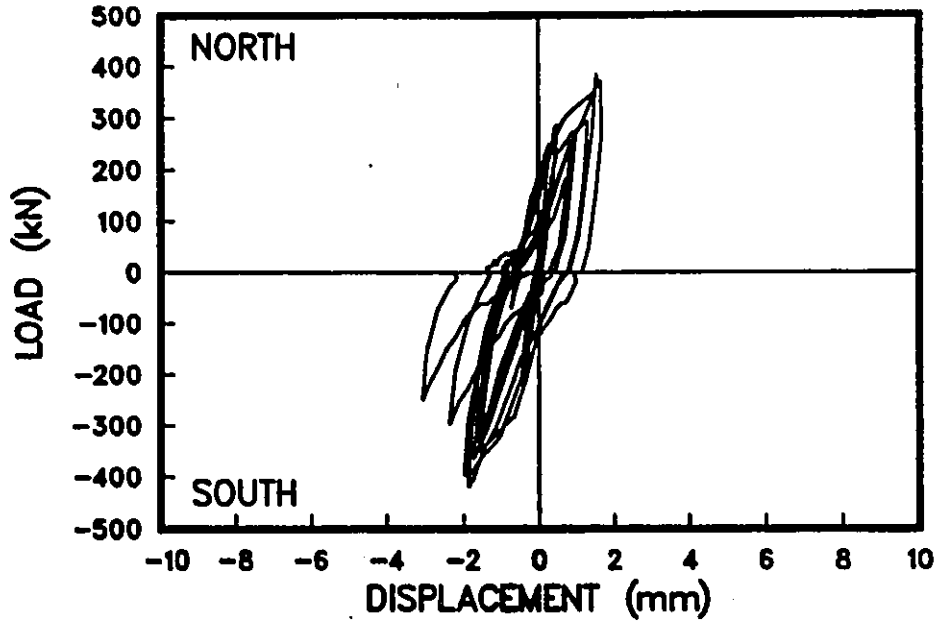

Figure 5.3: Wall 4 Load-Bar slip relationship

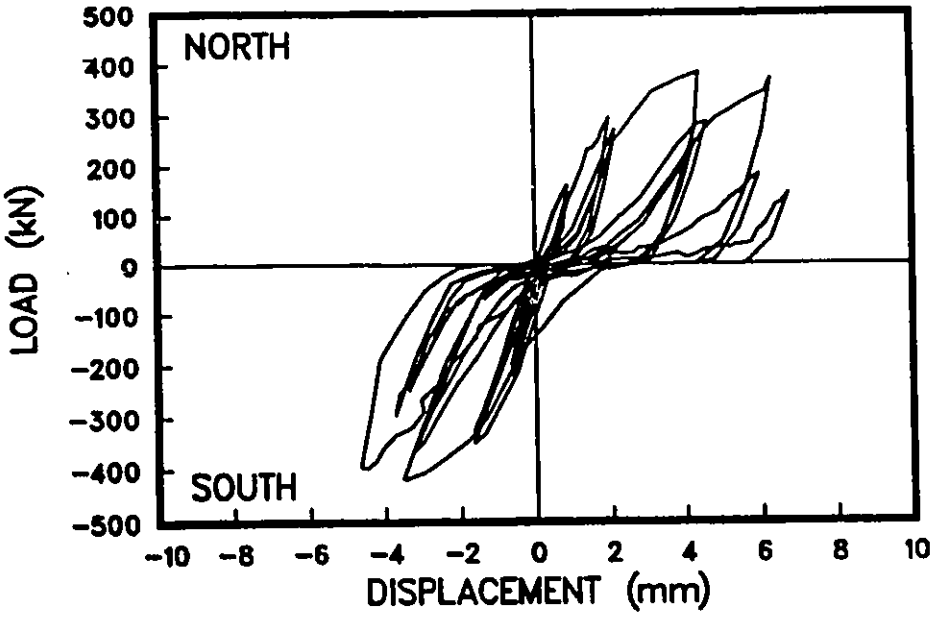

Figure 5.4: Wall 4 Load-Shear deformation relationship

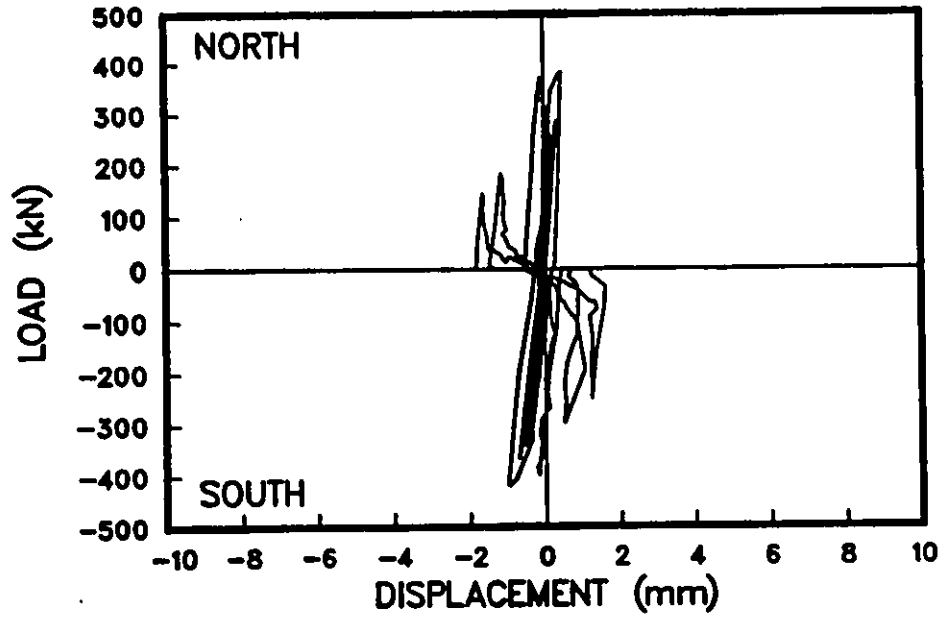

Figure 5.5: Wall 4 Load-Flexural deformation relationship

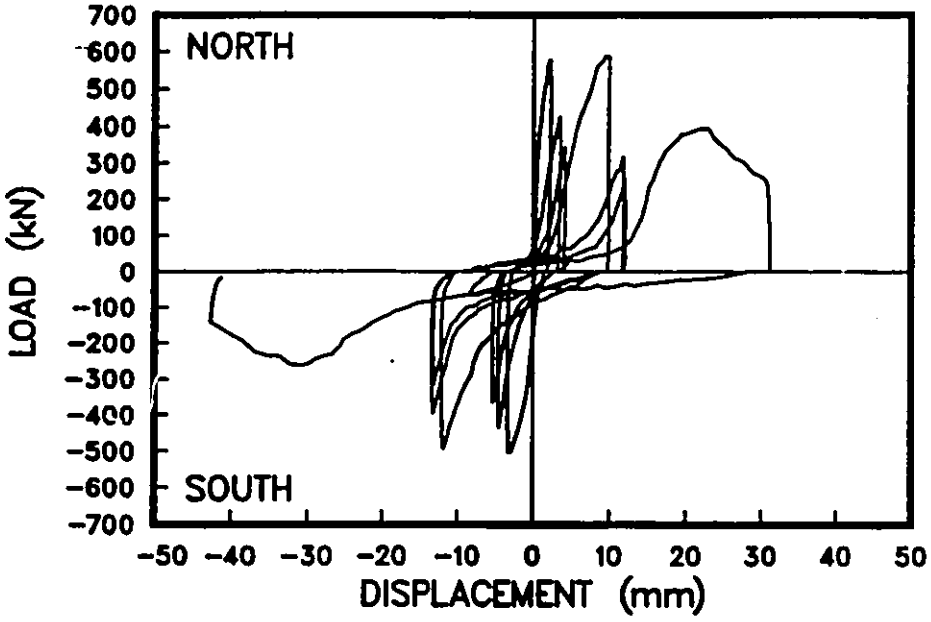

Figure 5.6: Wall 5 Load-Base slip relationship

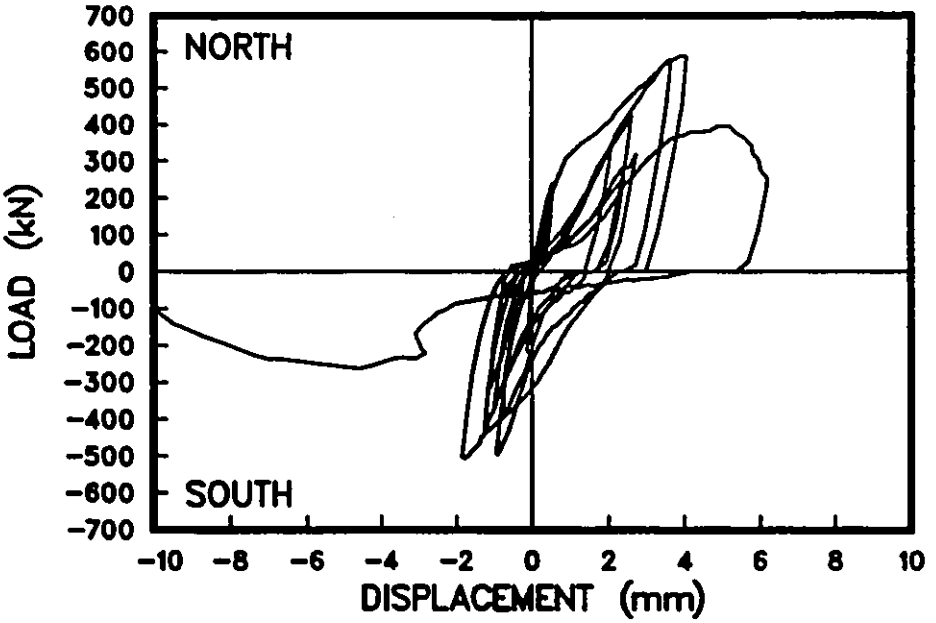

Figure 5.7: Wall 5 Load-Bar slip relationship

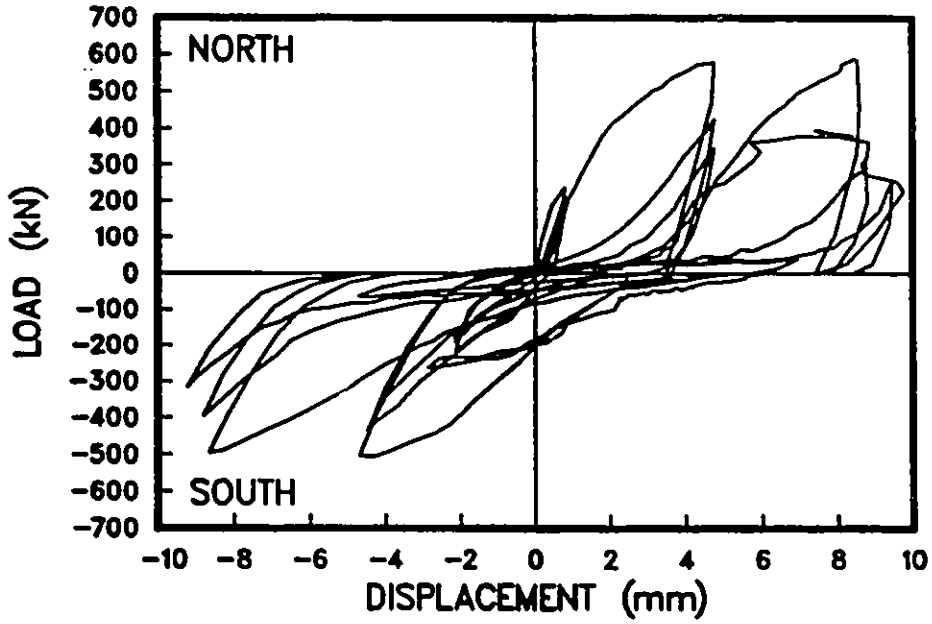

Figure 5.8: Wall 5 Load-Shear deformation relationship

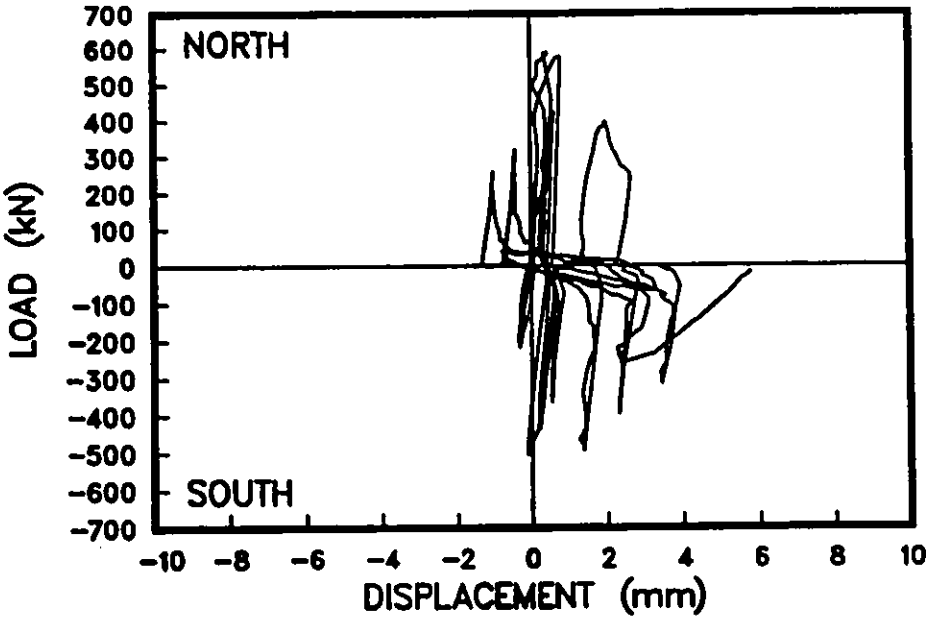

Figure 5.9: Wall 5 Load-Flexural deformation relationship

2 mm. Shear deformation hysteresis loops presented in Figure 5.4 show symmetrical behavior in the north and south directions. Inelastic shear deformation is noticeable at the first cycle at $+2\Delta_y$ which produced some pinching at low load level for the subsequent cycles. A comparison of the flexural deformation hysteresis loops presented in Figure 5.5 with shear deformations shows that flexural deformations remained small throughout the test and that no noticeable yielding took place within the wall element above the bottom LVDTs.

Wall 5 failed due to sliding shear as depicted in Figure 5.6 where a symmetrical behavior was observed in both directions. The bar slip hysteresis relationship presented in Figure 5.7 shows a symmetrical behavior in both directions. A permanent shift of the hysteresis loops was caused by the extensive yeilding of the flexural reinforcement at $1\Delta_y$. These permanent deformations at the base of the wall could not be recovered during the reloading process at $-1\Delta_y$. The shear deformation hysteresis behavior presented in Figure 5.8 shows a different behavior at $\pm\frac{1}{2}\Delta_y$ due to non-symmetrical cracking as depicted in Figure 4.29. However this phenomenon was not observed for the subsequent cycles. Inelastic shear deformation occurred at $+1\Delta_y$ creating some pinching in the hysteresis loops at low load levels. The pinching effect was mostly seen while loading in the north direction. The flexural deformation hysteresis loops presented in Figure 5.9 show a linear behavior throughout the loading program except at $\pm4\Delta_y$ where discrepancies are noticed due to excessive base slip. This linear behavior indicates that the wall element above the bottom LVDTs remained essentially elastic throughout the loading history.

To get an appreciation of the relative magnitude of each displacement component, Figures 5.10 to 5.13 were plotted. These figures show the displacement components of Wall 4 at selected load stages, namely 1, 7, 13 and 21. These load stages correspond to the first cycle at a given ductility displacement ratio, namely $\frac{1}{2}\Delta_y$, $1\Delta_y$, $2\Delta_y$ and $4\Delta_y$. As depicted in Figures 5.10 and 5.11, no base slip and bar slip was detected before $1\Delta_y$. Base slip became visible at $2\Delta_y$. Bar slip was considerably larger than the flexural deformation throughout the loading hystory. The ratio of shear deformation to the sum of shear and flexural deformations remained constant at about 70% for $\frac{1}{2}\Delta_y$ and $1\Delta_y$. At $2\Delta_y$and $4\Delta_y$this ratio increased to about

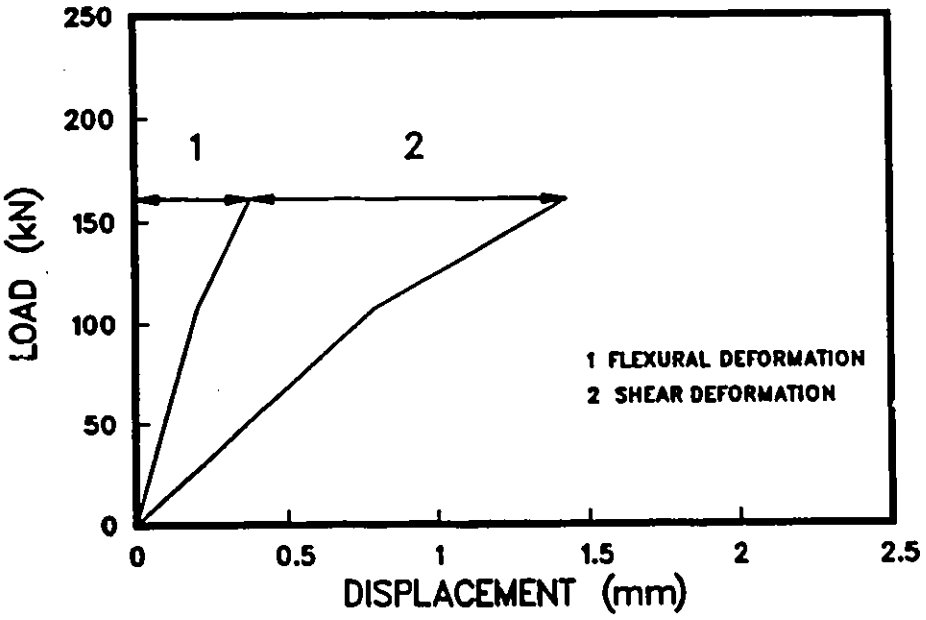

Figure 5.10: Wall 4 Load-Wall displacements history at $\frac{1}{2}\Delta_y$, load stage 1

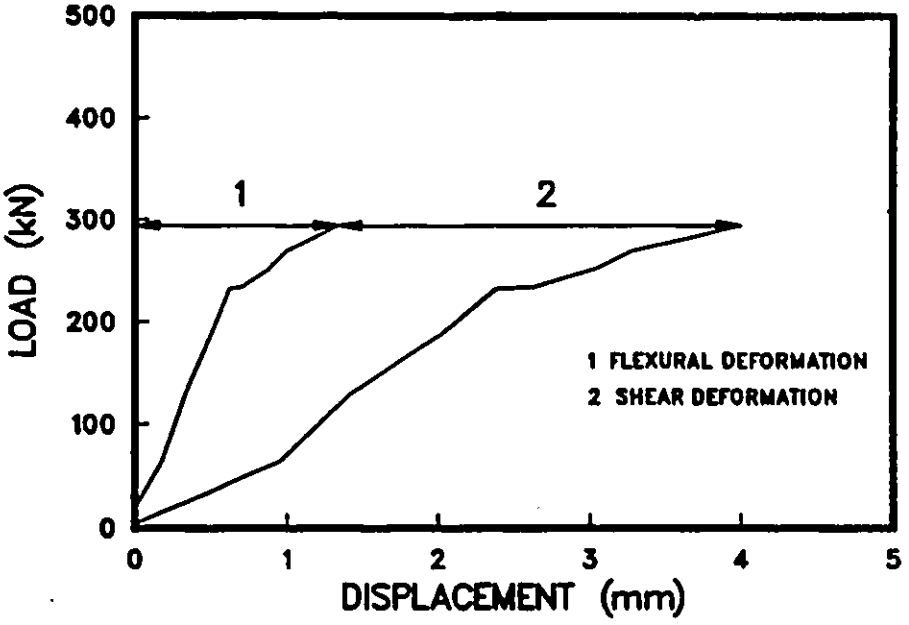

Figure 5.11: Wall 4 Load-Wall displacements history at $1\Delta_y$, load stage 7

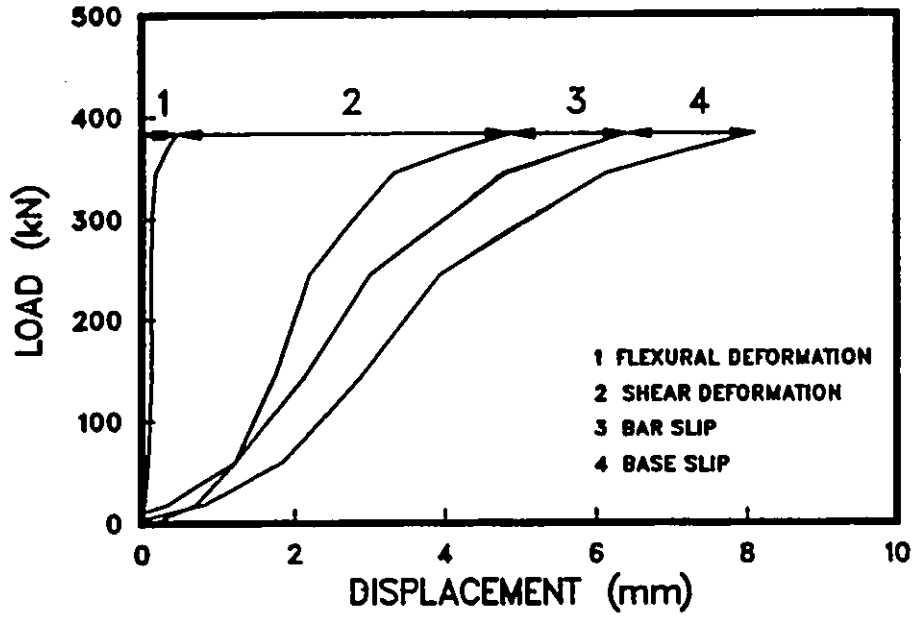

Figure 5.12: Wall 4 Load-Wall displacements history at $2\Delta_y$, load stage 13

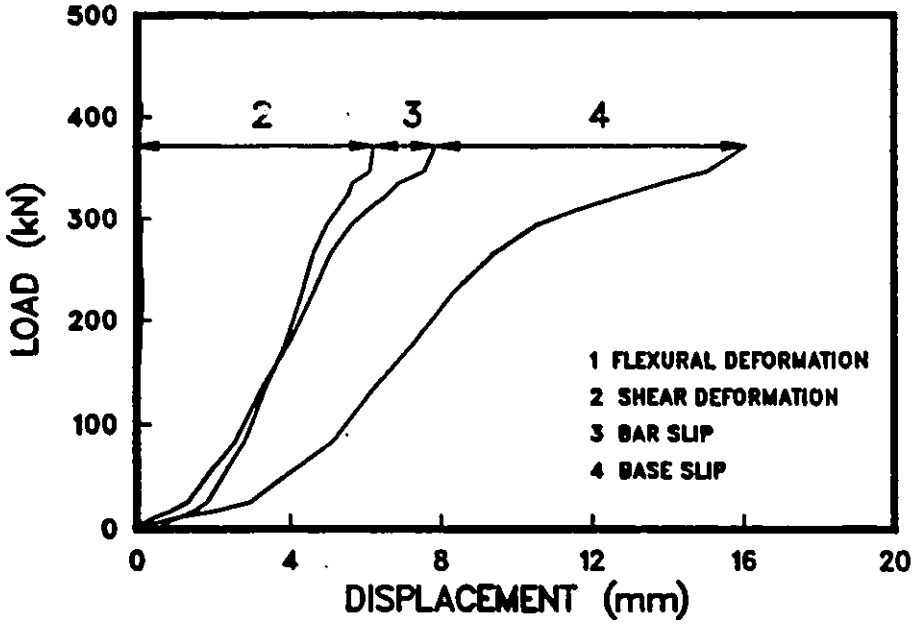

Figure 5.13: Wall 4 Load-Wall displacements history at $4\Delta_y$, load stage 21

95%.

Figures 5.14 to 5.17 present the same displacement components for Wall 5. As depicted in Figure 5.14, no base slip and bar slip was detected at $\frac{1}{2}\Delta_y$. Base slip and bar slip became visible at $1\Delta_y$ and became more pronounced as the displacement ductility ratio was increased. Figure 5.17 clearly shows that the mode of failure was due to the loss of strength in the base slip resistance mechanism. The bar slip component remained considerably large in comparison with the flexural deformation. The ratio of shear deformation to the sum of shear and flexural deformations remained constant at about 55% for $\frac{1}{2}\Delta_y$, increased to about 90% for $1\Delta_y$, $2\Delta_y$ and $4\Delta_y$.

5.4 Moment - Rotation relationship

Moment-rotation relationships were computed using the Beam Theory for monotonically increasing load. Assuming, these relationships would give the envelopes of the hysteresis curves, a comparison is made with the test results.

The first step in conducting a moment-rotation analysis involves the determination of a sectional moment-curvature relationship under monotonically increasing load. Using the material properties given in Table 3.1, the moment-curvature relationship for each wall was established up to its ultimate flexural capacity. These relationships are presented in Figure 5.18. In the derivation of these two curves, the actual stress-strain relationships of the concrete and the steel were used, including strength hardening in the reinforcing bars. Tensile strength of concrete and confinement of concrete in the compression zone were neglected.

The moment-rotation relationship of each wall was computed from the moment-curvature relationship presented in Figure 5.18. The rotation of the top beam with respect to the base was calculated by integrating the area of the curvature distribution along the height of the wall for a given base moment. The resulting primary moment-rotation relationships for Walls 4

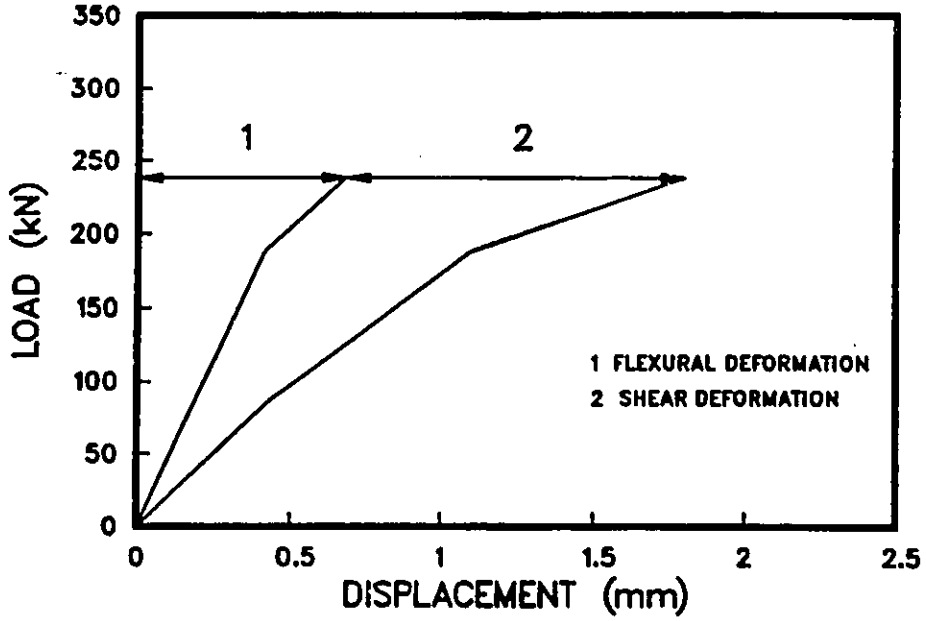

Figure 5.14: Wall 5 Load-Wall displacements history at $\frac{1}{2}\Delta_y$, load stage 1

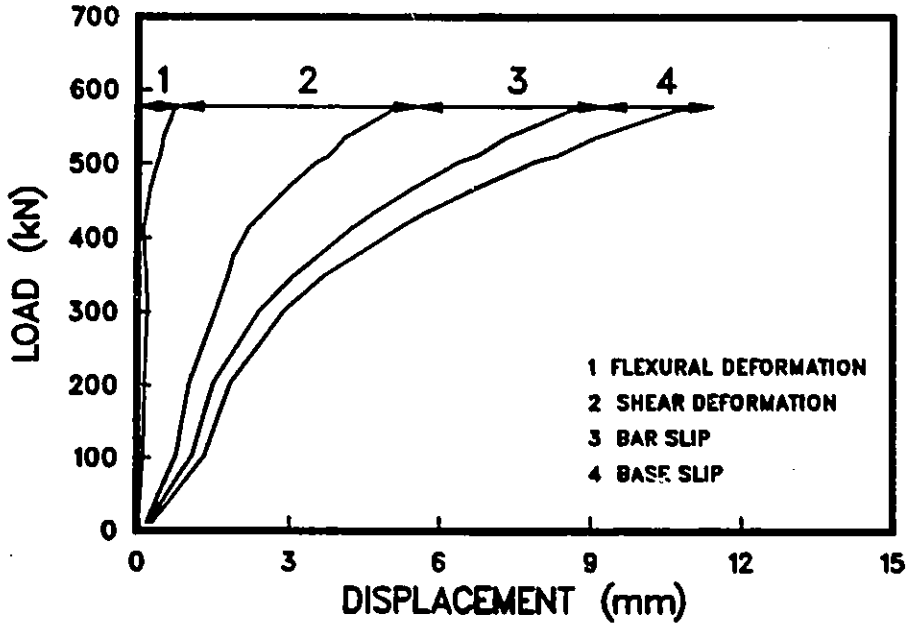

Figure 5.15: Wall 5 Load-Wall displacements history at $1\Delta_y$, load stage 7

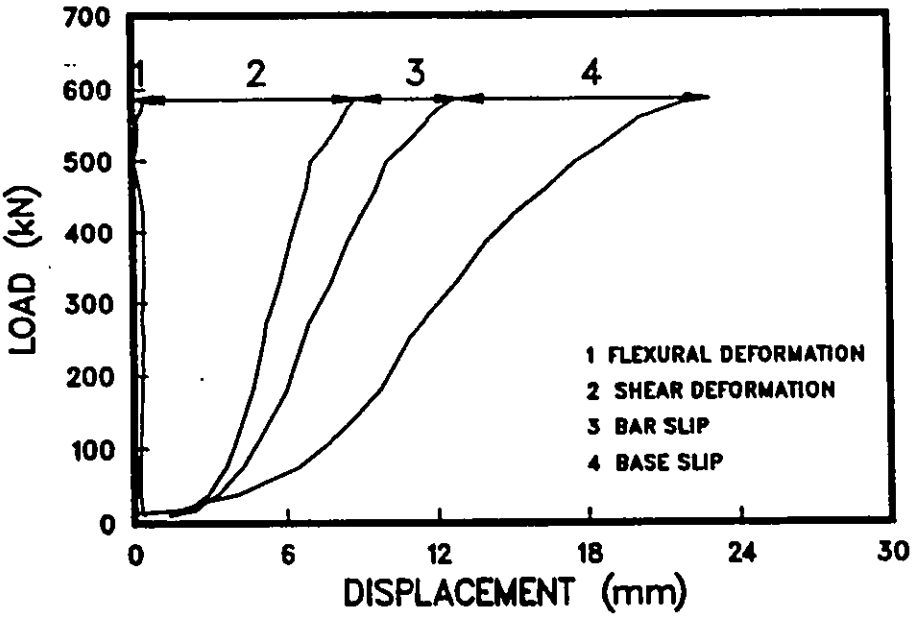

Figure 5.16: Wall 5 Load-Wall displacements history at $2\Delta_y$, load stage 13

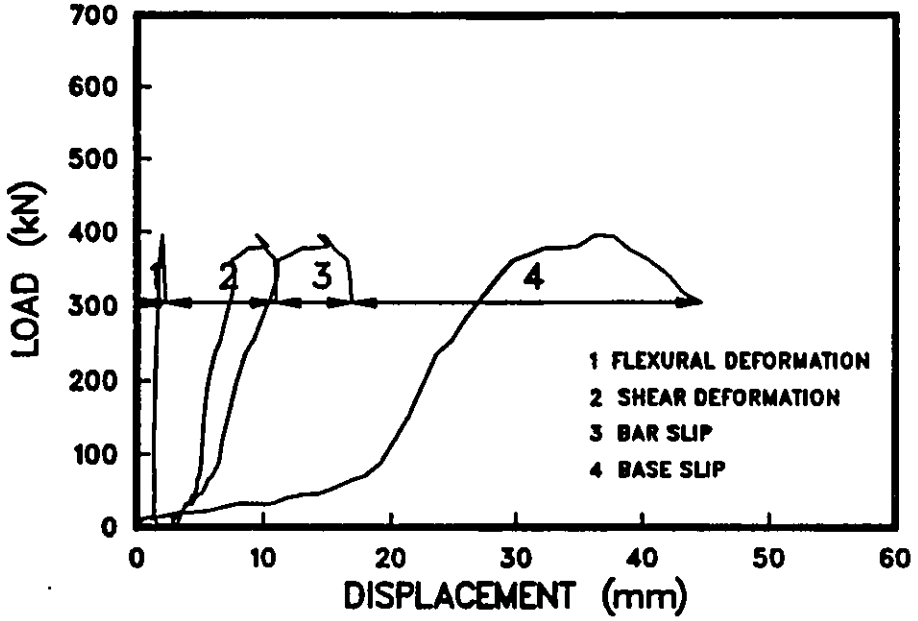

Figure 5.17: Wall 5 Load-Wall displacements history at $4\Delta_y$, load stage 21

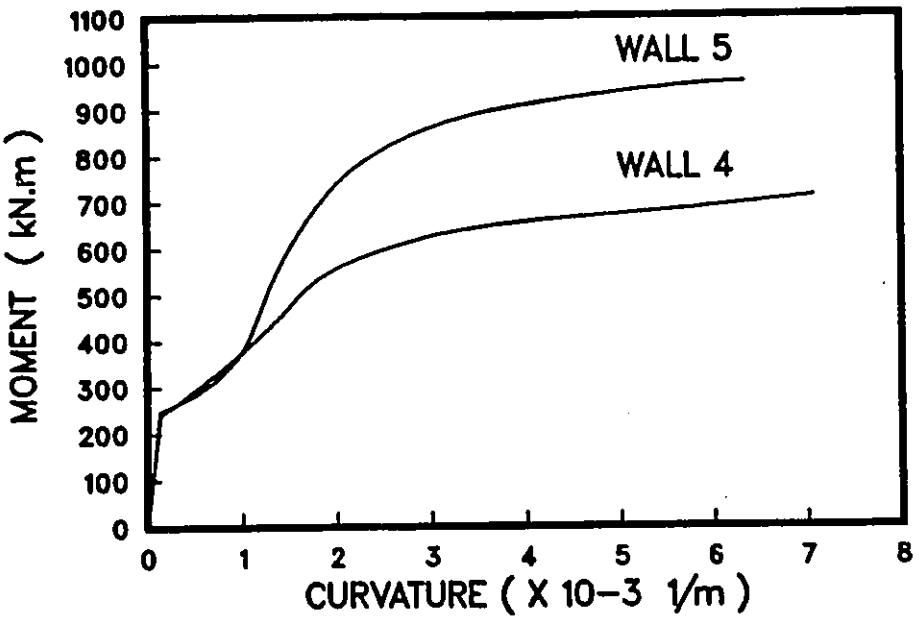

Figure 5.18: Moment-Curvature relationship for Walls 4 and 5

and 5 are presented in Figures 5.19 and 5.20 respectively. The experimental moment-rotation hysteresis curves are also shown in the same figures. The hysteresis loops were obtained by subtracting the base rotation presented in Figures 4.19 and 4.42 from the total top rotation shown in Figures 4.22 and 4.45 to obtain the observed rotation in the wall element.

As depicted from Figure 5.19 Wall 4 did not behave according to the analytical prediction based on the beam theory. The experimental results indicate reduced rotational stiffnesses of about 50% and 65% of the analytical prediction in the north and south direction respectively. The apparent discrepancy can be explained, in major part, by the base fixity condition of the specimen. The specimen was bolted on the laboratory strong floor at locations away from the wall base. This resulted in some flexibility in the wall, resulting from out-of-plane rotations. The effect of base fixity is illustrated in Chapter 6 and accounts for a large portion of the observed flexibility in response. The comparison of the observed responses between an earlier test where full fixity at the base was provided through a different set up, and the current tests, confirm the above point. This comparison is

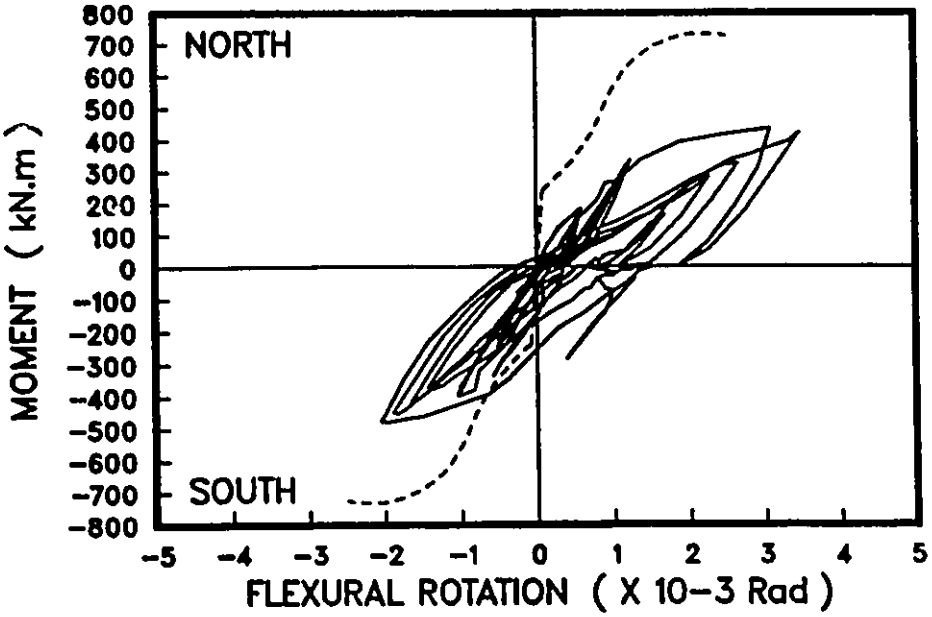

Figure 5.19: Wall 4 Analytical and experimental moment-rotation relationships

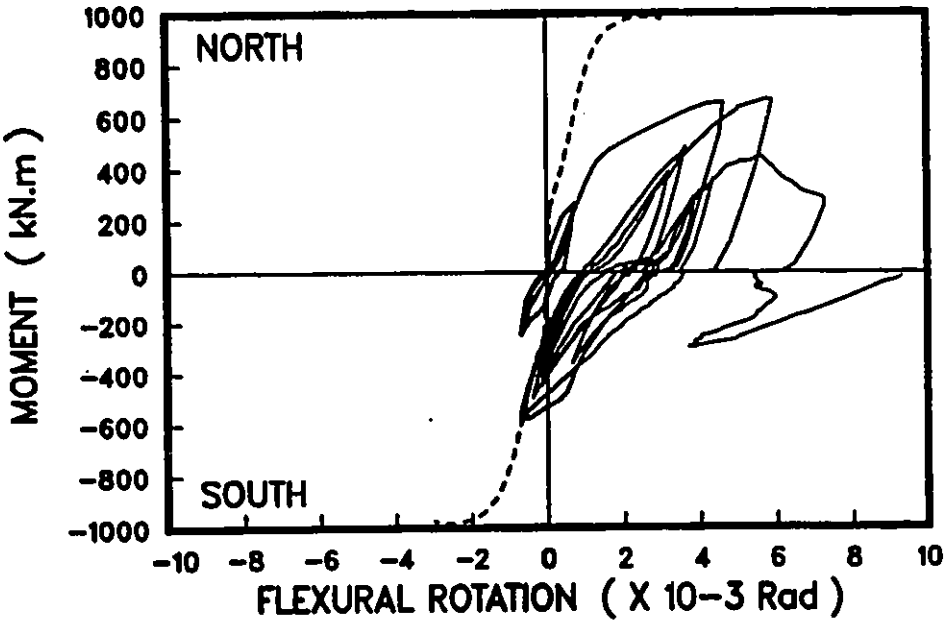

Figure 5.20: Wall 5 Analytical and experimental moment-rotation relationships

also presented in Chapter 6.

Some softening in flexural rigidity can be attributed to the presence of diagonal shear cracks. Shear flexure interaction is known to result in reduced flexural stiffness.

A similar softening was observed for Wall 5 as depicted in Figure 5.20. The observed rotational stiffnesses for Wall 5 were about 60% of the analytical prediction which is comparable with Wall 4. Furthermore the top displacement at $1\Delta_y$ in the north direction created a permanent shift in the axis of bending.

The analytical load-flexural displacement relationship of each wall was obtained by integrating the area of the rotation distribution along the height of the wall for a given base moment. It was observed that prior to the development of base slip, both walls showed a softening effect similar to the observed moment-rotation relationships. Upon the appearance of large base slip, the flexural displacements showed large scatter due to computational inaccuracies.

5.5 Shear force - Shear distortion relationship

The prediction of the analytical shear deformation in squat shear walls is complicated by the existence of cracks in the concrete and that plane section may not remain plane. However an approximation of the shear distorsion in cracked squat walls can be made by using a reduced value of the elastic shear modulus and a form factor. The elastic shear modulus for concrete can be approximated from the well-known relationship

$$G = \frac{E_c}{2(1+\nu)} \equiv 0.4\ E_c$$

Previous researchers [28,33] suggested that the shear modulus of diagonally cracked beams and flexural walls is approximately 10 to 30% of the

uncracked shear modulus, depending on the amount of web steel provided. Also the shear modulus of cracked deep beams, in which shear deformations dominate, is about 15% of the uncracked section when shear and flexure distortions are considered. Consequently it is expected that the cracked shear moduli for Walls 4 and 5 would be less than 15% of the uncracked moduli since arch action in deep beams enhances the shear modulus. Analytical shear force-shear deformation relationships are presented in Figures 5.21 and 5.22 for Walls 4 and 5 respectively where 5, 10 and 15% of the appropriate elastic shear modulus were used. The shear force - shear deformation history of the first cycle at $\frac{1}{2}\Delta_y$, $+1\Delta_y$, $+2\Delta_y$ and $+4\Delta_y$ are presented in Figures 5.21 and 5.22 for Walls 4 and 5 respectively. These relationships were obtained from the load-wall displacement relationships presented in Figures 5.10 to 5.13 and Figures 5.14 to 5.17.

Figure 5.21 shows that Wall 4 behaved in the effective elastic range of cracked reinforced concrete at $+\frac{1}{2}\Delta_y$ and $+1\Delta_y$ showing a shear modulus of about 10% of the uncracked modulus. However some inelastic shear deformation were recorded at $+2\Delta_y$ followed by some pinching of the force-deformation curve at $+4\Delta_y$ due to opening and closing of the diagonal shear cracks. Wall 5 showed a considerable amount of inelastic deformation at $+1\Delta_y$. The initial shear modulus was close to 15% of the uncracked modulus and decreased as diagonal shear cracks appeared during the loading process. Considerable pinching of the force-deformation curves at $+2\Delta_y$ and $+4\Delta_y$ resulted from the excessive shear distorsion at $+1\Delta_y$. The shear force-shear deformation curve at $+4\Delta_y$ is greatly affected by the extensive crushing of the concrete at the base due to base slip as depicted in Figure 5.17. It should be noted that inelastic shear deformations observed in Figures 5.21 and 5.22 at peak deformations did not necessarily correspond to yielding of the horizontal shear reinforcement.

5.6 Strain profiles

Strain in the vertical flexural bars were monitored at the base of the wall throughout the loading program. Strain distribution at different load levels

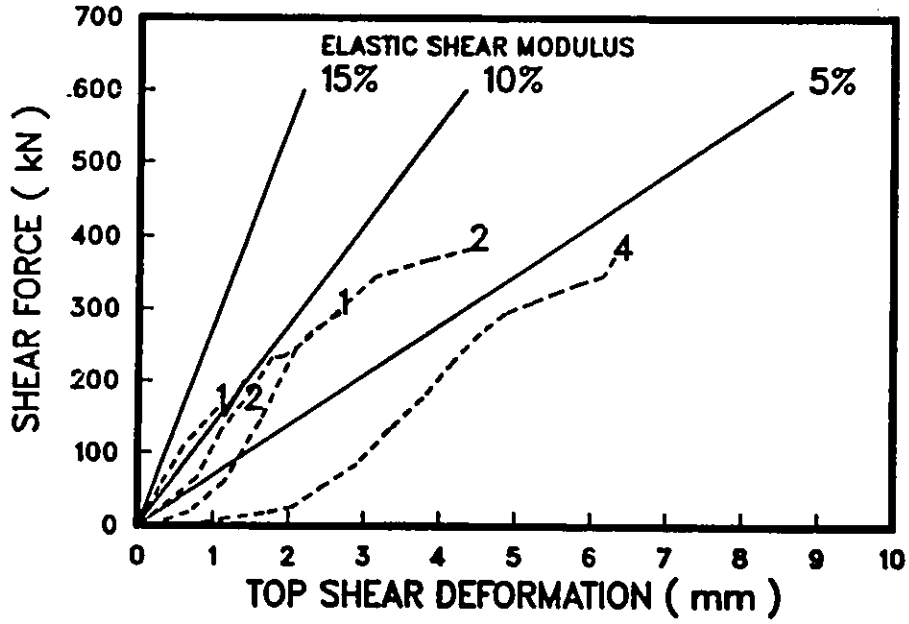

Figure 5.21: Wall 4 Analytical and experimental shear force-shear deformation relationships

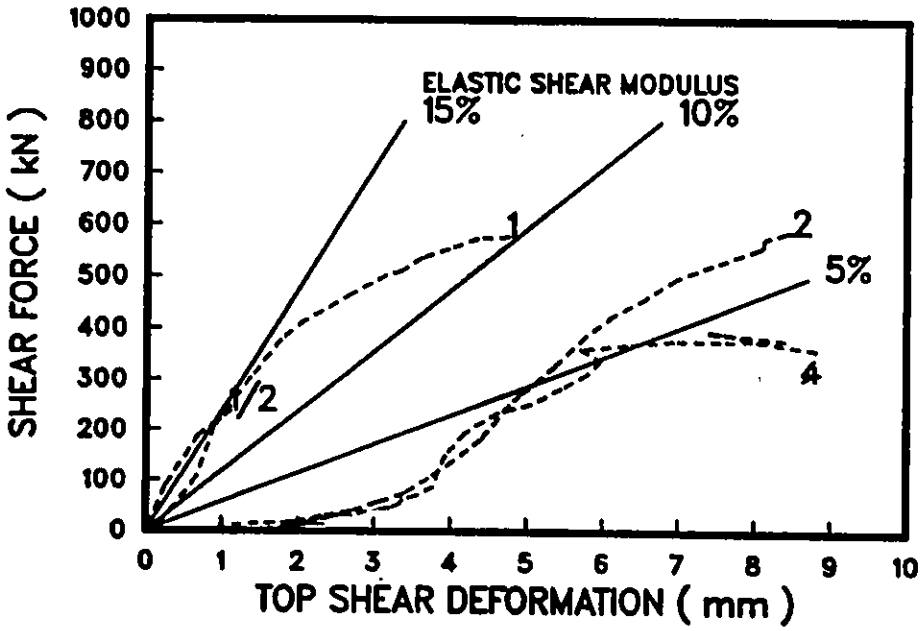

Figure 5.22: Wall 5 Analytical and experimental shear force-shear deformation relationships

of the first cycle at $+\frac{1}{2}\Delta_y, -\frac{1}{2}\Delta_y$ and $+1\Delta_y$ are presented. An average flexural strain was computed from the left and right bar at each row of bars and strain interpolation was made between rows when a defective strain gauge was encountered.

Figure 5.23 presents strain profiles at the base of Wall 4. As expected, at low load level the strain distribution is almost linear as depicted in Figure 5.23(a). The appearance of shear cracks and a flexural base crack at 161 kN can be seen on row No. 1 where the strain readings were slightly higher. The same phenomenon occurred at -120 kN as depicted in Figure 5.23(b) where shear and flexural cracks were formed. The appearance of shear cracks at 180 kN while loading towards $1\Delta_y$ highly stressed the first two rows of bars as shown in Figure 5.23(c). The flexural base crack was extending up to the third row of vertical bars. Strain readings in the compression zone were found to be low. However higher strain readings beyond the yield point of the reinforcing bar were noticed in Figure 5.23(c). This phenomenon is explained by a stress concentration at the gauge location due to a reduced diameter of the bar and the reliability of the gauges at high strain level. Also from the same figure it can be noticed that we did not reach the exact yield deflection since three rows of bars were required to yield as explained in Section 3.6. Yeilding of the first three rows occured at a top displacement of 5.0 mm, 295 kN, while loading towards load stage 13, at $2\Delta_y$.

Strain profiles at the base of Wall 5 are presented in Figure 5.24. The appearance of shear cracks at 155 kN did not appreciably affect the strain readings of Figure 5.24(a). The profiles remained essentially linear. However the profiles at $-\frac{1}{2}\Delta_y$, Figure 5.24(b), are not as linear as at $+\frac{1}{2}\Delta_y$. The formation of shear cracks at -145 kN affected the readings of row No. 12. No flexural base cracks were noticed at $\pm\frac{1}{2}\Delta_y$. Formation of shear cracks at 290 kN while loading towards load stage 13, at $1\Delta_y$, did not affect the strain profiles as shown in Figure 5.24(c). The appearance of a flexural base crack up to the sixth row at 415 kN yielded the first three rows of bars. Again higher strain readings were recorded beyond the yield strain of steel. Also from Figure 5.24(c) it can be noticed that we exceed the yeild deflection since only five bars were required to yeild. The yeild displacement should have been 5.7 mm at a load level of 433 kN.

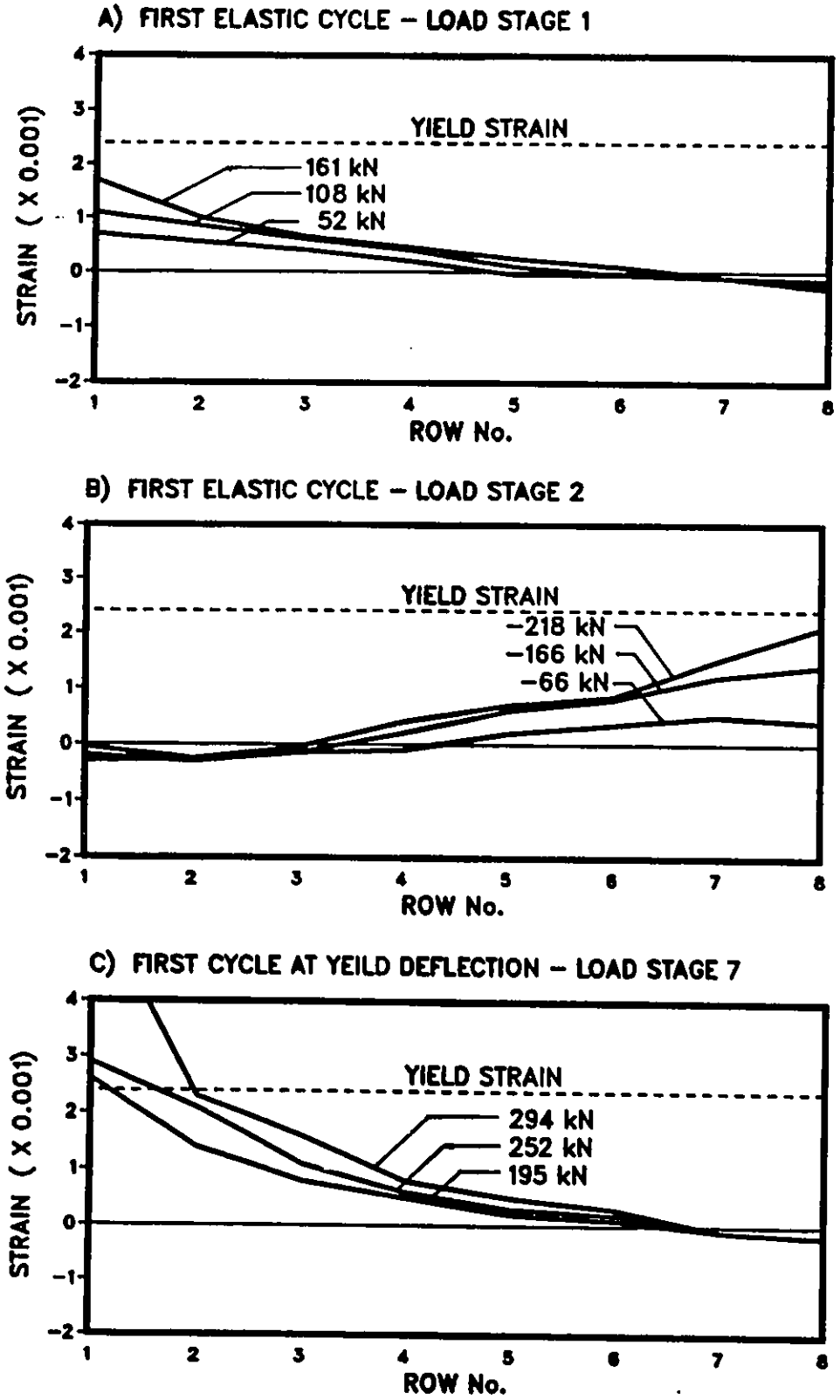

Figure 5.23: Wall 4 Base strain distributions in vertical reinforcement

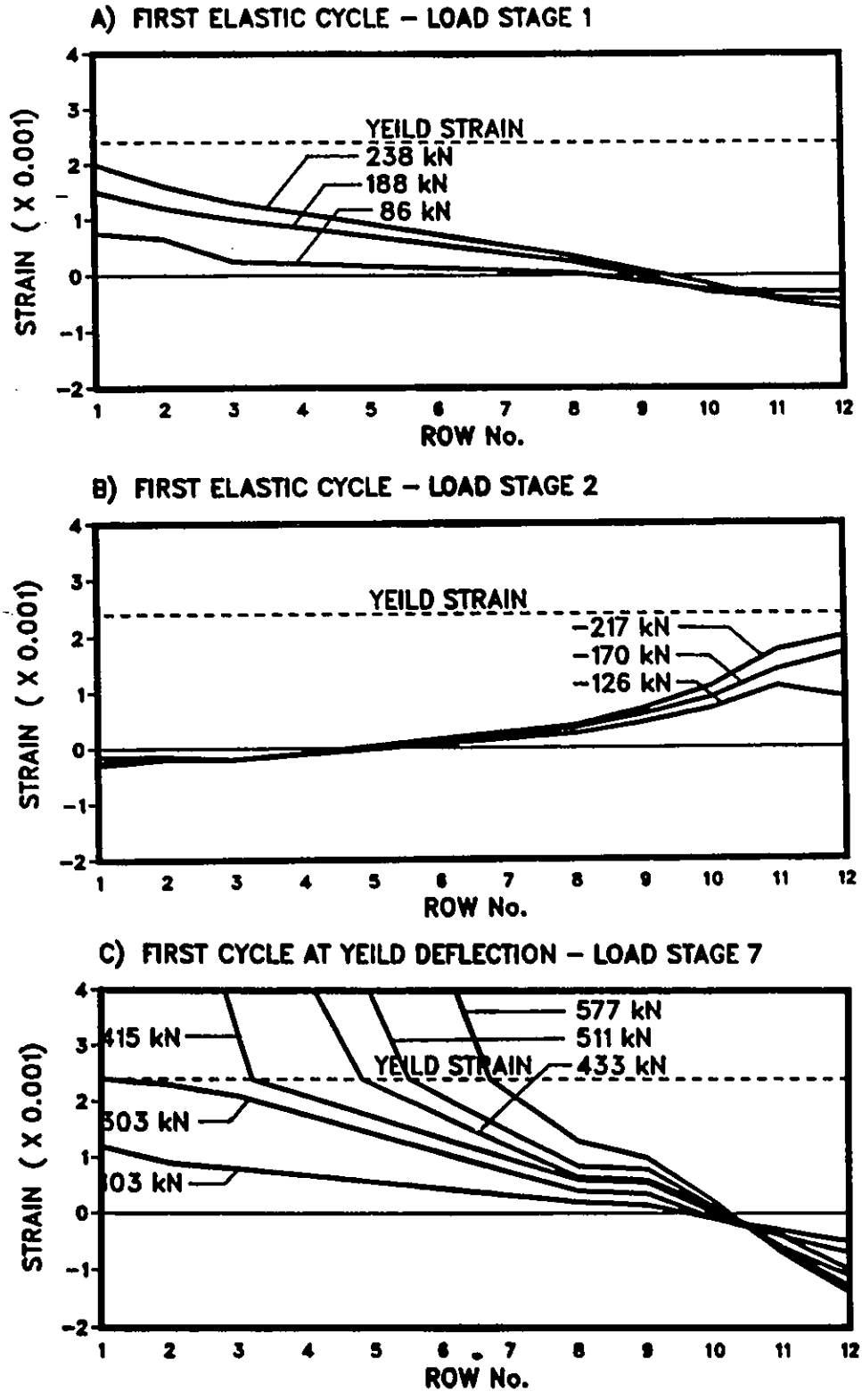

Figure 5.24: Wall 5 Base strain distributions in vertical reinforcement

An envelope of the observed moment-curvature relationship can be approximated using the load-strain profiles history at $+\frac{1}{2}\Delta_y$, $+1\Delta_y$ and $+2\Delta_y$. These approximate relationships are compared with the analytical moment-curvature relationships in Figures 5.25 and 5.26 for Walls 4 and 5 respectively.

The discrepancy between the analytical and the observed values is consistent with the previous comparison, done for flexural deformations. A possible explanation of this discrepancy, mostly related to the base fixity conditions of the test specimens, is provided in Section 5.4.

5.7 Energy dissipation

The energy dissipated by squat walls during displacement reversals is derived through inelastic deformations of the four wall displacement components. Inelastic flexural and bar slip deformations are usually preferred during strong ground motions since yeilding of the vertical reinforcement shows rounded hysteresis loops. Inelastic shear deformations however should be minimized since pinching of the hysteresis loops will follow after the first excursion into the inelastic range. This will usually reduced the energy dissipation capability of the wall. Base slip on the other hand should be avoided. The severe pinching of the hysteresis loops created by base slip offers a poor mean of energy dissipation mechanism especially at low load level.

The amount of energy dissipated by each wall displacement component can be calculated by integrating the area under the hysteresis loops. Figures 5.27 and 5.28 present the amount of energy dissipated by each wall as a function of the cumulative yeild displacement imposed on the wall. As depicted from these two figures, the base slip component dissipated approximately 65% and 50% of the total energy of Walls 4 and 5 respectively. The poor performances of the walls were due to the early onset of base slip during the loading program. The remaining energy was dissipated by the other displacement components, predominantly by inelastic shear deformations.

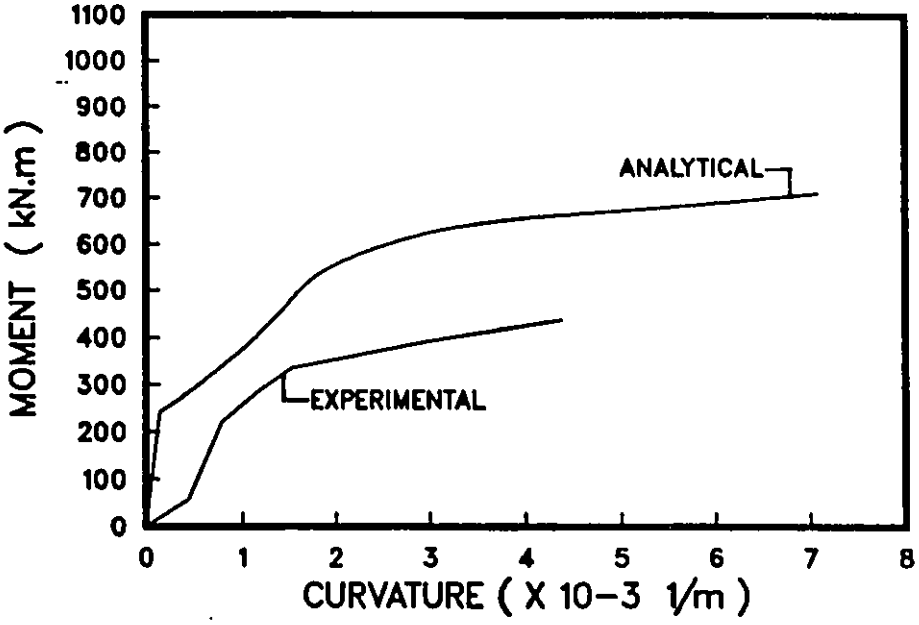

Figure 5.25: Wall 4 Analytical and experimental moment-curvature relationships

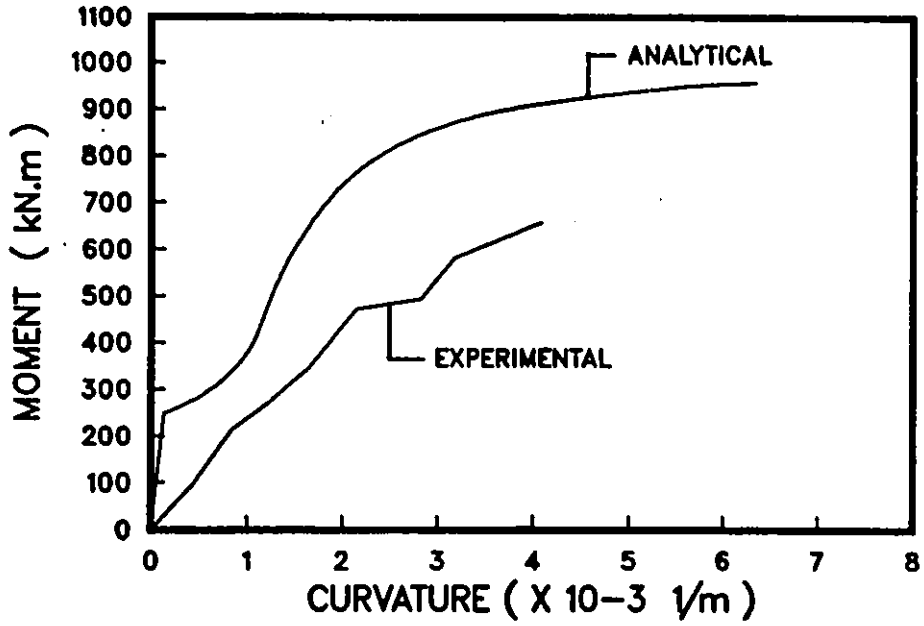

Figure 5.26: Wall 5 Analytical and experimental moment-curvature relationships

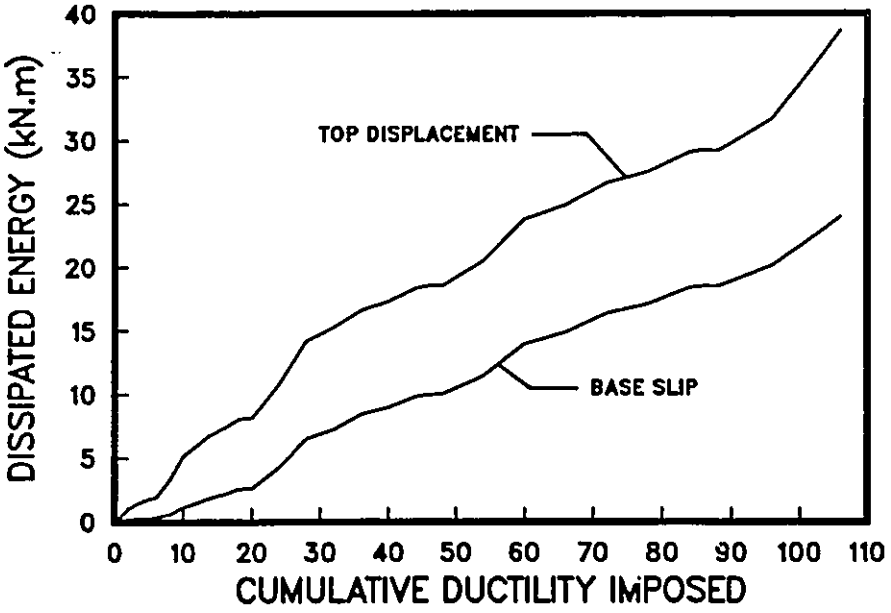

Figure 5.27: Wall 4 Energy dissipated-cumulative ductility imposed

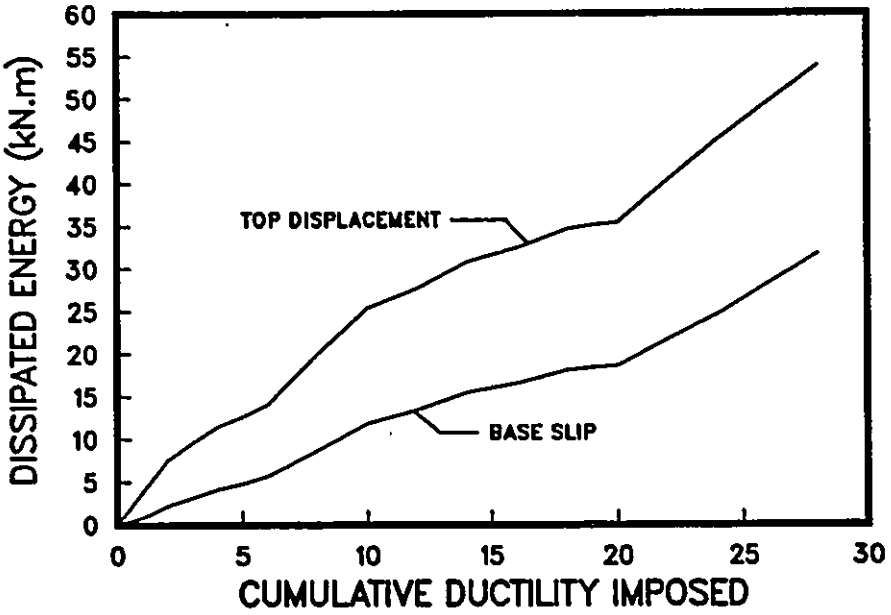

Figure 5.28: Wall 5 Energy dissipated-cumulative ductility imposed

Therefore both walls developed undesirable energy dissipation mechanisms which greatly affected their performances during testing.

Chapter 6

Finite element analysis

6.1 Introduction

The aim of this chapter is to discuss the development of a finite element computer program which could predict the structural behavior of squat shear walls under monotonic loading. The program should be able to predict the ultimate load carrying capacity of a wall and its behavior in the post-elastic range. Also the prediction of the crack patterns and the extent of steel yielding should be adequate.

A description of the constitutive models and the finite element formulation used in this study is made in the next two sections, followed by a description of the computer program develop by the author. Finally three case studies are examined to verify the adequacy of the program in predicting the behavior of squat shear walls.

The use of finite element techniques in modelling reinforced concrete shear walls has been employed by many researchers. However only a few investigations were focused on squat shear walls. Cervenka and Getstle [20] were among the first researchers to investigate the inelastic behavior of reinforced concrete panels subjected to in-plane forces. Using a rather simplified an-

alytical model, good correlations between the analytical and experimental load-displacement relationships and crack patterns were obtained. Since then many other researchers have duplicated their results using more sophisticated models and analyses. These new developments in finite element analysis has been summarized in a State-of-the-Art Report published by the American Society of Civil Engineers [5]. Also the recent Japanese work in the area of shear walls has been presented by Inoue et al. [26,27].

6.2 Constitutive model of reinforced concrete under monotonic loading

6.2.1 Compression field theory

The constitutive model used in the present study to represent the behavior of reinforced concrete under in-plane shear forces in a version of the Modified Compression Field theory presented by Vecchio and Collins [38]. This theory provides a simple tool for the analysis of reinforced concrete under general membrane loading. The theory is based on conditions of equilibrium and compatibility, and utilizes realistic stress-strain relationships for the reinforcement and for the concrete. It assumes that the concrete principal stress direction coincides with the principal strain direction. Stresses and strains are considered in terms of average values, smeared over an area of reinforced concrete which includes several cracks.

Figure 6.1 summarizes the main steps of the Modified Compression Field theory for reinforced concrete. For a given state of strain the average steel stresses f_{sx} and f_{sy} corresponding to the strains ϵ_x and ϵ_y are calculated from a bilinear steel model. These steel stresses do not include dowel action that may be present at the crack interface. The principal compressive stress, f_{c2}, in the cracked concrete is not only a function of the principal compressive strain, ϵ_2, but also depends on the principal tensile strain, ϵ_1, if cracks are present. An important series of tests performed by Vecchio and Collins [37] demonstrated that the concrete compressive strength is reduced

Given: $\epsilon_x, \epsilon_y, \gamma_{xy}$.
Require: f_x, f_y, v_{xy}.

- From ϵ_x, ϵ_y calculate the steel stresses f_{sx}, f_{sy}:

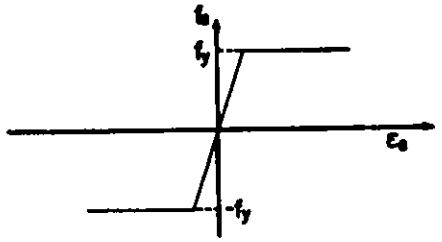

- Calculate the principal strains: $(\epsilon_x, \epsilon_y, \gamma_{xy}) \longrightarrow (\epsilon_1, \epsilon_2, \theta)$.
- Assume that the concrete principal stress direction coincides with the principal strain direction: $\theta_c = \theta$.
- Calculate the concrete principal stresses: $\epsilon_1 \rightarrow f_{c1}$, $\epsilon_2 \rightarrow f_{c2}$

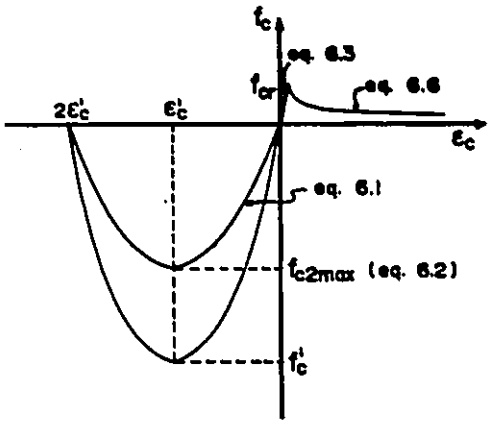

- Check that average concrete tensile stresses can be transmitted across the cracks and reduce them if necessary.
- Calculate the resultant stresses in X-Y coordinates:

$$(f_{c1}, f_{c2}, \theta_c, f_{sx}, f_{sy}) \longrightarrow (f_x, f_y, v_{xy})$$

Figure 6.1: Modified Compression Field theory for reinforced concrete

when coexisting principal tensile strains are high. The compressive stress-strain relationship for cracked concrete can be written as:

$$f_{c2} = f_{c2max}\left[2\left(\frac{\epsilon_2}{\epsilon'_c}\right) - \left(\frac{\epsilon_2}{\epsilon'_c}\right)^2\right] \tag{6.1}$$

where

$$f_{c2max} = \frac{f'_c}{0.8 - 0.34\frac{\epsilon_1}{\epsilon'_c}} \leq f'_c \tag{6.2}$$

Prior to cracking, $\epsilon_1 \leq \epsilon_{cr}$, the relationship between the average principal tensile stress in the concrete and the average principal tensile strain is nearly linear and is given by:

$$f_{c1} = E_c\epsilon_1 \tag{6.3}$$

where

$$E_c = 2\frac{f'_c}{\epsilon'_c} \tag{6.4}$$

$$\epsilon_{cr} = \frac{f_{cr}}{E_c} \tag{6.5}$$

However after cracking, $\epsilon_1 > \epsilon_{cr}$, the principal tensile stress in the concrete varies from zero at a crack location to a maximum value between the cracks and shows decreasing values of f_{c1} with increasing values of ϵ_1. The average principal tensile stress-strain relationship for concrete after cracking, as suggested by Vecchio and Collins [38], is given by:

$$f_{c1} = \frac{f_{cr}}{1 + \sqrt{200\epsilon_1}} \tag{6.6}$$

This average principal tensile stress, f_{c1}, may be limited by yielding of the steel reinforcement across the cracks where the tensile stress in the concrete is zero. This upper bound for tensile stresses as suggested by Vecchio and Collins [37] is given by:

$$f_{c1} \leq \rho_{sx}(f_{yx} - f_{sx})\cos^2\theta + \rho_{sy}(f_{yy} - f_{sy})\sin^2\theta \tag{6.7}$$

Also the principal tensile stress, f_{c1}, may be limited by sliding along the crack interface. This check involves a trial and error procedure which is presented in details elsewhere [38].

From the procedure presented in Figure 6.1, the Modified Compression Field theory is capable of predicting the response of reinforced concrete to membrane stresses by considering equilibrium conditions, compatibility requirements, and stress-strain relationships, all expressed in terms of average stresses and average strains. In the present study the original equation for the concrete principal compressive stress is modified to account for a better behavior at strains larger than ϵ'_c. Also strength hardening in the reinforcement is taken into account. These slight modifications were found to affect the response of squat shear walls in the plastic range.

6.2.2 Constitutive model for concrete

The concrete compressive response has been modified to include the actual stress-strain relationship of the concrete as presented in Figures 3.7 and 3.8. Vecchio and Collins used a simple parabola for the envelope curve as shown in Figure 6.1. It is proposed to replace this curve with the curves shown in Figure 6.2. The curve is the identical parabola on the rising portion which reaches a peak of f_{c2max} at ϵ'_c but on the falling portion is a straight line connecting the previous peak stress with a stress $f_{c2} = 0.3f_{c2max}$ at a strain $\epsilon_2 = -0.01$. Thereafter the stress f_{c2} levels off at $0.3f_{c2max}$. The stress-strain relationship of concrete for strains larger then ϵ'_c has been chosen arbitrary. Due to a lack of experimental evidence a simple bilinear model was retained. However similar models were used by other researchers [34,36].

The concrete tensile response given by equations 6.3 and 6.6 were retained in this study. However the determination of f_{cr} from split tests presented in Table 3.1 are usually too conservative. It was decided to follow Vecchio and Collins' recommendation to use the ACI equation [3] given as:

$$f_{cr} = 0.33\sqrt{f'_c}\, MPa \tag{6.8}$$

Equation 6.7 was also retained to limit the average principal tensile stress, f_{c1}, due to yielding of the reinforcement. However sliding along the crack interface was not considered in this study.

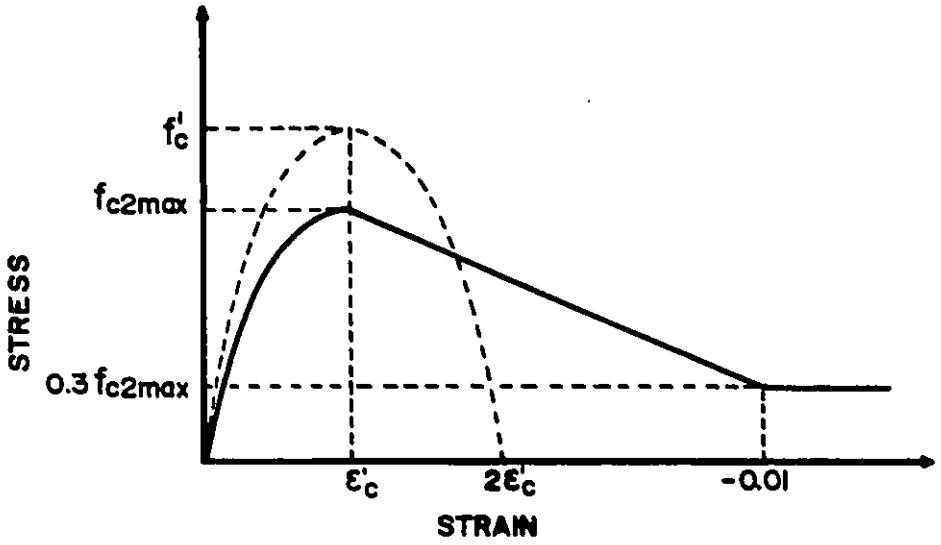

Figure 6.2: Constitutive model of compressive stress-strain relation of concrete

Upon cracking, an average crack width w over the cracked surface can be calculated as the product of the principal tensile strain and the crack spacing S_θ; that is

$$w = \epsilon_1 \cdot S_\theta \tag{6.9}$$

where

$$S_\theta = \frac{1}{\frac{\sin\theta}{S_{mx}} + \frac{\cos\theta}{S_{my}}} \tag{6.10}$$

$$S_{mx} = 1.5 \times x - bars\ spacing \tag{6.11}$$

$$S_{my} = 1.5 \times y - bars\ spacing \tag{6.12}$$

S_{mx} and S_{my} are the indicators of the crack control characteristics of the x-reinforcement and the y-reinforcement respectively. Equations 6.11 and 6.12 are empirical relations suggested by Vecchio and Collins [38].

6.2.3 Constitutive model for reinforcing steel

The bilinear model used in the compression field theory was modified to include the observed stress-strain relationship presented in Figure 3.9. Figure 6.3 presents a schematic of the steel model used in the present study. It includes the strain hardening region by fitting a parabola between the onset of strain hardening at ϵ_{sh} and the ultimate strain ϵ_u at f_u. This slight modification to the original model was done to investigate the effect of strain hardening on load-displacement relationship of squat shear walls.

6.3 Finite element formulation

6.3.1 Formulation selection

The choice of the finite element formulation to be used was based on the mode of application of the load on the wall. As previously described in Chapter 3, in-plane forces were generated in the wall which dictates the

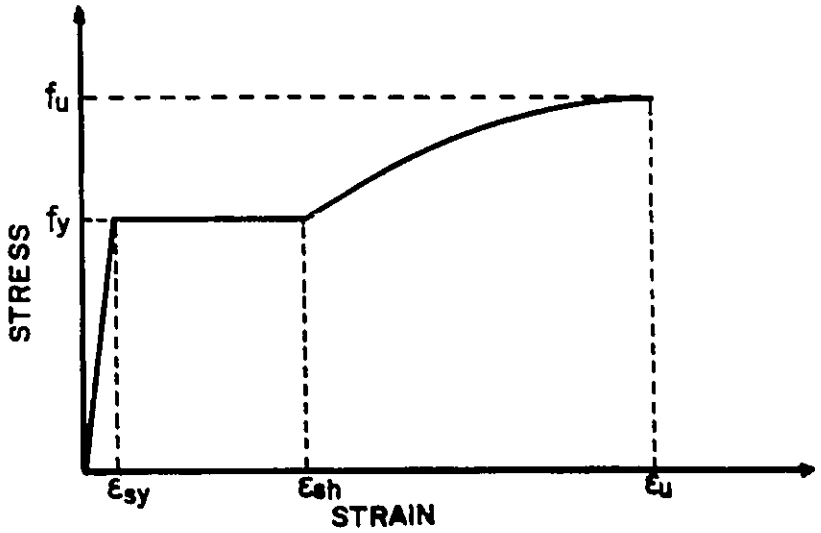

Figure 6.3: Constitutive model for stress-strain relationship of steel

use of two-dimensional plane stress elements. An eight node quadrilateral isoparametric element was selected. This type of element provides a parabolic distribution of displacement within the element and consequently a linear variation of strain. Elements with a quadratic displacement distribution model flexural behavior well and give acceptable results for shear behavior if sufficient elements are used throughout the depth of the member. The isoparametric formulation makes it possible to have nonrectangular elements with sides that may be curved. The exact order of quadrature used in the numerical integration of the stiffness matrix is a 2×2 point rule for elastic analyses, however higher order of quadrature may be needed for nonlinear analyses.

6.3.2 Evaluation of stresses for reinforced concrete

At each integration point within the element it is required to calculate the state of stress for a given state of strain ϵ_x, ϵ_y and γ_{xy}. The material

models described previously are then implemented to calculate the principal concrete stresses f_{c1} and f_{c2} acting at an angle $\theta_c = \theta$, where $-180° \leq \theta < 180°$. The concrete stresses are then rotated in the X-Y axes using the coordinate transformation as follows:

$$\begin{aligned} f_{cx} &= f_{c1}\cos^2\theta + f_{c2}\sin^2\theta \\ f_{cy} &= f_{c1}\sin^2\theta + f_{c2}\cos^2\theta \\ v_{cxy} &= (f_{c1} - f_{c2})\cos\theta\sin\theta \end{aligned} \tag{6.13}$$

The total stresses in the reinforced concrete at the integration point are found by adding the steel stresses to the concrete stresses.

$$\begin{aligned} f_x &= f_{cx} + \rho_{sx} f_{sx} \\ f_y &= f_{cy} + \rho_{sy} f_{sy} \\ v_{xy} &= v_{cxy} \end{aligned} \tag{6.14}$$

6.3.3 Solution of nonlinear equations

In analyzing a given structure with known geometry, material properties, boundary conditions and loading a linear set of equations can be established. By solving these equations, the displacements and reactions of the structure as a whole and the internal stresses in each element are found. However if the material properties show nonlinear stress-strain relations, the resulting equations are also nonlinear. These type of nonlinear problems are usually solved by taking a series of linear steps. A typical algorithm would increment the applied loading in steps and within each load step an iterative solution technique would be used until convergence requirements are met. The solution of nonlinear equations using an incremental load algorithm is well documented elsewhere [10].

In the incremental load algorithm previously described it often happens that the displacement solution does not converge, indicating no increase in load for a finite increase in displacement. This indicates that the structure reached its ultimate load and that the analysis must be stopped. However this study is concerned with the behavior of squat shear walls in the plastic

range which inevitably results in a plateau or even a decrease in the load carrying capacity of the structure especially at high displacement levels. To counteract this major drawback an incremental displacement algorithm is used. Instead of applying known nodal forces on the structure and solving the corresponding displacements, a given displacement is imposed at a node and the corresponding nodal force is solved. This technique has been successfully employed to trace the post-buckling configurations of curved beams including snap-through and multi-solution paths. A detailed outline of incremental displacement algorithms for nonlinear problems is presented by Batoz and Dhatt [11].

The solution of a set of nonlinear equations using an incremental displacement algorithm is obtained by linearizing the response of the finite element system about the conditions at a given displacement level. Three commonly used iterative solution techniques can be utilized and are designated as: (a) initial stiffness method; (b) secant stiffness method; and (c) tangent stiffness method. The initial stiffness method corresponds to a linearization of the response about the initial configuration of the finite element system. Consequently the construction and factorization of the global stiffness matrix is done once in the analysis. The secant and tangent stiffness methods, however, require the construction and factorization of the global stiffness matrix at each iteration within a given displacement increment based on the updated displacements. A modified iterative scheme can be used to update the stiffness matrix at the first iteration or at a prescribed number of iterations. The main advantage of these two iteration schemes over the initial stiffness method is that a faster convergence is achieved within the prescribed displacement increment. However this is usually counterbalanced by the major computational cost involved in constructing and factorizing the stiffness matrix. Also an ill-conditioned stiffness matrix can develop using the secant or tangent stiffness method as the structure approaches its ultimate load carrying capacity. To avoid this computational problem, the initial stiffness method was selected to be used with the incremental displacement algorithm as recommended by Zienkiewicz [42].

If an incremental displacement solution strategy based on iterative methods is to be effective, a realistic convergence criterion should be used for the termination of the iteration process. This convergence criterion is usually

based on the norms of out-of-balance nodal forces and/or incremental nodal displacements. The iteration process is stopped when the norms are within tolerance limits. These convergence criteria usually perform well before the attainment of the ultimate load. However severe inaccuracies were observed in the plastic range. Since the incremental displacement algorithm is solving for the externally applied force, it was decided to based the convergence criterion on the rate of change of this force. The iteration process is stopped when the ratio of the incremental externally applied force to the total force is within acceptable limits.

6.4 Finite element analysis program

Based on the constitutive models and finite element formulation presented in section 6.2 and 6.3, a computer program FEASSW, Finite Element Analysis of Squat Shear Walls, was written. Figure 6.4 presents a simplified flow chart of the program FEASSW. The listing of the computer program and a typical output is presented in Appendix C. A Gauss elimination equation solver for a symmetric and nonsingular stiffness matrix, stored in band form, is used. As depicted in Figure 6.4, the program can perform two types of analysis, a static linear analysis or a nonlinear incremental displacement analysis of a reinforced concrete structure subjected to monotonic loading history. For the latter analysis, the user specifies a control node on which the incremental displacements are imposed. Iteration is performed until the resulting force acting at the control node is within tolerable limits. Upon convergence, the program outputs the following results at each Gauss point of an element: average strains ($\epsilon_x, \epsilon_y, \gamma_{xy}$), steel stresses ($f_{sx}, f_{sy}$), concrete stresses ($f_{c1}, f_{c2}$), inclination of the principal strain direction (θ), cracking and crushing of concrete if present, and the average crack width (w).

The concrete constitutive model used in FEASSW is applicable to cracked concrete subjected to in-plane shear and normal stresses, that is, for values of ϵ_1 and ϵ_2 that are positive and negative respectively (tension-compression state of strain). Under biaxial compression, the effect of confinement which increases the strength of the concrete is not included in this study. The

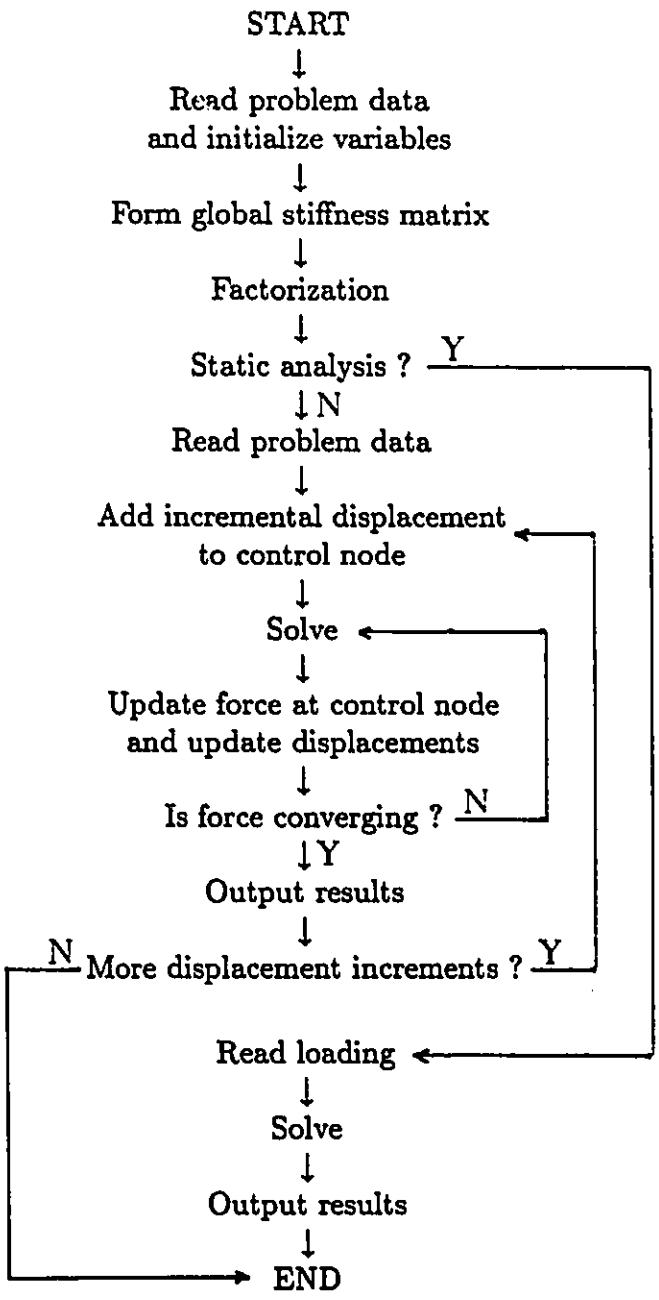

Figure 6.4: Simplified flow chart for FEASSW

compressive stresses acting on each of the principal direction are calculated from the stress-strain relations presented in Figure 6.2 using a value of $f_{c2max} = f'_c$. Under biaxial tension, the tensile stresses resulting on each of the principal direction are calculated independently using equation 6.3 or 6.6. These stress-strain relations for concrete under biaxial compression and tension are retained for simplicity. Consequently at low displacement levels where cracks are not present, the resulting externally applied force is usually overestimated. However squat shear walls are generally fully cracked beyond half of the ultimate load which indicates that the effect of biaxial compression or tension on the wall response is negligible.

Under extensive cracking of the concrete and yielding of the reinforcement, some portion of the structure may be subjected to unloading and reloading during the iteration process at a given imposed displacement due to stress redistribution. This unloading-reloading process should follow the observed behavior of steel and concrete under cyclic loading presented in Figures 3.7, 3.8 and 3.9. However no attempt was made to model this behavior. The stress-strain relationships under monotonic loading were used to model the unloading-reloading process.

6.5 Case studies

In this section three case studies are performed to evaluate the ability of FEASSW to reproduce the structural behavior of squat shear walls. First the effect of a flexible foundation beam, previously mentioned in section 4.4, on the wall response is presented for Walls 1 and 6. In the second case study, the prediction of the crack patterns for Wall 5 is made. Also a comparison of the crack widths and their orientation is made and yielding of the reinforcement is compared with the observed behavior. Finally the effect of the amount of horizontal reinforcement on the load carrying mechanism is investigated for Wall 1.

Wall No.	f'_c (MPa)	ϵ'_c (%)	f_{cr} (MPa)	ρ_{sx} (%)	ρ_{sy} (%)	f_y (MPa)	f_u (MPa)	ϵ_{sy} (%)	ϵ_{sh} (%)	ϵ_{su} (%)
1	-25	-0.20	1.65	0.25	0.80	430	650	0.215	1.6	11
5	-27	-0.18	1.71	1.20	1.20	480	770	0.240	1.0	10
6	-33	-0.17	1.90	0.80	0.80	480	770	0.240	1.0	10

Table 6.1: Material properties used in finite element analyses

6.5.1 Effect of foundation flexibility on wall response

The effect of a flexible foundation on the wall response is examined in this section. Base fixity in the prediction of shear and flexural deformations is generally granted. The purpose of this case study is to examine if the observed bending of the foundation significantly affects the load-top displacement relationship of squat shear walls.

Two wall specimens with an aspect ratio of one half were selected for this analysis, Walls 1 and 6. Wall 1 [40] was consider to have a fully fixed foundation beam whereas Wall 6 [39] was tested in the same manner as Walls 4 and 5. Wall 6 has an identical arrangement of steel reinforcement as Wall 4. However the sliding shear failure observed for Wall 4 was suppressed in Wall 6 by special detailing at the base of the wall. The resulting ductile behavior of Wall 6 was preferred over the sliding shear failure observed for Walls 4 and 5. The material properties of the walls use in the analyses are presented in Table 6.1.

The finite element meshes used in the analysis are presented in Figure 6.5. The shaded areas represent the top beam and foundation beam finite elements. The selection of the proper number of elements to be used was determined after a sensitivity analysis on different mesh sizes, that is, on the improvement of the solution by refining the finite element mesh.

The top beam was modeled with 14 plane stress elements having the appropriate thickness shown in Figure 3.1. Since cracking of the concrete in the top beam was not observed throughout the test, these elements were confined to remain elastic throughout the analysis. The control node and

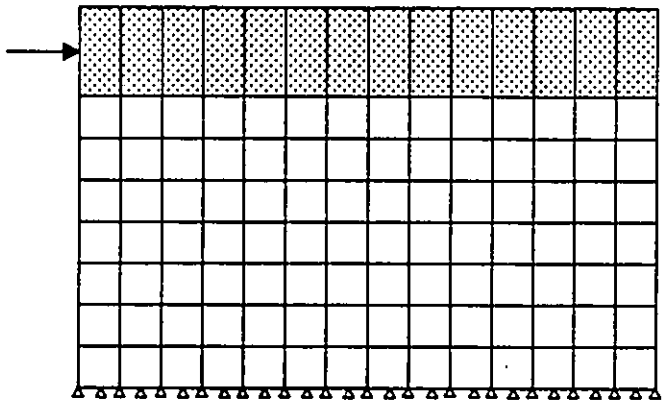

A) Rigid foundation

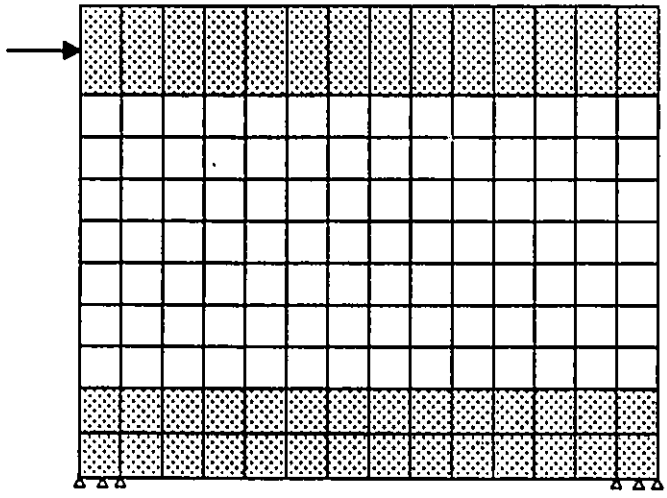

B) Flexible foundation

Figure 6.5: Finite element meshes

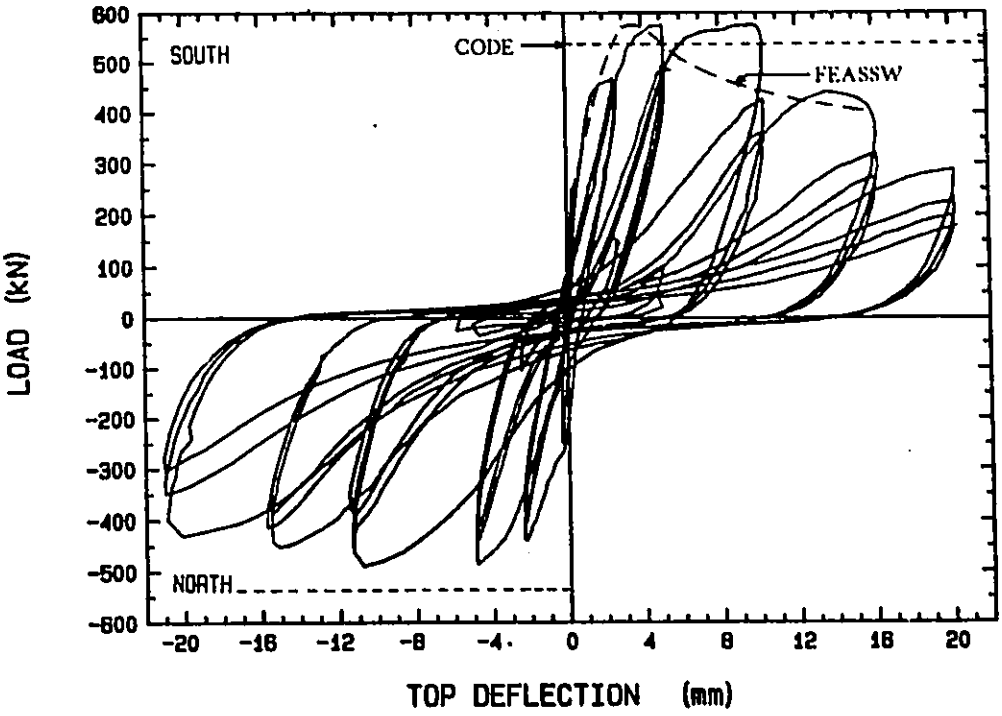

Figure 6.6: Wall 1 comparison between analytical and observed behavior

the resulting force are indicated on Figure 6.5 by an arrow.

The wall element was modeled with 98 plane stress elements using the constitutive relations presented in section 6.2. It was found that a 2×2 point rule used in the numerical integration gave the same results as a 4×4 point rule with only a slight increase in the number of iteration required to achieve the same accuracy. A convergence criterion of 0.5% was found to give a good trade off between the accuracy of the solution and the execution time.

The foundation beam of Figure 6.5(b) was modeled with 28 plane stress elements using the constitutive relations presented in section 6.2. The steel reinforcement shown in Figure 3.3 was assumed to be smeared throughout the height of the beam. Displacement constraints were applied only at the two extreme elements.

Figure 6.6 presents the load-top displacement hysteresis loops for Wall 1 along with the results of FEASSW and the code prediction based on the ultimate flexural capacity [17]. The FEASSW analysis was performed using the finite element mesh presented in Figure 6.5(a). The assumption that

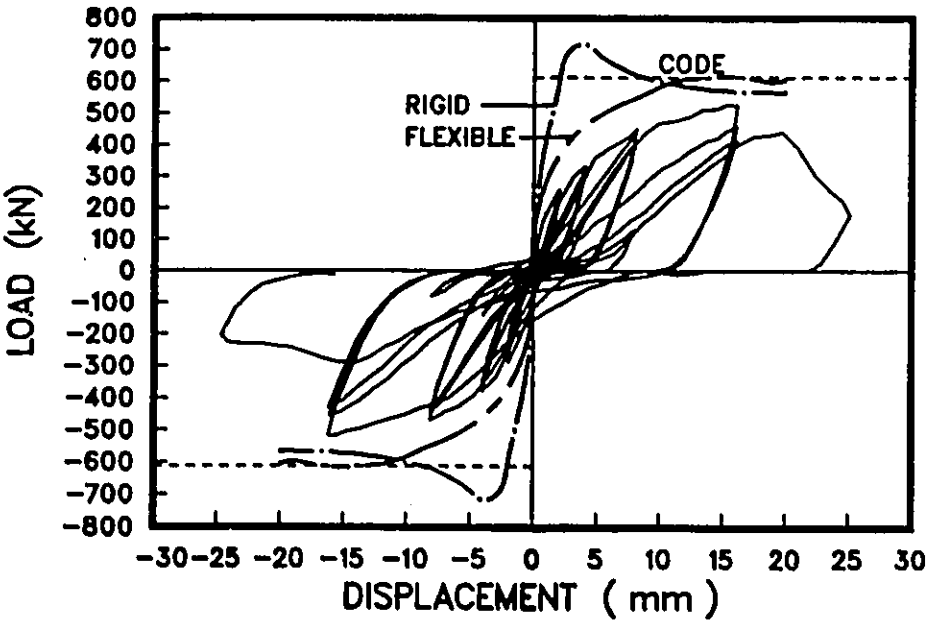

Figure 6.7: Wall 6 comparison between analytical and observed behavior

Wall 1 had a fully fixed foundation beam was adequate. The prediction of the load-top displacement relationship under monotonic loading is in good agreement with the observed behavior under cyclic loading if the stiffness degradation observed at $1\Delta_y$ and $2\Delta_y$, essentially caused by cyclic loading, is ignored. Also the relationship obtained from FEASSW shows a similar shape as that obtained from the walls tested by Barda [9] under monotonic loading. As expected, the ultimate load obtained from the code is slightly less than the observed and analytical ultimate loads in the south direction. However for an unknown reason Wall 1 showed to be weaker in the north direction.

Figure 6.7 presents the load-top displacement hysteresis loops for Wall 6 along with the results of FEASSW for a rigid and flexible foundations and the code prediction [17]. From this figure it can be seen that the foundation flexibility has a tremendous effect on the response of the wall under mono-

tonic loading. Although the load-top displacement curve obtained from the finite element mesh of Figure 6.5(b) does not agree well with the observed behavior, the shape of the analytical curve models adequately the envelop of the hysteresis loops. This disagreement was expected due to the complex behavior of the foundation beam reported in section 4.4 and the rather simplified model of the foundation beam used in the analysis. A vertical deflection of 9 mm was predicted by FEASSW in the middle region of the foundation beam with vertical crack widths less than 1 mm. This compare well with the observed behavior reported in section 4.4. In spite of the crude agreement obtained in Figure 6.7, the comparison clearly indicates that the wall response is affected by the foundation rigidity.

As depicted for Walls 1 and 6, the prediction of the ultimate load obtained for a fully fixed foundation is slightly overestimated by FEASSW when compared with the code. This overestimation is expected since the full stress-strain relation of the concrete is taken into account whereas the code limits the concrete strain at -0.003.

6.5.2 Comparison between observed and analytical behaviors of Wall 5

The behavior of Wall 5 reported in section 4.3 is compared with the analytical behavior obtained from FEASSW. Figure 6.8 presents the load-top displacement hysteresis loops of Wall 5 with the monotonic analytical prediction using the finite element mesh of Figure 6.5(b). As depicted in this figure, the simplified model of the foundation beam gave a better agreement for Wall 5 than for Wall 6. The material properties presented in Table 6.1 were used in the analysis.

The observed crack pattern obtained at load stage 1, $+\frac{1}{2}\Delta_y$, is compared with the analytical prediction in Figure 6.9. Both crack patterns are similar, showing an increase in the inclination of the cracks in the central region of the wall. A crack inclination of 38° in the central region of the wall was measured in both pictures of Figure 6.9 with crack widths less than 0.1 mm.

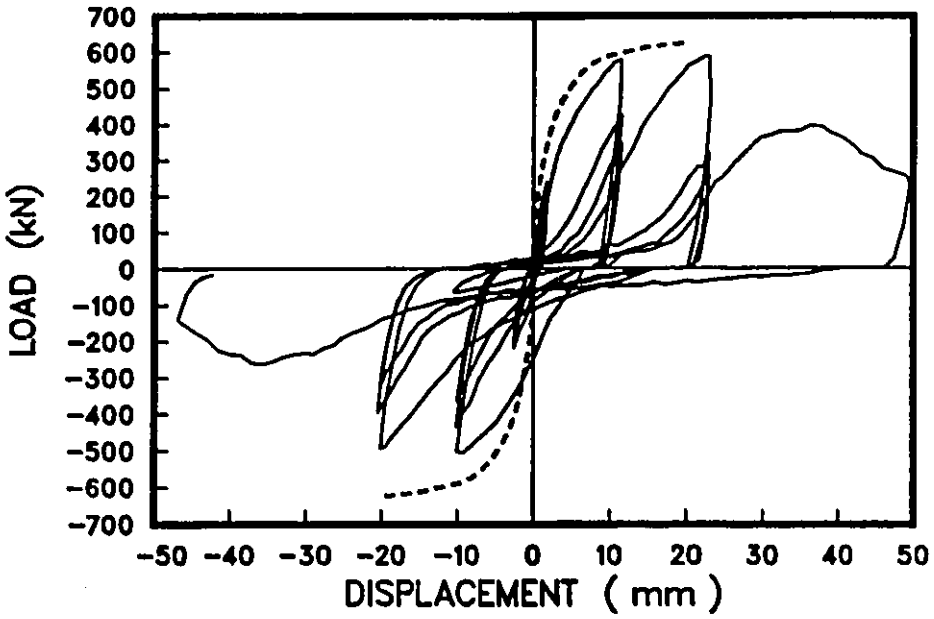

Figure 6.8: Wall 5 comparison between analytical and observed behavior

Figure 6.10 presents the observed crack pattern at the end of cycles at $\pm 1\Delta_y$ along with the predicted crack patterns at two different load levels. The vertical shading on Figure 6.10(b) and (c) indicates yielding of the vertical flexural bars. It was previously shown on Figure 5.24 that prior to the formation of the flexural base crack at approximately 415 kN, three vertical bars were yielding. Figure 6.10(b) shows the same hair line crack pattern and yielding of the reinforcement as observed during the test at approximately the same load level. Figure 6.10(c) shows the crack pattern and yielding of the reinforcement at $1\Delta_y$. As depicted in this figure, almost half of the vertical bar are yielding which is in good agreement with Figure 5.24. A base crack width of approximately 5 mm was obtained from FE-ASSW in the tension zone of the wall as depicted in Figure 6.10(c) which is comparable to a measured base crack width of 7 mm at 586 kN, $2\Delta_y$. The remaining cracks were essentially hair line cracks. Also a comparison of the crack pattern and their inclination between Figures 6.10(a)and (c) shows an excellent agreement. Diagonal 45° shear cracks were observed in the upper right section of the wall and reduced to 42° in the middle section. The tension zone of the wall was composed of flexural-shear cracks with in-

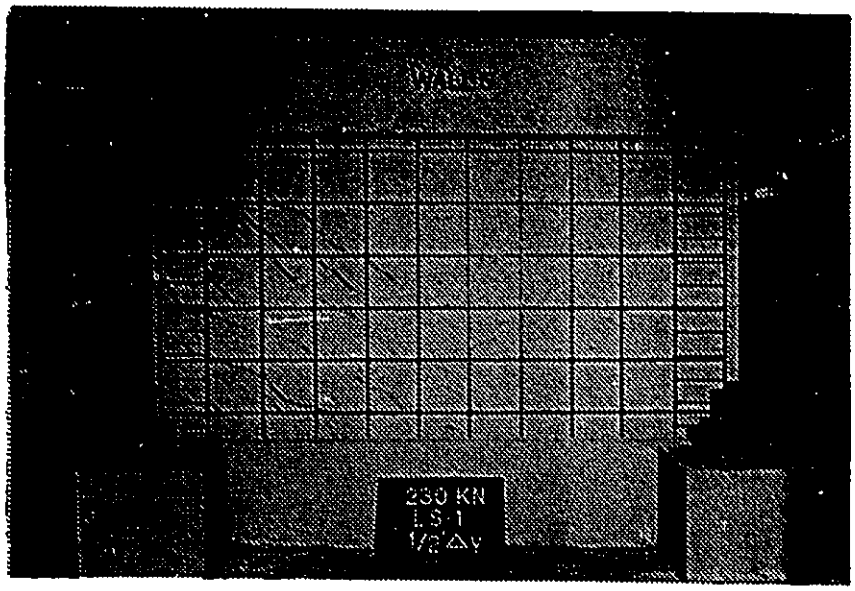

A) Observed crack pattern

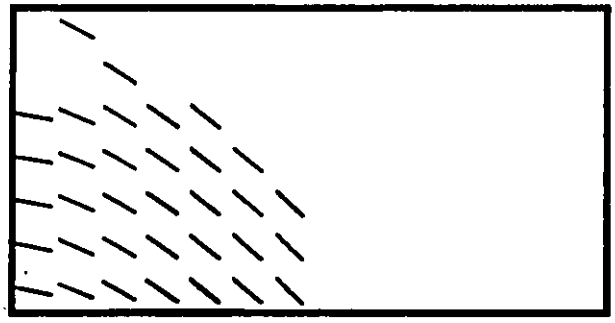

B) Analytical crack pattern

Figure 6.9: Wall 5 comparison of crack patterns at load stage 1, $+\frac{1}{2}\Delta_y$

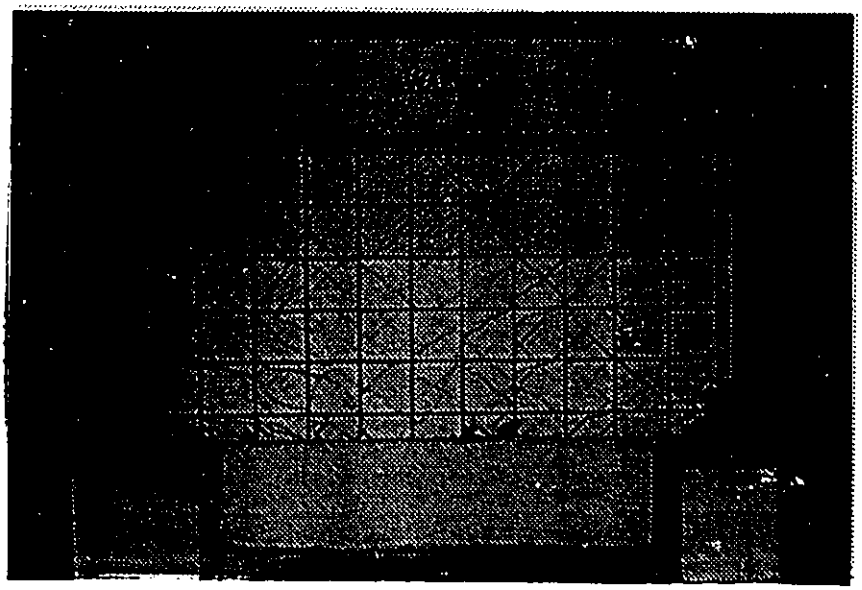

A) Observed crack pattern at 577 kN

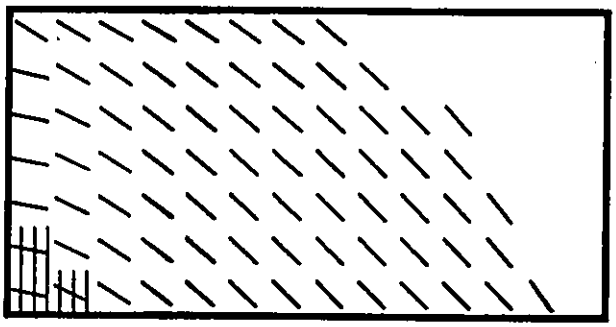

B) Analytical crack pattern at 432 kN

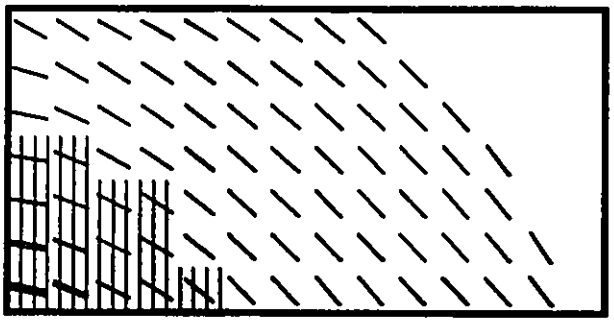

C) Analytical crack pattern at 593 kN

Figure 6.10: Wall 5 comparison of crack patterns at load stage 12, $1\Delta_y$

clination varying from almost 0° at the base to 38° in the upper left section of the wall. Yielding of the horizontal reinforcement was not observed in Figure 6.10.

In analyzing Figures 6.9 and 6.10, it becomes clear that crack patterns and the extent of steel yielding can be approximated in squat shear walls. A better modeling of the foundation beam would probably result in an even a better prediction of the wall behavior.

6.5.3 Effect of horizontal reinforcement on the behavior of Wall 1

The effect of the amount of horizontal reinforcement on the response of Wall 1 is analyzed in this section. The good agreement obtained in Figure 6.6 dictated the choice of Wall 1 over the other walls. Three different horizontal reinforcement ratios were analyzed while keeping the vertical reinforcement ratio constant. The finite element mesh presented in Figure 6.5(a) and the material properties shown in Table 6.1 were used.

Figure 6.11 presents the response of Wall 1 under monotonic loading for three different amount of horizontal reinforcement, that is, 0%, 0.25% and 0.8% along with the code prediction based on flexural capacity [17]. Wall 1 was designed with the minimum amount of horizontal reinforcement required by the Canadian code, that is, 0.25% while 0.8% corresponds to the required shear reinforcement based on the maximum load obtained at the development of the full flexural capacity. It is worth noting that Wall 1 with 0.8% horizontal steel ratio should behaved in a similar fashion as Walls 4 and 6. As depicted, in Figure 6.11, walls with steel ratios of 0.25% and 0.8% reached the ultimate load required by the code. As expected the absence of horizontal reinforcement drastically reduced the load carrying capacity of Wall 1 by approximately 20%.

To investigate the effect of the horizontal steel ratio on the load carrying mechanism, the crack patterns and the extent of steel yielding of all three walls are compared at different displacement levels. Figure 6.12 presents the

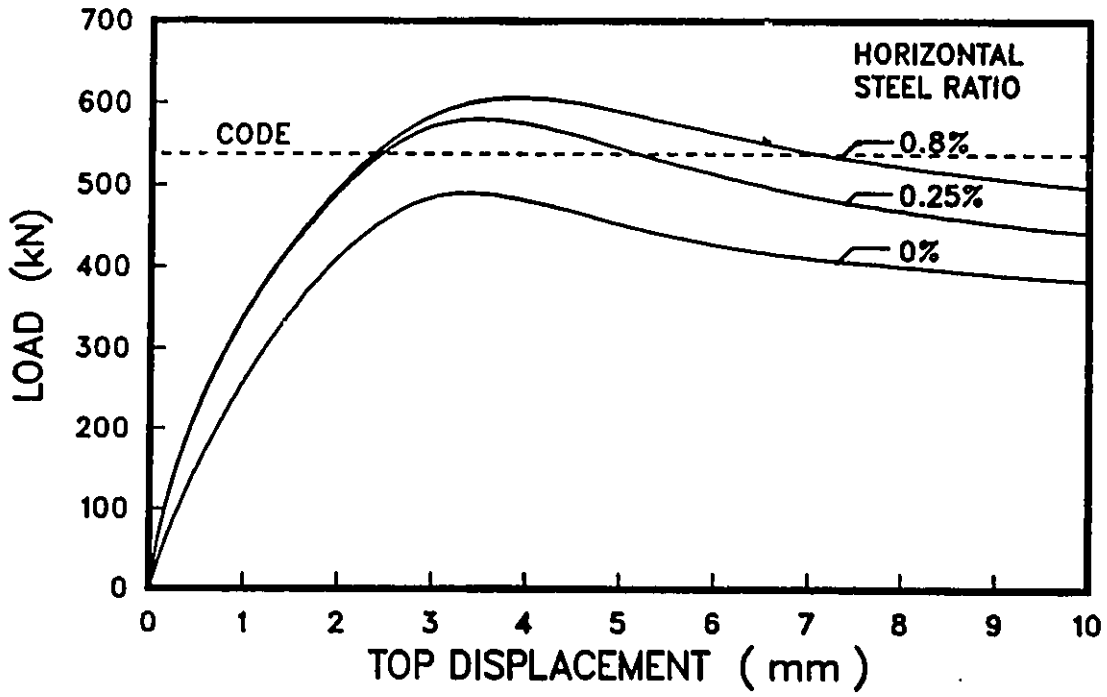

Figure 6.11: Wall 1 effect of horizontal reinforcement of wall behavior

analytical behavior of all walls at a top displacement of 4 mm which corresponds to the attainment of the ultimate load. Yielding of the vertical and horizontal reinforcement is represented by vertical and horizontal shadings respectively while crushing of the concrete (for $\epsilon_2 \leq -0.01$) is represented by triangles. In comparing Figures 6.12(b) and (c) it can be depicted that the amount of horizontal reinforcement do not significantly affect the crack patterns nor the extent of flexural yielding in the wall at 4 mm. The flexural base crack was estimated to be 2 mm in both analyses whereas the remaining cracks were essentially hair line cracks. However the absence of horizontal reinforcement in Figure 6.12(a) showed a pronounced effect on the crack pattern. Crack widths were estimated at 6 mm on the tension side of the wall whereas the remaining cracks were measured between 1 mm and 3 mm. The extensive cracking of the concrete had the effect of increasing the extent of flexural yielding which explains the reduction of the maximum load carried by this wall.

Figure 6.13 presents the behavior of the three walls at a top displacement of 10 mm. It can be depicted from Figure 6.13(a) that in the absence

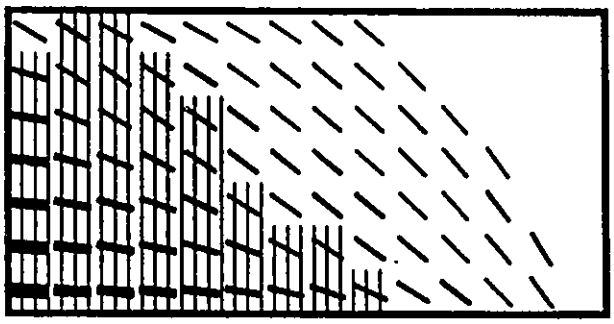

A) Horizontal steel ratio $\rho_{sx} = 0\%$

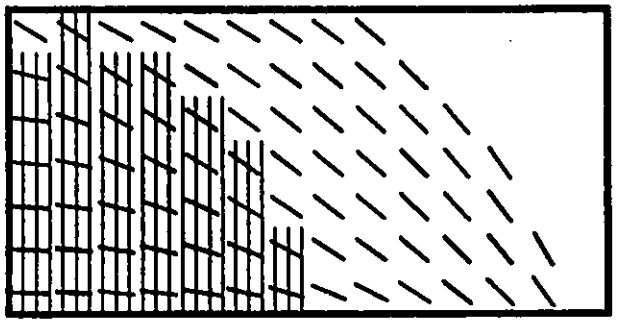

B) Horizontal steel ratio $\rho_{sx} = 0.25\%$

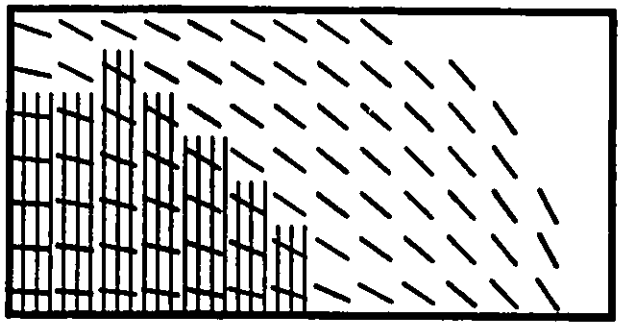

C) Horizontal steel ratio $\rho_{sx} = 0.8\%$

Figure 6.12: Wall 1 analytical crack patterns at 4 mm

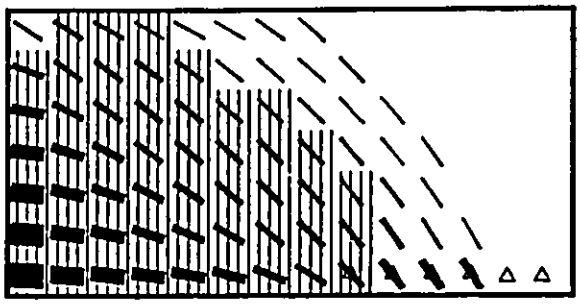

A) Horizontal steel ratio $\rho_{sx} = 0\%$

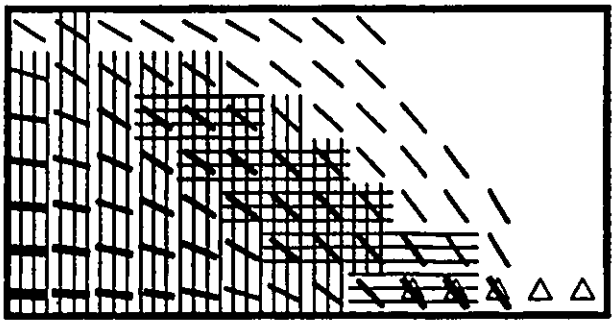

B) Horizontal steel ratio $\rho_{sx} = 0.25\%$

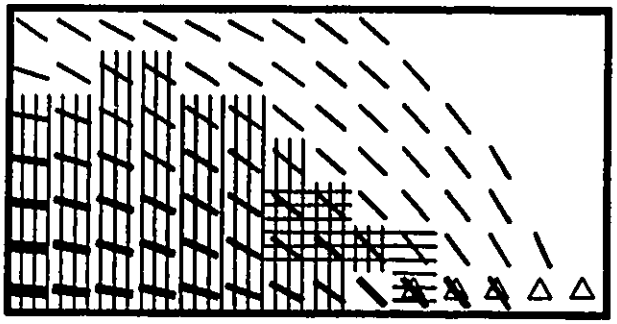

C) Horizontal steel ratio $\rho_{sx} = 0.8\%$

Figure 6.13: Wall 1 analytical crack patterns at 10 mm

of horizontal reinforcement the wall has a tendency to fail along a 45° diagonal crack. Also extensive cracking and crushing of the concrete is observed along the base of the wall. The effect of horizontal reinforcement on the crack pattern is clearly seen by comparing Figures 6.13(b) and (c). A diagonal tension mode of failure has a tendency to form in Figure 6.13(b) where the horizontal steel yielding and crack widths are more pronounced than in Figure 6.13(c). However it can be depicted from the latter figure that an increase in the amount of horizontal reinforcement has a tendency to reduce the extent of flexural yielding and to increase the crack width throughout the base of the wall which could lead to a sliding shear mode of failure. It should be noted that a ductile behavior was more pronounced in Figure 6.13(c) than (b). Crushing of concrete was not affected by the amount of horizontal reinforcement and no strength hardening was observed in all three analyses at a top displacement of 10 mm.

To emphasize the diagonal tension failure observed during the testing of Wall 1 (0.25% horizontal steel ratio), a comparison between the observed and analytical crack patterns is made in Figure 6.14. At a top displacement of 20 mm FEASSW adequately predicts the diagonal tension failure, showing extensive yielding of vertical and horizontal reinforcements in the central portion of the wall along with wide cracks as depicted in Figure 6.14(a). Figure 6.14(b) shows the observed crack pattern at 20 mm. The extent and orientation of the cracks show good agreement. Extensive strength hardening in the vertical bars was calculated by FEASSW whereas the horizontal bars remained essantially within the plateau range. This excessive yielding of the vertical bars can be seen in Figure 6.14(b) where the vertical bars show some sign of staggering across the wide diagonal crack.

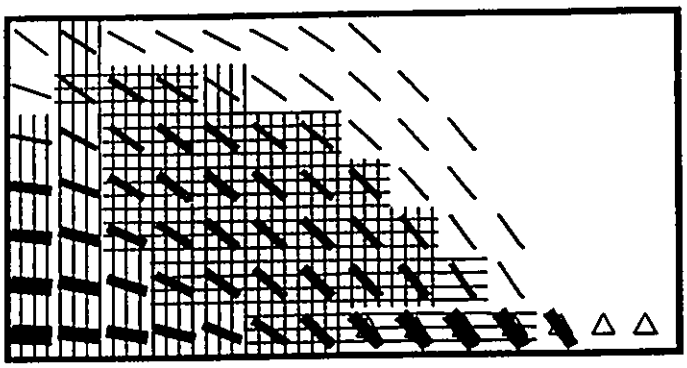

A) Analytical crack pattern ($\rho_{sx} = 0.25\%$)

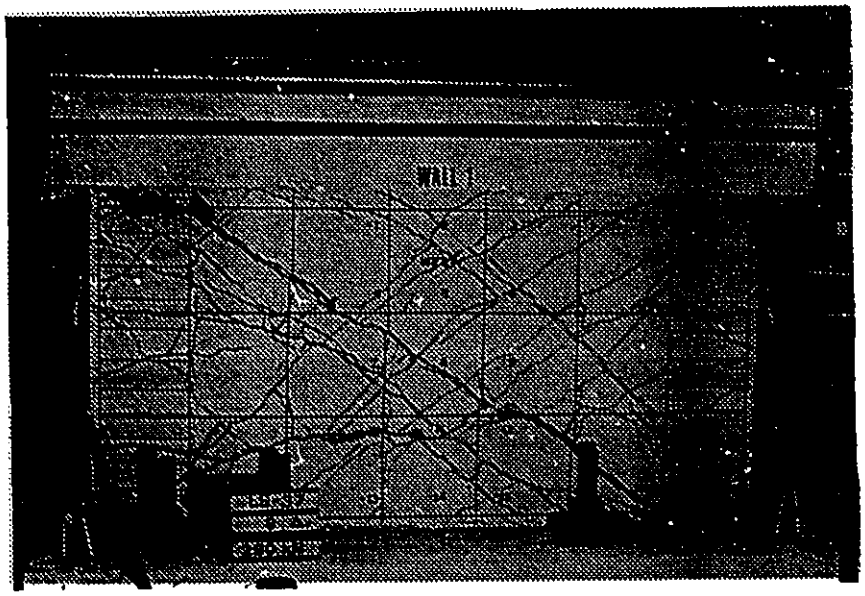

B) Observed crack pattern

Figure 6.14: Wall 1 comparison of crack patterns at 20 mm

Chapter 7

Conclusions

Based on the results of the experimental and analytical investigations carried out in this research program, the following conclusions can be made.

1. Squat shear walls designed in accordance with the current North American Building Codes [3,17] may fail due to sliding shear prior to the attainment of their ultimate design shear strengths.

2. The sliding shear in squat shear walls may take place prior to ultimate flexural capacity. The wall specimens tested in this investigation showed sliding shear failures at 68% and 70% of shear forces associated with their flexural capacities. These shear forces translate into $0.45\sqrt{f'_c}$MPa and $0.69\sqrt{f'_c}$MPa of nominal shear stress respectively.

3. The sliding shear failure mechanism is triggered by the formation of a continuous flexural crack at the base of the wall.

4. Ductility in squat shear walls with an aspect ratio of one-half can be attained if the diagonal tension capacity is limited to shear force producing sliding shear. Experimental and analytical results indicate that a squat wall with a minimum horizontal reinforcement ratio of 0.25% perform with a limited but acceptable ductility.

5. Cyclic loading produces approximately 35% to 50% reduction in the flexural rigidity of squat walls in the effective elastic range. The corresponding reduction in the shear rigidity can be as high as 85% to 90% of the uncracked stiffness.

6. Squat walls develop significant inelastic deformations. Walls that are critical in sliding shear also develop very high sliding shear deformations. The wall specimens tested in this investigation showed that approximately 35% of total inelastic displacement was due to shear. Displacements due to sliding shear and local slippage of vertical reinforcement in the foundation beam accounted for 50% and 15% of the total horizontal displacements. The flexural response of walls that failed by sliding shear was limited to the effective elastic range.

7. The degree of base fixity produces a significant effect on the wall response. This effect should be included in conducting dynamic analyses on squat shear walls.

8. The floor slabs, and/or top beams, when monolithically cast with shear walls are capable of preventing the 45° failure plane, enabling squat walls with an aspect ratio of less than one to resist higher shear stresses prior to the formation of the corner-to-corner failure plane.

Bibliography

[1] Aktan A. E. and Bertero V. V. , *RC Structural Walls: Seismic Design For Shear*, Journal of Structural Engineering, ASCE, Vol. 111, No. 8, August 1985, pp. 1775-1791.

[2] Aktan A. E. and Nelson G. E. , *Inelastic Analysis Of RC Sections*, Proceedings of the Third U. S. National Conference on Earthquake Engineering, August 24-28, 1986, Charleston, South Carolina, pp. 1015-1026.

[3] American Concrete Institute, *Building Code Requirements For Reinforced Concrete ACI 318-83*, Detroit, 1983, 111 p.

[4] American Concrete Institute, *Commentary on Building Code Requirements For Reinforced Concrete ACI 318-83*, Detroit, 1983, pp 151.

[5] American Society of Civil Engineers, *Finite Element Analysis of Reinforced Concrete*, New York, 1982, 545 p.

[6] Arnold C. , *Configuration And Seismic Design: A General Review*, Proceedings of the 2nd U. S. National Conference on Earthquake Engineering, August 22-24, 1979, Stanford, California, pp. 22-36.

[7] Associate Committe on the National Building Code, *National Building Code of Canada 1985*, National research Council of Canada, 1985, Part 4, pp. 151-180.

[8] Associate Committe on the National Building Code, *Supplement to the National Building Code of Canada 1985*, National Research Council of Canada, 1985, Chapter 4, Commentary J, pp. 221-241.

[9] Barda Felix, Hanson John M. and Corley W. Gene. , *Shear Strength Of Low-Rise Walls With Boundary Elements*, Reinforced Concrete Structures In Seismic Zones, Publication SP-53, American Concrete Institute, Detroit, 1977, pp.149-202.

[10] Bathe K. J., *Finite Element Procedures in Engineering Analysis*, Prentice-Hall, New Jersey, 1982, 735 p.

[11] Batoz J. L. and Dhatt G., *Incremental Displacement Algorithms for Nonlinear Problems*, International Journal for Numerical Methods in Engineering, Vol. 14, No. 8, 1979, pp. 1262-1267.

[12] Beekhuis W. J. , *An Experimental Study Of Squat Shear Walls*, Master of Engineering Report, Department of Civil Engineering, University of Canterbury, New Zealand, 1971, 132 pp.

[13] Benjamin J. R. and Williams H. A. , *The Behavior Of One-Storey Reinforced Concrete Shear Walls*, Journal of the Structural Division, Proceedings of ASCE, Vol. 83, May 1957, pp. 1-49.

[14] Bertero V. V. , *An Overwiew Of The State-Of-The-Art In Earthquake-Resistant Reinforced Concrete Building Construction*, Proceedings of the 2nd U. S. National Conference on Earthquake Engineering, August 22-24, 1979, Stanford, California, pp. 838-852.

[15] Bertero V. V. , *Seismic Behavior Of R/C Wall Structural Systems*, Proceedings of the 7th World Conference on Earthquake Engineering, September 8-13, 1980, Istanbul, Turkey, Part III, pp. 323-330.

[16] Bertero V. V. , *State Of The Art In The Seismic Resistant Construction Of Structures*, Third International Earthquake Microzonation Conference, Proceedings, Vol. 2, June 28-July 1, 1982, Seattle, U. S. A. ,pp.767-799.

[17] Canadian Standard Association, *Design Of Concrete Structures For Buildings CAN3-A23.3-M84*, Rexdale, 1984, 281 pp.

[18] Cardenas A. E. , Hanson J. M. , Corley W. G. and Hognestead E. , *Design Provisions For Shear Walls*, ACI Journal, Proceedings, Vol. 70, March 1973, pp. 221-230.

[19] Cardenas A. E. , Russell H. G. and Corley W. G. , *Strength Of Low-Rise Structural Walls*, Reinforced Concrete Structures Subjected To Wind And Earthquake Forces, Publication SP-63, American Concrete Institute, Detroit, 1980, pp. 221-241.

[20] Cervenka V. and Gerstle K. H., *Inelastic Analysis of Reinforced Concrete Panels Under In-Plane Loads*, Symposium: Inelasticity and Non-Linearity in Structural Concrete, Study No. 8, 1972, pp. 333-344.

[21] Collins M. P. , Mitchell D. and MacGregor J. G. , *Explanatory Notes On CSA Standard CAN3-A23.3-M84 Design Of Concrete Structures For Buildings*, Canadian Portland Cement Association, 1985, 140 pp.

[22] Derecho A. T., Iqbal M., Fintel M. and Corley W. G., *Loading History for Use in Quasi-Static Simulated Earthquake Loading Test*, Reinforced Concrete Structures Subjected to Wind and Eartquake Forces, Publication SP-63, American Concrete Institute, Detroit, 1980, pp. 329-356.

[23] Fiorato A. E. , Oesterle R. G. and Carpenter J. E. , *Reversing Load Tests Of Five Isolated Structural Walls*, Proceedings of the International Symposium on Earthquake Structural Engineering,St-Louis, Missouri, U. S. A. ,Vol. 1, August 1976, pp. 437-453.

[24] Oesterle R. G. , Fiorato A. E. , Aristizabal-Ochoa J. D. and Corley W. G. , *Hysteretic Response Of Reinforced Concrete Structural Walls*, Reinforced Concrete Structures Subjected To Wind And Earthquake Forces, Publication SP-63, American Concrete Institute, Detroit, 1980, pp. 243-273.

[25] Hernandez O. B. and Zermeno de L. M. E. , *Strength And Behavior of Structural Walls With Shear Failure*, Proceedings of the Seventh World Conference on Earthquake Engineering, Vol. 4, Istanbul, Turkey 1980, pp 121-124.

[26] Inoue N. and Noguchi H., *Finite Element Analysis of Reinforced Concrete in Japan*, Finite Element Analysis of RC Structure, American Society of Civil Engineers, New York, 1986, pp. 25-47.

[27] Inoue N., Koshika N. and Suzuki N., *Analysis of Shear Wall Based on Collins Panel Test*, Finite Element Analysis of RC Structure, American Society of Civil Engineers, New York, 1986, pp. 288-299.

[28] Park R. and Paulay T. , *Reinforced Concrete Structures*, John Wily and Sons Inc. , New York, 1975,769 p.

[29] Pauley T. , *The Design Of Reinforced Concrete Ductile Shear Walls For Earthquate Resistance*, Research Report 81-1, Department of Civil Engineering, University of Canterbury, New Zealand, February 1981, 72 p.

[30] Paulay T. , *Earthquake-Resisting Shearwalls — New Zealand Design Trends*, ACI Journal, Proceedings, Vol. 77, No. 3, May-June 1980, pp. 144-152.

[31] Paulay T. , *Design Aspects Of Shear Walls For Seismic Areas*, Canadian Journal of Civil Engineering, Vol. 2, No. 3, September 1975, pp. 321-344.

[32] Paulay T. and Uzumeri S. M. , *A Critical Review Of The Seismic Design Provisions For Ductile Shear Walls*, John Wily and Sons Inc. , New York, 1975, 769 p. Canadian Journal of Civil Engineering, Vol. 2, 1975, pp. 592-601.

[33] Saatcioglu M., Derecho A.T. and Corley W.G.,*Modelling Hysteretic Behavior of Coupled Walls For Dynamic Analysis*, Earthquake Engineering and Structural Dynamic Journal, Vol. 11, pp. 711-726, 1983.

[34] Stevens N. J., Uzumeri S. M. and Collins M. P., *Analytical Modelling of Reinforced Concrete Subjected to Monotonic and Reversed Loading*, University of Toronto, Department of Civil Engineering, Publication No. 87-1, January 1987, 201 p.

[35] Synge A. J. , *Ductility Of Squat Shear Walls*, Research report 80-8, Department of Civil Engineering, University of Canterbury, New Zealand, February 1980, 141 p.

[36] Vallnenas J. M., Bertero V. V. and Popov E. P., *Hysteresis Behavior of Reinforced Concrete Structural Walls*, Earthquake Engineering Research Center, Report No. UCB/EERC-79/20, August 1979, 234 p.

[37] Vecchio F. J. and Collins M. P., *The Response of Reinforced Concrete to In-Plane Shear and Normal Stresses*, University of Toronto, Department of Civil Engineering, Publication No. 82-03, March 1982, 332 p.

[38] Vecchio F. J. and Collins M. P., *The Modified Compression-Field Theory for Reinforced Concrete Elements Subjected to Shear*, Journal of the American Concrete Institute, Proceedings, Vol. 83, No. 2, March-April 1986, pp. 219-231.

[39] Wasiewicz Z. , *Sliding Shear In Squat Shear Walls*, M. A. Sc. Thesis, Department of Civil Engineering, University of Ottawa, 1987.

[40] Wiradinata S. , *Behavior Of Squat Walls Subjected To Load Reversals*, M. A. Sc. Thesis, Department of Civil Engineering, University of Toronto, January 1985, 171 p.

[41] Wiradianata S. and Saatcioglu M. , *Tests Of Squat Shear Wall Under Lateral Load Reversal*, Proceedings of the Third U. S. National Conference on Earthquake Engineering, August 24-28, 1986, Charleston, South Carolina, pp. 1395-1406.

[42] Zienkiewicz O. C., *Incremental Displacment in Non-Linear Analysis*, International Journal for Numerical Methods in Engineering, Vol. 3, 1971, pp. 587-588.

Appendix A

Design of Wall 4

A.1 Moment capacity of the section

The following material properties were used in the calculation of the ultimate moment capacity and were obtained from Table 3.1:

$$\begin{aligned} f'_c &= 33\ MPa \\ f_y &= 480\ MPa \\ \epsilon_y &= 0.24\% \\ E &= 200\ 000\ MPa \end{aligned}$$

Eight pairs of 10M deformed bars were used as depicted in Figure A.1:

$$A_{sv} = 16 \times 100\ mm^2 = 1600\ mm^2$$

$$\rho_{sv} = A_{sv}/A_g = 1600\ mm^2/(100\ mm \times 2000\ mm) = 0.8\%$$

From a strain compatibility analysis, the neutral axis is found to be at 225 mm from the compression face as depicted in Figure A.2.

$$T_s = (12 \times 100\ mm^2 \times 480\ MPa) + (0.00087 \times 2 \times 100\ mm^2 \times 200\ GPa)$$

$$T_s = 576\ kN + 34.7\ kN = 611\ kN$$

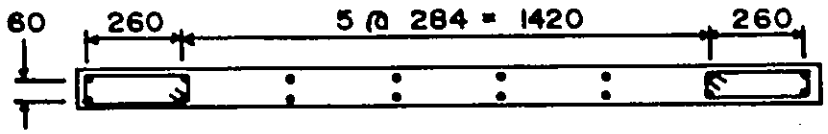

Figure A.1: Horizontal section of Wall 4

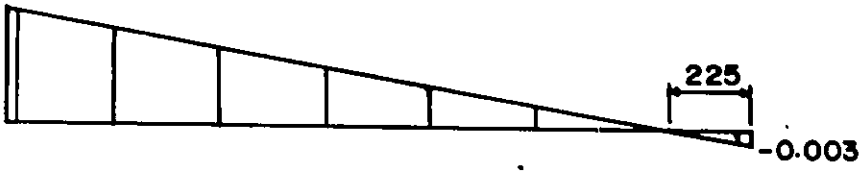

Figure A.2: Strain distribution at ultimate curvature

$$C_s = -(2 \times 100\ mm^2 \times 480\ MPa) = -96\ kN$$

$$C_c = -0.85 \times 33\ MPa \times (0.83 \times 225\ mm) \times 100\ mm = -524\ kN$$

$$\Sigma = 611 - 96 - 524 = -9\ kN \qquad OK.$$

$$M_u = (576\ kN \times 1.284\ m) + (34.7\ kN \times 0.290\ m) + (-96\ kN \times 0.030\ m)$$
$$+(-524\ kN \times 0.83 \times 0.225\ mm \times 0.5)$$

$$M_u = 698\ kN \cdot m$$

A.2 Shear capacity of the section

The shear force corresponding to the ultimate moment capacity is

$$V_u = M_u/h = 698\ kN \cdot m \div 1.14\ m = 612\ kN$$

where h is the distance from the line of action of the applied load to the base of the wall.

From the strain diagram presented in Figure A.2, the strain in the extreme tension bars is 2.3%. From Figure 3.9 some strain hardening is expected in the first four rows of tension steel increasing the value of T_s by 59 kN. This increase do not significantly change the ultimate capacity of the section. Therefore we neglect any strength hardening. Neglecting concrete contribution towards shear strength

$$V_c = 0\ kN$$

the minimum horizontal bar spacing is calculated as

$$S_{min} = \frac{A_s f_y d}{V_u} = 251\ mm$$

where d is the effective depth of the wall and is taken as 0.8 times the base length of the wall. Try 4 pairs of 10M bars at $S = 250\ mm$

$$\rho_{sh} = (8 \times 100\ mm^2)/(100\ mm \times 1000\ mm) = 0.8\%$$

for a design shear capacity of

$$V_r = \frac{A_s f_y d}{S} = \frac{200\ mm^2 \times 480\ MPa \times 0.8 \times 2000\ mm}{250\ mm} = 614\,kN\ >\ 612\,kN \quad OK.$$

The average shear stress applied to the section is

$$\tau_{shear} = \frac{612\ kN}{0.1\ m \times 0.8 \times 2\ m} = 3.83\ MPa = 0.67\sqrt{f'_c}MPa$$

A.3 Detailing

Stirrups made of 6.4 mm plain steel spaced at 80 mm were provided at both ends of the wall to prevent premature buckling of the vertical bars.

Appendix B

Design of Wall 5

B.1 Moment capacity of the section

The following material properties were used in the calculation of the ultimate moment capacity and were obtained from Table 3.1:

$$\begin{aligned} f'_c &= 27\ MPa \\ f_y &= 480\ MPa \\ \epsilon_y &= 0.24\% \\ E &= 200\ 000\ MPa \end{aligned}$$

Twelve pairs of 10M deformed bars were used as depicted in Figure B.1:

$$A_{sv} = 24 \times 100\ mm^2 = 2400\ mm^2$$

$$\rho_{sv} = A_{sv}/A_g = 2400\ mm^2/(100\ mm \times 2000\ mm) = 1.2\%$$

From a strain compatibility analysis, the neutral axis is found to be at 355 mm from the compression face as depicted in Figure B.2.

$$T_s = (16 \times 100\ mm^2 \times 480\ MPa) + (0.00176 \times 200\ GPa \times 2 \times 100\ mm^2)$$

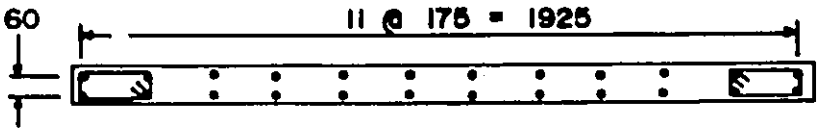

Figure B.1: Horizontal section of Wall 5

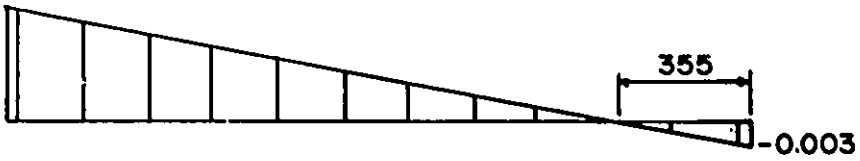

Figure B.2: Strain distribution at ultimate curvature

$$+(0.00028 \times 200\ GPa \times 2 \times 100\ mm^2)$$

$$T_s = 768\ kN + 70.4\ kN + 11.2\ kN = 850\ kN$$

$$C_s = -(2 \times 100\ mm^2 \times 480\ MPa) - (0.0012 \times 2 \times 100\ mm^2 \times 200\ GPa)$$

$$C_s = -144\ kN$$

$$C_c = -0.85 \times 27\ MPa \times (0.85 \times 355\ mm) \times 100\ mm = -693\ kN$$

$$\Sigma = 850 - 144 - 693 = 13\ kN \qquad OK.$$

$$M_u = (768\ kN \times 1.351\ m) + (70.4\ kN \times 0.563\ m) + (11.2\ kN \times 0.388\ m)$$

$$+(-144\ kN \times 0.038\ m) + (-693\ kN \times 0.85 \times 0.355\ mm \times 0.5)$$

$$M_u = 955\ kN \cdot m$$

B.2 Shear capacity of the section

The shear force corresponding to the ultimate moment capacity is

$$V_u = M_u/h = 955\ kN \cdot m \div 1.14\ m = 838\ kN$$

where h is the distance from the line of action of the applied load to the base of the wall.

From the strain diagram presented in Figure B.2, the strain in the extreme tension bars is 1.4%. From Figure 3.9 some strain hardening is expected but is negligeable. Neglecting concrete contribution towards shear strength

$$V_c = 0\ kN$$

the minimum horizontal bar spacing is calculated as

$$S_{min} = \frac{A_s f_y d}{V_u} = 183\ mm$$

where d is the effective depth of the wall and is taken as 0.8 times the base length of the wall. Try 6 pairs of 10M bars at $S = 175\ mm$

$$\rho_{sh} = (12 \times 100\ mm^2)/(100\ mm \times 1000\ mm) = 1.2\%$$

for a design shear capacity of

$$V_r = \frac{A_s f_y d}{S} = \frac{200\ mm^2 \times 480\ MPa \times 0.8 \times 2000\ mm}{175\ mm} = 878\ kN\ >\ 838\ kN \quad OK.$$

The average shear stress applied to the section is:

$$\tau_{shear} = \frac{838\ kN}{0.1\ m \times 0.8 \times 2\ m} = 5.24\ MPa = 1.01\sqrt{f'_c}MPa$$

B.3 Detailling

Stirrups made of 6.4 mm plain steel spaced at 80 mm were provided at both ends of the wall to prevent premature buckling of the vertical bars.

Appendix C

Computer Program Listing

The following appendix contains a copy of:

1. The BATCH EXEC program which compiles, sets up the input and output files and executes FEASSW using the CMS batch facility at the University of Ottawa.
2. A complete listing of FEASSW computer program.
3. The input file of the case study presented in Figure 6.6 for one displacement increment of 1 mm.
4. The results of FEASSW.

```
&TRACE ALL
GLOBAL TXTLIB VLNKMLIB VFORTLIB  PLOTLIB CMSLIB
GLOBAL LOADLIB DDBALL
FORTVS FEASSW (AUTODBL (DBLPAD4)       <--- COMPILE IN DOUBLE PRECISION
FI 1 DISK FEASSW DATA   A              <--- INPUT FILE
FI 2 DISK FEASSW OUTPUT A (LRECL 132   <--- OUTPUT FILE
FI 3 DISK FEASSW PLOT   A              <--- PLOT FILE
FI 4 DISK FEASSW RESULT A              <--- SUMMARY FORCE-DISPL. RESULTS
LOAD FEASSW (CLEAR START
EXEC SENDFILE FEASSW OUTPUT A TO 335757 AT UOTTAWA         SEND FILES
EXEC SENDFILE FEASSW PLOT   A TO 335757 AT UOTTAWA   <--- TO USER'S
EXEC SENDFILE FEASSW RESULT A TO 335757 AT UOTTAWA         ACCOUNT
&EXIT
```

```
                                                                      FEA00010
                                                                      FEA00020
                                                                      FEA00030
      CHARACTER TITLE*79                                              FEA00040
      OPEN(2)                                                         FEA00050
      WRITE(2,101)                                                    FEA00060
  101 FORMAT(T2,'FEASSW:  NON-LINEAR FINITE ELEMENT ANALYSIS OF REINFORCFEA00070
     *ED CONCRETE SQUAT SHEAR WALLS',/,'+',T2,84('_'),/,'-')          FEA00080
      READ(1,102) ICARD                                               FEA00090
  102 FORMAT(I10)                                                     FEA00100
      DO 10 I=1,ICARD                                                 FEA00110
         READ(1,103) TITLE                                            FEA00120
  103    FORMAT(A79)                                                  FEA00130
         WRITE(2,104) TITLE                                           FEA00140
  104    FORMAT(T2,A79)                                               FEA00150
   10 CONTINUE                                                        FEA00160
      WRITE(2,105)                                                    FEA00170
  105 FORMAT('-')                                                     FEA00180
      CALL MAIN1                                                      FEA00190
      STOP                                                            FEA00200
      END                                                             FEA00210
      BLOCK DATA                                                      FEA00220
      COMMON /D/ PTN(4,4),WGT(4,4),PTNOD(2,8),B(3,16),EB(3,16),NDOF(16) FEA00230
      DATA PTN /0.,0.,0.,0.,-.577350269189626,.577350269189626,0.,0., FEA00240
     *          -.77459669241483,0.,.77459669241483,0.,                FEA00250
     *          -.861136311594053,-.339981043584856,                   FEA00260
     *           .339981043584856,.861136311594053/                    FEA00270
      DATA WGT /2.,0.,0.,0.,1.,1.,0.,0.,                              FEA00280
     *          .555555555555556,.888888888888889,                    FEA00290
     *          .555555555555556,0.,                                  FEA00300
     *          .347854845137454,.652145154862546,.347854845137454,   FEA00310
     *          .652145154862546/                                     FEA00320
      DATA PTNOD /-1.,-1.,0.,-1.,1.,-1.,1.,0.,1.,1.,0.,1.,-1.,1.,-1.,0./FEA00330
      END                                                             FEA00340
      SUBROUTINE MAIN1                                                FEA00350
      COMMON /A/ ICHECK,IEXE,NN,NE,NMP                                FEA00360
      COMMON /C/ ID(1000,2),NEQ,ALOAD(1000),UF(1000),S(1000,80),MBAND FEA00370
      READ(1,101) ICHECK,IEXE,NN,NE,NMP                               FEA00380
  101 FORMAT(10I10)                                                   FEA00390
      WRITE(2,102) ICHECK,IEXE,NN,NE,NMP                              FEA00400
  102 FORMAT(T2,'PARAMETERS:',5X,10(I5,3X))                           FEA00410
      CALL NODGEN                                                     FEA00420
      CALL ELEGEN                                                     FEA00430
      CALL MATPRO                                                     FEA00440
      CALL BOUND                                                      FEA00450
      CALL LOD                                                        FEA00460
      IF (ICHECK.EQ.1) RETURN                                         FEA00470
      CALL STIFF                                                      FEA00480
      CALL SOLVE(1)                                                   FEA00490
      DO 10 I=1,NEQ                                                   FEA00500
         UF(I)=ALOAD(I)                                               FEA00510
   10 CONTINUE                                                        FEA00520
      IF (ICHECK.EQ.2) THEN                                           FEA00530
         CALL DISPLI                                                  FEA00540
         CALL STRLI                                                   FEA00550
         RETURN                                                       FEA00560
      END IF                                                          FEA00570
      CALL NONLIN                                                     FEA00580
      RETURN                                                          FEA00590
      END                                                             FEA00600
      SUBROUTINE NODGEN                                               FEA00610
C     NODE GENERATION                                                 FEA00620
      COMMON /A/ ICHECK,IEXE,NN,NE,NMP                                FEA00630
      COMMON /B/ X(1000),Y(1000),IEL(250,8),IELMAT(250),AMATP(10,10), FEA00640
     *           ITYPE(10)                                            FEA00650
      INODE=0                                                         FEA00660
      READ(1,101) ICARD                                               FEA00670
  101 FORMAT(I10)                                                     FEA00680
      DO 10 I=1,ICARD                                                 FEA00690
         READ(1,102) KOD,L,XL,YL                                      FEA00700
  102    FORMAT(2I10,2F10.0)                                          FEA00710
         IF (KOD.EQ.1) THEN                                           FEA00720
```

```
            X(L)=XL                                                          FEA00730
            Y(L)=YL                                                          FEA00740
         ELSE                                                                FEA00750
            READ(1,103) M,XM,YM,INC1                                         FEA00760
103         FORMAT(10X,I10,2F10.0,1I10)                                      FEA00770
            J=(M-L)/INC1                                                     FEA00780
            X1=(XM-XL)/J                                                     FEA00790
            Y1=(YM-YL)/J                                                     FEA00800
            IF (KOD.EQ.3) THEN                                               FEA00810
               READ(1,103) N,XN,YN,INC2                                      FEA00820
               K=(N-M)/INC2                                                  FEA00830
               X2=(XN-XM)/K                                                  FEA00840
               Y2=(YN-YM)/K                                                  FEA00850
            ELSE                                                             FEA00860
               K=0                                                           FEA00870
            END IF                                                           FEA00880
            DO 20 KK=0,K                                                     FEA00890
               DO 30 JJ=0,J                                                  FEA00900
                  ID=L+INC1*JJ+INC2*KK                                       FEA00910
                  X(ID)=XL+X1*JJ+X2*KK                                       FEA00920
                  Y(ID)=YL+Y1*JJ+Y2*KK                                       FEA00930
                  IF (ID.GT.INODE) INODE=ID                                  FEA00940
30             CONTINUE                                                      FEA00950
20          CONTINUE                                                         FEA00960
         END IF                                                              FEA00970
10     CONTINUE                                                              FEA00980
       WRITE(2,201)                                                          FEA00990
201    FORMAT('-','NODAL COORDINATES',/,'+',T2,17('_'),/,'-',T2,4('NODE',    FEA01000
     *        4X,'X-COOR',6X,'Y-COOR',6X),/,'+',T2,4(4('_'),4X,6('_'),      FEA01010
     *        6X,6('_'),6X),/,'-')                                          FEA01020
       Z=NN/4.+.999                                                          FEA01030
       I1=IFIX(Z)                                                            FEA01040
       DO 40 I=1,I1                                                          FEA01050
          IF (I1*3+I.LE.NN) THEN                                             FEA01060
             K=3                                                             FEA01070
          ELSE                                                               FEA01080
             K=2                                                             FEA01090
          END IF                                                             FEA01100
          WRITE(2,202) (J,X(J),Y(J),J=I,I+K*I1,I1)                           FEA01110
202       FORMAT(T2,4(I3,3X,1PE10.3E2,2X,1PE10.3E2,4X))                      FEA01120
40     CONTINUE                                                              FEA01130
       IF (INODE.NE.NN) THEN                                                 FEA01140
          WRITE(2,204)                                                       FEA01150
204       FORMAT(T2,'SUBROUTINE NODGEN:  INODE NOT EQUAL TO NN',10X,         FEA01160
     *           '***** EXECUTION STOPPED *****')                           FEA01170
          STOP                                                               FEA01180
       END IF                                                                FEA01190
       RETURN                                                                FEA01200
       END                                                                   FEA01210
       SUBROUTINE ELEGEN                                                     FEA01220
C      ELEMENT GENERATION                                                    FEA01230
       COMMON /A/ ICHECK,IEXE,NN,NE,NMP                                      FEA01240
       COMMON /B/ X(1000),Y(1000),IEL(250,8),IELMAT(250),AMATP(10,10),       FEA01250
     *            ITYPE(10)                                                 FEA01260
       IELEM=0                                                               FEA01270
       READ(1,101) ICARD                                                     FEA01280
101    FORMAT(1I10)                                                          FEA01290
       DO 10 I=1,ICARD                                                       FEA01300
          READ(1,102) KOD,IEL1,(IEL(IEL1,N),N=1,8),IELMAT(IEL1)             FEA01310
102       FORMAT(5X,11I5)                                                    FEA01320
          IF (KOD.NE.1) THEN                                                 FEA01330
             READ(1,103) IEL2,INCE1,INCN1                                    FEA01340
103          FORMAT(10X,3I5)                                                 FEA01350
             I1=(IEL2-IEL1)/INCE1                                            FEA01360
             IF (KOD.EQ.3) THEN                                              FEA01370
                READ(1,103) IEL3,INCE2,INCN2                                 FEA01380
                I2=(IEL3-IEL2)/INCE2                                         FEA01390
             ELSE                                                            FEA01400
                I2=0                                                         FEA01410
             END IF                                                          FEA01420
             DO 20 J=0,I2                                                    FEA01430
                DO 30 K=0,I1                                                 FEA01440
```

```
                  ID=IEL1+K*INCE1+J*INCE2                                    FEA01450
                  DO 40 L=1,8                                                FEA01460
                     IEL(ID,L)=IEL(IEL1,L)+K*INCN1+J*INCN2                   FEA01470
 40               CONTINUE                                                   FEA01480
                  IELMAT(ID)=IELMAT(IEL1)                                    FEA01490
                  IF (ID.GT.IELEM) IELEM=ID                                  FEA01500
 30            CONTINUE                                                      FEA01510
 20         CONTINUE                                                         FEA01520
         ELSE                                                               FEA01530
            IF (IEL1.GT.IELEM) IELEM=IEL1                                   FEA01540
         END IF                                                             FEA01550
 10   CONTINUE                                                             FEA01560
      WRITE(2,201)                                                         FEA01570
 201  FORMAT('-','ELEMENT CONNEXTIVITIES',/,'+',T2,22('_'),/,'-',         FEA01580
     *       'ELEMENT',20X,'NODES',22X,'MATERIAL INDEX',/,'+',7('_'),      FEA01590
     *       20X,5('_'),22X,14('_'),/,'-')                                 FEA01600
      DO 50 I=1,NE                                                         FEA01610
         WRITE(2,202) I,(IEL(I,J),J=1,8),IELMAT(I)                         FEA01620
 202     FORMAT(2X,I3,5X,8I5,12X,1I1)                                      FEA01630
 50   CONTINUE                                                             FEA01640
      IF (IELEM.NE.NE) THEN                                                FEA01650
         WRITE(2,204)                                                      FEA01660
 204     FORMAT(T2,'SUBROUTINE ELEGEN:  IELEM NOT EQUAL TO NE',10X,        FEA01670
     *          '***** EXECUTION STOPPED *****')                           FEA01680
         STOP                                                              FEA01690
      END IF                                                               FEA01700
      RETURN                                                               FEA01710
      END                                                                  FEA01720
      SUBROUTINE MATPRO                                                    FEA01730
C     MATERIAL PROPERTIES                                                  FEA01740
      COMMON /A/ ICHECK,IEXE,NN,NE,NMP                                     FEA01750
      COMMON /B/ X(1000),Y(1000),IEL(250,8),IELMAT(250),AMATP(10,10),      FEA01760
     *           ITYPE(10)                                                 FEA01770
      READ(1,101) ICARD                                                    FEA01780
 101  FORMAT(1I10)                                                         FEA01790
      IF (ICARD.NE.NMP) THEN                                               FEA01800
         WRITE(2,209)                                                      FEA01810
 209     FORMAT(T2,'SUBROUTINE MATPRO:  ICARD NOT EQUAL TO NMP',10X,       FEA01820
     *          '***** EXECUTION STOPPED *****')                           FEA01830
         STOP                                                              FEA01840
      END IF                                                               FEA01850
      DO 10 I=1,ICARD                                                      FEA01860
         READ(1,102) IMP,ITYPE(IMP),(AMATP(IMP,J),J=1,3)                   FEA01870
 102     FORMAT(5X,I5,I10,3F10.0)                                          FEA01880
         IF (ITYPE(IMP).EQ.2) THEN                                         FEA01890
            READ(1,103) (AMATP(IMP,J),J=4,10)                              FEA01900
 103        FORMAT(10X,7F10.0)                                             FEA01910
         END IF                                                            FEA01920
 10   CONTINUE                                                             FEA01930
      WRITE(2,201)                                                         FEA01940
 201  FORMAT('-','MATERIAL PROPERTIES',/,'+',19(' '),/,'-','INDEX',T20,    FEA01950
     *       'LINEAR ANALYSIS',T76,'NON-LINEAR ANALYSIS',/,'+',T2,5(' '),  FEA01960
     *       T11,32(' '),T51,76(' '),/,/,T14,'YOUNG',T24,'POISSON',T33,     FEA01970
     *       'THICKNESS',T55,'F','C',T66,'E0',T77,'FT',T88,'ES',T99,'EY',   FEA01980
     *       T110,'%H',T121,'%V',/,'+',T11,3(10('_'),1X),T51,7(10('_'),     FEA01990
     *       1X),/,'-')                                                    FEA02000
      DO 20 I=1,NMP                                                        FEA02010
         IF (ITYPE(I).EQ.1) THEN                                           FEA02020
            K=3                                                            FEA02030
         ELSE                                                              FEA02040
            K=10                                                           FEA02050
         END IF                                                            FEA02060
         WRITE(2,202) I,(AMATP(I,J),J=1,K)                                 FEA02070
 202     FORMAT(T3,I2,T11,3(1PE10.3E2,1X),T51,7(1PE10.3E2,1X))             FEA02080
 20   CONTINUE                                                             FEA02090
      RETURN                                                               FEA02100
      END                                                                  FEA02110
      SUBROUTINE BOUND                                                     FEA02120
C     BOUNDARY CONDITIONS                                                  FEA02130
      COMMON /A/ ICHECK,IEXE,NN,NE,NMP                                     FEA02140
      COMMON /B/ X(1000),Y(1000),IEL(250,8),IELMAT(250),AMATP(10,10),      FEA02150
     *           ITYPE(10)                                                 FEA02160
```

```
      COMMON /C/ ID(1000,2),NEQ,ALOAD(1000),UF(1000),S(1000,80),MBAND    FEA02170
      DO 5 I=1,1000                                                     FEA02180
         ID(I,1)=-1                                                     FEA02190
         ID(I,2)=-1                                                     FEA02200
 5    CONTINUE                                                          FEA02210
      READ(1,101) ICARD                                                 FEA02220
 101  FORMAT(I10)                                                       FEA02230
      DO 60 I=1,NE                                                      FEA02240
         DO 70 J=1,8                                                    FEA02250
            K=IEL(I,J)                                                  FEA02260
            ID(K,1)=1                                                   FEA02270
            ID(K,2)=1                                                   FEA02280
 70      CONTINUE                                                       FEA02290
 60   CONTINUE                                                          FEA02300
      DO 10 I=1,ICARD                                                   FEA02310
         READ(1,102) KOD,NOD1,IXY,NOD2,INC                              FEA02320
 102     FORMAT(5X,I5,4I10)                                             FEA02330
         IF (KOD.EQ.1) THEN                                             FEA02340
            NOD2=NOD1                                                   FEA02350
            INC=1                                                       FEA02360
         END IF                                                         FEA02370
         DO 20 J=NOD1,NOD2,INC                                          FEA02380
            ID(J,IXY)=0                                                 FEA02390
 20      CONTINUE                                                       FEA02400
10    CONTINUE                                                          FEA02410
      NEQ=0                                                             FEA02420
      DO 30 J=1,NN                                                      FEA02430
         DO 40 K=1,2                                                    FEA02440
            IF (ID(J,K).EQ.1) THEN                                      FEA02450
               NEQ=NEQ+1                                                FEA02460
               ID(J,K)=NEQ                                              FEA02470
            END IF                                                      FEA02480
 40      CONTINUE                                                       FEA02490
 30   CONTINUE                                                          FEA02500
      WRITE(2,201)                                                      FEA02510
 201  FORMAT('-','BOUNDARY CONDITIONS - ID MATRIX  (0 = CONSTRAINT    -1FEA02520
     * = UNCONNECTED',/,'+',31(' '),/,'-',4('NODE',5X,'X',4X,'Y',14X),  FEA02530
     * /,'+',T2,4(4('_'),5X,'_',4X,'_',14X),/,'_')                      FEA02540
      Z=NN/4.+.999                                                      FEA02550
      I1=IFIX(Z)                                                        FEA02560
      DO 50 I=1,I1                                                      FEA02570
         IF (I1*3+I.LE.NN) THEN                                         FEA02580
            K=3                                                         FEA02590
         ELSE                                                           FEA02600
            K=2                                                         FEA02610
         END IF                                                         FEA02620
         WRITE(2,202) (J,ID(J,1),ID(J,2),J=I,I+K*I1,I1)                 FEA02630
 202     FORMAT(T2,4(I3,5X,I3,2X,I3,13X))                               FEA02640
 50   CONTINUE                                                          FEA02650
      RETURN                                                            FEA02660
      END                                                               FEA02670
      SUBROUTINE LOD                                                    FEA02680
C     LOADING CONDITIONS                                                FEA02690
      COMMON /C/ ID(1000,2),NEQ,ALOAD(1000),UF(1000),S(1000,80),MBAND   FEA02700
      COMMON /E/ BLOAD(1000)                                            FEA02710
      READ(1,101) ICARD                                                 FEA02720
 101  FORMAT(I10)                                                       FEA02730
      WRITE(2,201)                                                      FEA02740
 201  FORMAT('-','LOADING CONDITIONS',/,'+',18('_'),/,'-',T2,'NODE',7X, FEA02750
     *       'LOAD-X',8X,'LOAD-Y',/,'+',T2,4('_'),7X,6('_'),8X,6('_'),  FEA02760
     *       /,'-')                                                     FEA02770
      DO 10 I=1,ICARD                                                   FEA02780
         READ(1,102) KOD,P,NOD1,IXY,NOD2,INC                            FEA02790
 102     FORMAT(5X,I5,F10.0,4I10)                                       FEA02800
         IF (KOD.EQ.1) THEN                                             FEA02810
            NOD2=NOD1                                                   FEA02820
            INC=1                                                       FEA02830
         END IF                                                         FEA02840
         DO 20 J=NOD1,NOD2,INC                                          FEA02850
            IF (ID(J,IXY).NE.0) THEN                                    FEA02860
               ALOAD(ID(J,IXY))=P                                       FEA02870
            ELSE                                                        FEA02880
```

```
            WRITE(2,204) P,J,IXY                                        FEA02890
204         FORMAT(T2,'*** WARNING ***    LOAD ',1PE10.3E2,             FEA02900
     *           ' APPLIED TO A CONSTRAINT OR UNEXISTANT NODE ',I4,     FEA02910
     *           ' DIRECTION ','"',I1,'"')                              FEA02920
         END IF                                                         FEA02930
         IF (IXY.EQ.1) THEN                                             FEA02940
            WRITE(2,202) J,P                                            FEA02950
202         FORMAT(T2,I3,T11,1PE10.3E2)                                 FEA02960
         ELSE                                                           FEA02970
            WRITE(2,203) J,P                                            FEA02980
203         FORMAT(T2,I3,T25,1PE10.3E2)                                 FEA02990
         END IF                                                         FEA03000
20    CONTINUE                                                          FEA03010
10    CONTINUE                                                          FEA03020
      DO 30 I=1,NEQ                                                     FEA03030
         BLOAD(I)=ALOAD(I)                                              FEA03040
30    CONTINUE                                                          FEA03050
      RETURN                                                            FEA03060
      END                                                               FEA03070
      SUBROUTINE STIFF                                                  FEA03080
C     INITIAL STIFFNESS MATRIX                                          FEA03090
      COMMON /A/ ICHECK,IEXE,NN,NE,NMP                                  FEA03100
      COMMON /B/ X(1000),Y(1000),IEL(250,8),IELMAT(250),AMATP(10,10),   FEA03110
     *           ITYPE(10)                                              FEA03120
      COMMON /C/ ID(1000,2),NEQ,ALOAD(1000),UF(1000),S(1000,80),MBAND   FEA03130
      COMMON /D/ PTN(4,4),WGT(4,4),PTNOD(2,8),B(3,16),EB(3,16),NDOF(16) FEA03140
      COMMON /F/ ALPHA,E1MAX,SMX,SMY,EX(16,3,3,250),IGAUSS,U(1000)      FEA03150
      REAL ST(16,16),E(3,3)                                             FEA03160
      MBAND=0                                                           FEA03170
      DO 10 I=1,NE                                                      FEA03180
         MIN=9999                                                       FEA03190
         MAX=0                                                          FEA03200
         DO 20 J=1,8                                                    FEA03210
            DO 30 K=1,2                                                 FEA03220
               L=ID(IEL(I,J),K)                                         FEA03230
               IF (L.GT.0) THEN                                         FEA03240
                  IF (L.LT.MIN) MIN=L                                   FEA03250
                  IF (L.GT.MAX) MAX=L                                   FEA03260
               END IF                                                   FEA03270
30          CONTINUE                                                   FEA03280
20       CONTINUE                                                      FEA03290
         MB=MAX-MIN+1                                                  FEA03300
         IF (MB.GT.MBAND) MBAND=MB                                     FEA03310
10    CONTINUE                                                         FEA03320
      IF (MBAND.GT.80) THEN                                            FEA03330
         WRITE(2,101) MBAND                                            FEA03340
101      FORMAT(T2,'SUBROUTINE STIFF:  SEMI-BANDWIDTH OF ',I3,         FEA03350
     *           ' EXCEEDING THE ALLOWABLE VALUE',10X,                 FEA03360
     *           '***** EXECUTION STOPPED *****')                      FEA03370
         STOP                                                          FEA03380
      END IF                                                           FEA03390
      DO 40 I=1,NEQ                                                    FEA03400
         DO 50 J=1,MBAND                                               FEA03410
            S(I,J)=0.                                                  FEA03420
50       CONTINUE                                                      FEA03430
40    CONTINUE                                                         FEA03440
      DO 100 I=1,NE                                                    FEA03450
         DO 110 J=1,16                                                 FEA03460
            DO 120 K=1,16                                              FEA03470
               ST(J,K)=0.                                              FEA03480
120         CONTINUE                                                   FEA03490
110      CONTINUE                                                      FEA03500
         IK=IELMAT(I)                                                  FEA03510
         APOIS=AMATP(IK,2)                                             FEA03520
         E(1,1)=AMATP(IK,1)/(1-APOIS**2)                               FEA03530
         E(1,2)=E(1,1)*APOIS                                           FEA03540
         E(3,3)=E(1,1)*(1-APOIS)/2                                     FEA03550
         E(1,3)=0.                                                     FEA03560
         E(2,1)=E(1,2)                                                 FEA03570
         E(2,3)=0.                                                     FEA03580
         E(3,1)=0.                                                     FEA03590
         E(3,2)=0.                                                     FEA03600
```

```
      E(2,2)=E(1,1)                                                     FEA03610
      THK=AMATP(IK,3)                                                   FEA03620
      NGAUSS=2                                                          FEA03630
      IF (IEXE.EQ.1.AND.ITYPE(IK).EQ.2) NGAUSS=IGAUSS                   FEA03640
      DO 130 NA=1,NGAUSS                                                FEA03650
         XA=PTN(NA,NGAUSS)                                              FEA03660
         DO 140 NB=1,NGAUSS                                             FEA03670
            YB=PTN(NB,NGAUSS)                                           FEA03680
            CALL SHAPE(XA,YB,I,DETJAC)                                  FEA03690
            IF (IEXE.EQ.1.AND.ITYPE(IK).EQ.2) THEN                      FEA03700
               KGAUSS=NB+(NA-1)*NGAUSS                                  FEA03710
               DO 500 J=1,3                                             FEA03720
                  DO 510 K=1,3                                          FEA03730
                     E(J,K)=EX(KGAUSS,J,K,I)                            FEA03740
510                CONTINUE                                             FEA03750
500            CONTINUE                                                 FEA03760
            END IF                                                      FEA03770
            DO 152 J=1,16                                               FEA03780
               DO 151 K=1,3                                             FEA03790
                  EB(K,J)=0.                                            FEA03800
                  DO 150 L=1,3                                          FEA03810
                     EB(K,J)=EB(K,J)+B(L,J)*E(K,L)                      FEA03820
150               CONTINUE                                              FEA03830
151            CONTINUE                                                 FEA03840
152         CONTINUE                                                    FEA03850
            DO 160 J=1,16                                               FEA03860
               DO 170 K=1,16                                            FEA03870
                  DUM=0.                                                FEA03880
                  DO 180 L=1,3                                          FEA03890
                     DUM=DUM+EB(L,J)*B(L,K)                             FEA03900
180               CONTINUE                                              FEA03910
                  ST(K,J)=ST(K,J)+WGT(NA,NGAUSS)*WGT(NB,NGAUSS)*        FEA03920
     *                    THK*DETJAC*DUM                                FEA03930
170            CONTINUE                                                 FEA03940
160         CONTINUE                                                    FEA03950
140      CONTINUE                                                       FEA03960
130   CONTINUE                                                          FEA03970
      DO 200 J=1,8                                                      FEA03980
         NDOF(J*2-1)=ID(IEL(I,J),1)                                     FEA03990
         NDOF(J*2)=ID(IEL(I,J),2)                                       FEA04000
200   CONTINUE                                                          FEA04010
      DO 210 J=1,16                                                     FEA04020
         JJ=NDOF(J)                                                     FEA04030
         IF (JJ.GT.0) THEN                                              FEA04040
            DO 220 K=1,16                                               FEA04050
               KK=NDOF(K)                                               FEA04060
               IF (KK.GE.JJ) THEN                                       FEA04070
                  LL=KK-JJ+1                                            FEA04080
                  S(JJ,LL)=S(JJ,LL)+ST(J,K)                             FEA04090
               END IF                                                   FEA04100
220         CONTINUE                                                    FEA04110
         END IF                                                         FEA04120
210   CONTINUE                                                          FEA04130
100   CONTINUE                                                          FEA04140
      RETURN                                                            FEA04150
      END                                                               FEA04160
      SUBROUTINE SHAPE(XA,YB,NEL,DETJAC)                                FEA04170
C     SHAPE FUNCTION, JACOBIAN AND B MATRIX FOR 8-NODE RECTANGULAR      FEA04180
C     ELEMENT                                                           FEA04190
      COMMON /B/ X(1000),Y(1000),IEL(250,8),IELMAT(250),AMATP(10,10),   FEA04200
     *           ITYPE(10)                                              FEA04210
      COMMON /D/ PTN(4,4),WGT(4,4),PTNOD(2,8),B(3,16),EB(3,16),NDOF(16) FEA04220
      REAL NXI(8),NET(8),JAC(2,2)                                       FEA04230
      NXI(1)=.25*(1-YB)*(2*XA+YB)                                       FEA04240
      NXI(2)=-(1-YB)*XA                                                 FEA04250
      NXI(3)=.25*(1-YB)*(2*XA-YB)                                       FEA04260
      NXI(4)=.5*(1-YB**2)                                               FEA04270
      NXI(5)=.25*(1+YB)*(2*XA+YB)                                       FEA04280
      NXI(6)=-(1+YB)*XA                                                 FEA04290
      NXI(7)=.25*(1+YB)*(2*XA-YB)                                       FEA04300
      NXI(8)=-.5*(1-YB**2)                                              FEA04310
      NET(1)=.25*(1-XA)*(XA+2*YB)                                       FEA04320
```

```
      NET(2)=-.5*(1-XA**2)                                                  FEA04330
      NET(3)=-.25*(1+XA)*(XA-2*YB)                                          FEA04340
      NET(4)=-(1+XA)*YB                                                     FEA04350
      NET(5)=.25*(1+XA)*(XA+2*YB)                                           FEA04360
      NET(6)=.5*(1-XA**2)                                                   FEA04370
      NET(7)=-.25*(1-XA)*(XA-2*YB)                                          FEA04380
      NET(8)=-(1-XA)*YB                                                     FEA04390
      JAC(1,1)=0.                                                           FEA04400
      JAC(1,2)=0.                                                           FEA04410
      JAC(2,1)=0.                                                           FEA04420
      JAC(2,2)=0.                                                           FEA04430
      DO 10 L=1,8                                                           FEA04440
         K=IEL(NEL,L)                                                       FEA04450
         JAC(1,1)=JAC(1,1)+NXI(L)*X(K)                                      FEA04460
         JAC(1,2)=JAC(1,2)+NXI(L)*Y(K)                                      FEA04470
         JAC(2,1)=JAC(2,1)+NET(L)*X(K)                                      FEA04480
         JAC(2,2)=JAC(2,2)+NET(L)*Y(K)                                      FEA04490
 10   CONTINUE                                                              FEA04500
      DETJAC=JAC(1,1)*JAC(2,2)-JAC(2,1)*JAC(1,2)                            FEA04510
      DUM1=JAC(1,1)/DETJAC                                                  FEA04520
      JAC(1,1)=JAC(2,2)/DETJAC                                              FEA04530
      JAC(1,2)=-JAC(1,2)/DETJAC                                             FEA04540
      JAC(2,1)=-JAC(2,1)/DETJAC                                             FEA04550
      JAC(2,2)=DUM1                                                         FEA04560
      DO 20 J=1,8                                                           FEA04570
         L=2*J                                                              FEA04580
         K=L-1                                                              FEA04590
         B(1,K)=JAC(1,1)*NXI(J)+JAC(1,2)*NET(J)                             FEA04600
         B(2,L)=JAC(2,1)*NXI(J)+JAC(2,2)*NET(J)                             FEA04610
         B(3,K)=B(2,L)                                                      FEA04620
         B(3,L)=B(1,K)                                                      FEA04630
 20   CONTINUE                                                              FEA04640
      RETURN                                                                FEA04650
      END                                                                   FEA04660
      SUBROUTINE SOLVE(IFLAG)                                               FEA04670
C     GAUSS ELIMINATION   SEE R.D. COOK (1981) P. 42                        FEA04680
      COMMON /C/ ID(1000,2),NEQ,ALOAD(1000),UF(1000),S(1000,80),MBAND       FEA04690
C-----FORWARD REDUCTION OF THE COEFFICIENT MATRIX                           FEA04700
      IF (IFLAG.EQ.1) THEN                                                  FEA04710
         DO 100 N=1,NEQ                                                     FEA04720
            DO 110 L=2,MBAND                                                FEA04730
               IF (S(N,L).NE.0.) THEN                                       FEA04740
                  I=N+L-1                                                   FEA04750
                  C=S(N,L)/S(N,1)                                           FEA04760
                  J=0                                                       FEA04770
                  DO 120 K=L,MBAND                                          FEA04780
                     J=J+1                                                  FEA04790
                     S(I,J)=S(I,J)-C*S(N,K)                                 FEA04800
 120              CONTINUE                                                  FEA04810
                  S(N,L)=C                                                  FEA04820
               END IF                                                       FEA04830
 110        CONTINUE                                                        FEA04840
 100     CONTINUE                                                           FEA04850
      END IF                                                                FEA04860
C-----FORWARD REDUCTION OF THE VECTOR OF CONSTANTS                          FEA04870
      DO 130 N=1,NEQ                                                        FEA04880
         DO 140 L=2,MBAND                                                   FEA04890
            IF (S(N,L).NE.0.) THEN                                          FEA04900
               I=N+L-1                                                      FEA04910
               ALOAD(I)=ALOAD(I)-S(N,L)*ALOAD(N)                            FEA04920
            END IF                                                          FEA04930
 140     CONTINUE                                                           FEA04940
         ALOAD(N)=ALOAD(N)/S(N,1)                                           FEA04950
 130  CONTINUE                                                              FEA04960
C-----SOLVE FOR UNKNOWNS BY BACK-SUBSTITUTION                               FEA04970
      DO 150 M=2,NEQ                                                        FEA04980
         N=NEQ+1-M                                                          FEA04990
         DO 160 L=2,MBAND                                                   FEA05000
            IF (S(N,L).NE.0.) THEN                                          FEA05010
               K=N+L-1                                                      FEA05020
               ALOAD(N)=ALOAD(N)-S(N,L)*ALOAD(K)                            FEA05030
            END IF                                                          FEA05040
```

```
160      CONTINUE                                                       FEA05050
150   CONTINUE                                                          FEA05060
      RETURN                                                            FEA05070
      END                                                               FEA05080
      SUBROUTINE DISPLI                                                 FEA05090
C     DISPLACEMENT PRINTOUT                                             FEA05100
      COMMON /A/ ICHECK,IEXE,NN,NE,NMP                                  FEA05110
      COMMON /B/ X(1000),Y(1000),IEL(250,8),IELMAT(250),AMATP(10,10),   FEA05120
     *           ITYPE(10)                                              FEA05130
      COMMON /C/ ID(1000,2),NEQ,ALOAD(1000),UF(1000),S(1000,80),MBAND   FEA05140
      COMMON /D/ PTN(4,4),WGT(4,4),PTNOD(2,8),B(3,16),EB(3,16),NDOF(16) FEA05150
      COMMON /F/ ALPHA,E1MAX,SMX,SMY,EX(16,3,3,250),IGAUSS,U(1000)      FEA05160
      REAL D(8)                                                         FEA05170
      INTEGER NOD(4)                                                    FEA05180
      WRITE(2,101)                                                      FEA05190
101   FORMAT('1***** DISPLACEMENT SOLUTION *****  (-9.999E03 = UNCONNECTFEA05200
     *ED NODE)',/,'+',T8,22(' '),/,'-',T2,                              FEA05210
     *4('NODE',3X,'X DISPL',5X,'Y DISPL',7X),/,'+',T2,4(4('_'),2X,      FEA05220
     *10(' '),2X,10('_'),5X),/,'-')                                     FEA05230
      I1=NN/4.+.999                                                     FEA05240
      DO 10 I=1,I1                                                      FEA05250
         IF (I1*3+I.LE.NN) THEN                                         FEA05260
            K=3                                                         FEA05270
         ELSE                                                           FEA05280
            K=2                                                         FEA05290
         END IF                                                         FEA05300
         II=0                                                           FEA05310
         JJ=0                                                           FEA05320
         DO 20 J=I,I+K*I1,I1                                            FEA05330
            JJ=JJ+1                                                     FEA05340
            NOD(JJ)=J                                                   FEA05350
            DO 30 L=1,2                                                 FEA05360
               II=II+1                                                  FEA05370
               IF (ID(J,L).GT.0) THEN                                   FEA05380
                  IF (ICHECK.EQ.2) THEN                                 FEA05390
                     D(II)=UF(ID(J,L))                                  FEA05400
                  ELSE                                                  FEA05410
                     D(II)=U(ID(J,L))                                   FEA05420
                  END IF                                                FEA05430
               ELSE IF (ID(J,L).EQ.0) THEN                              FEA05440
                  D(II)=0.                                              FEA05450
               ELSE                                                     FEA05460
                  D(II)=-9999.                                          FEA05470
               END IF                                                   FEA05480
30          CONTINUE                                                    FEA05490
20       CONTINUE                                                       FEA05500
         WRITE(2,201) (NOD(J),D(J*2-1),D(J*2),J=1,K+1)                  FEA05510
201      FORMAT(T2,4(I3,3X,1PE10.3E2,2X,1PE10.3E2,5X))                  FEA05520
10    CONTINUE                                                          FEA05530
      RETURN                                                            FEA05540
      END                                                               FEA05550
      SUBROUTINE STRLI                                                  FEA05560
C     STRESS PRINTOUT (ELASTIC ANALYSIS)                                FEA05570
      COMMON /A/ ICHECK,IEXE,NN,NE,NMP                                  FEA05580
      COMMON /B/ X(1000),Y(1000),IEL(250,8),IELMAT(250),AMATP(10,10),   FEA05590
     *           ITYPE(10)                                              FEA05600
      COMMON /C/ ID(1000,2),NEQ,ALOAD(1000),UF(1000),S(1000,80),MBAND   FEA05610
      COMMON /D/ PTN(4,4),WGT(4,4),PTNOD(2,8),B(3,16),EB(3,16),NDOF(16) FEA05620
      REAL D(16),SS(3)                                                  FEA05630
      WRITE(2,101)                                                      FEA05640
101   FORMAT('1***** STRESS OUTPUT FOR STATIC LINEAR ANALYSIS *****',/, FEA05650
     *       '+',T8,40(' '),/,'-',T2,'ELEMENT',3X,'NODE',9X,'STRESS  XX',FEA05660
     *       5X,'STRESS  YY',5X,'STRESS  XY',/,'+',T2,7('_'),3X,4('_'),  FEA05670
     *       9X,3(10('_'),5X),/,'-')                                    FEA05680
      DO 10 I=1,NE                                                      FEA05690
         IK=IELMAT(I)                                                   FEA05700
         APOIS=AMATP(IK,2)                                              FEA05710
         E11=AMATP(IK,1)/(1-APOIS**2)                                   FEA05720
         E12=E11*APOIS                                                  FEA05730
         E33=E11*(1-APOIS)/2                                            FEA05740
         DO 20 J=1,8                                                    FEA05750
            DO 30 K=1,2                                                 FEA05760
```

```
                KK=ID(IEL(I,J),K)                                                FEA05770
                JJ=J*2-2+K                                                       FEA05780
                IF (KK.GT.0) THEN                                                FEA05790
                   D(JJ)=UF(KK)                                                  FEA05800
                ELSE                                                             FEA05810
                   D(JJ)=0.                                                      FEA05820
                END IF                                                           FEA05830
30           CONTINUE                                                            FEA05840
20        CONTINUE                                                               FEA05850
          DO 40 J=1,8                                                            FEA05860
             XA=PTNOD(1,J)                                                       FEA05870
             YB=PTNOD(2,J)                                                       FEA05880
             CALL SHAPE(XA,YB,I,DETJAC)                                          FEA05890
             DO 50 JJ=1,8                                                        FEA05900
                LL=2*JJ                                                          FEA05910
                KK=LL-1                                                          FEA05920
                EB(1,KK)=B(1,KK)*E11                                             FEA05930
                EB(2,KK)=B(1,KK)*E12                                             FEA05940
                EB(3,KK)=B(3,KK)*E33                                             FEA05950
                EB(1,LL)=B(2,LL)*E12                                             FEA05960
                EB(2,LL)=B(2,LL)*E11                                             FEA05970
                EB(3,LL)=B(3,LL)*E33                                             FEA05980
50           CONTINUE                                                            FEA05990
             DO 60 K=1,3                                                         FEA06000
                SS(K)=0.                                                         FEA06010
                DO 70 L=1,16                                                     FEA06020
                SS(K)=SS(K)+EB(K,L)*D(L)                                         FEA06030
70              CONTINUE                                                         FEA06040
60           CONTINUE                                                            FEA06050
             WRITE(2,201) IEL(I,J),SS                                            FEA06060
201          FORMAT(T12,I3,10X,3(1PE10.3E2,5X))                                  FEA06070
             IF (J.EQ.1) WRITE(2,202) I                                          FEA06080
202          FORMAT('+',2X,I3)                                                   FEA06090
40        CONTINUE                                                               FEA06100
          WRITE(2,203)                                                           FEA06110
203       FORMAT(/)                                                              FEA06120
10     CONTINUE                                                                  FEA06130
       RETURN                                                                    FEA06140
       END                                                                       FEA06150
       SUBROUTINE NONLIN                                                         FEA06160
C      NONLINEAR ANALYSIS                                                        FEA06170
       COMMON /A/ ICHECK,IEXE,NN,NE,NMP                                          FEA06180
       COMMON /B/ X(1000),Y(1000),IEL(250,8),IELMAT(250),AMATP(10,10),           FEA06190
      *           ITYPE(10)                                                      FEA06200
       COMMON /C/ ID(1000,2),NEQ,ALOAD(1000),UF(1000),S(1000,80),MBAND           FEA06210
       COMMON /D/ PTN(4,4),WGT(4,4),PTNOD(2,8),B(3,16),EB(3,16),NDOF(16)         FEA06220
       COMMON /E/ BLOAD(1000)                                                    FEA06230
       COMMON /F/ ALPHA,E1MAX,SMX,SMY,EX(16,3,3,250),IGAUSS,U(1000)              FEA06240
       REAL D(16),STRAIN(3),STRESS(3),RLOAD(16),E(3,3),                          FEA06250
      *     CLOAD(1000),AVERAG(11)                                             FEA06260
       READ(1,101) IDNOD,IXY,NINC,NITE,ISOFT,IGAUSS,CONV,DINC                    FEA06270
101    FORMAT(6I5,2F10.0)                                                        FEA06280
       WRITE(2,102) IDNOD,IXY,NINC,NITE,ISOFT,IGAUSS,DINC,CONV                   FEA06290
102    FORMAT('1','PARAMETERS FOR NON-LINEAR ANALYSIS',/,'+',34('_'),            FEA06300
      */,/,/,T2,'CONTROL NODE',T30,I5,T40,'DIRECTION',I2,/,T2,                   FEA06310
      *'LOAD STEPS',T30,I5,/,T2,'MAX. ITERATION',T30,I5,/,T2,                    FEA06320
      *'SOFTENING MODEL',T30,I5,/,T2,'GAUSS POINTS',T30,I5,/,T2,                 FEA06330
      *'DISPLACEMENT INCREMENT',T25,1PE10.3E2,/,T2,                              FEA06340
      *'CONVERGENCE CRITERIA',T25,1PE10.3E2)                                     FEA06350
       READ(1,401) ALPHA,E1MAX,SMX,SMY,ESH,EU,FU                                 FEA06360
401    FORMAT(3F10.0)                                                            FEA06370
       WRITE(2,402) ALPHA,E1MAX,SMX,SMY,ESH,EU,FU                                FEA06380
402    FORMAT(/,T2,'ALPHA (ISOFT=1)',T25,1PE10.3E2,                              FEA06390
      *       /,T2,'BETA  (ISOFT=1)',T25,1PE10.3E2,                             FEA06400
      *       /,T2,'SMX',T25,1PE10.3E2,/,T2,'SMY',T25,1PE10.3E2,                FEA06410
      *       /,T2,'E SH',T25,1PE10.3E2,/,T2,'E U',T25,1PE10.3E2,               FEA06420
      *       /,T2,'FU',T25,1PE10.3E2)                                          FEA06430
       IF (ICHECK.EQ.4) CALL PLOT1(NINC)                                         FEA06440
       SMX=SMX*1.5                                                               FEA06450
       SMY=SMY*1.5                                                               FEA06460
       IUL=ID(IDNOD,IXY)                                                         FEA06470
       IF (IUL.LE.0) THEN                                                        FEA06480
```

```
      WRITE(2,103) IDNOD,IXY                                            FEA06490
103   FORMAT(T2,'CONTROL NODE IS CONSTRAINT OR UNEXISTANT',10X,         FEA06500
     *       '*****  EXECUTION STOPPED  *****')                        FEA06510
      STOP                                                              FEA06520
     END IF                                                             FEA06530
     DO 10 I=1,NEQ                                                      FEA06540
      U(I)=0.                                                           FEA06550
10   CONTINUE                                                           FEA06560
     FORCE=0.                                                           FEA06570
     DO 20 IINC=1,NINC                                                  FEA06580
      U(IUL)=IINC*DINC                                                  FEA06590
      KFLAG=0                                                           FEA06600
      WRITE(2,104) IINC,U(IUL)                                          FEA06610
104   FORMAT('1',10('*'),5X,'DISPLACEMENT INCREMENT  ',I2,10X,          FEA06620
     *       1PE10.3E2,5X,10('*'),/,/,T2,'ITERATION',T15,               FEA06630
     *       'CONVERGENCE RATIO',T35,'DELTA',T49,'FORCE',/)             FEA06640
      DO 30 ITE=1,NITE                                                  FEA06650
       DO 40 I=1,NEQ                                                    FEA06660
        ALOAD(I)=0.                                                     FEA06670
40     CONTINUE                                                         FEA06680
       IF (KFLAG.EQ.1) THEN                                             FEA06690
        WRITE(2,106)                                                    FEA06700
106     FORMAT(/,/,/,T2,'ELEMENT',T10,'GAUSS',T26,'STRAIN',T49,         FEA06710
     *       'STEEL STRESSES',T86,'CONCRETE STRESSES',/,T10,'POINT',    FEA06720
     *       T17,'XX',T28,'YY',T39,'XY',T46,'HORIZONTAL',T58,           FEA06730
     *       'VERTICAL',T71,'THETA',T84,'FC1',T91,'CODE',T100,          FEA06740
     *       'FC2',T107,'CODE',T112,'CRACK WIDTH',/,'+',121('_'),/)     FEA06750
       END IF                                                           FEA06760
       DO 50 I=1,NE                                                     FEA06770
        DO 60 J=1,8                                                     FEA06780
         DO 70 K=1,2                                                    FEA06790
          KK=ID(IEL(I,J),K)                                             FEA06800
          JJ=J*2-2+K                                                    FEA06810
          NDOF(JJ)=KK                                                   FEA06820
          IF (KK.GT.0) THEN                                             FEA06830
           D(JJ)=U(KK)                                                  FEA06840
          ELSE                                                          FEA06850
           D(JJ)=0.                                                     FEA06860
          END IF                                                        FEA06870
70       CONTINUE                                                       FEA06880
60      CONTINUE                                                        FEA06890
        IK=IELMAT(I)                                                    FEA06900
        IF (ITYPE(IK).EQ.1) THEN                                        FEA06910
         NGAUSS=2                                                       FEA06920
        ELSE                                                            FEA06930
         NGAUSS=IGAUSS                                                  FEA06940
        END IF                                                          FEA06950
        IF (KFLAG.EQ.1) WRITE(2,107)                                    FEA06960
107     FORMAT(T2,/)                                                    FEA06970
        DO 80 NA=1,NGAUSS                                               FEA06980
         XA=PTN(NA,NGAUSS)                                              FEA06990
         DO 90 NB=1,NGAUSS                                              FEA07000
          YB=PTN(NB,NGAUSS)                                             FEA07010
          CALL SHAPE(XA,YB,I,DETJAC)                                    FEA07020
          DO 100 J=1,3                                                  FEA07030
           STRAIN(J)=0.                                                 FEA07040
           DO 110 K=1,16                                                FEA07050
            STRAIN(J)=STRAIN(J)+B(J,K)*D(K)                             FEA07060
110        CONTINUE                                                     FEA07070
100       CONTINUE                                                      FEA07080
          IF (ITYPE(IK).EQ.1) THEN                                      FEA07090
           APOIS=AMATP(IK,2)                                            FEA07100
           E(1,1)=AMATP(IK,1)/(1-APOIS**2)                              FEA07110
           E(1,2)=E(1,1)*APOIS                                          FEA07120
           E(3,3)=E(1,1)*(1-APOIS)/2                                    FEA07130
           E(1,3)=0.                                                    FEA07140
           E(2,1)=E(1,2)                                                FEA07150
           E(2,3)=0.                                                    FEA07160
           E(3,1)=0.                                                    FEA07170
           E(3,2)=0.                                                    FEA07180
           E(2,2)=E(1,1)                                                FEA07190
           DO 120 J=1,3                                                 FEA07200
```

```
                        STRESS(J)=0.                                                    FEA07210
                        DO 130 K=1,3                                                    FEA07220
                           STRESS(J)=STRESS(J)+E(J,K)*STRAIN(K)                         FEA07230
130                     CONTINUE                                                        FEA07240
120                  CONTINUE                                                         FEA07250
                     ELSE                                                             FEA07260
                        CALL FIELD(STRAIN,STRESS,IK,STH,STV,ANG,STRX,                 FEA07270
     *                          K1,STRY,K2,ISOFT,W,KFLAG,E,ESH,EU,FU)                FEA07280
                     END IF                                                           FEA07290
                     IF (KFLAG.EQ.1) THEN                                             FEA07300
                        KGAUSS=NB+(NA-1)*NGAUSS                                       FEA07310
                        IF (ITYPE(IK).EQ.1) THEN                                      FEA07320
                           WRITE(2,201) KGAUSS,STRAIN,STRESS                          FEA07330
201                        FORMAT(T11,I2,6(1PE10.3E2,1X))                             FEA07340
                           IF (KGAUSS.EQ.1) WRITE(2,202) I                            FEA07350
202                        FORMAT('+',T3,I3,T80,                                      FEA07360
     *                          'ELASTIC STRESSES XX YY XY')                         FEA07370
                        ELSE                                                          FEA07380
                           WRITE(2,203) KGAUSS,STRAIN,STH,STV,ANG*57.29,              FEA07390
     *                                STRX,K1,STRY,K2,W                             FEA07400
203                        FORMAT(T11,I2,6(1PE10.3E2,1X),T80,                         FEA07410
     *                          3(1PE10.3E2,2X,I2,2X))                               FEA07420
                           IF (KGAUSS.EQ.1) WRITE(2,204) I                            FEA07430
204                        FORMAT('+',T3,I3)                                          FEA07440
                           IF (ICHECK.EQ.4) THEN                                      FEA07450
                              IF (KGAUSS.EQ.1) THEN                                   FEA07460
                                 DO 620 J=1,11                                        FEA07470
                                    AVERAG(J)=0.                                      FEA07480
620                              CONTINUE                                             FEA07490
                                 FAC=NGAUSS**2                                        FEA07500
                              END IF                                                  FEA07510
                              AVERAG(1)=STRAIN(1)/FAC+AVERAG(1)                       FEA07520
                              AVERAG(2)=STRAIN(2)/FAC+AVERAG(2)                       FEA07530
                              AVERAG(3)=STRAIN(3)/FAC+AVERAG(3)                       FEA07540
                              AVERAG(4)=STH/FAC+AVERAG(4)                             FEA07550
                              AVERAG(5)=STV/FAC+AVERAG(5)                             FEA07560
                              IF (ANG.LT.0.) ANG=ANG+1.5708                           FEA07570
                              AVERAG(6)=ANG/FAC+AVERAG(6)                             FEA07580
                              AVERAG(7)=STRX/FAC+AVERAG(7)                            FEA07590
                              AVERAG(8)=K1/FAC+AVERAG(8)                              FEA07600
                              AVERAG(9)=STRY/FAC+AVERAG(9)                            FEA07610
                              AVERAG(10)=K2/FAC+AVERAG(10)                            FEA07620
                              AVERAG(11)=W/FAC+AVERAG(11)                             FEA07630
                              IF (KGAUSS.EQ.NGAUSS**2) THEN                           FEA07640
                                 WRITE(3,304) I,AVERAG                                FEA07650
                                 FORMAT(I10,5(1PE10.3E2),/,T10,                       FEA07660
304                                    6(1PE10.3E2))                                  FEA07670
     *                        END IF                                                  FEA07680
                           END IF                                                     FEA07690
                        END IF                                                        FEA07700
                     END IF                                                           FEA07710
                     DO 140 J=1,16                                                    FEA07720
                        DUM=0.                                                        FEA07730
                        DO 150 K=1,3                                                  FEA07740
                           DUM=DUM+B(K,J)*STRESS(K)                                   FEA07750
                        CONTINUE                                                      FEA07760
150                     RLOAD(J)=DUM*WGT(NA,NGAUSS)*WGT(NB,NGAUSS)*                   FEA07770
     *                          DETJAC*AMATP(IK,3)                                   FEA07780
                                                                                      FEA07790
                     CONTINUE                                                         FEA07800
140                  DO 160 J=1,16                                                    FEA07810
                        K=NDOF(J)                                                     FEA07820
                        IF (K.GT.0) ALOAD(K)=ALOAD(K)-RLOAD(J)                        FEA07830
160                  CONTINUE                                                         FEA07840
90                 CONTINUE                                                         FEA07850
80                 CONTINUE                                                         FEA07860
50              CONTINUE                                                            FEA07870
                IF (KFLAG.EQ.1) THEN                                                FEA07880
                   CALL DISPLI                                                      FEA07890
                   GOTO 20                                                          FEA07900
                END IF                                                              FEA07910
                DO 165 I=1,NEQ                                                      FEA07920
```

```
               ALOAD(I)=ALOAD(I)+BLOAD(I)*FORCE                                 FEA07930
               CLOAD(I)=ALOAD(I)                                                FEA07940
  165        CONTINUE                                                           FEA07950
             IF (ITE.EQ.1) DUNORM=0.                                            FEA07960
             UNORM=0.                                                           FEA07970
             CALL SOLVE(2)                                                      FEA07980
             DELTA=-ALOAD(IUL)/UF(IUL)                                          FEA07990
             DO 170 I=1,NEQ                                                     FEA08000
               U(I)=U(I)+ALOAD(I)+DELTA*UF(I)                                   FEA08010
               IF (ITE.EQ.1) DUNORM=DUNORM+(ALOAD(I)+DELTA*UF(I))*              FEA08020
     *                                CLOAD(I)                                  FEA08030
               UNORM=UNORM+(ALOAD(I)+DELTA*UF(I))*CLOAD(I)                      FEA08040
  170        CONTINUE                                                           FEA08050
             FORCE=FORCE+DELTA                                                  FEA08060
             RATIO=UNORM/DUNORM                                                 FEA08070
             WRITE(2,301) ITE,RATIO,DELTA,FORCE                                 FEA08080
  301        FORMAT(T5,I2,T19,3(1PE10.3E2,4X))                                  FEA08090
             IF (ABS(DELTA).LT.CONV*FORCE) THEN                                 FEA08100
               KFLAG=1                                                          FEA08110
               WRITE(2,302) FORCE                                               FEA08120
  302          FORMAT(/,/,/,T2,'EXTERNAL TOTAL FORCE = ',1PE10.3E2)           FEA08130
               WRITE(4,333) U(IUL),FORCE                                        FEA08140
  333          FORMAT(T2,'DISPL = ',1PE10.3E2,10X,'FORCE = ',1PE10.3E2)       FEA08150
               IF (ICHECK.EQ.4) THEN                                            FEA08160
                 WRITE(3,303) U(IUL),FORCE                                      FEA08170
                 DO 500 J=1,2                                                   FEA08180
                   DO 510 K=1,NN                                                FEA08190
                     IF (ID(K,J).GT.0) THEN                                     FEA08200
                       CLOAD(K)=U(ID(K,J))                                      FEA08210
                     ELSE                                                       FEA08220
                       CLOAD(K)=0.                                              FEA08230
                     END IF                                                     FEA08240
  510                CONTINUE                                                   FEA08250
  303                FORMAT(8(1PE10.3E2))                                       FEA08260
  500              CONTINUE                                                     FEA08270
               END IF                                                           FEA08280
             END IF                                                             FEA08290
   30      CONTINUE                                                           FEA08300
           WRITE(2,306)                                                       FEA08310
  306      FORMAT(T2,'*****  CONVERGENCE NOT ACHEIVED - EXECUTION STOPPED     FEA08320
     * *****')                                                                 FEA08330
           STOP                                                               FEA08340
   20    CONTINUE                                                           FEA08350
         RETURN                                                             FEA08360
         END                                                                FEA08370
         SUBROUTINE PLOT1(NINC)                                             FEA08380
C        GENERATE PLOTTING FILE                                             FEA08390
         COMMON /A/ ICHECK,IEXE,NN,NE,NMP                                   FEA08400
         COMMON /B/ X(1000),Y(1000),IEL(250,8),IELMAT(250),AMATP(10,10),    FEA08410
     *              ITYPE(10)                                               FEA08420
         WRITE(3,101) NN,NE,NINC                                            FEA08430
  101    FORMAT(5I5)                                                        FEA08440
         WRITE(3,102) (X(I),I=1,NN)                                         FEA08450
         WRITE(3,102) (Y(I),I=1,NN)                                         FEA08460
  102    FORMAT(8(1PE10.3E2))                                               FEA08470
         DO 10 I=1,NE                                                       FEA08480
           K=ITYPE(IELMAT(I))                                               FEA08490
           WRITE(3,103) I,K,(IEL(I,J),J=1,8)                                FEA08500
  103      FORMAT(10I5)                                                     FEA08510
   10    CONTINUE                                                           FEA08520
         RETURN                                                             FEA08530
         END                                                                FEA08540
         SUBROUTINE FIELD(STRAIN,STRESS,IK,STH,STV,ANG,F1,K1,F2,K2,         FEA08550
C        COMPRESSION FIELD THEORY                                           FEA08560
     *                   ISOFT,W,KFLAG,E,ESH,EU,FU)                         FEA08570
         COMMON /B/ X(1000),Y(1000),IEL(250,8),IELMAT(250),AMATP(10,10),    FEA08580
     *              ITYPE(10)                                               FEA08590
         COMMON /F/ ALPHA,E1MAX,SMX,SMY,EX(16,3,3,250),IGAUSS,U(1000)       FEA08600
         REAL STRAIN(3),STRESS(3),ANG,M,E(3,3),TE(3,3),ETE(3,3)             FEA08610
         EL=STRAIN(1)                                                       FEA08620
         ET=STRAIN(2)                                                       FEA08630
         GM=STRAIN(3)                                                       FEA08640
```

```
      SQ=SQRT(((EL-ET)*.5)**2+(GM*.5)**2)                                FEA08650
      AVG=(EL+ET)*.5                                                     FEA08660
      E1=AVG+SQ                                                          FEA08670
      E2=AVG-SQ                                                          FEA08680
      ELT=EL-ET                                                          FEA08690
      IF (ELT.EQ.0..AND.GM.EQ.0.) THEN                                   FEA08700
         ANG=0.                                                          FEA08710
      ELSE                                                               FEA08720
         ANG=.5*ATAN2(GM,ELT)                                            FEA08730
      END IF                                                             FEA08740
      FC=AMATP(IK,4)                                                     FEA08750
      E0=AMATP(IK,5)                                                     FEA08760
      FT=AMATP(IK,6)                                                     FEA08770
      ES=AMATP(IK,7)                                                     FEA08780
      EY=AMATP(IK,8)                                                     FEA08790
      RH=AMATP(IK,9)                                                     FEA08800
      RV=AMATP(IK,10)                                                    FEA08810
      FY=ES*EY                                                           FEA08820
      EC=2*FC/E0                                                         FEA08830
      EPCR=FT/EC                                                         FEA08840
      C=COS(ANG)                                                         FEA08850
      S=SIN(ANG)                                                         FEA08860
      M=-ALPHA*FT/(E1MAX-1.)/EPCR                                        FEA08870
      B=-M*E1MAX*EPCR                                                    FEA08880
      W=0.                                                               FEA08890
C-----STRESSES IN REINFORCEMENT                                          FEA08900
      IF (ABS(EL).LE.EY) THEN                                            FEA08910
         STH=EL*ES                                                       FEA08920
      ELSE IF (ABS(EL).LT.ESH) THEN                                      FEA08930
         STH=SIGN(FY,EL)                                                 FEA08940
      ELSE                                                               FEA08950
        DE=EU-ESH                                                        FEA08960
        DF=FU-FY                                                         FEA08970
        A1=DF/(DE**2-2*DE**2)                                            FEA08980
        A2=-2*A1*DE                                                      FEA08990
        XX=ABS(EL)-ESH                                                   FEA09000
        YY=A1*XX**2+A2*XX                                                FEA09010
        STH=(YY+FY)*SIGN(1.,EL)                                          FEA09020
      END IF                                                             FEA09030
      IF (ABS(ET).LE.EY) THEN                                            FEA09040
         STV=ET*ES                                                       FEA09050
      ELSE IF (ABS(ET).LT.ESH) THEN                                      FEA09060
         STV=SIGN(FY,ET)                                                 FEA09070
      ELSE                                                               FEA09080
        DE=EU-ESH                                                        FEA09090
        DF=FU-FY                                                         FEA09100
        A1=DF/(DE**2-2*DE**2)                                            FEA09110
        A2=-2*A1*DE                                                      FEA09120
        XX=ABS(ET)-ESH                                                   FEA09130
        YY=A1*XX**2+A2*XX                                                FEA09140
        STV=(YY+FY)*SIGN(1.,ET)                                          FEA09150
      END IF                                                             FEA09160
C-----CALCULATE F1                                                       FEA09170
      IF (E1.LT.0.) THEN                                                 FEA09180
         E10=E1/E0                                                       FEA09190
         F1=FC*(2*E10-E10**2)                                            FEA09200
         IF (F1.GT.0.) F1=0.                                             FEA09210
         IF (E1.GE.E0) THEN                                              FEA09220
            K1=-1                                                        FEA09230
         ELSE IF (E1.GE.2*E0) THEN                                       FEA09240
            K1=-2                                                        FEA09250
         ELSE                                                            FEA09260
            K1=-3                                                        FEA09270
         END IF                                                          FEA09280
      ELSE IF (E1.LT.EPCR) THEN                                          FEA09290
         F1=EC*E1                                                        FEA09300
         K1=1                                                            FEA09310
      ELSE                                                               FEA09320
         W=E1/(S/SMX+C/SMY)                                              FEA09330
         IF (ISOFT.EQ.0) THEN                                            FEA09340
            F1=FT/(1+SQRT(200*E1))                                       FEA09350
         ELSE                                                            FEA09360
```

```
            F1=M*E1+B                                                   FEA09370
            IF (F1.LT.0.) F1=0.                                         FEA09380
         END IF                                                         FEA09390
         K1=2                                                           FEA09400
         F1MAX=RH*(FY-STH)*S**2+RV*(FY-STV)*C**2                        FEA09410
         IF (F1.GT.F1MAX) THEN                                          FEA09420
            F1=F1MAX                                                    FEA09430
            IF (F1.LT.0.) F1=0.                                         FEA09440
            K1=3                                                        FEA09450
         END IF                                                         FEA09460
      END IF                                                            FEA09470
C-----CALCULATE F2                                                      FEA09480
      IF (E2.GT.EPCR) THEN                                              FEA09490
         IF (ISOFT.EQ.0) THEN                                           FEA09500
            F2=FT/(1+SQRT(200*E2))                                      FEA09510
         ELSE                                                           FEA09520
            F2=M*E2+B                                                   FEA09530
            IF (F2.LT.0.) F2=0.                                         FEA09540
         END IF                                                         FEA09550
         K2=-2                                                          FEA09560
         F2MAX=RH*(FY-STH)*C**2+RV*(FY-STV)*S**2                        FEA09570
         IF (F2.GT.F2MAX) THEN                                          FEA09580
            F2=F2MAX                                                    FEA09590
            IF (F2.LT.0.) F2=0.                                         FEA09600
            K2=-3                                                       FEA09610
         END IF                                                         FEA09620
      ELSE IF (E2.LT.EPCR.AND.E2.GT.0.) THEN                            FEA09630
         F2=EC*E2                                                       FEA09640
         K2=-1                                                          FEA09650
      ELSE                                                              FEA09660
         E20=E2/E0                                                      FEA09670
         FMAX=FC/(.8-.34*E1/E0)                                         FEA09680
         IF (FMAX.LT.FC) FMAX=FC                                        FEA09690
         IF (E1.LT.0.) FMAX=FC                                          FEA09700
         IF (E2.GE.E0) THEN                                             FEA09710
            F2=FMAX*(2*E20-E20**2)                                      FEA09720
         ELSE IF (E2.LT.E0.AND.E2.GE.-.010) THEN                        FEA09730
            M=(1-.3)*FMAX/(E0+.010)                                     FEA09740
            B=FMAX-M*E0                                                 FEA09750
            F2=M*E2+B                                                   FEA09760
         ELSE                                                           FEA09770
            F2=.3*FMAX                                                  FEA09780
         END IF                                                         FEA09790
         IF (E2.GE.E0) THEN                                             FEA09800
            K2=1                                                        FEA09810
         ELSE IF (E2.GE.-.010) THEN                                     FEA09820
            K2=2                                                        FEA09830
         ELSE                                                           FEA09840
            K2=3                                                        FEA09850
         END IF                                                         FEA09860
      END IF                                                            FEA09870
      STRESS(1)=F1*C**2+F2*S**2+RH*STH                                  FEA09880
      STRESS(2)=F1*S**2+F2*C**2+RV*STV                                  FEA09890
      STRESS(3)=(F1-F2)*C*S                                             FEA09900
      RETURN                                                            FEA09910
      END                                                               FEA09920
```

```
          2
WALL 1 - 0.25% HORIZONTAL REINFORCEMENT - FIXED BASE
7 X 14 WALL ELEMENTS AND 1 X 14 ELASTIC TOP BEAM ELEMENTS
          4              0          493          112            3
          2
          3              1
                        15           0.           1.            1
                       491           2.           1.           17
          3             16           0.        1.15
                        17           0.        1.30            1
                       493           2.        1.30           17
          4
          2     8       15          32           49          50          51          34          17          16           1
              112        8          34
          3     1        1          18           35          36          37          20           3           2           2
                7        1           2
               15        8          34
          3    97      409         426          443         444         445         428         411         410           2
              103        1           2
              111        8          34
          3    17       69          86          103         104         105          88          71          70           3
               23        1           2
               95        8          34
          3
          1              1         25E9          .15          .50
          2              2         25E9          .15          .10
                    -25E6        -.0020       1.65E6         2E11       .00215       .0025       .0080
          3              2         25E9          .15          .10
                    -25E6        -.0020       1.65E6         2E11       .00215       .0025      .00800
          2
          2              1            1          477           17
          2              1            2          477           17
          1
          1             1.           16            1
   16     1      1      50            0            2        .0050        .0010
        .50             10.         .250         .284         .016         .110       650E6
```

WALL 1 - 0.25% HORIZONTAL REINFORCEMENT - FIXED BASE
7 X 14 WALL ELEMENTS AND 1 X 14 ELASTIC TOP BEAM ELEMENTS

PARAMETERS: 4 0 493 112 3

NODAL COORDINATES

NODE	X-COOR	Y-COOR	NODE	X-COOR	Y-COOR	NODE	X-COOR	Y-COOR	NODE	X-COOR	Y-COOR
1	0.000E+00	0.000E+00	125	5.000E-01	3.571E-01	249	1.000E+00	7.143E-01	373	1.500E+00	1.150E+00
2	0.000E+00	7.143E-02	126	5.000E-01	4.286E-01	250	1.000E+00	7.857E-01	374	1.500E+00	1.300E+00
3	0.000E+00	1.429E-01	127	5.000E-01	5.000E-01	251	1.000E+00	8.571E-01	375	1.571E+00	0.000E+00
4	0.000E+00	2.143E-01	128	5.000E-01	5.714E-01	252	1.000E+00	9.286E-01	376	1.571E+00	7.143E-02
5	0.000E+00	2.857E-01	129	5.000E-01	6.429E-01	253	1.000E+00	1.000E+00	377	1.571E+00	1.429E-01
6	0.000E+00	3.571E-01	130	5.000E-01	7.143E-01	254	1.000E+00	1.150E+00	378	1.571E+00	2.143E-01
7	0.000E+00	4.286E-01	131	5.000E-01	7.857E-01	255	1.000E+00	1.300E+00	379	1.571E+00	2.857E-01
8	0.000E+00	5.000E-01	132	5.000E-01	8.571E-01	256	1.071E+00	0.000E+00	380	1.571E+00	3.571E-01
9	0.000E+00	5.714E-01	133	5.000E-01	9.286E-01	257	1.071E+00	7.143E-02	381	1.571E+00	4.286E-01
10	0.000E+00	6.429E-01	134	5.000E-01	1.000E+00	258	1.071E+00	1.429E-01	382	1.571E+00	5.000E-01
11	0.000E+00	7.143E-01	135	5.000E-01	1.150E+00	259	1.071E+00	2.143E-01	383	1.571E+00	5.714E-01
12	0.000E+00	7.857E-01	136	5.000E-01	1.300E+00	260	1.071E+00	2.857E-01	384	1.571E+00	6.429E-01
13	0.000E+00	8.571E-01	137	5.714E-01	0.000E+00	261	1.071E+00	3.571E-01	385	1.571E+00	7.143E-01
14	0.000E+00	9.286E-01	138	5.714E-01	7.143E-02	262	1.071E+00	4.286E-01	386	1.571E+00	7.857E-01
15	0.000E+00	1.000E+00	139	5.714E-01	1.429E-01	263	1.071E+00	5.000E-01	387	1.571E+00	8.571E-01
16	0.000E+00	1.150E+00	140	5.714E-01	2.143E-01	264	1.071E+00	5.714E-01	388	1.571E+00	9.286E-01
17	0.000E+00	1.300E+00	141	5.714E-01	2.857E-01	265	1.071E+00	6.429E-01	389	1.571E+00	1.000E+00
18	7.143E-02	0.000E+00	142	5.714E-01	3.571E-01	266	1.071E+00	7.143E-01	390	1.571E+00	1.150E+00
19	7.143E-02	7.143E-02	143	5.714E-01	4.286E-01	267	1.071E+00	7.857E-01	391	1.571E+00	1.300E+00
20	7.143E-02	1.429E-01	144	5.714E-01	5.000E-01	268	1.071E+00	8.571E-01	392	1.643E+00	0.000E+00
21	7.143E-02	2.143E-01	145	5.714E-01	5.714E-01	269	1.071E+00	9.286E-01	393	1.643E+00	7.143E-02
22	7.143E-02	2.857E-01	146	5.714E-01	6.429E-01	270	1.071E+00	1.000E+00	394	1.643E+00	1.429E-01
23	7.143E-02	3.571E-01	147	5.714E-01	7.143E-01	271	1.071E+00	1.150E+00	395	1.643E+00	2.143E-01
24	7.143E-02	4.286E-01	148	5.714E-01	7.857E-01	272	1.071E+00	1.300E+00	396	1.643E+00	2.857E-01
25	7.143E-02	5.000E-01	149	5.714E-01	8.571E-01	273	1.143E+00	0.000E+00	397	1.643E+00	3.571E-01
26	7.143E-02	5.714E-01	150	5.714E-01	9.286E-01	274	1.143E+00	7.143E-02	398	1.643E+00	4.286E-01
27	7.143E-02	6.429E-01	151	5.714E-01	1.000E+00	275	1.143E+00	1.429E-01	399	1.643E+00	5.000E-01
28	7.143E-02	7.143E-01	152	5.714E-01	1.150E+00	276	1.143E+00	2.143E-01	400	1.643E+00	5.714E-01
29	7.143E-02	7.857E-01	153	5.714E-01	1.300E+00	277	1.143E+00	2.857E-01	401	1.643E+00	6.429E-01
30	7.143E-02	8.571E-01	154	6.429E-01	0.000E+00	278	1.143E+00	3.571E-01	402	1.643E+00	7.143E-01
31	7.143E-02	9.286E-01	155	6.429E-01	7.143E-02	279	1.143E+00	4.286E-01	403	1.643E+00	7.857E-01
32	7.143E-02	1.000E+00	156	6.429E-01	1.429E-01	280	1.143E+00	5.000E-01	404	1.643E+00	8.571E-01
33	7.143E-02	1.150E+00	157	6.429E-01	2.143E-01	281	1.143E+00	5.714E-01	405	1.643E+00	9.286E-01
34	7.143E-02	1.300E+00	158	6.429E-01	2.857E-01	282	1.143E+00	6.429E-01	406	1.643E+00	1.000E+00
35	1.429E-01	0.000E+00	159	6.429E-01	3.571E-01	283	1.143E+00	7.143E-01	407	1.643E+00	1.150E+00
36	1.429E-01	7.143E-02	160	6.429E-01	4.286E-01	284	1.143E+00	7.857E-01	408	1.643E+00	1.300E+00
37	1.429E-01	1.429E-01	161	6.429E-01	5.000E-01	285	1.143E+00	8.571E-01	409	1.714E+00	0.000E+00
38	1.429E-01	2.143E-01	162	6.429E-01	5.714E-01	286	1.143E+00	9.286E-01	410	1.714E+00	7.143E-02
39	1.429E-01	2.857E-01	163	6.429E-01	6.429E-01	287	1.143E+00	1.000E+00	411	1.714E+00	1.429E-01
40	1.429E-01	3.571E-01	164	6.429E-01	7.143E-01	288	1.143E+00	1.150E+00	412	1.714E+00	2.143E-01
41	1.429E-01	4.286E-01	165	6.429E-01	7.857E-01	289	1.143E+00	1.300E+00	413	1.714E+00	2.857E-01
42	1.429E-01	5.000E-01	166	6.429E-01	8.571E-01	290	1.214E+00	0.000E+00	414	1.714E+00	3.571E-01
43	1.429E-01	5.714E-01	167	6.429E-01	9.286E-01	291	1.214E+00	7.143E-02	415	1.714E+00	4.286E-01
44	1.429E-01	6.429E-01	168	6.429E-01	1.000E+00	292	1.214E+00	1.429E-01	416	1.714E+00	5.000E-01
45	1.429E-01	7.143E-01	169	6.429E-01	1.150E+00	293	1.214E+00	2.143E-01	417	1.714E+00	5.714E-01
46	1.429E-01	7.857E-01	170	6.429E-01	1.300E+00	294	1.214E+00	2.857E-01	418	1.714E+00	6.429E-01
47	1.429E-01	8.571E-01	171	7.143E-01	0.000E+00	295	1.214E+00	3.571E-01	419	1.714E+00	7.143E-01
48	1.429E-01	9.286E-01	172	7.143E-01	7.143E-02	296	1.214E+00	4.286E-01	420	1.714E+00	7.857E-01
49	1.429E-01	1.000E+00	173	7.143E-01	1.429E-01	297	1.214E+00	5.000E-01	421	1.714E+00	8.571E-01
50	1.429E-01	1.150E+00	174	7.143E-01	2.143E-01	298	1.214E+00	5.714E-01	422	1.714E+00	9.286E-01
51	1.429E-01	1.300E+00	175	7.143E-01	2.857E-01	299	1.214E+00	6.429E-01	423	1.714E+00	1.000E+00
52	2.143E-01	0.000E+00	176	7.143E-01	3.571E-01	300	1.214E+00	7.143E-01	424	1.714E+00	1.150E+00
53	2.143E-01	7.143E-02	177	7.143E-01	4.286E-01	301	1.214E+00	7.857E-01	425	1.714E+00	1.300E+00
54	2.143E-01	1.429E-01	178	7.143E-01	5.000E-01	302	1.214E+00	8.571E-01	426	1.786E+00	0.000E+00

55	2.143E-01	2.143E-01	179	7.143E-01	5.714E-01	303	1.214E+00	9.286E-01	427	1.786E+00	7.143E-02
56	2.143E-01	2.857E-01	180	7.143E-01	6.429E-01	304	1.214E+00	1.000E+00	428	1.786E+00	1.429E-01
57	2.143E-01	3.571E-01	181	7.143E-01	7.143E-01	305	1.214E+00	1.150E+00	429	1.786E+00	2.143E-01
58	2.143E-01	4.286E-01	182	7.143E-01	7.857E-01	306	1.214E+00	1.300E+00	430	1.786E+00	2.857E-01
59	2.143E-01	5.000E-01	183	7.143E-01	8.571E-01	307	1.286E+00	0.000E+00	431	1.786E+00	3.571E-01
60	2.143E-01	5.714E-01	184	7.143E-01	9.286E-01	308	1.286E+00	7.143E-02	432	1.786E+00	4.286E-01
61	2.143E-01	6.429E-01	185	7.143E-01	1.000E+00	309	1.286E+00	1.429E-01	433	1.786E+00	5.000E-01
62	2.143E-01	7.143E-01	186	7.143E-01	1.150E+00	310	1.286E+00	2.143E-01	434	1.786E+00	5.714E-01
63	2.143E-01	7.857E-01	187	7.143E-01	1.300E+00	311	1.286E+00	2.857E-01	435	1.786E+00	6.429E-01
64	2.143E-01	8.571E-01	188	7.857E-01	0.000E+00	312	1.286E+00	3.571E-01	436	1.786E+00	7.143E-01
65	2.143E-01	9.286E-01	189	7.857E-01	7.143E-02	313	1.286E+00	4.286E-01	437	1.786E+00	7.857E-01
66	2.143E-01	1.000E+00	190	7.857E-01	1.429E-01	314	1.286E+00	5.000E-01	438	1.786E+00	8.571E-01
67	2.143E-01	1.150E+00	191	7.857E-01	2.143E-01	315	1.286E+00	5.714E-01	439	1.786E+00	9.286E-01
68	2.143E-01	1.300E+00	192	7.857E-01	2.857E-01	316	1.286E+00	6.429E-01	440	1.786E+00	1.000E+00
69	2.857E-01	0.000E+00	193	7.857E-01	3.571E-01	317	1.286E+00	7.143E-01	441	1.786E+00	1.150E+00
70	2.857E-01	7.143E-02	194	7.857E-01	4.286E-01	318	1.286E+00	7.857E-01	442	1.786E+00	1.300E+00
71	2.857E-01	1.429E-01	195	7.857E-01	5.000E-01	319	1.286E+00	8.571E-01	443	1.857E+00	0.000E+00
72	2.857E-01	2.143E-01	196	7.857E-01	5.714E-01	320	1.286E+00	9.286E-01	444	1.857E+00	7.143E-02
73	2.857E-01	2.857E-01	197	7.857E-01	6.429E-01	321	1.286E+00	1.000E+00	445	1.857E+00	1.429E-01
74	2.857E-01	3.571E-01	198	7.857E-01	7.143E-01	322	1.286E+00	1.150E+00	446	1.857E+00	2.143E-01
75	2.857E-01	4.286E-01	199	7.857E-01	7.857E-01	323	1.286E+00	1.300E+00	447	1.857E+00	2.857E-01
76	2.857E-01	5.000E-01	200	7.857E-01	8.571E-01	324	1.357E+00	0.000E+00	448	1.857E+00	3.571E-01
77	2.857E-01	5.714E-01	201	7.857E-01	9.286E-01	325	1.357E+00	7.143E-02	449	1.857E+00	4.286E-01
78	2.857E-01	6.429E-01	202	7.857E-01	1.000E+00	326	1.357E+00	1.429E-01	450	1.857E+00	5.000E-01
79	2.857E-01	7.143E-01	203	7.857E-01	1.150E+00	327	1.357E+00	2.143E-01	451	1.857E+00	5.714E-01
80	2.857E-01	7.857E-01	204	7.857E-01	1.300E+00	328	1.357E+00	2.857E-01	452	1.857E+00	6.429E-01
81	2.857E-01	8.571E-01	205	8.571E-01	0.000E+00	329	1.357E+00	3.571E-01	453	1.857E+00	7.143E-01
82	2.857E-01	9.286E-01	206	8.571E-01	7.143E-02	330	1.357E+00	4.286E-01	454	1.857E+00	7.857E-01
83	2.857E-01	1.000E+00	207	8.571E-01	1.429E-01	331	1.357E+00	5.000E-01	455	1.857E+00	8.571E-01
84	2.857E-01	1.150E+00	208	8.571E-01	2.143E-01	332	1.357E+00	5.714E-01	456	1.857E+00	9.286E-01
85	2.857E-01	1.300E+00	209	8.571E-01	2.857E-01	333	1.357E+00	6.429E-01	457	1.857E+00	1.000E+00
86	3.571E-01	0.000E+00	210	8.571E-01	3.571E-01	334	1.357E+00	7.143E-01	458	1.857E+00	1.150E+00
87	3.571E-01	7.143E-02	211	8.571E-01	4.286E-01	335	1.357E+00	7.857E-01	459	1.857E+00	1.300E+00
88	3.571E-01	1.429E-01	212	8.571E-01	5.000E-01	336	1.357E+00	8.571E-01	460	1.929E+00	0.000E+00
89	3.571E-01	2.143E-01	213	8.571E-01	5.714E-01	337	1.357E+00	9.286E-01	461	1.929E+00	7.143E-02
90	3.571E-01	2.857E-01	214	8.571E-01	6.429E-01	338	1.357E+00	1.000E+00	462	1.929E+00	1.429E-01
91	3.571E-01	3.571E-01	215	8.571E-01	7.143E-01	339	1.357E+00	1.150E+00	463	1.929E+00	2.143E-01
92	3.571E-01	4.286E-01	216	8.571E-01	7.857E-01	340	1.357E+00	1.300E+00	464	1.929E+00	2.857E-01
93	3.571E-01	5.000E-01	217	8.571E-01	8.571E-01	341	1.429E+00	0.000E+00	465	1.929E+00	3.571E-01
94	3.571E-01	5.714E-01	218	8.571E-01	9.286E-01	342	1.429E+00	7.143E-02	466	1.929E+00	4.286E-01
95	3.571E-01	6.429E-01	219	8.571E-01	1.000E+00	343	1.429E+00	1.429E-01	467	1.929E+00	5.000E-01
96	3.571E-01	7.143E-01	220	8.571E-01	1.150E+00	344	1.429E+00	2.143E-01	468	1.929E+00	5.714E-01
97	3.571E-01	7.857E-01	221	8.571E-01	1.300E+00	345	1.429E+00	2.857E-01	469	1.929E+00	6.429E-01
98	3.571E-01	8.571E-01	222	9.286E-01	0.000E+00	346	1.429E+00	3.571E-01	470	1.929E+00	7.143E-01
99	3.571E-01	9.286E-01	223	9.286E-01	7.143E-02	347	1.429E+00	4.286E-01	471	1.929E+00	7.857E-01
100	3.571E-01	1.000E+00	224	9.286E-01	1.429E-01	348	1.429E+00	5.000E-01	472	1.929E+00	8.571E-01
101	3.571E-01	1.150E+00	225	9.286E-01	2.143E-01	349	1.429E+00	5.714E-01	473	1.929E+00	9.286E-01
102	3.571E-01	1.300E+00	226	9.286E-01	2.857E-01	350	1.429E+00	6.429E-01	474	1.929E+00	1.000E+00
103	4.286E-01	0.000E+00	227	9.286E-01	3.571E-01	351	1.429E+00	7.143E-01	475	1.929E+00	1.150E+00
104	4.286E-01	7.143E-02	228	9.286E-01	4.286E-01	352	1.429E+00	7.857E-01	476	1.929E+00	1.300E+00
105	4.286E-01	1.429E-01	229	9.286E-01	5.000E-01	353	1.429E+00	8.571E-01	477	2.000E+00	0.000E+00
106	4.286E-01	2.143E-01	230	9.286E-01	5.714E-01	354	1.429E+00	9.286E-01	478	2.000E+00	7.143E-02
107	4.286E-01	2.857E-01	231	9.286E-01	6.429E-01	355	1.429E+00	1.000E+00	479	2.000E+00	1.429E-01
108	4.286E-01	3.571E-01	232	9.286E-01	7.143E-01	356	1.429E+00	1.150E+00	480	2.000E+00	2.143E-01
109	4.286E-01	4.286E-01	233	9.286E-01	7.857E-01	357	1.429E+00	1.300E+00	481	2.000E+00	2.857E-01
110	4.286E-01	5.000E-01	234	9.286E-01	8.571E-01	358	1.500E+00	0.000E+00	482	2.000E+00	3.571E-01
111	4.286E-01	5.714E-01	235	9.286E-01	9.286E-01	359	1.500E+00	7.143E-02	483	2.000E+00	4.286E-01
112	4.286E-01	6.429E-01	236	9.286E-01	1.000E+00	360	1.500E+00	1.429E-01	484	2.000E+00	5.000E-01
113	4.286E-01	7.143E-01	237	9.286E-01	1.150E+00	361	1.500E+00	2.143E-01	485	2.000E+00	5.714E-01
114	4.286E-01	7.857E-01	238	9.286E-01	1.300E+00	362	1.500E+00	2.857E-01	486	2.000E+00	6.429E-01
115	4.286E-01	8.571E-01	239	1.000E+00	0.000E+00	363	1.500E+00	3.571E-01	487	2.000E+00	7.143E-01
116	4.286E-01	9.286E-01	240	1.000E+00	7.143E-02	364	1.500E+00	4.286E-01	488	2.000E+00	7.857E-01
117	4.286E-01	1.000E+00	241	1.000E+00	1.429E-01	365	1.500E+00	5.000E-01	489	2.000E+00	8.571E-01
118	4.286E-01	1.150E+00	242	1.000E+00	2.143E-01	366	1.500E+00	5.714E-01	490	2.000E+00	9.286E-01
119	4.286E-01	1.300E+00	243	1.000E+00	2.857E-01	367	1.500E+00	6.429E-01	491	2.000E+00	1.000E+00
120	5.000E-01	0.000E+00	244	1.000E+00	3.571E-01	368	1.500E+00	7.143E-01	492	2.000E+00	1.150E+00
121	5.000E-01	7.143E-02	245	1.000E+00	4.286E-01	369	1.500E+00	7.857E-01	493	2.000E+00	1.300E+00
122	5.000E-01	1.429E-01	246	1.000E+00	5.000E-01	370	1.500E+00	8.571E-01			
123	5.000E-01	2.143E-01	247	1.000E+00	5.714E-01	371	1.500E+00	9.286E-01			
124	5.000E-01	2.857E-01	248	1.000E+00	6.429E-01	372	1.500E+00	1.000E+00			

ELEMENT CONNEXTIVITIES

ELEMENT	NODES								MATERIAL INDEX
1	1	18	35	36	37	20	3	2	2
2	3	20	37	38	39	22	5	4	2
3	5	22	39	40	41	24	7	6	2
4	7	24	41	42	43	26	9	8	2
5	9	26	43	44	45	28	11	10	2
6	11	28	45	46	47	30	13	12	2
7	13	30	47	48	49	32	15	14	2
8	15	32	49	50	51	34	17	16	1
9	35	52	69	70	71	54	37	36	2
10	37	54	71	72	73	56	39	38	2
11	39	56	73	74	75	58	41	40	2
12	41	58	75	76	77	60	43	42	2
13	43	60	77	78	79	62	45	44	2
14	45	62	79	80	81	64	47	46	2
15	47	64	81	82	83	66	49	48	2
16	49	66	83	84	85	68	51	50	1
17	69	86	103	104	105	88	71	70	3
18	71	88	105	106	107	90	73	72	3
19	73	90	107	108	109	92	75	74	3
20	75	92	109	110	111	94	77	76	3
21	77	94	111	112	113	96	79	78	3
22	79	96	113	114	115	98	81	80	3
23	81	98	115	116	117	100	83	82	3
24	83	100	117	118	119	102	85	84	1
25	103	120	137	138	139	122	105	104	3
26	105	122	139	140	141	124	107	106	3
27	107	124	141	142	143	126	109	108	3
28	109	126	143	144	145	128	111	110	3
29	111	128	145	146	147	130	113	112	3
30	113	130	147	148	149	132	115	114	3
31	115	132	149	150	151	134	117	116	3
32	117	134	151	152	153	136	119	118	1
33	137	154	171	172	173	156	139	138	3
34	139	156	173	174	175	158	141	140	3
35	141	158	175	176	177	160	143	142	3
36	143	160	177	178	179	162	145	144	3
37	145	162	179	180	181	164	147	146	3
38	147	164	181	182	183	166	149	148	3
39	149	166	183	184	185	168	151	150	3
40	151	168	185	186	187	170	153	152	1
41	171	188	205	206	207	190	173	172	3
42	173	190	207	208	209	192	175	174	3
43	175	192	209	210	211	194	177	176	3
44	177	194	211	212	213	196	179	178	3
45	179	196	213	214	215	198	181	180	3
46	181	198	215	216	217	200	183	182	3
47	183	200	217	218	219	202	185	184	3
48	185	202	219	220	221	204	187	186	1
49	205	222	239	240	241	224	207	206	3
50	207	224	241	242	243	226	209	208	3
51	209	226	243	244	245	228	211	210	3
52	211	228	245	246	247	230	213	212	3
53	213	230	247	248	249	232	215	214	3
54	215	232	249	250	251	234	217	216	3
55	217	234	251	252	253	236	219	218	3
56	219	236	253	254	255	238	221	220	1
57	239	256	273	274	275	258	241	240	3
58	241	258	275	276	277	260	243	242	3
59	243	260	277	278	279	262	245	244	3
60	245	262	279	280	281	264	247	246	3
61	247	264	281	282	283	266	249	248	3
62	249	266	283	284	285	268	251	250	3
63	251	268	285	286	287	270	253	252	3
64	253	270	287	288	289	272	255	254	1
65	273	290	307	308	309	292	275	274	3
66	275	292	309	310	311	294	277	276	3

67	277	294	311	312	313	296	279	278	3
68	279	296	313	314	315	298	281	280	3
69	281	298	315	316	317	300	283	282	3
70	283	300	317	318	319	302	285	284	3
71	285	302	319	320	321	304	287	286	3
72	287	304	321	322	323	306	289	288	1
73	307	324	341	342	343	326	309	308	3
74	309	326	343	344	345	328	311	310	3
75	311	328	345	346	347	330	313	312	3
76	313	330	347	348	349	332	315	314	3
77	315	332	349	350	351	334	317	316	3
78	317	334	351	352	353	336	319	318	3
79	319	336	353	354	355	338	321	320	3
80	321	338	355	356	357	340	323	322	1
81	341	358	375	376	377	360	343	342	3
82	343	360	377	378	379	362	345	344	3
83	345	362	379	380	381	364	347	346	3
84	347	364	381	382	383	366	349	348	3
85	349	366	383	384	385	368	351	350	3
86	351	368	385	386	387	370	353	352	3
87	353	370	387	388	389	372	355	354	3
88	355	372	389	390	391	374	357	356	1
89	375	392	409	410	411	394	377	376	3
90	377	394	411	412	413	396	379	378	3
91	379	396	413	414	415	398	381	380	3
92	381	398	415	416	417	400	383	382	3
93	383	400	417	418	419	402	385	384	3
94	385	402	419	420	421	404	387	386	3
95	387	404	421	422	423	406	389	388	3
96	389	406	423	424	425	408	391	390	1
97	409	426	443	444	445	428	411	410	2
98	411	428	445	446	447	430	413	412	2
99	413	430	447	448	449	432	415	414	2
100	415	432	449	450	451	434	417	416	2
101	417	434	451	452	453	436	419	418	2
102	419	436	453	454	455	438	421	420	2
103	421	438	455	456	457	440	423	422	2
104	423	440	457	458	459	442	425	424	1
105	443	460	477	478	479	462	445	444	2
106	445	462	479	480	481	464	447	446	2
107	447	464	481	482	483	466	449	448	2
108	449	466	483	484	485	468	451	450	2
109	451	468	485	486	487	470	453	452	2
110	453	470	487	488	489	472	455	454	2
111	455	472	489	490	491	474	457	456	2
112	457	474	491	492	493	476	459	458	1

MATERIAL PROPERTIES

INDEX	LINEAR ANALYSIS			NON-LINEAR ANALYSIS						
	YOUNG	POISSON	THICKNESS	F'C	E0	FT	ES	EY	%H	%V
1	2.500E+10	1.500E-01	5.000E-01							
2	2.500E+10	1.500E-01	1.000E-01	-2.500E+07	-2.000E-03	1.650E+06	2.000E+11	2.150E-03	2.500E-03	8.000E-03
3	2.500E+10	1.500E-01	1.000E-01	-2.500E+07	-2.000E-03	1.650E+06	2.000E+11	2.150E-03	2.500E-03	8.000E-03

BOUNDARY CONDITIONS - ID MATRIX (0 = CONSTRAINT -1 = UNCONNECTED

NODE	X	Y	NODE	X	Y	NODE	X	Y	NODE	X	Y
1	0	0	125	-1	-1	249	355	356	373	-1	-1
2	1	2	126	181	182	250	357	358	374	527	528
3	3	4	127	-1	-1	251	359	360	375	0	0
4	5	6	128	183	184	252	361	362	376	529	530

5	7	8
6	9	10
7	11	12
8	13	14
9	15	16
10	17	18
11	19	20
12	21	22
13	23	24
14	25	26
15	27	28
16	29	30
17	31	32
18	0	0
19	-1	-1
20	33	34
21	-1	-1
22	35	36
23	-1	-1
24	37	38
25	-1	-1
26	39	40
27	-1	-1
28	41	42
29	-1	-1
30	43	44
31	-1	-1
32	45	46
33	-1	-1
34	47	48
35	0	0
36	49	50
37	51	52
38	53	54
39	55	56
40	57	58
41	59	60
42	61	62
43	63	64
44	65	66
45	67	68
46	69	70
47	71	72
48	73	74
49	75	76
50	77	78
51	79	80
52	0	0
53	-1	-1
54	81	82
55	-1	-1
56	83	84
57	-1	-1
58	85	86
59	-1	-1
60	87	88
61	-1	-1
62	89	90
63	-1	-1
64	91	92
65	-1	-1
66	93	94
67	-1	-1
68	95	96
69	0	0
70	97	98
71	99	100
72	101	102
73	103	104
74	105	106
75	107	108
76	109	110

129	-1	-1
130	185	186
131	-1	-1
132	187	188
133	-1	-1
134	189	190
135	-1	-1
136	191	192
137	0	0
138	193	194
139	195	196
140	197	198
141	199	200
142	201	202
143	203	204
144	205	206
145	207	208
146	209	210
147	211	212
148	213	214
149	215	216
150	217	218
151	219	220
152	221	222
153	223	224
154	0	0
155	-1	-1
156	225	226
157	-1	-1
158	227	228
159	-1	-1
160	229	230
161	-1	-1
162	231	232
163	-1	-1
164	233	234
165	-1	-1
166	235	236
167	-1	-1
168	237	238
169	-1	-1
170	239	240
171	0	0
172	241	242
173	243	244
174	245	246
175	247	248
176	249	250
177	251	252
178	253	254
179	255	256
180	257	258
181	259	260
182	261	262
183	263	264
184	265	266
185	267	268
186	269	270
187	271	272
188	0	0
189	-1	-1
190	273	274
191	-1	-1
192	275	276
193	-1	-1
194	277	278
195	-1	-1
196	279	280
197	-1	-1
198	281	282
199	-1	-1
200	283	284

253	363	364
254	365	366
255	367	368
256	0	0
257	-1	-1
258	369	370
259	-1	-1
260	371	372
261	-1	-1
262	373	374
263	-1	-1
264	375	376
265	-1	-1
266	377	378
267	-1	-1
268	379	380
269	-1	-1
270	381	382
271	-1	-1
272	383	384
273	0	0
274	385	386
275	387	388
276	389	390
277	391	392
278	393	394
279	395	396
280	397	398
281	399	400
282	401	402
283	403	404
284	405	406
285	407	408
286	409	410
287	411	412
288	413	414
289	415	416
290	0	0
291	-1	-1
292	417	418
293	-1	-1
294	419	420
295	-1	-1
296	421	422
297	-1	-1
298	423	424
299	-1	-1
300	425	426
301	-1	-1
302	427	428
303	-1	-1
304	429	430
305	-1	-1
306	431	432
307	0	0
308	433	434
309	435	436
310	437	438
311	439	440
312	441	442
313	443	444
314	445	446
315	447	448
316	449	450
317	451	452
318	453	454
319	455	456
320	457	458
321	459	460
322	461	462
323	463	464
324	0	0

377	531	532
378	533	534
379	535	536
380	537	538
381	539	540
382	541	542
383	543	544
384	545	546
385	547	548
386	549	550
387	551	552
388	553	554
389	555	556
390	557	558
391	559	560
392	0	0
393	-1	-1
394	561	562
395	-1	-1
396	563	564
397	-1	-1
398	565	566
399	-1	-1
400	567	568
401	-1	-1
402	569	570
403	-1	-1
404	571	572
405	-1	-1
406	573	574
407	-1	-1
408	575	576
409	0	0
410	577	578
411	579	580
412	581	582
413	583	584
414	585	586
415	587	588
416	589	590
417	591	592
418	593	594
419	595	596
420	597	598
421	599	600
422	601	602
423	603	604
424	605	606
425	607	608
426	0	0
427	-1	-1
428	609	610
429	-1	-1
430	611	612
431	-1	-1
432	613	614
433	-1	-1
434	615	616
435	-1	-1
436	617	618
437	-1	-1
438	619	620
439	-1	-1
440	621	622
441	-1	-1
442	623	624
443	0	0
444	625	626
445	627	628
446	629	630
447	631	632
448	633	634

77	111	112	201	-1	-1	325	-1	-1	449	635	636
78	113	114	202	285	286	326	465	466	450	637	638
79	115	116	203	-1	-1	327	-1	-1	451	639	640
80	117	118	204	287	288	328	467	468	452	641	642
81	119	120	205	0	0	329	-1	-1	453	643	644
82	121	122	206	289	290	330	469	470	454	645	646
83	123	124	207	291	292	331	-1	-1	455	647	648
84	125	126	208	293	294	332	471	472	456	649	650
85	127	128	209	295	296	333	-1	-1	457	651	652
86	0	0	210	297	298	334	473	474	458	653	654
87	-1	-1	211	299	300	335	-1	-1	459	655	656
88	129	130	212	301	302	336	475	476	460	0	0
89	-1	-1	213	303	304	337	-1	-1	461	-1	-1
90	131	132	214	305	306	338	477	478	462	657	658
91	-1	-1	215	307	308	339	-1	-1	463	-1	-1
92	133	134	216	309	310	340	479	480	464	659	660
93	-1	-1	217	311	312	341	0	0	465	-1	-1
94	135	136	218	313	314	342	481	482	466	661	662
95	-1	-1	219	315	316	343	483	484	467	-1	-1
96	137	138	220	317	318	344	485	486	468	663	664
97	-1	-1	221	319	320	345	487	488	469	-1	-1
98	139	140	222	0	0	346	489	490	470	665	666
99	-1	-1	223	-1	-1	347	491	492	471	-1	-1
100	141	142	224	321	322	348	493	494	472	667	668
101	-1	-1	225	-1	-1	349	495	496	473	-1	-1
102	143	144	226	323	324	350	497	498	474	669	670
103	0	0	227	-1	-1	351	499	500	475	-1	-1
104	145	146	228	325	326	352	501	502	476	671	672
105	147	148	229	-1	-1	353	503	504	477	0	0
106	149	150	230	327	328	354	505	506	478	673	674
107	151	152	231	-1	-1	355	507	508	479	675	676
108	153	154	232	329	330	356	509	510	480	677	678
109	155	156	233	-1	-1	357	511	512	481	679	680
110	157	158	234	331	332	358	0	0	482	681	682
111	159	160	235	-1	-1	359	-1	-1	483	683	684
112	161	162	236	333	334	360	513	514	484	685	686
113	163	164	237	-1	-1	361	-1	-1	485	687	688
114	165	166	238	335	336	362	515	516	486	689	690
115	167	168	239	0	0	363	-1	-1	487	691	692
116	169	170	240	337	338	364	517	518	488	693	694
117	171	172	241	339	340	365	-1	-1	489	695	696
118	173	174	242	341	342	366	519	520	490	697	698
119	175	176	243	343	344	367	-1	-1	491	699	700
120	0	0	244	345	346	368	521	522	492	701	702
121	-1	-1	245	347	348	369	-1	-1	493	703	704
122	177	178	246	349	350	370	523	524			
123	-1	-1	247	351	352	371	-1	-1			
124	179	180	248	353	354	372	525	526			

LOADING CONDITIONS

NODE	LOAD-X	LOAD-Y
16	1.000E+00	

PARAMETERS FOR NON-LINEAR ANALYSIS

CONTROL NODE	16	DIRECTION 1
LOAD STEPS	1	
MAX. ITERATION	50	
SOFTENING MODEL	0	
GAUSS POINTS	2	
DISPLACEMENT INCREMENT	1.000E-03	

CONVERGENCE CRITERIA	5.000E-03
ALPHA (ISOFT=1)	5.000E-01
BETA (ISOFT=1)	1.000E+01
SMX	2.500E-01
SMY	2.840E-01
E SH	1.600E-02
E U	1.100E-01
FU	6.500E+08

********** DISPLACEMENT INCREMENT 1 1.000E-03 **********

ITERATION	CONVERGENCE RATIO	DELTA	FORCE
1	1.000E+00	9.059E+05	9.059E+05
2	5.879E-03	-2.671E+05	6.389E+05
3	1.981E-03	-1.085E+05	5.303E+05
4	8.736E-04	-6.072E+04	4.696E+05
5	4.422E-04	-3.793E+04	4.317E+05
6	2.439E-04	-2.544E+04	4.062E+05
7	1.428E-04	-1.783E+04	3.884E+05
8	8.701E-05	-1.297E+04	3.754E+05
9	5.565E-05	-9.594E+03	3.658E+05
10	3.720E-05	-7.207E+03	3.586E+05
11	2.550E-05	-5.517E+03	3.531E+05
12	1.791E-05	-4.296E+03	3.488E+05
13	1.325E-05	-3.338E+03	3.455E+05
14	9.888E-06	-2.669E+03	3.428E+05
15	7.553E-06	-2.117E+03	3.407E+05
16	6.248E-06	-1.636E+03	3.391E+05

EXTERNAL TOTAL FORCE = 3.391E+05

ELEMENT	GAUSS POINT	STRAIN XX	STRAIN YY	STRAIN XY	STEEL STRESSES HORIZONTAL	STEEL STRESSES VERTICAL	THETA	CONCRETE STRESSES FC1	CODE	CONCRETE STRESSES FC2	CODE	CRACK WIDTH
1	1	1.944E-06	1.368E-03	1.267E-04	3.889E+05	2.737E+08	8.734E+01	1.074E+06	3	-2.386E+04	1	4.946E-04
	2	1.944E-06	1.290E-03	8.062E-05	3.887E+05	2.579E+08	8.820E+01	1.074E+06	3	1.707E+04	-1	4.713E-04
	3	3.785E-06	1.173E-03	1.663E-04	7.570E+05	2.347E+08	8.594E+01	1.076E+06	3	-5.239E+04	1	4.174E-04
	4	8.814E-06	1.141E-03	2.033E-04	1.763E+06	2.282E+08	8.490E+01	1.075E+06	3	-5.920E+03	1	4.015E-04
2	1	7.766E-08	1.234E-03	6.110E-05	1.553E+04	2.468E+08	8.857E+01	1.075E+06	3	-1.679E+04	1	4.533E-04
	2	7.319E-07	1.162E-03	6.786E-05	1.464E+05	2.323E+08	8.832E+01	1.075E+06	3	-6.478E+03	1	4.252E-04
	3	8.855E-06	1.114E-03	2.158E-04	1.771E+06	2.228E+08	8.447E+01	1.076E+06	3	-3.942E+04	1	3.904E-04
	4	9.691E-06	1.059E-03	2.150E-04	1.938E+06	2.118E+08	8.420E+01	1.077E+06	3	-3.021E+04	1	3.703E-04
3	1	3.392E-07	1.108E-03	7.098E-05	6.785E+04	2.217E+08	8.816E+01	1.075E+06	3	-1.991E+04	1	4.048E-04
	2	1.162E-06	1.030E-03	6.492E-05	2.325E+05	2.060E+08	8.819E+01	1.075E+06	3	3.487E+03	-1	3.765E-04
	3	9.959E-06	1.012E-03	2.194E-04	1.992E+06	2.023E+08	8.382E+01	1.079E+06	3	-4.777E+04	1	3.525E-04
	4	1.240E-05	9.446E-04	2.337E-04	2.481E+06	1.889E+08	8.296E+01	1.082E+06	3	-5.040E+04	1	3.268E-04
4	1	-1.441E-07	9.690E-04	7.387E-05	-2.882E+04	1.938E+08	8.781E+01	1.076E+06	3	-3.873E+04	1	3.524E-04
	2	1.328E-06	8.809E-04	8.196E-05	2.656E+05	1.762E+08	8.733E+01	1.076E+06	3	-1.442E+04	1	3.184E-04
	3	1.248E-05	8.924E-04	2.341E-04	2.496E+06	1.785E+08	8.254E+01	1.085E+06	3	-7.056E+04	1	3.078E-04
	4	1.611E-05	8.097E-04	2.371E-04	3.223E+06	1.619E+08	8.167E+01	1.089E+06	3	-3.043E+04	1	2.777E-04
5	1	-8.181E-08	8.132E-04	8.280E-05	-1.636E+04	1.626E+08	8.708E+01	1.078E+06	3	-5.457E+04	1	2.930E-04

	2	7.532E-06	7.043E-04	1.680E-05	1.506E+06	1.409E+08	8.930E+01	1.071E+06	3	1.858E+05	-1	2.614E-04
	3	1.700E-05	7.367E-04	2.477E-04	3.401E+06	1.473E+08	8.050E+01	1.099E+06	3	-9.271E+04	1	2.510E-04
	4	2.874E-05	6.346E-04	3.002E-04	5.749E+06	1.269E+08	7.682E+01	1.131E+06	3	-1.595E+05	1	2.139E-04
6	1	-7.313E-06	5.934E-04	9.823E-05	-1.463E+06	1.187E+08	8.535E+01	1.088E+06	3	-2.818E+05	1	2.098E-04
	2	9.312E-06	4.319E-04	1.613E-04	1.862E+06	8.638E+07	7.955E+01	1.126E+06	3	-1.386E+05	1	1.466E-04
	3	1.632E-05	5.733E-04	2.557E-04	3.265E+06	1.147E+08	7.766E+01	1.133E+06	3	-2.899E+05	1	1.935E-04
	4	3.544E-05	4.175E-04	2.095E-04	7.088E+06	8.349E+07	7.562E+01	1.163E+06	3	2.150E+05	-1	1.403E-04
7	1	8.570E-06	3.711E-04	1.056E-05	1.714E+06	7.422E+07	8.916E+01	1.071E+06	3	2.123E+05	-1	1.374E-04
	2	4.129E-04	4.137E-04	-8.039E-04	8.258E+07	8.273E+07	-4.502E+01	1.175E+06	2	2.836E+05	-1	-3.585E-03
	3	2.422E-05	1.647E-04	2.068E-04	4.843E+06	3.294E+07	6.209E+01	1.364E+06	2	-7.578E+05	1	6.351E-05
	4	3.974E-04	4.024E-04	9.578E-04	7.949E+07	8.049E+07	4.514E+01	1.163E+06	2	-1.936E+06	1	2.478E-04
8	1	-7.904E-05	-9.447E-05	1.377E-04	-2.384E+06	-2.719E+06	1.497E+06	ELASTIC STRESSES XX YY XY				
	2	-7.142E-05	-1.014E-04	-1.299E-04	-2.216E+06	-2.867E+06	-1.412E+06					
	3	-1.095E-04	1.533E-04	9.839E-05	-2.212E+06	3.501E+06	1.069E+06					
	4	-1.116E-04	1.603E-04	-9.394E-05	-2.239E+06	3.671E+06	-1.021E+06					
9	1	4.743E-06	1.085E-03	1.945E-04	9.486E+05	2.171E+08	8.489E+01	1.078E+06	3	-9.843E+04	1	3.819E-04
	2	1.233E-05	1.067E-03	2.458E-04	2.466E+06	2.135E+08	8.343E+01	1.077E+06	3	-4.494E+04	1	3.707E-04
	3	6.031E-06	9.957E-04	2.173E-04	1.206E+06	1.991E+08	8.380E+01	1.081E+06	3	-1.438E+05	1	3.469E-04
	4	1.714E-05	9.706E-04	2.868E-04	3.428E+06	1.941E+08	8.162E+01	1.084E+06	3	-9.905E+04	1	3.328E-04
10	1	1.461E-05	1.033E-03	2.641E-04	2.921E+06	2.067E+08	8.272E+01	1.079E+06	3	-5.587E+04	1	3.570E-04
	2	1.799E-05	9.866E-04	2.878E-04	3.599E+06	1.973E+08	8.172E+01	1.082E+06	3	-7.340E+04	1	3.385E-04
	3	2.195E-05	9.466E-04	3.193E-04	4.390E+06	1.893E+08	8.047E+01	1.088E+06	3	-1.208E+05	1	3.225E-04
	4	2.876E-05	9.045E-04	3.544E-04	5.751E+06	1.809E+08	7.898E+01	1.095E+06	3	-1.431E+05	1	3.062E-04
11	1	2.055E-05	9.486E-04	2.997E-04	4.109E+06	1.897E+08	8.104E+01	1.085E+06	3	-7.622E+04	1	3.241E-04
	2	2.286E-05	8.871E-04	3.149E-04	4.571E+06	1.774E+08	7.998E+01	1.092E+06	3	-1.233E+05	1	3.015E-04
	3	3.420E-05	8.683E-04	3.754E-04	6.841E+06	1.737E+08	7.788E+01	1.102E+06	3	-1.522E+05	1	2.931E-04
	4	4.100E-05	8.111E-04	3.973E-04	8.199E+06	1.622E+08	7.635E+01	1.115E+06	3	-1.805E+05	1	2.732E-04
12	1	2.732E-05	8.356E-04	3.218E-04	5.465E+06	1.671E+08	7.914E+01	1.098E+06	3	-8.827E+04	1	2.831E-04
	2	3.382E-05	7.570E-04	3.456E-04	6.764E+06	1.514E+08	7.722E+01	1.115E+06	3	-1.336E+05	1	2.552E-04
	3	4.625E-05	7.661E-04	4.118E-04	9.250E+06	1.532E+08	7.511E+01	1.129E+06	3	-2.117E+05	1	2.581E-04
	4	5.041E-05	6.930E-04	4.226E-04	1.008E+07	1.386E+08	7.333E+01	1.155E+06	3	-3.197E+05	1	2.343E-04
13	1	3.581E-05	6.993E-04	3.387E-04	7.161E+06	1.399E+08	7.647E+01	1.126E+06	3	-1.229E+05	1	2.356E-04
	2	2.941E-05	6.025E-04	3.505E-04	5.882E+06	1.205E+08	7.427E+01	1.164E+06	3	-4.961E+05	1	2.035E-04
	3	6.002E-05	6.316E-04	4.344E-04	1.200E+07	1.263E+08	7.138E+01	1.186E+06	3	-3.275E+05	1	2.151E-04
	4	7.678E-05	5.422E-04	4.557E-04	1.536E+07	1.084E+08	6.780E+01	1.216E+06	2	-4.032E+05	1	1.893E-04
14	1	5.694E-05	4.921E-04	3.346E-04	1.139E+07	9.843E+07	7.121E+01	1.213E+06	3	1.234E+03	-1	1.674E-04
	2	8.908E-05	3.700E-04	4.488E-04	1.782E+07	7.400E+07	6.102E+01	1.255E+06	2	-8.724E+05	1	1.424E-04
	3	9.158E-05	4.819E-04	5.148E-04	1.832E+07	9.638E+07	6.358E+01	1.223E+06	2	-8.987E+05	1	1.776E-04
	4	6.580E-05	4.460E-04	5.851E-04	1.316E+07	8.921E+07	6.150E+01	1.224E+06	2	-2.270E+06	1	1.746E-04
15	1	1.679E-04	4.104E-04	5.826E-04	3.358E+07	8.208E+07	5.629E+01	1.224E+06	2	-6.548E+05	1	1.717E-04
	2	-4.586E-05	6.360E-04	1.216E-03	-9.172E+06	1.272E+08	5.963E+01	1.142E+06	2	-9.039E+06	1	2.845E-04
	3	1.340E-04	5.463E-04	8.135E-04	2.681E+07	1.093E+08	5.843E+01	1.179E+06	2	-2.812E+06	1	2.274E-04
	4	-5.073E-05	5.435E-04	5.111E-04	-1.015E+07	1.087E+08	6.964E+01	1.216E+06	2	-3.505E+06	1	1.925E-04
16	1	-5.340E-05	9.121E-06	-8.547E-05	-1.331E+06	2.841E+04	-9.290E+05	ELASTIC STRESSES XX YY XY				
	2	-1.001E-04	1.720E-05	7.259E-05	-2.494E+06	5.580E+04	7.890E+05					
	3	-4.723E-05	-2.910E-05	-4.489E-06	-1.319E+06	-9.255E+05	-4.879E+04					
	4	-9.276E-05	-3.192E-05	1.860E-05	-2.495E+06	-1.172E+06	2.022E+05					
17	1	5.882E-06	9.433E-04	2.309E-04	1.176E+06	1.887E+08	8.307E+01	1.085E+06	3	-2.029E+05	1	3.267E-04

	2	1.929E-05	9.152E-04	3.063E-04	3.858E+06	1.830E+08	8.055E+01	1.090E+06	3	-1.538E+05	1	3.119E-04
	3	6.728E-06	8.787E-04	2.509E-04	1.346E+06	1.757E+08	8.197E+01	1.090E+06	3	-2.732E+05	1	3.020E-04
	4	2.245E-05	8.490E-04	3.316E-04	4.489E+06	1.698E+08	7.906E+01	1.100E+06	3	-2.389E+05	1	2.876E-04
18	1	2.665E-05	8.915E-04	3.470E-04	5.330E+06	1.783E+08	7.906E+01	1.096E+06	3	-1.711E+05	1	3.020E-04
	2	3.613E-05	8.506E-04	3.887E-04	7.227E+06	1.701E+08	7.724E+01	1.107E+06	3	-1.961E+05	1	2.868E-04
	3	3.192E-05	8.238E-04	3.766E-04	6.385E+06	1.648E+08	7.728E+01	1.111E+06	3	-2.633E+05	1	2.779E-04
	4	4.488E-05	7.815E-04	4.247E-04	8.976E+06	1.563E+08	7.501E+01	1.129E+06	3	-2.975E+05	1	2.634E-04
19	1	4.263E-05	8.150E-04	4.129E-04	8.526E+06	1.630E+08	7.593E+01	1.118E+06	3	-2.269E+05	1	2.745E-04
	2	5.185E-05	7.600E-04	4.375E-04	1.037E+07	1.520E+08	7.414E+01	1.137E+06	3	-2.564E+05	1	2.564E-04
	3	5.358E-05	7.460E-04	4.511E-04	1.072E+07	1.492E+08	7.345E+01	1.145E+06	3	-3.341E+05	1	2.521E-04
	4	6.536E-05	6.927E-04	4.814E-04	1.307E+07	1.385E+08	7.124E+01	1.176E+06	3	-4.074E+05	1	2.361E-04
20	1	5.748E-05	7.133E-04	4.526E-04	1.150E+07	1.427E+08	7.269E+01	1.157E+06	3	-3.245E+05	1	2.416E-04
	2	6.758E-05	6.456E-04	4.683E-04	1.352E+07	1.291E+08	7.049E+01	1.194E+06	3	-3.830E+05	1	2.209E-04
	3	7.399E-05	6.508E-04	5.005E-04	1.480E+07	1.302E+08	6.952E+01	1.191E+06	2	-4.839E+05	1	2.242E-04
	4	8.974E-05	5.921E-04	5.362E-04	1.795E+07	1.184E+08	6.656E+01	1.199E+06	2	-6.572E+05	1	2.095E-04
21	1	7.825E-05	5.968E-04	4.971E-04	1.565E+07	1.194E+08	6.810E+01	1.202E+06	2	-5.383E+05	1	2.080E-04
	2	9.501E-05	5.206E-04	5.345E-04	1.900E+07	1.041E+08	6.426E+01	1.213E+06	2	-8.387E+05	1	1.898E-04
	3	9.785E-05	5.493E-04	5.598E-04	1.957E+07	1.099E+08	6.443E+01	1.205E+06	2	-8.926E+05	1	1.998E-04
	4	1.019E-04	5.017E-04	5.971E-04	2.039E+07	1.003E+08	6.189E+01	1.210E+06	2	-1.416E+06	1	1.912E-04
22	1	8.832E-05	4.878E-04	5.872E-04	1.766E+07	9.756E+07	6.211E+01	1.214E+06	2	-1.647E+06	1	1.862E-04
	2	9.470E-05	4.807E-04	5.832E-04	1.894E+07	9.613E+07	6.174E+01	1.216E+06	2	-1.526E+06	1	1.842E-04
	3	8.697E-05	4.720E-04	5.983E-04	1.739E+07	9.440E+07	6.137E+01	1.216E+06	2	-1.870E+06	1	1.833E-04
	4	8.341E-05	4.571E-04	6.412E-04	1.668E+07	9.141E+07	6.011E+01	1.215E+06	2	-2.457E+06	1	1.842E-04
23	1	2.180E-05	4.880E-04	7.076E-04	4.359E+06	9.760E+07	6.168E+01	1.206E+06	2	-4.042E+06	1	1.961E-04
	2	-1.498E-05	4.182E-04	3.074E-04	-2.996E+06	8.364E+07	7.231E+01	1.238E+06	3	-1.574E+06	1	1.436E-04
	3	1.194E-05	4.202E-04	5.641E-04	2.388E+06	8.403E+07	6.294E+01	1.235E+06	2	-3.193E+06	1	1.639E-04
	4	-1.098E-05	3.957E-04	5.423E-04	-2.195E+06	7.915E+07	6.343E+01	1.244E+06	2	-3.530E+06	1	1.547E-04
24	1	-5.640E-05	1.782E-05	5.444E-05	-1.374E+06	2.395E+05	5.917E+05	ELASTIC STRESSES XX YY XY				
	2	-9.651E-05	1.398E-05	-2.553E-05	-2.415E+06	-1.272E+04	-2.774E+05					
	3	-4.986E-05	2.870E-05	3.351E-05	-1.165E+06	5.428E+05	3.642E+05					
	4	-9.692E-05	3.293E-05	-3.493E-08	-2.352E+06	4.703E+05	-3.796E+02					
25	1	6.990E-06	8.372E-04	2.663E-04	1.398E+06	1.674E+08	8.110E+01	1.096E+06	3	-3.448E+05	1	2.862E-04
	2	2.438E-05	8.053E-04	3.486E-04	4.877E+06	1.611E+08	7.796E+01	1.110E+06	3	-3.178E+05	1	2.720E-04
	3	7.755E-06	7.840E-04	2.871E-04	1.551E+06	1.568E+08	7.984E+01	1.106E+06	3	-4.464E+05	1	2.665E-04
	4	2.724E-05	7.478E-04	3.699E-04	5.447E+06	1.496E+08	7.641E+01	1.127E+06	3	-4.346E+05	1	2.521E-04
26	1	3.577E-05	7.775E-04	3.944E-04	7.153E+06	1.555E+08	7.599E+01	1.124E+06	3	-3.337E+05	1	2.620E-04
	2	5.031E-05	7.343E-04	4.444E-04	1.006E+07	1.469E+08	7.349E+01	1.148E+06	3	-3.870E+05	1	2.482E-04
	3	4.054E-05	7.174E-04	4.180E-04	8.108E+06	1.435E+08	7.414E+01	1.147E+06	3	-4.677E+05	1	2.423E-04
	4	5.822E-05	6.732E-04	4.714E-04	1.164E+07	1.346E+08	7.126E+01	1.182E+06	3	-5.404E+05	1	2.297E-04
27	1	6.078E-05	6.990E-04	4.733E-04	1.216E+07	1.398E+08	7.171E+01	1.170E+06	3	-4.326E+05	1	2.378E-04
	2	7.511E-05	6.480E-04	5.111E-04	1.502E+07	1.296E+08	6.912E+01	1.190E+06	2	-5.547E+05	1	2.240E-04
	3	7.103E-05	6.409E-04	5.051E-04	1.421E+07	1.282E+08	6.922E+01	1.192E+06	2	-6.158E+05	1	2.215E-04
	4	8.857E-05	5.943E-04	5.478E-04	1.771E+07	1.189E+08	6.635E+01	1.197E+06	2	-7.776E+05	1	2.110E-04
28	1	8.720E-05	6.106E-04	5.360E-04	1.744E+07	1.221E+08	6.715E+01	1.195E+06	2	-6.376E+05	1	2.147E-04
	2	1.000E-04	5.578E-04	5.715E-04	2.000E+07	1.116E+08	6.434E+01	1.202E+06	2	-9.214E+05	1	2.032E-04
	3	1.004E-04	5.592E-04	5.775E-04	2.007E+07	1.118E+08	6.423E+01	1.201E+06	2	-9.657E+05	1	2.042E-04
	4	1.091E-04	5.140E-04	6.104E-04	2.182E+07	1.028E+08	6.177E+01	1.206E+06	2	-1.349E+06	1	1.959E-04
29	1	1.064E-04	5.182E-04	5.944E-04	2.127E+07	1.036E+08	6.235E+01	1.207E+06	2	-1.217E+06	1	1.952E-04

	2	9.906E-05	4.818E-04	6.254E-04	1.981E+07	9.635E+07	6.072E+01	1.211E+06	2	-1.869E+06	1	1.891E-04
	3	1.114E-04	4.851E-04	6.333E-04	2.228E+07	9.702E+07	6.027E+01	1.209E+06	2	-1.705E+06	1	1.914E-04
	4	9.712E-05	4.507E-04	6.397E-04	1.942E+07	9.013E+07	5.946E+01	1.215E+06	2	-2.236E+06	1	1.832E-04
30	1	9.440E-05	4.538E-04	6.134E-04	1.888E+07	9.076E+07	6.018E+01	1.218E+06	2	-1.993E+06	1	1.809E-04
	2	5.550E-05	4.336E-04	6.557E-04	1.110E+07	8.671E+07	5.998E+01	1.220E+06	2	-3.235E+06	1	1.788E-04
	3	8.970E-05	4.317E-04	6.511E-04	1.794E+07	8.634E+07	5.885E+01	1.218E+06	2	-2.604E+06	1	1.797E-04
	4	5.024E-05	4.047E-04	6.169E-04	1.005E+07	8.093E+07	5.993E+01	1.230E+06	2	-3.104E+06	1	1.674E-04
31	1	3.149E-05	4.115E-04	5.508E-04	6.298E+06	8.229E+07	6.229E+01	1.237E+06	2	-2.747E+06	1	1.611E-04
	2	-1.486E-05	3.931E-04	5.953E-04	-2.971E+06	7.862E+07	6.221E+01	1.239E+06	2	-4.109E+06	1	1.592E-04
	3	2.712E-05	3.900E-04	5.856E-04	5.424E+06	7.799E+07	6.088E+01	1.238E+06	2	-3.283E+06	1	1.593E-04
	4	-1.623E-05	3.429E-04	4.964E-04	-3.247E+06	6.858E+07	6.293E+01	1.263E+06	2	-3.448E+06	1	1.364E-04
32	1	-4.304E-05	1.019E-05	1.792E-05	-1.062E+06	9.549E+04	1.948E+05	ELASTIC STRESSES XX YY XY				
	2	-9.166E-05	1.619E-05	2.027E-05	-2.282E+06	6.231E+04	2.203E+05					
	3	-4.126E-05	4.831E-06	3.140E-05	-1.037E+06	-3.473E+04	3.413E+05					
	4	-8.425E-05	7.594E-06	1.656E-05	-2.126E+06	-1.290E+05	1.800E+05					
33	1	8.074E-06	7.468E-04	3.032E-04	1.615E+06	1.494E+08	7.884E+01	1.115E+06	3	-5.426E+05	1	2.529E-04
	2	2.936E-05	7.072E-04	3.859E-04	5.873E+06	1.414E+08	7.517E+01	1.142E+06	3	-5.397E+05	1	2.386E-04
	3	8.981E-06	6.971E-04	3.267E-04	1.797E+06	1.394E+08	7.729E+01	1.131E+06	3	-6.908E+05	1	2.354E-04
	4	3.276E-05	6.528E-04	4.094E-04	6.552E+06	1.306E+08	7.327E+01	1.169E+06	3	-7.132E+05	1	2.212E-04
34	1	4.416E-05	6.758E-04	4.345E-04	8.832E+06	1.352E+08	7.273E+01	1.168E+06	3	-5.799E+05	1	2.292E-04
	2	6.415E-05	6.325E-04	4.914E-04	1.283E+07	1.265E+08	6.957E+01	1.195E+06	2	-6.791E+05	1	2.182E-04
	3	4.954E-05	6.222E-04	4.596E-04	9.908E+06	1.244E+08	7.062E+01	1.200E+06	2	-7.758E+05	1	2.134E-04
	4	7.245E-05	5.823E-04	5.214E-04	1.449E+07	1.165E+08	6.717E+01	1.203E+06	2	-9.227E+05	1	2.055E-04
35	1	7.904E-05	6.019E-04	5.296E-04	1.581E+07	1.204E+08	6.731E+01	1.198E+06	2	-7.850E+05	1	2.117E-04
	2	9.665E-05	5.583E-04	5.738E-04	1.933E+07	1.117E+08	6.440E+01	1.202E+06	2	-1.008E+06	1	2.035E-04
	3	8.790E-05	5.525E-04	5.605E-04	1.758E+07	1.105E+08	6.482E+01	1.204E+06	2	-1.083E+06	1	2.005E-04
	4	1.041E-04	5.127E-04	6.046E-04	2.082E+07	1.025E+08	6.202E+01	1.207E+06	2	-1.391E+06	1	1.948E-04
36	1	1.067E-04	5.260E-04	6.030E-04	2.133E+07	1.052E+08	6.240E+01	1.205E+06	2	-1.256E+06	1	1.981E-04
	2	1.132E-04	4.860E-04	6.333E-04	2.263E+07	9.721E+07	6.024E+01	1.209E+06	2	-1.667E+06	1	1.917E-04
	3	1.118E-04	4.846E-04	6.306E-04	2.236E+07	9.692E+07	6.029E+01	1.209E+06	2	-1.673E+06	1	1.910E-04
	4	1.134E-04	4.515E-04	6.557E-04	2.267E+07	9.029E+07	5.863E+01	1.212E+06	2	-2.115E+06	1	1.862E-04
37	1	1.092E-04	4.619E-04	6.505E-04	2.185E+07	9.237E+07	5.922E+01	1.211E+06	2	-2.066E+06	1	1.877E-04
	2	9.860E-05	4.296E-04	6.481E-04	1.972E+07	8.591E+07	5.852E+01	1.218E+06	2	-2.432E+06	1	1.794E-04
	3	1.063E-04	4.291E-04	6.618E-04	2.126E+07	8.582E+07	5.800E+01	1.216E+06	2	-2.448E+06	1	1.814E-04
	4	9.205E-05	4.007E-04	6.588E-04	1.841E+07	8.014E+07	5.755E+01	1.223E+06	2	-2.848E+06	1	1.738E-04
38	1	7.856E-05	4.126E-04	6.555E-04	1.571E+07	8.252E+07	5.850E+01	1.222E+06	2	-2.963E+06	1	1.753E-04
	2	4.810E-05	3.815E-04	5.941E-04	9.620E+06	7.631E+07	5.965E+01	1.238E+06	2	-3.047E+06	1	1.593E-04
	3	7.214E-05	3.792E-04	6.370E-04	1.443E+07	7.584E+07	5.786E+01	1.231E+06	2	-3.096E+06	1	1.652E-04
	4	4.560E-05	3.438E-04	5.907E-04	9.121E+06	6.877E+07	5.839E+01	1.246E+06	2	-3.288E+06	1	1.501E-04
39	1	2.091E-05	3.549E-04	5.728E-04	4.183E+06	7.098E+07	6.012E+01	1.248E+06	2	-3.462E+06	1	1.492E-04
	2	-1.343E-05	3.015E-04	4.617E-04	-2.685E+06	6.029E+07	6.214E+01	1.278E+06	2	-3.270E+06	1	1.226E-04
	3	1.973E-05	3.080E-04	5.379E-04	3.945E+06	6.159E+07	5.909E+01	1.263E+06	2	-3.407E+06	1	1.342E-04
	4	-1.498E-05	2.660E-04	4.722E-04	-2.996E+06	5.320E+07	6.037E+01	1.286E+06	2	-3.592E+06	1	1.151E-04
40	1	-4.210E-05	1.021E-05	4.093E-05	-1.038E+06	9.957E+04	4.449E+05	ELASTIC STRESSES XX YY XY				
	2	-7.937E-05	1.216E-05	1.249E-05	-1.983E+06	6.492E+03	1.358E+05					
	3	-4.125E-05	1.042E-05	4.035E-05	-1.015E+06	1.082E+05	4.386E+05					
	4	-7.158E-05	1.338E-05	1.717E-05	-1.779E+06	6.772E+04	1.866E+05					
41	1	9.341E-06	6.602E-04	3.435E-04	1.868E+06	1.320E+08	7.608E+01	1.146E+06	3	-8.232E+05	1	2.229E-04

	2	3.508E-05	6.152E-04	4.274E-04	7.017E+06	1.230E+08	7.180E+01	1.194E+06	3	-8.707E+05	1	2.099E-04
	3	1.051E-05	6.098E-04	3.715E-04	2.102E+06	1.220E+08	7.410E+01	1.174E+06	3	-1.049E+06	1	2.066E-04
	4	3.945E-05	5.677E-04	4.579E-04	7.890E+06	1.135E+08	6.953E+01	1.212E+06	2	-1.136E+06	1	1.968E-04
42	1	5.435E-05	5.861E-04	4.815E-04	1.087E+07	1.172E+08	6.891E+01	1.206E+06	2	-9.525E+05	1	2.037E-04
	2	7.785E-05	5.479E-04	5.441E-04	1.557E+07	1.096E+08	6.541E+01	1.207E+06	2	-1.152E+06	1	1.977E-04
	3	5.992E-05	5.396E-04	5.121E-04	1.198E+07	1.079E+08	6.656E+01	1.213E+06	2	-1.261E+06	1	1.925E-04
	4	8.351E-05	5.026E-04	5.726E-04	1.670E+07	1.005E+08	6.309E+01	1.213E+06	2	-1.520E+06	1	1.883E-04
43	1	9.282E-05	5.189E-04	5.818E-04	1.856E+07	1.038E+08	6.310E+01	1.209E+06	2	-1.349E+06	1	1.937E-04
	2	1.074E-04	4.821E-04	6.240E-04	2.148E+07	9.642E+07	6.049E+01	1.211E+06	2	-1.700E+06	1	1.894E-04
	3	9.723E-05	4.762E-04	6.086E-04	1.945E+07	9.524E+07	6.095E+01	1.214E+06	2	-1.762E+06	1	1.859E-04
	4	1.083E-04	4.438E-04	6.458E-04	2.166E+07	8.875E+07	5.872E+01	1.215E+06	2	-2.148E+06	1	1.829E-04
44	1	1.124E-04	4.573E-04	6.473E-04	2.249E+07	9.145E+07	5.902E+01	1.212E+06	2	-2.005E+06	1	1.865E-04
	2	1.106E-04	4.272E-04	6.665E-04	2.212E+07	8.545E+07	5.770E+01	1.216E+06	2	-2.437E+06	1	1.818E-04
	3	1.112E-04	4.219E-04	6.645E-04	2.223E+07	8.438E+07	5.753E+01	1.217E+06	2	-2.443E+06	1	1.804E-04
	4	1.070E-04	3.935E-04	6.741E-04	2.140E+07	7.869E+07	5.651E+01	1.221E+06	2	-2.815E+06	1	1.752E-04
45	1	1.041E-04	4.054E-04	6.668E-04	2.083E+07	8.107E+07	5.715E+01	1.220E+06	2	-2.700E+06	1	1.766E-04
	2	8.685E-05	3.774E-04	6.580E-04	1.737E+07	7.548E+07	5.691E+01	1.228E+06	2	-3.086E+06	1	1.683E-04
	3	9.979E-05	3.729E-04	6.713E-04	1.996E+07	7.459E+07	5.607E+01	1.226E+06	2	-3.050E+06	1	1.700E-04
	4	8.284E-05	3.422E-04	6.484E-04	1.657E+07	6.843E+07	5.589E+01	1.236E+06	2	-3.299E+06	1	1.594E-04
46	1	7.082E-05	3.524E-04	6.270E-04	1.416E+07	7.047E+07	5.709E+01	1.238E+06	2	-3.192E+06	1	1.580E-04
	2	4.299E-05	3.147E-04	5.844E-04	8.597E+06	6.294E+07	5.746E+01	1.253E+06	2	-3.456E+06	1	1.427E-04
	3	6.747E-05	3.170E-04	6.205E-04	1.349E+07	6.340E+07	5.595E+01	1.246E+06	2	-3.428E+06	1	1.495E-04
	4	4.111E-05	2.774E-04	5.647E-04	8.222E+06	5.548E+07	5.635E+01	1.264E+06	2	-3.536E+06	1	1.322E-04
47	1	2.114E-05	2.818E-04	5.271E-04	4.227E+06	5.635E+07	5.815E+01	1.271E+06	2	-3.437E+06	1	1.271E-04
	2	-1.648E-05	2.407E-04	4.637E-04	-3.295E+06	4.814E+07	5.950E+01	1.294E+06	2	-3.679E+06	1	1.081E-04
	3	1.929E-05	2.458E-04	5.131E-04	3.858E+06	4.916E+07	5.690E+01	1.282E+06	2	-3.561E+06	1	1.175E-04
	4	-1.972E-05	1.958E-04	4.215E-04	-3.943E+06	3.915E+07	5.853E+01	1.315E+06	2	-3.578E+06	1	9.278E-05
48	1	-4.060E-05	7.454E-06	3.930E-05	-1.010E+06	3.488E+04	4.271E+05	ELASTIC STRESSES XX YY XY				
	2	-6.480E-05	1.032E-05	2.039E-05	-1.618E+06	1.528E+04	2.216E+05					
	3	-4.080E-05	6.139E-06	4.156E-05	-1.020E+06	4.861E+02	4.518E+05					
	4	-5.529E-05	7.706E-06	2.036E-05	-1.385E+06	-1.502E+04	2.213E+05					
49	1	1.196E-05	5.743E-04	3.945E-04	2.392E+06	1.149E+08	7.247E+01	1.201E+06	3	-1.243E+06	1	1.959E-04
	2	4.252E-05	5.343E-04	4.816E-04	8.505E+06	1.069E+08	6.779E+01	1.217E+06	2	-1.374E+06	1	1.885E-04
	3	1.290E-05	5.280E-04	4.288E-04	2.579E+06	1.056E+08	7.011E+01	1.224E+06	2	-1.590E+06	1	1.832E-04
	4	4.602E-05	4.904E-04	5.150E-04	9.204E+06	9.808E+07	6.539E+01	1.223E+06	2	-1.765E+06	1	1.788E-04
50	1	6.321E-05	5.070E-04	5.347E-04	1.264E+07	1.014E+08	6.484E+01	1.217E+06	2	-1.534E+06	1	1.854E-04
	2	8.631E-05	4.715E-04	5.929E-04	1.726E+07	9.431E+07	6.150E+01	1.217E+06	2	-1.831E+06	1	1.826E-04
	3	6.683E-05	4.640E-04	5.650E-04	1.337E+07	9.281E+07	6.255E+01	1.223E+06	2	-1.958E+06	1	1.771E-04
	4	8.773E-05	4.317E-04	6.182E-04	1.755E+07	8.634E+07	5.954E+01	1.222E+06	2	-2.296E+06	1	1.759E-04
51	1	9.835E-05	4.474E-04	6.266E-04	1.967E+07	8.948E+07	5.955E+01	1.217E+06	2	-2.098E+06	1	1.810E-04
	2	1.077E-04	4.173E-04	6.590E-04	2.154E+07	8.347E+07	5.758E+01	1.219E+06	2	-2.475E+06	1	1.785E-04
	3	9.821E-05	4.095E-04	6.470E-04	1.964E+07	8.190E+07	5.784E+01	1.222E+06	2	-2.560E+06	1	1.748E-04
	4	1.055E-04	3.816E-04	6.725E-04	2.109E+07	7.632E+07	5.616E+01	1.224E+06	2	-2.909E+06	1	1.724E-04
52	1	1.090E-04	3.967E-04	6.733E-04	2.179E+07	7.933E+07	5.656E+01	1.221E+06	2	-2.752E+06	1	1.759E-04
	2	1.045E-04	3.688E-04	6.769E-04	2.089E+07	7.376E+07	5.566E+01	1.225E+06	2	-3.067E+06	1	1.702E-04
	3	1.057E-04	3.617E-04	6.805E-04	2.115E+07	7.234E+07	5.530E+01	1.226E+06	2	-3.140E+06	1	1.693E-04
	4	1.006E-04	3.339E-04	6.769E-04	2.012E+07	6.678E+07	5.450E+01	1.232E+06	2	-3.395E+06	1	1.628E-04
53	1	9.642E-05	3.480E-04	6.701E-04	1.928E+07	6.961E+07	5.528E+01	1.231E+06	2	-3.277E+06	1	1.644E-04

	2	8.049E-05	3.160E-04	6.409E-04	1.610E+07	6.321E+07	5.508E+01	1.242E+06	2	-3.451E+06	1	1.529E-04
	3	9.230E-05	3.124E-04	6.627E-04	1.846E+07	6.247E+07	5.418E+01	1.239E+06	2	-3.536E+06	1	1.560E-04
	4	7.642E-05	2.798E-04	6.281E-04	1.528E+07	5.597E+07	5.397E+01	1.251E+06	2	-3.656E+06	1	1.437E-04
54	1	6.469E-05	2.909E-04	6.114E-04	1.294E+07	5.817E+07	5.515E+01	1.252E+06	2	-3.567E+06	1	1.427E-04
	2	3.894E-05	2.503E-04	5.483E-04	7.789E+06	5.006E+07	5.554E+01	1.273E+06	2	-3.590E+06	1	1.243E-04
	3	6.083E-05	2.530E-04	5.904E-04	1.217E+07	5.060E+07	5.401E+01	1.264E+06	2	-3.691E+06	1	1.321E-04
	4	3.560E-05	2.119E-04	5.242E-04	7.121E+06	4.238E+07	5.429E+01	1.286E+06	2	-3.674E+06	1	1.132E-04
55	1	1.716E-05	2.160E-04	4.942E-04	3.432E+06	4.319E+07	5.595E+01	1.292E+06	2	-3.604E+06	1	1.087E-04
	2	-2.115E-05	1.611E-04	3.908E-04	-4.231E+06	3.222E+07	5.750E+01	1.332E+06	2	-3.508E+06	1	8.135E-05
	3	1.386E-05	1.746E-04	4.615E-04	2.772E+06	3.492E+07	5.460E+01	1.309E+06	2	-3.612E+06	1	9.582E-05
	4	-2.486E-05	1.155E-04	3.504E-04	-4.973E+06	2.309E+07	5.591E+01	1.357E+06	2	-3.457E+06	1	6.641E-05
56	1	-4.133E-05	6.309E-06	4.267E-05	-1.033E+06	2.794E+03	4.639E+05	ELASTIC STRESSES XX YY XY				
	2	-4.830E-05	7.184E-06	1.980E-05	-1.208E+06	-1.571E+03	2.152E+05					
	3	-4.161E-05	5.554E-06	4.178E-05	-1.043E+06	-1.759E+04	4.541E+05					
	4	-3.880E-05	5.831E-06	1.978E-05	-9.700E+05	2.652E+02	2.150E+05					
57	1	1.444E-05	4.958E-04	4.563E-04	2.889E+06	9.915E+07	6.826E+01	1.229E+06	2	-1.876E+06	1	1.753E-04
	2	4.794E-05	4.595E-04	5.396E-04	9.588E+06	9.189E+07	6.366E+01	1.227E+06	2	-2.095E+06	1	1.728E-04
	3	1.472E-05	4.537E-04	4.953E-04	2.943E+06	9.074E+07	6.577E+01	1.235E+06	2	-2.359E+06	1	1.665E-04
	4	4.896E-05	4.185E-04	5.718E-04	9.792E+06	8.370E+07	6.143E+01	1.232E+06	2	-2.596E+06	1	1.657E-04
58	1	6.754E-05	4.343E-04	5.863E-04	1.351E+07	8.685E+07	6.101E+01	1.226E+06	2	-2.316E+06	1	1.719E-04
	2	8.778E-05	4.036E-04	6.351E-04	1.756E+07	8.073E+07	5.822E+01	1.225E+06	2	-2.649E+06	1	1.714E-04
	3	6.815E-05	3.948E-04	6.134E-04	1.363E+07	7.896E+07	5.901E+01	1.231E+06	2	-2.816E+06	1	1.657E-04
	4	8.652E-05	3.656E-04	6.543E-04	1.730E+07	7.313E+07	5.655E+01	1.230E+06	2	-3.134E+06	1	1.653E-04
59	1	9.713E-05	3.826E-04	6.598E-04	1.943E+07	7.652E+07	5.669E+01	1.226E+06	2	-2.900E+06	1	1.704E-04
	2	1.033E-04	3.555E-04	6.794E-04	2.065E+07	7.110E+07	5.518E+01	1.228E+06	2	-3.214E+06	1	1.676E-04
	3	9.488E-05	3.453E-04	6.729E-04	1.898E+07	6.906E+07	5.520E+01	1.231E+06	2	-3.352E+06	1	1.641E-04
	4	1.002E-04	3.181E-04	6.837E-04	2.003E+07	6.362E+07	5.383E+01	1.234E+06	2	-3.602E+06	1	1.605E-04
60	1	1.033E-04	3.355E-04	6.829E-04	2.067E+07	6.710E+07	5.438E+01	1.231E+06	2	-3.406E+06	1	1.641E-04
	2	9.768E-05	3.073E-04	6.733E-04	1.954E+07	6.146E+07	5.364E+01	1.238E+06	2	-3.612E+06	1	1.568E-04
	3	9.970E-05	2.979E-04	6.811E-04	1.994E+07	5.957E+07	5.311E+01	1.238E+06	2	-3.745E+06	1	1.563E-04
	4	9.352E-05	2.687E-04	6.620E-04	1.870E+07	5.374E+07	5.240E+01	1.247E+06	2	-3.870E+06	1	1.477E-04
61	1	8.947E-05	2.850E-04	6.542E-04	1.789E+07	5.700E+07	5.331E+01	1.245E+06	2	-3.706E+06	1	1.493E-04
	2	7.300E-05	2.520E-04	6.141E-04	1.460E+07	5.039E+07	5.312E+01	1.259E+06	2	-3.779E+06	1	1.362E-04
	3	8.502E-05	2.457E-04	6.370E-04	1.700E+07	4.914E+07	5.207E+01	1.255E+06	2	-3.912E+06	1	1.393E-04
	4	6.830E-05	2.118E-04	5.885E-04	1.366E+07	4.236E+07	5.185E+01	1.272E+06	2	-3.905E+06	1	1.249E-04
62	1	5.799E-05	2.247E-04	5.724E-04	1.160E+07	4.493E+07	5.311E+01	1.273E+06	2	-3.766E+06	1	1.241E-04
	2	3.178E-05	1.825E-04	5.013E-04	6.356E+06	3.651E+07	5.336E+01	1.298E+06	2	-3.715E+06	1	1.042E-04
	3	5.237E-05	1.840E-04	5.417E-04	1.047E+07	3.681E+07	5.182E+01	1.287E+06	2	-3.853E+06	1	1.119E-04
	4	2.389E-05	1.397E-04	4.587E-04	4.778E+06	2.794E+07	5.208E+01	1.318E+06	2	-3.719E+06	1	8.976E-05
63	1	1.071E-05	1.456E-04	4.364E-04	2.143E+06	2.911E+07	5.358E+01	1.323E+06	2	-3.615E+06	1	8.660E-05
	2	-2.720E-05	8.104E-05	3.158E-04	-5.439E+06	1.621E+07	5.445E+01	1.379E+06	2	-3.377E+06	1	5.484E-05
	3	3.234E-06	1.086E-04	3.980E-04	6.467E+05	2.172E+07	5.241E+01	1.343E+06	2	-3.608E+06	1	7.385E-05
	4	-3.128E-05	3.357E-05	2.608E-04	-6.256E+06	6.715E+06	5.198E+01	1.417E+06	2	-3.219E+06	1	3.821E-05
64	1	-4.167E-05	4.512E-06	4.057E-05	-1.048E+06	-4.445E+04	4.409E+05	ELASTIC STRESSES XX YY XY				
	2	-3.192E-05	4.396E-06	1.931E-05	-7.995E+05	-1.003E+04	2.099E+05					
	3	-4.138E-05	3.289E-06	3.891E-05	-1.046E+06	-7.465E+04	4.230E+05					
	4	-2.309E-05	2.695E-06	1.737E-05	-5.801E+05	-1.963E+04	1.888E+05					
65	1	1.514E-05	4.241E-04	5.244E-04	3.027E+06	8.483E+07	6.397E+01	1.238E+06	2	-2.742E+06	1	1.611E-04

	2	4.908E-05	3.895E-04	5.946E-04	9.817E+06	7.790E+07	5.989E+01	1.236E+06	2	-2.988E+06	1	1.613E-04
	3	1.497E-05	3.846E-04	5.638E-04	2.995E+06	7.692E+07	6.162E+01	1.243E+06	2	-3.314E+06	1	1.551E-04
	4	4.847E-05	3.504E-04	6.239E-04	9.694E+06	7.009E+07	5.791E+01	1.240E+06	2	-3.542E+06	1	1.557E-04
66	1	6.739E-05	3.666E-04	6.317E-04	1.348E+07	7.332E+07	5.767E+01	1.234E+06	2	-3.203E+06	1	1.614E-04
	2	8.518E-05	3.376E-04	6.659E-04	1.704E+07	6.753E+07	5.538E+01	1.234E+06	2	-3.486E+06	1	1.608E-04
	3	6.620E-05	3.269E-04	6.533E-04	1.324E+07	6.538E+07	5.587E+01	1.240E+06	2	-3.729E+06	1	1.556E-04
	4	8.283E-05	2.970E-04	6.767E-04	1.657E+07	5.940E+07	5.378E+01	1.241E+06	2	-3.954E+06	1	1.540E-04
67	1	9.297E-05	3.171E-04	6.795E-04	1.859E+07	6.342E+07	5.412E+01	1.235E+06	2	-3.672E+06	1	1.591E-04
	2	9.774E-05	2.894E-04	6.835E-04	1.955E+07	5.788E+07	5.283E+01	1.239E+06	2	-3.871E+06	1	1.548E-04
	3	8.993E-05	2.759E-04	6.826E-04	1.799E+07	5.519E+07	5.262E+01	1.243E+06	2	-4.088E+06	1	1.514E-04
	4	9.396E-05	2.469E-04	6.763E-04	1.879E+07	4.939E+07	5.137E+01	1.248E+06	2	-4.212E+06	1	1.457E-04
68	1	9.697E-05	2.686E-04	6.755E-04	1.939E+07	5.371E+07	5.212E+01	1.244E+06	2	-3.971E+06	1	1.498E-04
	2	9.024E-05	2.386E-04	6.493E-04	1.805E+07	4.773E+07	5.143E+01	1.254E+06	2	-4.037E+06	1	1.402E-04
	3	9.250E-05	2.252E-04	6.602E-04	1.850E+07	4.504E+07	5.068E+01	1.255E+06	2	-4.249E+06	1	1.396E-04
	4	8.463E-05	1.942E-04	6.236E-04	1.693E+07	3.884E+07	4.998E+01	1.267E+06	2	-4.233E+06	1	1.284E-04
69	1	8.127E-05	2.153E-04	6.193E-04	1.625E+07	4.307E+07	5.110E+01	1.264E+06	2	-4.035E+06	1	1.310E-04
	2	6.299E-05	1.808E-04	5.633E-04	1.260E+07	3.617E+07	5.090E+01	1.283E+06	2	-3.973E+06	1	1.154E-04
	3	7.454E-05	1.702E-04	5.853E-04	1.491E+07	3.404E+07	4.964E+01	1.280E+06	2	-4.164E+06	1	1.179E-04
	4	5.437E-05	1.349E-04	5.180E-04	1.087E+07	2.698E+07	4.941E+01	1.302E+06	2	-4.011E+06	1	1.004E-04
70	1	4.611E-05	1.532E-04	5.132E-04	9.222E+06	3.065E+07	5.089E+01	1.300E+06	2	-3.896E+06	1	1.019E-04
	2	2.183E-05	1.089E-04	4.285E-04	4.366E+06	2.179E+07	5.074E+01	1.332E+06	2	-3.684E+06	1	7.999E-05
	3	3.466E-05	1.084E-04	4.609E-04	6.932E+06	2.169E+07	4.954E+01	1.323E+06	2	-3.882E+06	1	8.584E-05
	4	4.544E-06	6.645E-05	3.693E-04	9.089E+05	1.329E+07	4.975E+01	1.362E+06	2	-3.649E+06	1	6.271E-05
71	1	-7.855E-06	7.469E-05	3.531E-04	-1.571E+06	1.494E+07	5.157E+01	1.367E+06	2	-3.561E+06	1	6.052E-05
	2	-4.365E-06	5.184E-06	2.186E-04	-8.730E+06	1.037E+06	5.129E+01	1.452E+06	2	-3.173E+06	1	2.614E-05
	3	-2.325E-05	2.384E-05	2.786E-04	-4.651E+06	4.767E+06	4.979E+01	1.412E+06	2	-3.401E+06	1	3.986E-05
	4	-4.807E-05	-2.006E-05	1.820E-04	-9.614E+06	-4.012E+06	4.937E+01	1.450E+06	1	-3.054E+06	1	0.000E+00
72	1	-4.013E-05	2.488E-06	3.755E-05	-1.017E+06	-9.032E+04	4.082E+05	ELASTIC STRESSES XX YY XY				
	2	-1.727E-05	1.467E-06	1.515E-05	-4.360E+05	-2.874E+04	1.646E+05					
	3	-3.853E-05	2.150E-06	3.409E-05	-9.771E+05	-9.282E+04	3.705E+05					
	4	-1.019E-05	4.364E-07	1.223E-05	-2.590E+05	-2.795E+04	1.329E+05					
73	1	1.482E-05	3.565E-04	5.927E-04	2.963E+06	7.129E+07	5.997E+01	1.245E+06	2	-3.758E+06	1	1.515E-04
	2	4.773E-05	3.212E-04	6.438E-04	9.546E+06	6.424E+07	5.650E+01	1.244E+06	2	-3.961E+06	1	1.518E-04
	3	1.456E-05	3.169E-04	6.299E-04	2.913E+06	6.339E+07	5.782E+01	1.249E+06	2	-4.379E+06	1	1.469E-04
	4	4.679E-05	2.781E-04	6.672E-04	9.359E+06	5.563E+07	5.456E+01	1.249E+06	2	-4.538E+06	1	1.459E-04
74	1	6.506E-05	2.967E-04	6.664E-04	1.301E+07	5.933E+07	5.458E+01	1.244E+06	2	-4.112E+06	1	1.510E-04
	2	8.091E-05	2.653E-04	6.809E-04	1.618E+07	5.307E+07	5.257E+01	1.246E+06	2	-4.289E+06	1	1.484E-04
	3	6.315E-05	2.510E-04	6.787E-04	1.263E+07	5.020E+07	5.273E+01	1.251E+06	2	-4.638E+06	1	1.437E-04
	4	7.703E-05	2.167E-04	6.776E-04	1.541E+07	4.333E+07	5.082E+01	1.256E+06	2	-4.729E+06	1	1.388E-04
75	1	8.731E-05	2.432E-04	6.803E-04	1.746E+07	4.864E+07	5.145E+01	1.249E+06	2	-4.382E+06	1	1.449E-04
	2	9.039E-05	2.132E-04	6.653E-04	1.808E+07	4.265E+07	5.023E+01	1.257E+06	2	-4.444E+06	1	1.380E-04
	3	8.229E-05	1.929E-04	6.677E-04	1.646E+07	3.857E+07	4.970E+01	1.261E+06	2	-4.768E+06	1	1.340E-04
	4	8.422E-05	1.616E-04	6.389E-04	1.684E+07	3.232E+07	4.845E+01	1.271E+06	2	-4.724E+06	1	1.252E-04
76	1	8.852E-05	1.906E-04	6.426E-04	1.770E+07	3.813E+07	4.951E+01	1.264E+06	2	-4.429E+06	1	1.309E-04
	2	7.918E-05	1.591E-04	5.969E-04	1.584E+07	3.183E+07	4.881E+01	1.279E+06	2	-4.342E+06	1	1.183E-04
	3	8.046E-05	1.377E-04	6.051E-04	1.609E+07	2.754E+07	4.770E+01	1.282E+06	2	-4.633E+06	1	1.163E-04
	4	6.710E-05	1.058E-04	5.439E-04	1.342E+07	2.117E+07	4.703E+01	1.301E+06	2	-4.438E+06	1	1.011E-04
77	1	6.738E-05	1.345E-04	5.525E-04	1.348E+07	2.691E+07	4.846E+01	1.294E+06	2	-4.236E+06	1	1.067E-04

	2	4.597E-05	9.906E-05	4.783E-04	9.194E+06	1.981E+07	4.816E+01	1.320E+06	2	-4.026E+06	1	8.814E-05
	3	5.254E-05	8.345E-05	4.917E-04	1.051E+07	1.669E+07	4.679E+01	1.319E+06	2	-4.260E+06	1	8.853E-05
	4	2.765E-05	4.821E-05	4.086E-04	5.530E+06	9.643E+06	4.644E+01	1.352E+06	2	-3.992E+06	1	6.830E-05
78	1	2.509E-05	7.229E-05	4.141E-04	5.019E+06	1.446E+07	4.825E+01	1.345E+06	2	-3.833E+06	1	7.236E-05
	2	-1.096E-05	3.196E-05	3.157E-04	-2.192E+06	6.393E+06	4.887E+01	1.393E+06	2	-3.581E+06	1	4.779E-05
	3	5.075E-06	2.032E-05	3.358E-04	1.015E+06	4.063E+06	4.629E+01	1.386E+06	2	-3.734E+06	1	5.093E-05
	4	-3.214E-05	-1.781E-05	2.282E-04	-6.429E+06	-3.563E+06	4.679E+01	1.455E+06	2	-3.362E+06	1	2.517E-05
79	1	-3.653E-05	-6.978E-06	2.300E-04	-7.306E+06	-1.396E+06	4.866E+01	1.451E+06	2	-3.324E+06	1	2.652E-05
	2	-4.753E-05	-3.195E-05	1.642E-04	-9.507E+06	-6.389E+06	4.771E+01	1.069E+06	1	-2.962E+06	1	0.000E+00
	3	-5.269E-05	-3.401E-05	1.718E-04	-1.054E+07	-6.801E+06	4.810E+01	1.077E+06	1	-3.139E+06	1	0.000E+00
	4	-4.880E-05	-3.286E-05	1.505E-04	-9.761E+06	-6.573E+06	4.802E+01	8.712E+05	1	-2.828E+06	1	0.000E+00
80	1	-3.591E-05	2.018E-06	3.246E-05	-9.106E+05	-8.615E+04	3.529E+05	ELASTIC STRESSES XX YY XY				
	2	-6.042E-06	2.605E-07	1.007E-05	-1.535E+05	-1.652E+04	1.094E+05					
	3	-3.157E-05	7.999E-07	2.785E-05	-8.043E+05	-1.006E+05	3.028E+05					
	4	-1.266E-06	-3.846E-07	7.806E-06	-3.387E+04	-1.469E+04	8.485E+04					
81	1	1.467E-05	2.866E-04	6.570E-04	2.934E+06	5.732E+07	5.624E+01	1.252E+06	2	-4.859E+06	1	1.437E-04
	2	4.645E-05	2.439E-04	6.816E-04	9.290E+06	4.879E+07	5.307E+01	1.254E+06	2	-4.966E+06	1	1.412E-04
	3	1.386E-05	2.382E-04	6.900E-04	2.773E+06	4.764E+07	5.400E+01	1.257E+06	2	-5.568E+06	1	1.382E-04
	4	4.345E-05	1.885E-04	6.923E-04	8.690E+06	3.770E+07	5.091E+01	1.263E+06	2	-5.589E+06	1	1.323E-04
82	1	6.032E-05	2.132E-04	6.808E-04	1.206E+07	4.263E+07	5.132E+01	1.258E+06	2	-5.022E+06	1	1.368E-04
	2	7.221E-05	1.766E-04	6.683E-04	1.444E+07	3.532E+07	4.943E+01	1.265E+06	2	-5.059E+06	1	1.302E-04
	3	5.518E-05	1.506E-04	6.700E-04	1.104E+07	3.011E+07	4.905E+01	1.272E+06	2	-5.541E+06	1	1.242E-04
	4	6.341E-05	1.109E-04	6.400E-04	1.268E+07	2.219E+07	4.712E+01	1.283E+06	2	-5.501E+06	1	1.149E-04
83	1	7.800E-05	1.518E-04	6.504E-04	1.560E+07	3.036E+07	4.823E+01	1.272E+06	2	-5.028E+06	1	1.245E-04
	2	7.681E-05	1.191E-04	6.084E-04	1.536E+07	2.383E+07	4.699E+01	1.285E+06	2	-4.906E+06	1	1.135E-04
	3	6.575E-05	8.488E-05	6.052E-04	1.315E+07	1.698E+07	4.590E+01	1.294E+06	2	-5.362E+06	1	1.065E-04
	4	5.877E-05	4.985E-05	5.377E-04	1.175E+07	9.971E+06	4.452E+01	1.316E+06	2	-5.077E+06	1	9.121E-05
84	1	7.118E-05	9.511E-05	5.673E-04	1.424E+07	1.902E+07	4.620E+01	1.298E+06	2	-4.767E+06	1	1.034E-04
	2	5.682E-05	6.298E-05	4.959E-04	1.136E+07	1.260E+07	4.535E+01	1.322E+06	2	-4.480E+06	1	8.680E-05
	3	4.889E-05	3.467E-05	4.888E-04	9.778E+06	6.934E+06	4.416E+01	1.331E+06	2	-4.811E+06	1	8.082E-05
	4	2.868E-05	2.247E-06	4.034E-04	5.737E+06	4.493E+05	4.312E+01	1.365E+06	2	-4.449E+06	1	6.153E-05
85	1	3.767E-05	4.051E-05	4.321E-04	7.535E+06	8.102E+06	4.518E+01	1.346E+06	2	-4.228E+06	1	7.195E-05
	2	5.777E-06	9.295E-06	3.388E-04	1.155E+06	1.859E+06	4.529E+01	1.389E+06	2	-3.883E+06	1	4.988E-05
	3	6.575E-06	-2.393E-05	3.300E-04	1.315E+06	-4.786E+06	4.236E+01	1.402E+06	2	-4.170E+06	1	4.447E-05
	4	-2.759E-05	-4.442E-05	2.341E-04	-5.517E+06	-8.885E+06	4.294E+01	1.463E+06	2	-3.687E+06	1	2.301E-05
86	1	-2.167E-05	-2.002E-05	2.600E-04	-4.334E+06	-4.004E+06	4.518E+01	1.438E+06	2	-3.630E+06	1	3.079E-05
	2	-4.506E-05	-4.661E-05	1.754E-04	-9.012E+06	-9.321E+06	4.474E+01	1.047E+06	1	-3.227E+06	1	0.000E+00
	3	-4.552E-05	-5.426E-05	1.795E-04	-9.104E+06	-1.085E+07	4.360E+01	9.988E+05	1	-3.371E+06	1	0.000E+00
	4	-4.065E-05	-5.151E-05	1.539E-04	-8.130E+06	-1.030E+07	4.298E+01	7.768E+05	1	-2.986E+06	1	0.000E+00
87	1	-4.470E-05	-3.976E-05	1.602E-04	-8.941E+06	-7.951E+06	4.588E+01	9.472E+05	1	-2.965E+06	1	0.000E+00
	2	-4.056E-05	-2.943E-05	1.500E-04	-8.112E+06	-5.887E+06	4.712E+01	1.006E+06	1	-2.680E+06	1	0.000E+00
	3	-3.198E-05	-4.295E-05	1.488E-04	-6.397E+06	-8.589E+06	4.289E+01	9.286E+05	1	-2.723E+06	1	0.000E+00
	4	-3.339E-05	-3.365E-05	1.322E-04	-6.678E+06	-6.730E+06	4.494E+01	8.142E+05	1	-2.428E+06	1	0.000E+00
88	1	-2.898E-05	-1.228E-07	2.359E-05	-7.416E+05	-1.143E+05	2.564E+05	ELASTIC STRESSES XX YY XY				
	2	1.723E-06	-1.051E-06	5.994E-06	4.004E+04	-2.026E+04	6.516E+04					
	3	-2.449E-05	-7.955E-07	1.909E-05	-6.294E+05	-1.143E+05	2.075E+05					
	4	4.444E-06	-1.594E-06	2.829E-06	1.075E+05	-2.373E+04	3.076E+04					
89	1	1.939E-05	2.013E-04	7.224E-04	3.878E+06	4.027E+07	5.206E+01	1.259E+06	2	-6.124E+06	1	1.362E-04

	2	4.237E-05	1.369E-04	6.913E-04	8.474E+06	2.737E+07	4.889E+01	1.273E+06	2	-6.061E+06	1	1.234E-04
	3	1.265E-05	1.262E-04	7.422E-04	2.529E+06	2.525E+07	4.935E+01	1.271E+06	2	-7.064E+06	1	1.252E-04
	4	1.721E-05	2.840E-05	6.235E-04	3.442E+06	5.681E+06	4.551E+01	1.311E+06	2	-6.703E+06	1	9.432E-05
90	1	4.407E-05	9.298E-05	6.478E-04	8.814E+06	1.860E+07	4.715E+01	1.289E+06	2	-5.997E+06	1	1.108E-04
	2	5.044E-05	5.281E-05	5.980E-04	1.009E+07	1.056E+07	4.511E+01	1.305E+06	2	-5.802E+06	1	9.888E-05
	3	1.251E-05	-9.136E-07	5.783E-04	2.501E+06	-1.827E+05	4.433E+01	1.328E+06	2	-6.583E+06	1	8.327E-05
	4	1.979E-05	-3.950E-05	5.079E-04	3.958E+06	-7.901E+06	4.167E+01	1.351E+06	2	-6.198E+06	1	6.971E-05
91	1	4.904E-05	2.884E-05	5.504E-04	9.809E+06	5.769E+06	4.394E+01	1.319E+06	2	-5.562E+06	1	8.878E-05
	2	4.312E-05	-1.201E-06	4.794E-04	8.625E+06	-2.403E+05	4.235E+01	1.343E+06	2	-5.193E+06	1	7.411E-05
	3	9.289E-06	-6.825E-05	4.237E-04	1.858E+06	-1.365E+07	3.981E+01	1.383E+06	2	-5.746E+06	1	5.295E-05
	4	-2.242E-05	-8.229E-05	3.211E-04	-4.484E+06	-1.646E+07	3.972E+01	1.436E+06	2	-5.102E+06	1	3.162E-05
92	1	2.420E-05	-2.728E-05	4.028E-04	4.840E+06	-5.455E+06	4.135E+01	1.374E+06	2	-4.853E+06	1	5.718E-05
	2	-1.352E-05	-5.026E-05	2.952E-04	-2.705E+06	-1.005E+07	4.145E+01	1.431E+06	2	-4.312E+06	1	3.315E-05
	3	-3.733E-05	-9.530E-05	2.495E-04	-7.465E+06	-1.906E+07	3.845E+01	1.544E+06	1	-4.623E+06	1	0.000E+00
	4	-3.829E-05	-9.223E-05	2.094E-04	-7.658E+06	-1.845E+07	3.777E+01	1.072E+06	1	-4.147E+06	1	0.000E+00
93	1	-3.045E-05	-5.959E-05	2.387E-04	-6.089E+06	-1.192E+07	4.152E+01	1.470E+06	2	-3.960E+06	1	2.133E-05
	2	-3.747E-05	-6.908E-05	1.848E-04	-7.494E+06	-1.382E+07	4.014E+01	1.012E+06	1	-3.540E+06	1	0.000E+00
	3	-3.651E-05	-8.226E-05	1.875E-04	-7.302E+06	-1.645E+07	3.814E+01	9.277E+05	1	-3.745E+06	1	0.000E+00
	4	-2.921E-05	-7.243E-05	1.612E-04	-5.841E+06	-1.449E+07	3.749E+01	8.161E+05	1	-3.244E+06	1	0.000E+00
94	1	-3.459E-05	-6.023E-05	1.689E-04	-6.918E+06	-1.205E+07	4.068E+01	9.506E+05	1	-3.211E+06	1	0.000E+00
	2	-3.120E-05	-4.729E-05	1.497E-04	-6.241E+06	-9.458E+06	4.193E+01	9.005E+05	1	-2.781E+06	1	0.000E+00
	3	-2.180E-05	-6.303E-05	1.500E-04	-4.359E+06	-1.261E+07	3.731E+01	8.849E+05	1	-2.915E+06	1	0.000E+00
	4	-2.036E-05	-5.160E-05	1.290E-04	-4.072E+06	-1.032E+07	3.819E+01	7.591E+05	1	-2.493E+06	1	0.000E+00
95	1	-2.943E-05	-4.506E-05	1.300E-04	-5.886E+06	-9.013E+06	4.157E+01	7.051E+05	1	-2.502E+06	1	0.000E+00
	2	-2.837E-05	-3.599E-05	1.157E-04	-5.674E+06	-7.199E+06	4.311E+01	6.445E+05	1	-2.203E+06	1	0.000E+00
	3	-2.005E-05	-4.405E-05	1.132E-04	-4.010E+06	-8.810E+06	3.901E+01	6.458E+05	1	-2.198E+06	1	0.000E+00
	4	-2.104E-05	-3.457E-05	9.620E-05	-4.208E+06	-6.913E+06	4.099E+01	5.192E+05	1	-1.873E+06	1	0.000E+00
96	1	-2.084E-05	-1.280E-06	1.561E-05	-5.378E+05	-1.127E+05	1.697E+05	ELASTIC STRESSES XX YY XY				
	2	5.575E-06	-1.722E-06	5.301E-07	1.360E+05	-2.265E+04	5.761E+03					
	3	-1.590E-05	-1.968E-06	9.865E-06	-4.142E+05	-1.113E+05	1.072E+05					
	4	6.024E-06	-1.566E-06	-2.156E-06	1.481E+05	-1.694E+04	-2.344E+04					
97	1	-1.519E-05	3.229E-05	7.105E-04	-3.038E+06	6.458E+06	4.691E+01	1.299E+06	2	-7.933E+06	1	1.027E-04
	2	-2.442E-05	-6.543E-05	5.540E-04	-4.883E+06	-1.309E+07	4.288E+01	1.357E+06	2	-7.416E+06	1	6.587E-05
	3	-3.143E-05	-1.859E-04	6.199E-04	-6.285E+06	-3.719E+07	3.800E+01	1.369E+06	2	-9.557E+06	1	6.035E-05
	4	-8.501E-05	-2.500E-04	4.132E-04	-1.700E+07	-5.000E+07	3.411E+01	1.374E+06	1	-8.799E+06	1	0.000E+00
98	1	-2.403E-05	-1.041E-04	4.757E-04	-4.807E+06	-2.083E+07	4.022E+01	1.389E+06	2	-7.050E+06	1	5.040E-05
	2	-4.926E-05	-1.267E-04	3.551E-04	-9.853E+06	-2.535E+07	3.884E+01	1.451E+06	2	-6.289E+06	1	2.678E-05
	3	-8.048E-05	-2.343E-04	3.385E-04	-1.610E+07	-4.685E+07	3.278E+01	7.131E+05	1	-7.845E+06	1	0.000E+00
	4	-5.003E-05	-2.148E-04	2.854E-04	-1.001E+07	-4.295E+07	3.000E+01	8.091E+05	1	-6.877E+06	1	0.000E+00
99	1	-5.524E-05	-1.319E-04	2.871E-04	-1.105E+07	-2.639E+07	3.752E+01	1.375E+06	1	-5.688E+06	1	0.000E+00
	2	-4.463E-05	-1.289E-04	2.451E-04	-8.927E+06	-2.578E+07	3.551E+01	1.071E+06	1	-5.116E+06	1	0.000E+00
	3	-3.588E-05	-1.926E-04	2.525E-04	-7.177E+06	-3.852E+07	2.909E+01	8.591E+05	1	-6.140E+06	1	0.000E+00
	4	-2.600E-05	-1.590E-04	2.020E-04	-5.200E+06	-3.180E+07	2.832E+01	7.103E+05	1	-5.050E+06	1	0.000E+00
100	1	-3.746E-05	-1.153E-04	2.203E-04	-7.491E+06	-2.306E+07	3.526E+01	1.011E+06	1	-4.597E+06	1	0.000E+00
	2	-2.921E-05	-9.878E-05	1.898E-04	-5.841E+06	-1.976E+07	3.493E+01	9.271E+05	1	-3.956E+06	1	0.000E+00
	3	-2.044E-05	-1.374E-04	1.757E-04	-4.087E+06	-2.749E+07	2.817E+01	6.655E+05	1	-4.400E+06	1	0.000E+00
	4	-1.587E-05	-1.102E-04	1.472E-04	-3.174E+06	-2.203E+07	2.867E+01	6.095E+05	1	-3.619E+06	1	0.000E+00
101	1	-2.454E-05	-8.938E-05	1.680E-04	-4.908E+06	-1.788E+07	3.444E+01	8.266E+05	1	-3.539E+06	1	0.000E+00

	2-1.989E-05	-7.125E-05	1.461E-04	-3.978E+06	-1.425E+07	3.531E+01	7.962E+05	1	-2.980E+06	1	0.000E+00
	3-1.306E-05	-9.310E-05	1.299E-04	-2.613E+06	-1.862E+07	2.917E+01	5.798E+05	1	-3.129E+06	1	0.000E+00
	4-9.813E-06	-7.160E-05	1.098E-04	-1.963E+06	-1.432E+07	3.032E+01	5.574E+05	1	-2.525E+06	1	0.000E+00
102	1-1.698E-05	-6.304E-05	1.282E-04	-3.396E+06	-1.261E+07	3.511E+01	7.020E+05	1	-2.630E+06	1	0.000E+00
	2-1.322E-05	-5.091E-05	1.106E-04	-2.644E+06	-1.018E+07	3.559E+01	6.588E+05	1	-2.211E+06	1	0.000E+00
	3-7.959E-06	-5.835E-05	9.754E-05	-1.592E+06	-1.167E+07	3.134E+01	5.435E+05	1	-2.153E+06	1	0.000E+00
	4-5.677E-06	-4.280E-05	8.290E-05	-1.135E+06	-8.559E+06	3.294E+01	5.295E+05	1	-1.711E+06	1	0.000E+00
103	1-1.267E-05	-4.201E-05	9.859E-05	-2.534E+06	-8.403E+06	3.671E+01	6.022E+05	1	-1.931E+06	1	0.000E+00
	2-1.579E-05	-3.226E-05	8.100E-05	-3.158E+06	-6.451E+06	3.925E+01	4.326E+05	1	-1.607E+06	1	0.000E+00
	3-5.583E-06	-3.259E-05	7.331E-05	-1.117E+06	-6.518E+06	3.488E+01	4.994E+05	1	-1.433E+06	1	0.000E+00
	4-8.482E-06	-2.250E-05	6.133E-05	-1.696E+06	-4.500E+06	3.856E+01	3.991E+05	1	-1.160E+06	1	0.000E+00
104	1-1.209E-05	-2.118E-06	5.822E-06	-3.174E+05	-1.006E+05	6.329E+04	ELASTIC STRESSES XX YY XY				
	2 5.477E-06	-1.376E-06	-4.012E-06	1.348E+05	-1.419E+04	-4.361E+04					
	3-7.127E-06	-1.488E-06	1.197E-06	-1.880E+05	-6.540E+04	1.301E+04					
	4 3.815E-06	-6.642E-07	-5.699E-06	9.502E+04	-2.352E+03	-6.194E+04					
105	1-4.928E-05	-4.134E-04	4.946E-04	-9.857E+06	-8.269E+07	2.682E+01	1.469E+06	2	-1.165E+07	1	2.297E-05
	2-8.020E-05	-3.715E-04	3.686E-04	-1.604E+07	-7.430E+07	2.584E+01	2.264E+05	1	-1.019E+07	1	0.000E+00
	3-3.733E-05	-8.750E-04	3.373E-04	-7.465E+06	-1.750E+08	1.096E+01	-1.162E+05	-1	-1.754E+07	1	0.000E+00
	4-3.557E-05	-5.772E-04	1.805E-04	-7.114E+06	-1.154E+08	9.212E+00	-5.207E+05	-1	-1.261E+07	1	0.000E+00
106	1-4.392E-05	-3.333E-04	3.493E-04	-8.784E+06	-6.666E+07	2.518E+01	9.548E+05	1	-9.307E+06	1	0.000E+00
	2-2.384E-05	-2.739E-04	2.289E-04	-4.768E+06	-5.478E+07	2.123E+01	5.159E+05	1	-7.326E+06	1	0.000E+00
	3 3.953E-06	-4.441E-04	8.798E-05	7.906E+05	-8.883E+07	5.553E+00	2.058E+05	1	-9.954E+06	1	0.000E+00
	4 2.357E-07	-3.179E-04	7.406E-05	4.714E+04	-6.357E+07	6.552E+00	1.122E+05	1	-7.405E+06	1	0.000E+00
107	1-1.737E-05	-2.289E-04	1.762E-04	-3.474E+06	-4.579E+07	1.989E+01	3.631E+05	1	-6.096E+06	1	0.000E+00
	2-1.329E-05	-1.785E-04	1.484E-04	-2.658E+06	-3.570E+07	2.096E+01	3.785E+05	1	-4.906E+06	1	0.000E+00
	3-3.265E-06	-2.579E-04	6.507E-05	-6.531E+05	-5.157E+07	7.168E+00	2.066E+04	1	-6.120E+06	1	0.000E+00
	4-2.630E-06	-1.921E-04	4.539E-05	-5.260E+05	-3.843E+07	6.735E+00	1.269E+03	1	-4.633E+06	1	0.000E+00
108	1-9.983E-06	-1.503E-04	1.282E-04	-1.997E+06	-3.006E+07	2.121E+01	3.726E+05	1	-4.188E+06	1	0.000E+00
	2-6.800E-06	-1.158E-04	1.034E-04	-1.360E+06	-2.316E+07	2.175E+01	3.457E+05	1	-3.294E+06	1	0.000E+00
	3-1.345E-06	-1.529E-04	3.625E-05	-2.691E+05	-3.059E+07	6.724E+00	1.980E+04	1	-3.726E+06	1	0.000E+00
	4-2.416E-07	-1.094E-04	2.968E-05	-4.832E+04	-2.188E+07	7.605E+00	4.350E+04	1	-2.707E+06	1	0.000E+00
109	1-5.846E-06	-9.245E-05	8.992E-05	-1.169E+06	-1.849E+07	2.304E+01	3.319E+05	1	-2.711E+06	1	0.000E+00
	2-4.382E-06	-6.757E-05	7.536E-05	-8.764E+05	-1.351E+07	2.501E+01	3.299E+05	1	-2.083E+06	1	0.000E+00
	3-5.564E-07	-8.380E-05	2.650E-05	-1.113E+05	-1.676E+07	8.828E+00	3.755E+04	1	-2.101E+06	1	0.000E+00
	4-4.800E-07	-5.310E-05	2.228E-05	-9.601E+04	-1.062E+07	1.147E+01	4.454E+04	1	-1.365E+06	1	0.000E+00
110	1-3.475E-06	-5.038E-05	6.859E-05	-6.949E+05	-1.008E+07	2.781E+01	3.654E+05	1	-1.683E+06	1	0.000E+00
	2-2.213E-06	-3.175E-05	6.102E-05	-4.425E+05	-6.349E+06	3.208E+01	4.229E+05	1	-1.256E+06	1	0.000E+00
	3-4.550E-07	-3.433E-05	1.943E-05	-9.099E+04	-6.865E+06	1.492E+01	5.336E+04	1	-9.144E+05	1	0.000E+00
	4-2.163E-07	-1.070E-05	1.687E-05	-4.326E+04	-2.140E+06	2.907E+01	1.119E+05	1	-3.832E+05	1	0.000E+00
111	1-4.452E-07	-2.180E-05	5.417E-05	-8.903E+04	-4.359E+06	3.424E+01	4.499E+05	1	-9.958E+05	1	0.000E+00
	2-4.819E-06	-9.033E-06	4.363E-05	-9.638E+05	-1.807E+06	4.224E+01	3.747E+05	1	-7.158E+05	1	0.000E+00
	3 1.645E-06	5.660E-06	1.899E-05	3.289E+05	1.132E+06	5.096E+01	3.339E+05	1	-1.511E+05	1	0.000E+00
	4-1.450E-06	2.539E-05	1.810E-05	-2.901E+05	5.078E+06	7.300E+01	7.039E+05	1	-1.053E+05	1	0.000E+00
112	1-3.735E-06	9.973E-08	-5.201E-07	-9.515E+04	-1.178E+04	-5.654E+03	ELASTIC STRESSES XX YY XY				
	2 2.071E-06	-3.448E-07	-6.606E-06	5.164E+04	-8.731E+02	-7.180E+04					
	3-1.500E-06	6.636E-06	-1.160E-06	-1.291E+04	1.640E+05	-1.261E+04					
	4-6.967E-08	2.643E-06	-2.928E-06	8.359E+03	6.734E+04	-3.183E+04					

***** DISPLACEMENT SOLUTION ***** (-9.999E03 = UNCONNECTED NODE)

NODE	X DISPL	Y DISPL	NODE	X DISPL	Y DISPL	NODE	X DISPL	Y DISPL	NODE	X DISPL	Y DISPL
1	0.000E+00	0.000E+00	125	-9.999E+03	-9.999E+03	249	5.617E-04	2.752E-04	373	-9.999E+03	-9.999E+03
2	1.631E-05	1.040E-04	126	2.434E-04	3.090E-04	250	6.280E-04	2.920E-04	374	9.625E-04	6.679E-05
3	4.337E-05	2.021E-04	127	-9.999E+03	-9.999E+03	251	6.925E-04	3.063E-04	375	0.000E+00	0.000E+00
4	7.825E-05	2.928E-04	128	3.741E-04	3.889E-04	252	7.540E-04	3.174E-04	376	5.184E-05	1.532E-05
5	1.201E-04	3.787E-04	129	-9.999E+03	-9.999E+03	253	8.111E-04	3.248E-04	377	1.071E-04	2.740E-05
6	1.686E-04	4.603E-04	130	5.216E-04	4.580E-04	254	8.888E-04	3.255E-04	378	1.642E-04	3.607E-05
7	2.227E-04	5.368E-04	131	-9.999E+03	-9.999E+03	255	9.643E-04	3.263E-04	379	2.238E-04	4.223E-05
8	2.826E-04	6.073E-04	132	6.774E-04	5.196E-04	256	0.000E+00	0.000E+00	380	2.848E-04	4.611E-05
9	3.467E-04	6.721E-04	133	-9.999E+03	-9.999E+03	257	-9.999E+03	-9.999E+03	381	3.460E-04	4.778E-05
10	4.166E-04	7.332E-04	134	8.288E-04	5.750E-04	258	7.884E-05	6.523E-05	382	4.071E-04	4.848E-05
11	4.889E-04	7.875E-04	135	-9.999E+03	-9.999E+03	259	-9.999E+03	-9.999E+03	383	4.665E-04	4.716E-05
12	5.690E-04	8.254E-04	136	1.001E-03	5.771E-04	260	1.829E-04	1.223E-04	384	5.236E-04	4.369E-05
13	6.439E-04	8.532E-04	137	0.000E+00	0.000E+00	261	-9.999E+03	-9.999E+03	385	5.783E-04	3.919E-05
14	7.204E-04	8.996E-04	138	2.304E-05	5.448E-05	262	3.037E-04	1.724E-04	386	6.317E-04	3.508E-05
15	7.616E-04	9.442E-04	139	5.447E-05	1.066E-04	263	-9.999E+03	-9.999E+03	387	6.843E-04	3.179E-05
16	1.000E-03	8.894E-04	140	9.352E-05	1.562E-04	264	4.339E-04	2.156E-04	388	7.354E-04	2.863E-05
17	9.613E-04	8.331E-04	141	1.395E-04	2.030E-04	265	-9.999E+03	-9.999E+03	389	7.858E-04	2.602E-05
18	0.000E+00	0.000E+00	142	1.918E-04	2.471E-04	266	5.664E-04	2.512E-04	390	8.757E-04	2.586E-05
19	-9.999E+03	-9.999E+03	143	2.501E-04	2.885E-04	267	-9.999E+03	-9.999E+03	391	9.636E-04	2.562E-05
20	4.341E-05	1.760E-04	144	3.137E-04	3.270E-04	268	6.939E-04	2.773E-04	392	0.000E+00	0.000E+00
21	-9.999E+03	-9.999E+03	145	3.819E-04	3.629E-04	269	-9.999E+03	-9.999E+03	393	-9.999E+03	-9.999E+03
22	1.203E-04	3.393E-04	146	4.539E-04	3.965E-04	270	8.078E-04	2.905E-04	394	1.098E-04	1.838E-05
23	-9.999E+03	-9.999E+03	147	5.277E-04	4.281E-04	271	-9.999E+03	-9.999E+03	395	-9.999E+03	-9.999E+03
24	2.229E-04	4.852E-04	148	6.043E-04	4.582E-04	272	9.623E-04	2.916E-04	396	2.273E-04	2.237E-05
25	-9.999E+03	-9.999E+03	149	6.786E-04	4.865E-04	273	0.000E+00	0.000E+00	397	-9.999E+03	-9.999E+03
26	3.471E-04	6.124E-04	150	7.540E-04	5.130E-04	274	3.801E-05	3.117E-05	398	3.485E-04	1.852E-05
27	-9.999E+03	-9.999E+03	151	8.247E-04	5.359E-04	275	8.307E-05	6.020E-05	399	-9.999E+03	-9.999E+03
28	4.903E-04	7.140E-04	152	9.111E-04	5.372E-04	276	1.339E-04	8.724E-05	400	4.647E-04	8.031E-06
29	-9.999E+03	-9.999E+03	153	9.915E-04	5.386E-04	277	1.894E-04	1.125E-04	401	-9.999E+03	-9.999E+03
30	6.474E-04	7.903E-04	154	0.000E+00	0.000E+00	278	2.487E-04	1.360E-04	402	5.757E-04	-2.359E-06
31	-9.999E+03	-9.999E+03	155	-9.999E+03	-9.999E+03	279	3.108E-04	1.579E-04	403	-9.999E+03	-9.999E+03
32	8.149E-04	8.239E-04	156	5.713E-05	1.001E-04	280	3.750E-04	1.780E-04	404	6.821E-04	-1.034E-05
33	-9.999E+03	-9.999E+03	157	-9.999E+03	-9.999E+03	281	4.403E-04	1.963E-04	405	-9.999E+03	-9.999E+03
34	1.015E-03	8.596E-04	158	1.446E-04	1.898E-04	282	5.058E-04	2.126E-04	406	7.837E-04	-1.608E-05
35	0.000E+00	0.000E+00	159	-9.999E+03	-9.999E+03	283	5.707E-04	2.268E-04	407	-9.999E+03	-9.999E+03
36	1.703E-05	8.027E-05	160	2.574E-04	2.692E-04	284	6.341E-04	2.386E-04	408	9.648E-04	-1.658E-05
37	4.399E-05	1.596E-04	161	-9.999E+03	-9.999E+03	285	6.948E-04	2.476E-04	409	0.000E+00	0.000E+00
38	7.893E-05	2.356E-04	162	3.900E-04	3.387E-04	286	7.527E-04	2.541E-04	410	5.589E-05	5.747E-06
39	1.210E-04	3.087E-04	163	-9.999E+03	-9.999E+03	287	8.043E-04	2.556E-04	411	1.105E-04	4.687E-06
40	1.694E-04	3.784E-04	164	5.344E-04	4.002E-04	288	8.839E-04	2.561E-04	412	1.689E-04	1.758E-06
41	2.239E-04	4.443E-04	165	-9.999E+03	-9.999E+03	289	9.610E-04	2.564E-04	413	2.289E-04	-3.522E-06
42	2.834E-04	5.053E-04	166	6.816E-04	4.545E-04	290	0.000E+00	0.000E+00	414	2.876E-04	-1.151E-05
43	3.486E-04	5.613E-04	167	-9.999E+03	-9.999E+03	291	-9.999E+03	-9.999E+03	415	3.464E-04	-2.001E-05
44	4.179E-04	6.130E-04	168	8.234E-04	4.982E-04	292	8.727E-05	5.530E-05	416	4.046E-04	-2.751E-05
45	4.931E-04	6.585E-04	169	-9.999E+03	-9.999E+03	293	-9.999E+03	-9.999E+03	417	4.622E-04	-3.423E-05
46	5.687E-04	6.940E-04	170	9.857E-04	5.019E-04	294	1.958E-04	1.028E-04	418	5.186E-04	-4.035E-05
47	6.526E-04	7.200E-04	171	0.000E+00	0.000E+00	295	-9.999E+03	-9.999E+03	419	5.740E-04	-4.542E-05
48	7.372E-04	7.424E-04	172	2.588E-05	4.830E-05	296	3.178E-04	1.432E-04	420	6.279E-04	-4.990E-05
49	8.665E-04	7.841E-04	173	6.005E-05	9.374E-05	297	-9.999E+03	-9.999E+03	421	6.805E-04	-5.371E-05
50	9.275E-04	7.939E-04	174	1.017E-04	1.367E-04	298	4.464E-04	1.763E-04	422	7.320E-04	-5.674E-05
51	1.067E-03	8.053E-04	175	1.503E-04	1.772E-04	299	-9.999E+03	-9.999E+03	423	7.821E-04	-5.918E-05
52	0.000E+00	0.000E+00	176	2.050E-04	2.153E-04	300	5.746E-04	2.015E-04	424	8.747E-04	-5.949E-05
53	-9.999E+03	-9.999E+03	177	2.651E-04	2.510E-04	301	-9.999E+03	-9.999E+03	425	9.659E-04	-5.972E-05
54	4.496E-05	1.466E-04	178	3.298E-04	2.844E-04	302	6.956E-04	2.172E-04	426	0.000E+00	0.000E+00
55	-9.999E+03	-9.999E+03	179	3.980E-04	3.160E-04	303	-9.999E+03	-9.999E+03	427	-9.999E+03	-9.999E+03
56	1.224E-04	2.847E-04	180	4.684E-04	3.456E-04	304	8.008E-04	2.200E-04	428	1.090E-04	-1.501E-05
57	-9.999E+03	-9.999E+03	181	5.407E-04	3.736E-04	305	-9.999E+03	-9.999E+03	429	-9.999E+03	-9.999E+03
58	2.256E-04	4.100E-04	182	6.126E-04	3.996E-04	306	9.604E-04	2.204E-04	430	2.248E-04	-4.058E-05
59	-9.999E+03	-9.999E+03	183	6.845E-04	4.232E-04	307	0.000E+00	0.000E+00	431	-9.999E+03	-9.999E+03
60	3.511E-04	5.191E-04	184	7.538E-04	4.440E-04	308	4.277E-05	2.629E-05	432	3.435E-04	-6.234E-05
61	-9.999E+03	-9.999E+03	185	8.221E-04	4.624E-04	309	9.142E-05	5.047E-05	433	-9.999E+03	-9.999E+03
62	4.951E-04	6.071E-04	186	9.019E-04	4.638E-04	310	1.448E-04	7.259E-05	434	4.603E-04	-7.893E-05
63	-9.999E+03	-9.999E+03	187	9.806E-04	4.655E-04	311	2.020E-04	9.284E-05	435	-9.999E+03	-9.999E+03
64	6.580E-04	6.702E-04	188	0.000E+00	0.000E+00	312	2.622E-04	1.113E-04	436	5.727E-04	-9.064E-05

65	-9.999E+03	-9.999E+03	189	-9.999E+03	-9.999E+03	313	3.245E-04	1.279E-04	437	-9.999E+03	-9.999E+03
66	8.457E-04	7.513E-04	190	6.326E-05	8.756E-05	314	3.881E-04	1.426E-04	438	6.797E-04	-9.841E-05
67	-9.999E+03	-9.999E+03	191	-9.999E+03	-9.999E+03	315	4.522E-04	1.554E-04	439	-9.999E+03	-9.999E+03
68	1.040E-03	7.424E-04	192	1.565E-04	1.652E-04	316	5.157E-04	1.661E-04	440	7.808E-04	-1.032E-04
69	0.000E+00	0.000E+00	193	-9.999E+03	-9.999E+03	317	5.778E-04	1.746E-04	441	-9.999E+03	-9.999E+03
70	1.861E-05	6.910E-05	194	2.730E-04	2.338E-04	318	6.379E-04	1.809E-04	442	9.668E-04	-1.037E-04
71	4.631E-05	1.365E-04	195	-9.999E+03	-9.999E+03	319	6.952E-04	1.847E-04	443	0.000E+00	0.000E+00
72	8.192E-05	2.019E-04	196	4.056E-04	2.945E-04	320	7.478E-04	1.850E-04	444	4.947E-05	-2.097E-05
73	1.245E-04	2.647E-04	197	-9.999E+03	-9.999E+03	321	7.972E-04	1.833E-04	445	1.027E-04	-4.515E-05
74	1.736E-04	3.246E-04	198	5.462E-04	3.480E-04	322	8.802E-04	1.836E-04	446	1.617E-04	-6.382E-05
75	2.286E-04	3.810E-04	199	-9.999E+03	-9.999E+03	323	9.603E-04	1.837E-04	447	2.218E-04	-8.034E-05
76	2.892E-04	4.334E-04	200	6.866E-04	3.930E-04	324	0.000E+00	0.000E+00	448	2.819E-04	-9.559E-05
77	3.546E-04	4.815E-04	201	-9.999E+03	-9.999E+03	325	-9.999E+03	-9.999E+03	449	3.418E-04	-1.081E-04
78	4.254E-04	5.249E-04	202	8.195E-04	4.276E-04	326	9.548E-05	4.550E-05	450	4.010E-04	-1.182E-04
79	5.004E-04	5.629E-04	203	-9.999E+03	-9.999E+03	327	-9.999E+03	-9.999E+03	451	4.592E-04	-1.264E-04
80	5.811E-04	5.978E-04	204	9.751E-04	4.298E-04	328	2.080E-04	8.240E-05	452	5.162E-04	-1.330E-04
81	6.607E-04	6.325E-04	205	0.000E+00	0.000E+00	329	-9.999E+03	-9.999E+03	453	5.719E-04	-1.381E-04
82	7.564E-04	6.699E-04	206	2.925E-05	4.208E-05	330	3.309E-04	1.115E-04	454	6.264E-04	-1.420E-04
83	8.253E-04	7.019E-04	207	6.681E-05	8.162E-05	331	-9.999E+03	-9.999E+03	455	6.793E-04	-1.448E-04
84	9.352E-04	7.017E-04	208	1.117E-04	1.188E-04	332	4.574E-04	1.328E-04	456	7.305E-04	-1.467E-04
85	1.014E-03	7.005E-04	209	1.629E-04	1.538E-04	333	-9.999E+03	-9.999E+03	457	7.801E-04	-1.479E-04
86	0.000E+00	0.000E+00	210	2.197E-04	1.866E-04	334	5.804E-04	1.459E-04	458	8.743E-04	-1.481E-04
87	-9.999E+03	-9.999E+03	211	2.809E-04	2.175E-04	335	-9.999E+03	-9.999E+03	459	9.674E-04	-1.481E-04
88	4.798E-05	1.279E-04	212	3.457E-04	2.466E-04	336	6.932E-04	1.497E-04	460	0.000E+00	0.000E+00
89	-9.999E+03	-9.999E+03	213	4.130E-04	2.739E-04	337	-9.999E+03	-9.999E+03	461	-9.999E+03	-9.999E+03
90	1.274E-04	2.474E-04	214	4.820E-04	2.996E-04	338	7.941E-04	1.456E-04	462	9.915E-05	-7.664E-05
91	-9.999E+03	-9.999E+03	215	5.515E-04	3.232E-04	339	-9.999E+03	-9.999E+03	463	-9.999E+03	-9.999E+03
92	2.326E-04	3.549E-04	216	6.208E-04	3.447E-04	340	9.608E-04	1.459E-04	464	2.205E-04	-1.276E-04
93	-9.999E+03	-9.999E+03	217	6.886E-04	3.638E-04	341	0.000E+00	0.000E+00	465	-9.999E+03	-9.999E+03
94	3.599E-04	4.476E-04	218	7.544E-04	3.801E-04	342	4.739E-05	2.137E-05	466	3.410E-04	-1.584E-04
95	-9.999E+03	-9.999E+03	219	8.167E-04	3.930E-04	343	9.948E-05	4.025E-05	467	-9.999E+03	-9.999E+03
96	5.077E-04	5.251E-04	220	8.950E-04	3.940E-04	344	1.552E-04	5.670E-05	468	4.587E-04	-1.776E-04
97	-9.999E+03	-9.999E+03	221	9.704E-04	3.951E-04	345	2.137E-04	7.095E-05	469	-9.999E+03	-9.999E+03
98	6.687E-04	5.932E-04	222	0.000E+00	0.000E+00	346	2.746E-04	8.314E-05	470	5.717E-04	-1.884E-04
99	-9.999E+03	-9.999E+03	223	-9.999E+03	-9.999E+03	347	3.369E-04	9.336E-05	471	-9.999E+03	-9.999E+03
100	8.288E-04	6.535E-04	224	7.061E-05	7.593E-05	348	3.995E-04	1.015E-04	472	6.792E-04	-1.930E-04
101	-9.999E+03	-9.999E+03	225	-9.999E+03	-9.999E+03	349	4.617E-04	1.077E-04	473	-9.999E+03	-9.999E+03
102	1.013E-03	6.628E-04	226	1.696E-04	1.428E-04	350	5.227E-04	1.121E-04	474	7.794E-04	-1.933E-04
103	0.000E+00	0.000E+00	227	-9.999E+03	-9.999E+03	351	5.817E-04	1.144E-04	475	-9.999E+03	-9.999E+03
104	2.062E-05	6.110E-05	228	2.887E-04	2.019E-04	352	6.376E-04	1.143E-04	476	9.675E-04	-1.928E-04
105	4.991E-05	1.203E-04	229	-9.999E+03	-9.999E+03	353	6.899E-04	1.118E-04	477	0.000E+00	0.000E+00
106	8.690E-05	1.773E-04	230	4.202E-04	2.541E-04	354	7.407E-04	1.091E-04	478	3.953E-05	-7.596E-05
107	1.309E-04	2.316E-04	231	-9.999E+03	-9.999E+03	355	7.911E-04	1.070E-04	479	9.910E-05	-1.277E-04
108	1.812E-04	2.829E-04	232	5.567E-04	2.990E-04	356	8.774E-04	1.070E-04	480	1.596E-04	-1.595E-04
109	2.376E-04	3.310E-04	233	-9.999E+03	-9.999E+03	357	9.616E-04	1.069E-04	481	2.202E-04	-1.821E-04
110	2.994E-04	3.758E-04	234	6.907E-04	3.350E-04	358	0.000E+00	0.000E+00	482	2.806E-04	-2.007E-04
111	3.667E-04	4.172E-04	235	-9.999E+03	-9.999E+03	359	-9.999E+03	-9.999E+03	483	3.408E-04	-2.150E-04
112	4.387E-04	4.549E-04	236	8.140E-04	3.588E-04	360	1.034E-04	3.437E-05	484	4.004E-04	-2.254E-04
113	5.152E-04	4.904E-04	237	-9.999E+03	-9.999E+03	361	-9.999E+03	-9.999E+03	485	4.587E-04	-2.329E-04
114	5.925E-04	5.233E-04	238	9.669E-04	3.607E-04	362	2.191E-04	5.788E-05	486	5.158E-04	-2.384E-04
115	6.758E-04	5.551E-04	239	0.000E+00	0.000E+00	363	-9.999E+03	-9.999E+03	487	5.717E-04	-2.418E-04
116	7.512E-04	5.844E-04	240	3.335E-05	3.637E-05	364	3.420E-04	7.262E-05	488	6.261E-04	-2.436E-04
117	8.330E-04	6.134E-04	241	7.469E-05	7.047E-05	365	-9.999E+03	-9.999E+03	489	6.792E-04	-2.439E-04
118	9.180E-04	6.161E-04	242	1.227E-04	1.024E-04	366	4.650E-04	7.962E-05	490	7.305E-04	-2.423E-04
119	1.011E-03	6.197E-04	243	1.763E-04	1.324E-04	367	-9.999E+03	-9.999E+03	491	7.790E-04	-2.393E-04
120	0.000E+00	0.000E+00	244	2.344E-04	1.605E-04	368	5.810E-04	7.896E-05	492	8.744E-04	-2.378E-04
121	-9.999E+03	-9.999E+03	245	2.963E-04	1.870E-04	369	-9.999E+03	-9.999E+03	493	9.673E-04	-2.370E-04
122	5.208E-05	1.133E-04	246	3.608E-04	2.118E-04	370	6.866E-04	7.222E-05			
123	-9.999E+03	-9.999E+03	247	4.272E-04	2.348E-04	371	-9.999E+03	-9.999E+03			
124	1.349E-04	2.169E-04	248	4.944E-04	2.560E-04	372	7.883E-04	6.707E-05			